A NOVEL LIQUID DESICCANT AIR CONDITIONING SYSTEM WITH MEMBRANE EXCHANGERS AND VARIOUS HEAT SOURCES

A Thesis Submitted to the College of

Graduate Studies and Research

in Partial Fulfillment of the Requirements

for the Degree of Doctor of Philosophy

in the Department of Mechanical Engineering

University of Saskatchewan

Saskatoon

By

Ahmed Hamdi Abdel-Salam

PERMISSION TO USE

In presenting this thesis in partial fulfillment of the requirements for a Postgraduate degree from the University of Saskatchewan, I agree that the Libraries of this University may make it freely available for inspection. I further agree that permission for copying of this thesis in any manner, in whole or in part, for scholarly purposes may be granted by the professors who supervised my thesis work or, in their absence, by the Head of the Department or the Dean of the College in which my thesis work was done. It is understood that any copying, publication, or use of this thesis or parts thereof for financial gain shall not be allowed without my written permission. It is also understood that due recognition shall be given to me and to the University of Saskatchewan in any scholarly use which may be made of any material in my thesis.

Requests for permission to copy or to make other use of material in this thesis in whole or in part should be addressed to:

Head of the Department of Mechanical Engineering

University of Saskatchewan

57 Campus Drive, Saskatoon, Saskatchewan, S7N 5A9

ABSTRACT

Liquid desiccant air conditioning (LDAC) has received much attention in recent years. This is mainly because LDAC systems are able to control latent loads in a more energy efficient way than conventional air conditioning systems. Although many research studies have been conducted on LDAC technologies, the following gaps in the scientific literature are addressed in this thesis: (1) carryover of desiccant droplets in air streams, (2) direct comparisons between different configurations of LDAC systems, (3) fundamentals of capacity matching in heat-pump LDAC systems, (4) optimal-control strategies for heat-pump LDAC systems, and (5) importance of transients in evaluating the performance of a LDAC system. Items (1) to (4) are addressed using TRNSYS simulations, and item (5) is addressed using data collected from a field test.

The use of liquid-to-air membrane energy exchangers (LAMEEs) as dehumidifiers and regenerators in LDAC systems eliminate the desiccant droplets carryover problem in air streams. This is because LAMEE separate the air and solution streams using semi-permeable membranes, which allow the transfer of heat and moisture but do not allow the transfer of the liquid desiccant. A preliminary configuration for a membrane LDAC system, which uses LAMEEs as the dehumidifier and regenerator, is proposed and investigated under fixed operating conditions in this thesis. The influences of key design and operating parameters on the heat and mass transfer performances of the membrane LDAC system are evaluated. Results show that the membrane LDAC technology is able to effectively remove latent loads in applications that the humidity to be controlled.

A comprehensive evaluation is conducted in this thesis for the thermal, economic and environmental performances of several configurations of membrane LDAC systems. The solution cooling load is covered using a cooling heat pump in all systems studied, while the solution heating load is covered using one of the following five different heating systems: (1) a gas boiler, (2) a heating heat pump, (3) a solar thermal system with gas boiler backup, (4) a solar thermal system with heat pump backup, and (5) the condenser of the solution cooling heating pump. Each of the membrane LDAC systems studied is evaluated

with/without an energy recovery ventilator (ERV) installed in the air handling system. The influence of operating the ERV under balanced/unbalanced operating conditions is studied. It is found that the most economic membrane LDAC system is the one which uses the evaporator and condenser of the same heat pump to cover the solution cooling and heating loads, respectively (i.e. heat-pump membrane LDAC system).

No clear guidance was found in the literature for sizing the evaporator and condenser in a heat-pump LDAC system to simultaneously meet the solution cooling and heating loads. When the heating and cooling provided by the heat pump exactly match the heating and cooling requirements of the solution, the system is "capacity matched". A parametric study is conducted on a heat-pump membrane LDAC system to identify the influence of key operating and design parameters on achieving capacity matching. It is concluded that the solution inlet temperatures to the dehumidifier and regenerator are the most influential parameters on the moisture removal rate, capacity matching and coefficient of performance (COP). Three control strategies are developed for heat-pump membrane LDAC systems, where these strategies meet the latent loads and achieve one of the following three objectives: (1) meet the sensible loads, (2) achieve capacity matching, or (3) optimize the COP. Results show that the COP of a heat-pump LDAC system can be doubled by selecting the right combination of solution inlet temperatures to the regenerator and dehumidifier.

The importance of transients in evaluating the performance of a LDAC system is addressed in the thesis using a data collected from a field test on a solar LDAC system. It is found that the sensible, latent and total cooling energy, and the total primary energy consumption of the LDAC system are changed by less than 10% during an entire test day when transients are considered. Thus, it can be concluded that steady-state models are reliable to evaluate the energy performances of LDAC systems.

ACKNOWLEDGEMENT

This thesis would not have been possible without the help and support of many great minds and kind hearts for whom I will be indebted forever.

I am grateful beyond words to my supervisor Professor Carey Simonson for the unlimited training, support, motivation and friendship he has provided me with throughout my Ph.D. studies. I am much honored that I have worked under his distinguished supervision over the last four years, which enabled me to learn many life-time professional and personal lessons. The success of this Ph.D. project would not have been possible without his dedication to the mission of training and empowering his graduate students to become HQP with many opportunities open for them. I wish more scholars would follow Professor Simonson's ethics and philosophy in training graduate students.

I would like to extend my gratitude to Professor Robert Besant for the knowledge and game-changing ideas he has shared with me during our many discussions. Professor Besant has inspired me in many ways by his passion about inventing leading-edge technologies to conquer global warming and secure the planet for future generations.

I wish to thank my brother and fellow Ph.D. Candidate Rani for all the support and motivation he has provided me with, and for the long-productive nights we spent working hard at the university. The warm welcome and hospitality extended to me by Mohamed Beshr and Radia Eldeeb when I first arrived in Saskatoon is highly appreciated. Many thanks are due to Doctor Ge Gaoming for his help and support throughout my research project, and for the many interesting discussions we have had about air conditioning technologies. I would also like to thank my fellow graduate students/post-doctoral fellows who have conducted their research either before me or during my studies as their work has been of great help for me – Doctor Melanie Fauchoux, Doctor Gazi Mahmood, Doctor Davood Moghaddam, Mohammad Rafati, Farhad Fathieh, Blake Erb, Mohammad Afshin, Shirin Niroomand, Adesola Olufade, Ashkan Oghabi, Houman Kamili and Devin Storle.

I sincerely thank my committee members Professors Greg Schoenau, Jaafar Sultan and Robert Besant, my external examiner Professor Wasim Saman, and the chair of the examining committee Professor David Torvi. The time they spent reviewing my work is highly appreciated, and their constructive feedback has been beneficial.

The strong dedication of all the faculty and staff at the Department of Mechanical Engineering is strongly appreciated. I would like to thank Professors David Torvi, James Bugg and Reza Fotouhi for always having their doors open when they served as Department Head and/or Graduate Chair. Many thanks are due to Kelley Georgeson for all her great work as a graduate student secretary. She has always impressed me by her patience in helping graduate students from the moment they submit their applications until they graduate.

Special thanks are to be extended to Doctor Stephen Harrison, Chris McNevin and Danial Salimizad from the Solar Calorimetry Laboratory at Queen's University for their cooperation and for the hospitality extended to me during my visit to their research group.

I would like to acknowledge the financial assistance from the National Science and Engineering Research Council of Canada (NSERC) – Smart Net-zero Energy Building strategic Research Network (SNEBRN), the Department of Mechanical Engineering at University of Saskatchewan, the American Society of Heating, Refrigerating, and Air-Conditioning Engineers (ASHRAE) Grant-In-Aid, the Government of Saskatchewan's Innovative & Opportunity Scholarship, the George Ira Hanson Scholarship, and the Loretta Schoenau Scholarship.

DEDICATION

I dedicate this thesis to my parents.

Thank you both for all the love, support and care you have given me throughout my life. You have never failed me and have always been willing to provide more under any circumstances. Your unconditional love has always been a strong motivation for me, and it will always be.

TABLE OF CONTENTS

LIST OF FIGURES

LIST OF TABLES

NOMENCLATURE

ACRONYMS

AHRI	Air-Conditioning, Heating and Refrigeration Institute
ASHRAE	American Society of Heating, Refrigerating and Air Conditioning Engineers
AC	air conditioning
CAC	conventional air conditioning
CAC-ERV	conventional air conditioning with energy recovery ventilator
C/R	collector/regenerator
CC	cooling capacity
CMI	capacity matching index
COP	coefficient of performance
ECOP	electrical coefficient of performance
EEI	energy exchange inequality
ERV	energy recovery ventilator
H-M-LDAC	heat-pump membrane liquid desiccant air conditioning
HP	heat pump
HR	heat ratio
HRR	heat recovery rate
IAQ	indoor air quality
IC	initial cost
LAMEE	liquid-to-air membrane energy exchanger
LCC	life cycle cost
LDAC	liquid desiccant air conditioning
LiCl	lithium chloride
MEI	mass exchange inequality
M-LDAC	membrane liquid desiccant air-conditioning
M-LDAC-ERV	membrane liquid desiccant air-conditioning with energy recovery ventilator

M-LDAC-ERV-HP	membrane liquid desiccant air-conditioning with energy recovery ventilator and electrical heat pump for solution heating.
M-LDAC-ERV-NG	membrane liquid desiccant air-conditioning with energy recovery ventilator and natural gas boiler for solution heating.
M-LDAC-HP	membrane liquid desiccant air-conditioning with electrical heat pump for solution heating
M-LDAC-NG	membrane liquid desiccant air-conditioning with natural gas boiler for solution heating
MRR	moisture removal rate
NG	natural gas
OC	operating cost
PBP	payback period
PWF	present worth factor
RH	relative humidity
SDAC	solar desiccant air conditioning system
SHR	sensible heat ratio
SHX	sensible heat exchanger
S-M-LDAC	membrane liquid desiccant air-conditioning
S-M-LDAC-ERV	solar membrane liquid desiccant air-conditioning with energy recovery ventilator
S-M-LDAC-ERV-HP	membrane liquid desiccant air-conditioning with energy recovery ventilator and electrical heat pump for solution heating.
S-M-LDAC-ERV-NG	membrane liquid desiccant air-conditioning with energy recovery ventilator and natural gas boiler for solution heating.
S-M-LDAC-HP	solar membrane liquid desiccant air-conditioning with electrical heat pump for solution heating
S-M-LDAC-NG	solar membrane liquid desiccant air-conditioning with natural gas boiler for solution heating
STS	solar thermal system
TCOP	thermal coefficient of performance

SYMBOLS

A	surface area of the semi-permeable membranes (m^2)
A_c	solar collector surface area (m^2)
C	thermal capacity rate (W/K)
C^*	air-to-air thermal capacity rate ratio
$CF_{electrical\text{-}thermal}$	equivalent conversion coefficient of electric to thermal energy
c_p	specific heat capacity (kJ/(kg·K))
Cr^*	solution-to-air heat capacity ratio
C_{sol}	concentration of desiccant solution (%)
d	discount rate (%)
D_h	hydraulic diameter (m)
E	energy consumption (J)
E_T	slope of equilibrium humidity to temperature of solution (g/(kg·K))
F	air pollution emissions (kg/year)
F_{CO2}	annual carbon dioxide emissions (ton/year)
h	specific enthalpy (kJ/kg)
H^*	operating condition factor
h_c	convective heat transfer coefficient (W/(m^2·K))
h_m	convective mass transfer coefficient (kg/(m^2·s))
i	interest rate (%)
I_T	total solar radiation on a tilted surface (W/m^2)
k	thermal conductivity of the membrane (W/(m·K))
k_f	thermal conductivity of the fluid (W/(m·K))
k_m	water vapor permeability of the membrane (kg/(m·s))
L	length of the LAMEE (m)
Le	Lewis number
$\dot{m}$	mass flow rate (kg/s)
N	life cycle of the system (years)
NTU	number of heat transfer units
NTU_m	number of mass transfer units
Nu	Nusselt number

P	energy consumption rate (W)
Pr	pressure (Pa)
q	heat/energy transfer rate (W)
R	calculated parameter
Re	Reynold's number
$R_{exhaust}$	exhaust airflow rate ratio of ERV
SF_{annual}	annual solar fraction of solar collector (%)
T	temperature (°C)
U	overall heat transfer coefficient ($W/m^2 \cdot K$)
U_m	overall mass transfer coefficient ($kg/m^2 \cdot s$)
U_R	uncertainty in a calculated parameter R
$U_{\bar{x}_i}$	uncertainty in a measured parameter x_i
V_t	thermal storage tank volume relative to collector area (L/m^2)
W	humidity ratio (g/kg)
x_i	measured parameter

GREEK SYMBOLS

Δ	difference between two values
α	percent of electricity generated using a given type of power plant with respect to the total electricity generated
δ	thickness of the semi-permeable membrane (m)
ε	effectiveness
η	efficiency
φ	mass of pollutant emitted from a given power plant (kg/GJ)

SUBSCRIPTS

air	airflow
amb	ambient air
aux	auxiliary
c	solar collector
comp	compressor

cond	condenser
cool	cooling
db	dry bulb
deh	dehumidifier
evap	evaporator
exhaust	exhaust airflow
fresh	fresh airflow
heat	heating
i	type of pollutant
in	inlet
j	type of power plant
lat	latent
min	minimum
out	outlet
p	pumping
reg	regenerator
sen	sensible
sol	desiccant solution
th	thermal
tot	total
wat	wat

CHAPTER 1

INTRODUCTION

1.1 MOTIVATION

Building technologies have been of great interest to all civilizations starting from the ancient Egyptians thousands of years ago reaching to today's modern world. Initially, the main focus of research in building technologies was on developing new materials and construction techniques. Shortly after, attention has been given to air conditioning technologies which started with simple ideas such as hanging a wet cloth on a window to cool outdoor air when the wind blows. In 1902, a break-through was achieved by Willis Carrier when he invented the vapor compression technology. Millions of vapor compression systems have been installed all over the world since then due to their ability to achieve cooling and dehumidification under a wide range of operating conditions. Although vapor compression systems are reliable and very well-developed, they do not achieve air dehumidification in the most energy efficient way.

In a world where a majority of the financial and political tensions are driven by energy resources, there is an increasing urge to develop more energy efficient technologies. Among the technologies which have promising energy performance in achieving air dehumidification compared to vapor compression systems is the liquid desiccant technology. The main goal of this Ph.D. research is to propose and investigate solutions to the issues that currently hinder the use of the liquid desiccant technology on a wide scale in commercial and residential buildings.

1.2 BACKGROUND

1.2.1 Air conditioning processes

Two interconnected processes are required to take place in an air conditioner in order to achieve comfortable and healthy indoor air conditions. These processes are sensible and latent cooling. Sensible cooling is the reduction of dry bulb temperature at a constant

humidity ratio, while latent cooling is the reduction of humidity ratio at a constant dry bulb temperature. In a majority of air conditioning applications, sensible and latent loads have to be simultaneously controlled in order to have healthy and comfortable indoor air conditions. Although conventional air conditioning systems can efficiently achieve sensible cooling, it is more challenging to achieve latent cooling.

1.2.2 Why moisture control?

Inefficient control of indoor humidity (latent loads) results in the degradation of indoor air quality (IAQ) and affects occupants' comfort, wellbeing and productivity. In addition, inefficient control of humidity may result in several undesirable consequences on human health as shown in Figure 1.1 (Sterling et al., 1985). Moisture control problems becomes even more serious in buildings located in hot-humid climates, especially in buildings that require large amounts of fresh air such as hospitals, educational facilities and office buildings.

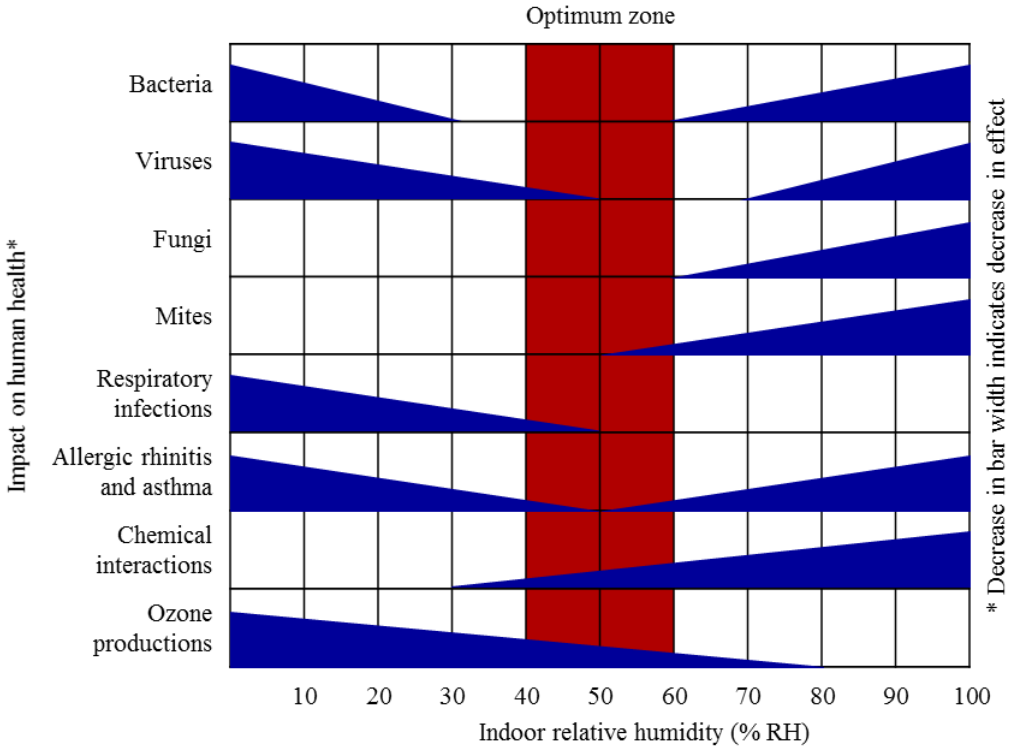

FIGURE 1.1. Impacts of indoor humidity on human health, and recommended optimum humidity levels (Sterling et al., 1985).

1.2.3 Moisture control in conventional air conditioning

In a vapor compression system, moisture control is achieved by cooling the hot-humid air below its dew point temperature in order to condense the water vapor from the air. For example, if a supply humidity ratio of 6 g/kg is required, the air has to be cooled to around 7ºC as shown in the psychrometric chart presented in Figure 1.2. The overcooled air is not directly delivered to the conditioned space but should be reheated to a reasonable temperature in order to avoid the thermal discomfort (cold draft). The overcooling and reheating processes, which take place in a vapor compression system, are energy intensive. In addition, the condensation of water droplets results in wet cooling coils which may lead to the growth of mold and bacteria on the coils, and consequently affects the IAQ.

It can be concluded that although the vapor compression system is the most well-developed air conditioning technology, it does not achieve dehumidification in energy efficient way. Thus, there is high demand for an air conditioning technology which efficiently covers the latent loads.

1.2.4 Moisture control in solid desiccant air conditioning

A solid desiccant air conditioning system uses solid desiccants to achieve dehumidification by adsorbtion. As shown in Figure 1.2, the air stream is simultaneously heated and dehumidified in solid desiccant systems, and thus the air stream leaving the desiccant wheel has to be sensibly cooled. It was mentioned in a review article by Hwang et al. (2008) that although solid desiccant air conditioning can achieve dehumidification in a more energy efficient way than a conventional air conditioning system, a liquid desiccant air conditioning (LDAC) system is capable of achieving dehumidification at higher efficiency than a solid desiccant air conditioning system. Neverhtless, solid desiccant systems are more common in practice than liquid desiccant systems.

1.2.5 Moisture control in liquid desiccant air conditioning

A liquid desiccant solution is used in a LDAC system to absorb moisture from humid air and thus there is no need to overcool the air below its dew point temperature (nor to over heat it) as can be seen in the LDAC process lines in Figure 1.2. Although not all the sensible

load is usually covered during the dehumidification process in a LDAC system, a dry cooling coil is commonly used to cover the additional sensible loads not covered during the dehumidification process as presented in Figure 1.2.

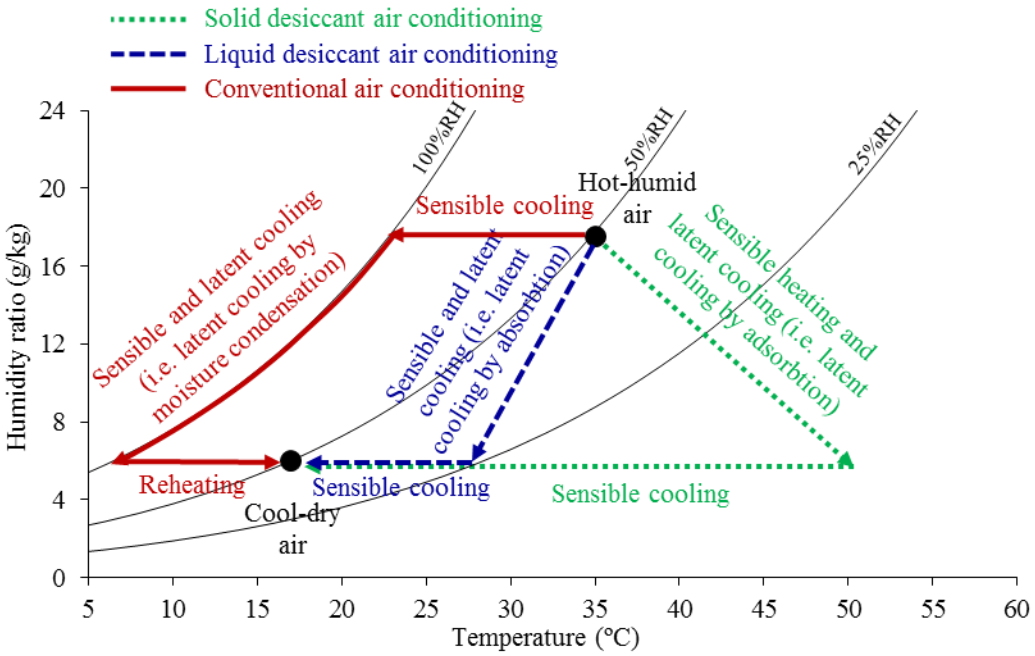

FIGURE 1.2. A psychrometric chart shows cooling/dehumidification processes in conventional, solid and liquid desiccant air conditioning.

Figure 1.3 shows the core components of a LDAC system which are: a dehumidifier, a regenerator, cooling equipment, and heating equipment. The processes take place in a LDAC cycle are as follows. Hot-humid air enters the dehumidifier, where it is dried (and possibly cooled) by a cold and concentrated desiccant solution (see state (a) in Figure 1.3). The desiccant solution leaves the dehumidifier (state (b)) at a lower concentration (and possibly higher temperature) than it entered the dehumidifier, and thus it should be regenerated before it can be reused in the dehumidifier. The regeneration of the dilute desiccant solution takes place in a regenerator, where water vapor transfers from the dilute desiccant solution stream to a regeneration air stream. In order to ensure that water vapor transfers from the dilute solution stream to the regeneration air stream and not vice versa, the vapor pressure of the dilute solution should be higher than the vapor pressure of the regeneration air. Thus, the dilute solution is heated to a specific set point temperature

before it is delivered to the regenerator (state (c)). The concentrated desiccant solution leaving the regenerator (state (d)) is warm and has high surface vapor, and therefore it needs to be cooled to a specific set point temperature in order to reduce its vapor pressure below the vapor pressure of the hot-humid air that is to be dehumidified.

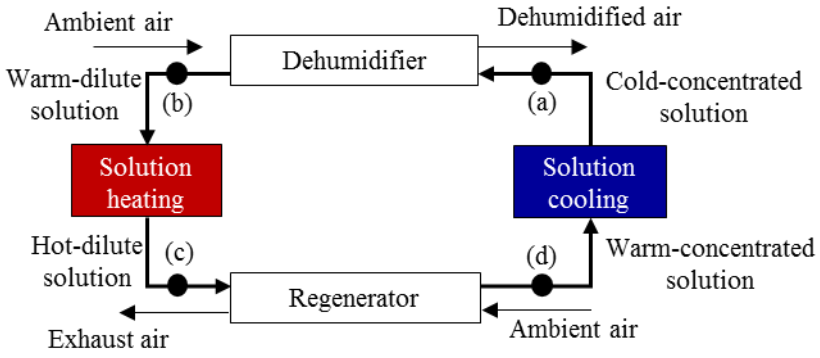

FIGURE 1.3. Core components of a liquid desiccant air conditioning (LDAC) system.

Although LDAC systems are capable of achieving efficient indoor humidity control, there are concerns about LDAC systems which hinder their wide spread use in residential and commercial buildings (Abdel-Salam and Simonson, 2015a). Solutions for these concerns are proposed and investigated in this Ph.D. thesis.

1.3 LITERATURE REVIEW

To get an insight on the research conducted in previous LDAC papers, the journal papers result when "liquid desiccant" is searched for in a scientific engineering database (www.engineeringvillage.com) are classified as presented in Figure 1.4. The period between 1980 and 2014 is investigated, and the journal papers are classified either based on the methodology or the objective. In general, it can be seen from Figure 1.4 that the attention to LDAC is increasing at considerable rate over the past 35 years, especially during the last decade. Figure 1.4(a) shows that around 60% of the journal papers conducted on LDAC are theoretical, 20% are laboratory, 15% are both theoretical and laboratory, and less than 5% are field studies. Figure 1.4(b) shows that majority of the focus of journal papers is on dehumidifiers/regenerators, followed by the whole system, and that

only a few studies focus on the thermodynamic properties of liquid desiccants and on reviewing LDAC. In addition, it can be seen that the number of review papers is considerably increasing in the last few years.

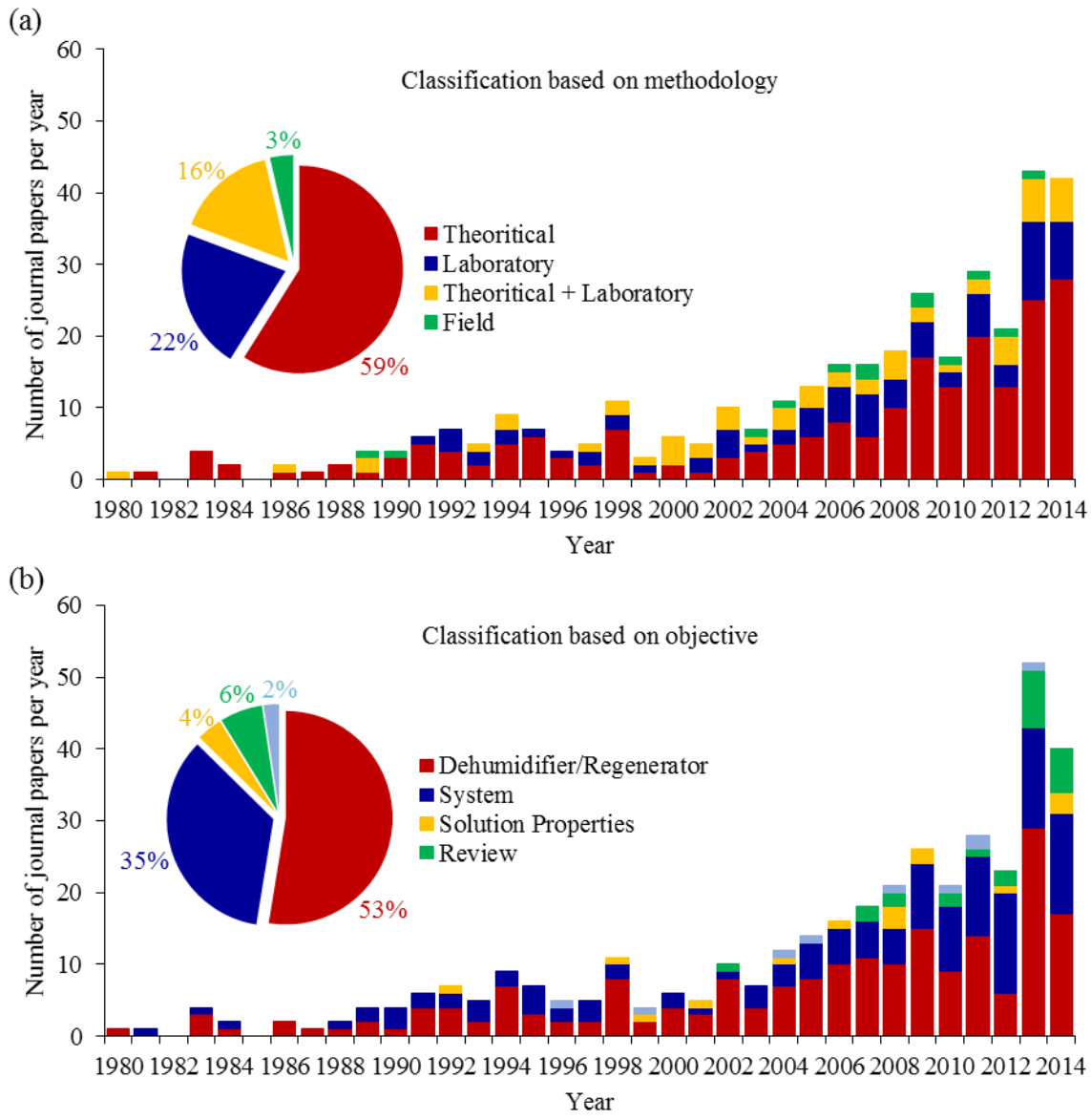

Figure 1.4. Classification of majority of LDAC journal papers published between 1980 and 2014 (Abdel-Salam and Simonson, 2015a).

A breakdown for the major topics investigated in previous studies about LDAC technologies over the past three decades is presented in Figure 1.5. A detailed review for

research performed on these topics, and some practical installations/limitations of LDAC, is presented in a comprehensive review article by Abdel-Salam and Simonson (2015a). Research related to the topics investigated in this thesis is reviewed and presented in the following chapters.

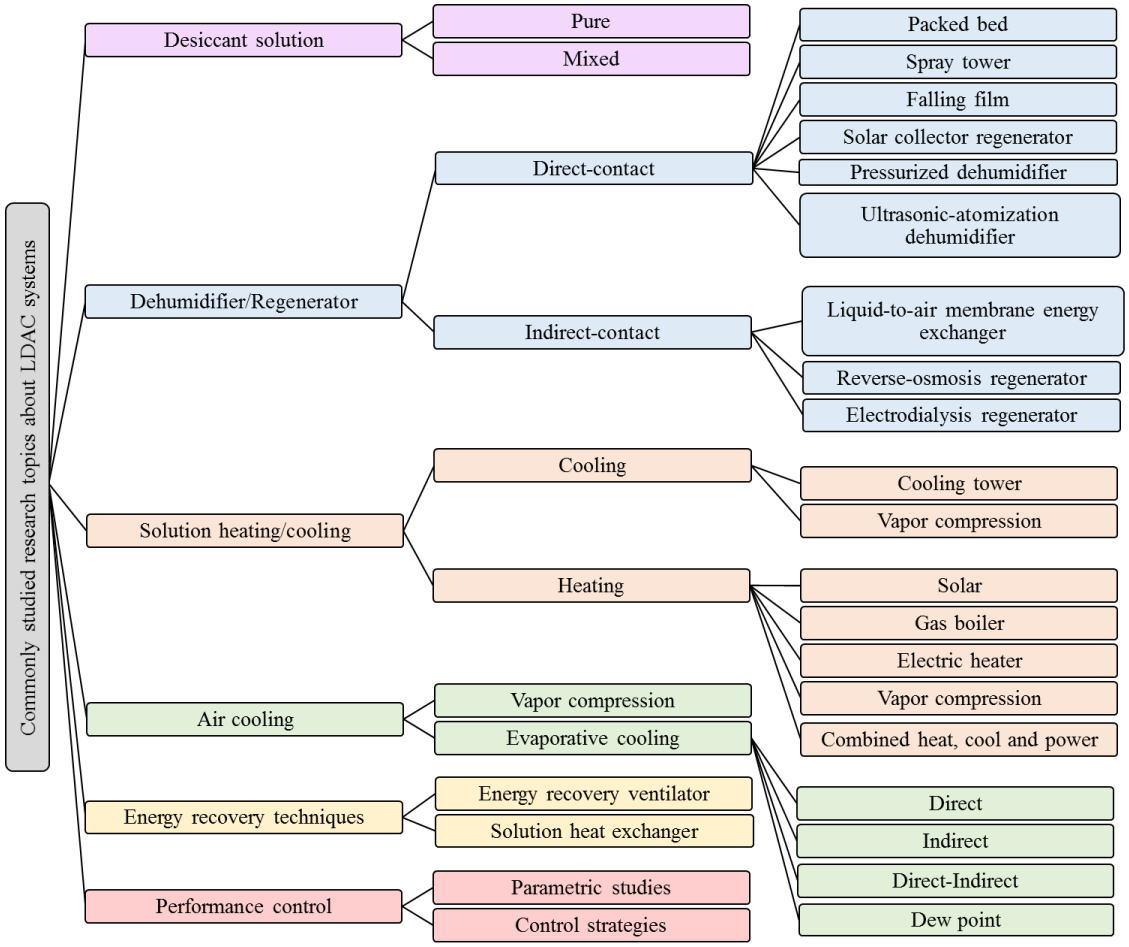

Figure 1.5. A breakdown of commonly studied research topics about LDAC systems (Abdel-Salam and Simonson, 2015a).

1.4 OBJECTIVES AND OVERVIEW

The main goal of this Ph.D. research is to rectify the current limitations and gaps in the LDAC literature to enable the wide spread use of LDAC systems in commercial and residential buildings. The major objectives of this thesis are to:

(1) quantify the heat and mass transfer performance of a membrane LDAC system;

(2) investigate the feasibility of several configurations of a membrane LDAC system;

(3) define the fundamentals of capacity matching in heat-pump LDAC systems;
(4) develop novel strategies for optimal-control of LDAC systems, and
(5) evaluate the importance of transients in estimating the performance of a LDAC system.
Motivations for the objectives are presented in Sections 1.4.1 to 1.4.5.

1.4.1 Quantify the heat and mass transfer performance of a membrane LDAC system

Previous studies on LDAC systems have mainly used direct-contact exchangers which are subject to the direct transfer of liquid desiccant into the air stream. Although there are several designs of direct-contact exchangers with promising heat and mass transfer performances (Oberg and Goswami, 1998; Kessling et al., 1998; Dai et al., 2001; Fumo and Goswami, 2002; Gommed et al., 2004; Jain and Bansal, 2007; Gommed and Grossman, 2007; Katejanekarn and Kumar, 2008; Liu et al., 2009a; Min et al., 2010; Niu et al., 2010), the entrainment of desiccant droplets in air streams has not been completely eliminated. The carryover of corrosive desiccant droplets in air streams might lead to corrosion and indoor chemical pollution and has limited the wide spread of LDAC technology in residential and commercial buildings. A promising solution for the problem of desiccant droplets entrainment in air streams is the use of a liquid-to-air membrane energy exchanger (LAMEE) as the dehumidifier/regenerator. In a LAMEE, air and solution streams are separated using semi-permeable membranes. These membranes allow the transfer of moisture but prevent the transfer of desiccant.

Although many studies have been conducted on the heat and mass transfer performance of direct-contact LDAC systems, no detailed information is available in the literature about the heat and mass transfer performance of a membrane LDAC (M-LDAC) system which uses LAMEEs as the dehumidifier and regenerator (Abdel-Salam et al., 2013a). Thus, the performance of a membrane LDAC system is investigated in Chapter 2 under various fixed design and operating conditions in order to determine if it could be a promising replacement for direct-contact LDAC systems.

1.4.2 Investigate the feasibility of several configurations of a membrane LDAC system

The energy efficiency of a LDAC system is strongly dependent on its configuration; however, there is no available information in the literature about direct comparisons between different configurations of membrane LDAC systems (Abdel-Salam and Simonson, 2014a; Abdel-Salam et al., 2014a, 2014d). Thus, the second objective of this thesis is to evaluate the feasibility (thermal, environmental and economic) of possible configurations of a membrane LDAC system by conducting annual building-energy modelling to determine the most promising configuration for future research. This objective is addressed in Chapters 3, 4 and 5.

1.4.3 Define the fundamentals of capacity matching in heat-pump LDAC systems

A heat-pump LDAC system uses the evaporator and condenser of a heat pump to cover the solution cooling and heating loads, respectively. This system has several advantages, and it is among the most promising configurations of LDAC systems. The continuous operation of a heat-pump LDAC system requires that the capacities of the condenser and evaporator of the heat pump cover the solution heating and cooling loads, respectively. When the heating and cooling provided by the heat pump exactly match the heating and cooling requirements of the solution, the system is "capacity matched". In previous studies, researchers have added auxiliary condensers, auxiliary heaters or auxiliary coolers in heat-pump LDAC systems in order to achieve capacity matching (Yadav, 1995; Li et al., 2005; Zhang et al., 2010a; Begero and Chiara, 2011; Zhao et al., 2011; Yamaguchi et al., 2011; Niu et al., 2012; Zhang et al., 2012a; Zhang et al., 2013a; Zhang and Zhang, 2014). However, there is no information in the literature on when an auxiliary equipment is required, and where it should be installed; in addition, there is no understanding for the influence of key operating and design parameters on capacity matching (Abdel-Salam and Simonson, 2014b). The third objective of this thesis, which is addressed in Chapter 6, is to define the fundamentals of capacity matching in heat-pump LDAC systems.

1.4.4 Develop novel strategies for optimal-control of LDAC systems

Many parametric studies and annual energy simulations have been conducted on LDAC systems (Ge et al., 2011a, 2011b, 2014a; Radhwan et al., 1993; Abdel-Salam et al., 2013a,

2013c; Abdel-Salam and Simonson, 2014a, 2014b; Fumo and Goswami, 2002; Martin and Goswami, 1999; Moon et al., 2009; Liu et al., 2006; Liu et al., 2007). Meanwhile, no optimal-control strategies have been developed for LDAC systems (Abdel-Salam and Simonson, 2015b). Novel control strategies are developed in Chapter 7 to address the fourth objective of this thesis. These strategies enable the control of a heat-pump LDAC system to meet the entire latent loads and to achieve one of the following additional objectives: (1) meet the entire sensible loads, (2) optimize the COP, or (3) achieve capacity matching.

1.4.5 Evaluate the importance of transients on the performance of a LDAC system

Steady-state theoretical models are commonly used to evaluate the heat and mass transfer performance of LDAC systems. However, no studies have been conducted to quantify the errors that result when a steady-state model is used to evaluate the performance of a LDAC system. The fifth objective of this thesis, presented in Chapter 8, addresses this point by quantifying the effect of transients on the performance of a LDAC system.

1.5 PUBLICATIONS

The work conducted during this Ph.D. research has resulted in 9 journal papers and 6 conference papers. All these publications are published, except four journal papers which are currently under review.

1.5.1 Papers in referred journals

(1) Abdel-Salam, A.H., Ge, G., Simonson, C.J., 2013a. Performance analysis of a membrane liquid desiccant air-conditioning system. *Energy and Buildings*, **62**, 559-569.

(2) Abdel-Salam, A.H., Simonson, C.J., 2014a. Annual evaluation of energy, environmental and economic performances of a membrane liquid desiccant air conditioning system with/without ERV. *Applied Energy*, **116**, 134-148.

(3) Abdel-Salam, A.H., Ge, G., Simonson, C.J., 2014a. Thermo-economic performance of a solar membrane liquid desiccant air conditioning system. *Solar Energy*, **102**, 56-73.

(4) Abdel-Salam, A.H., Simonson, C.J., 2014b. Capacity matching in heat-pump membrane liquid desiccant air conditioning systems. *International Journal of Refrigeration*, **48**, 166-177.

(5) Abdel-Salam, A.H., Simonson, C.J., 2015a. State-of-the-art in liquid desiccant air conditioning equipment and systems. *Renewable Energy and Sustainable Reviews*, submitted.

(6) Abdel-Salam, A.H., Simonson, C.J., 2015b. A novel control strategy for a heat-pump membrane liquid desiccant air conditioning system. *International Journal of Refrigeration*, submitted.

(7) Abdel-Salam, A.H., McNevin, C., Crofoot, L., Harrison, S.J., Simonson, C.J., 2015b. A field study of a solar liquid desiccant air conditioning system: Quasi-steady and transient. *ASME Journal of Solar Energy Engineering*, submitted.

(8) Ge, G., Moghaddam, D.G., Abdel-Salam, A.H., Besant, R.W., Simonson, C.J., 2014b. Comparison of experimental data and a model for heat and mass transfer performance of a liquid-to-air membrane energy exchanger (LAMEE) when used for air dehumidification and salt solution regeneration. *International Journal of Heat and Mass Transfer*, **68**, 119–131.

(9) Ge, G., Abdel-Salam, A.H., Abdel-Salam, M.R.H., Besant, R.W., Simonson, C.J., 2015. Heat and mass transfer performance comparison between a direct-contact packed bed and a liquid-to-air membrane energy exchanger for air dehumidification. *Science and Technology for the Built Environment*, under final internal review.

1.5.2 Papers in conference proceedings

(1) Abdel-Salam, A.H., Ge, G., Fauchoux, M.T., Simonson, C.J., 2013b. Annual energy simulation of a novel membrane liquid desiccant air conditioning system in an office building located in a hot humid climate. Proceedings of the 5th International Conference on Solar Air-Conditioning, Bad Krozingen, Black Forest, Germany.

(2) Abdel-Salam, A.H., Ge, G., Fauchoux, M.T., Moghaddam, D.G., Simonson, C.J., 2013c. Effectiveness evaluation of a liquid-to-air membrane energy exchangers as dehumidifier/regenerator in a liquid desiccant air-conditioning system. Proceedings

of the 24th Canadian Conference of Applied Mechanics (CANCAM 2013), Saskatoon, SK, Canada.

(3) Abdel-Salam, A.H., Abdel-Salam, M.R.H., Ge, G., Fauchoux, M.T., Simonson C.J., 2013d. Impacts of different air conditioning schemes on indoor air quality, energy consumption, environmental emissions and economics of a small office building in a hot-humid climate. Proceedings of the 17th ASHRAE IAQ Conference, Vancouver, Canada.

(4) Moghaddam, D.G., Ge, G., Abdel-Salam, A.H., Besant, R.W., Simonson, C.J., 2013e. Effects of solution inlet temperature on the effectiveness and moisture removal rate of a liquid-to-air membrane energy exchanger (LAMEE) during regenerator operating conditions. Proceedings of the 24th Canadian Conference of Applied Mechanics (CANCAM 2013), Saskatoon, SK, Canada.

(5) Abdel-Salam, A.H., Ge, G., Simonson, C.J., 2014d. TRNSYS modelling of a hybrid membrane liquid desiccant air conditioning system. Proceedings of IBPSA-Canada's 8th biennial conference (eSim 2014), Ottawa, ON, Canada.

(6) Abdel-Salam, A.H., Simonson, C.J., 2015c. COP evaluation for a membrane liquid desiccant air conditioning system using four different heating equipment. Proceedings of 2015 REHVA Annual Conference: Advanced HVAC & Natural Gas Technologies, Riga, Latvia.

1.6 STRUCTURE

This thesis is structured as a manuscript style, where each chapter is a separate publication as shown in Figure 1.6. Slight editions have been implemented on the published manuscripts presented in this thesis. Each major objective is addressed in one chapter except the second objective which is addressed in three chapters. Each chapter begins with a brief overview of the manuscript presented in the chapter and its logical connection to the overall thesis.

Chapter 1: Introduction

Objective #1: To quantify the heat and mass transfer performance of a membrane LDAC system

Chapter 2: Heat and Mass transfer performance of a membrane LDAC system

Title of manuscript: Performance analysis of a membrane liquid desiccant air-conditioning system
Manuscript #1 in Section 1.5.1

Objective #2: To investigate the feasibility of several configurations for a membrane LDAC system

Chapter 3: Thermal, economic and environmental performances of a basic membrane LDAC system

Title of manuscript: Annual energy, environmental and economic performances of a membrane liquid desiccant air conditioning system evaluation of with/without ERV
Manuscript #2 in Section 1.5.1

Chapter 4: Thermal, economic and environmental performances of a solar membrane LDAC system

Title of manuscript: Thermo-economic performance of a solar membrane liquid desiccant air conditioning system
Manuscript #3 in Section 1.5.1

Chapter 5: Thermal, economic and environmental performances of a heat-pump membrane LDAC system

Title of manuscript: TRNSYS Modelling of a hybrid membrane liquid desiccant air conditioning system
Manuscript #5 in Section 1.5.2

Objective #3: To define the fundamentals of capacity matching in heat-pump LDAC systems

Chapter 6: Fundamentals of capacity matching in heat-pump LDAC systems

Title of manuscript: Capacity matching in heat-pump membrane liquid desiccant air conditioning systems
Manuscript #4 in Section 1.5.1

Objective #4: To develop novel strategies for optimal-control of LDAC systems

Chapter 7: Control Strategy for optimal-control of LDAC systems

Title of manuscript: A field test for a solar LDAC system: Quasi-steady and transients
Manuscript #6 in Section 1.5.1

Objective #5: To evaluate the importance of transients in estimating the performance of a LDAC system

Chapter 8: Importance of transients in evaluating the performance of a LDAC system

Title of manuscript: A field study of a solar liquid desiccant air conditioning system: Quasi-steady and transient performance
Manuscript #7 in Section 1.5.1

Chapter 9: Summary, conclusions and recommended topics for future work

Appendix A: Copyright permissions

FIGURE 1.6. Overview of the thesis showing the objectives, chapters and manuscripts in the thesis.

CHAPTER 2

HEAT AND MASS TRANSFER PERFORMANCE OF A MEMBRANE LDAC SYSTEM

2.1 OVERVIEW

This Chapter addresses the first objective of the thesis (i.e. to quantify the heat and mass transfer performance of a membrane LDAC system). A steady-state TRNSYS model is developed for a membrane LDAC system. A parametric study is conducted to evaluate the influences of the key design and operating parameters on the performance of the membrane LDAC system. The parametric study identified the key control parameters, and their recommended operating ranges, to be used in the design, sizing and operation of membrane LDAC systems.

The manuscript presented in this chapter is published in Energy and Buildings. A Post-Doctoral Fellow "Dr. Gaoming Ge" has contributed to this manuscript by developing the analytical model used to predict the LAMEE performance. In addition, he proof read the paper and provided guidance to clarify the physical meaning of the results. As the lead author of the paper, I conducted the research, analyzed the results, wrote the manuscript, incorporated co-authors comments and addressed the reviewers' comments.

It is worth mentioning that in addition to the results presented in this chapter, I have co-authored a research paper in the Internation Jounral of Heat and Mass Transfer (Ge et al., 2014a) that provides experimental data on the performance of a LAMEE (when it is not installed in a system). The heat and mass transfer performance of the LAMEE has been experimentally and analytically evaluated under air dehumidification and solution regeneration operating modes. This paper is not included in the thesis, but it is recommended to be consulted for more information about the heat and mass transfer performance of LAMEEs and verification of the analytical model used in this thesis.

Performance analysis of a membrane liquid desiccant air-conditioning system

(Energy and Buildings, 2013, Volume 62)

Ahmed H. Abdel-Salam, Gaoming Ge, Carey. J. Simonson

2.2 ABSTRACT

A new membrane liquid desiccant air-conditioning (LDAC) system is proposed and investigated in this paper. Liquid-to-air membrane energy exchangers (LAMEEs) are used as a dehumidifier and a regenerator in the proposed LDAC system, which can eliminate the desiccant droplets carryover problem occurring in most direct-contact LDAC systems. A parametric study on steady-state performance of the membrane LDAC system is performed using the TRNSYS energy simulation platform. The impacts of various climatic conditions and key system parameters on the system performance are evaluated. Results show that the proposed membrane LDAC system is capable of achieving recommended supply air conditions for productive, comfort and healthy environments if the key system parameters are effectively controlled. The system coefficient of performance (COP) at the design condition is 0.68, and the sensible heat ratio (SHR) for the dehumidifier lies in the range between 0.3 and 0.5 under different climatic, operating and design conditions. The proposed LDAC system is able to effectively remove latent load in applications that require efficient humidity control.

2.3 INTRODUCTION

The world energy consumption has increased significantly in past decades, due to population growth and economic development. Since air conditioning (AC) systems make up to 50% of building energy consumption (Perez-Lombard et al., 2008), there should be energy efficient AC systems that are able to provide healthy environments with acceptable indoor air quality (IAQ) in order to improve the health and productivity of building occupants. Desiccant dehumidification AC systems show promise as energy efficient AC systems (ASHRAE, 2008).

Although there are several advantages for the widely used conventional AC systems and they are able to effectively remove sensible loads within conditioned spaces, they are

inefficient in terms of conditioning latent loads. When indoor humidity control is required in some cases, the cooling coil temperature in conventional AC systems must be lower than the dew point temperature of the process air stream in order to remove moisture by condensation. This results in wet cooling coil surfaces that may lead to the growth of mold and bacteria; consequently, lead to undesirable health issues and poor IAQ within conditioned spaces (Ge et al., 2012). Moreover, after moisture is removed from the process air stream, the overcooled air often needs to be reheated before it is supplied to the occupied spaces. A large amount of energy consumed in the overcooling and reheating processes makes conventional AC systems energy intensive (Qi et al., 2012). It is clear that the latent load treatment is a challenge for conventional AC systems. Since latent load is dominant over sensible load in ventilation air in hot and humid regions, according to the ventilation cooling load index developed by Harriman et al. (1997), efficient AC systems that can handle the latent load effectively are required.

The aforementioned drawbacks of conventional AC systems can be avoided by using liquid desiccant air-conditioning (LDAC) systems. LDAC systems are considered as a promising alternative to other AC systems especially in the applications that require efficient humidity control such as: supermarkets, green buildings and greenhouses (Burns et al, 1985; Ma et al., 2006; Davies, 2005). Although many studies have been performed on this topic since the 1950s, most of them focused on direct-contact liquid-to-air conditioners (Oberg and Goswami, 1998; Kessling et al., 1998; Dai et al., 2001; Fumo and Goswami, 2002; Gommed et al., 2004; Jain and Bansal, 2007; Gommed and Grossman, 2007; Katejanekarn and Kumar, 2008; Liu et al., 2009a; Min et al., 2010; Niu et al., 2010). These systems have been found to be more energy efficient than conventional AC systems, but entrainment of desiccant droplets in the air streams is a significant drawback of the direct-contact LDAC systems. The carryover of liquid desiccant by the supply air stream can lead to the corrosion of downstream ducting and equipment which results in high maintenance requirements, short life cycles and high costs. In addition, desiccant carryover may affect IAQ within the conditioned space and health of occupants. These drawbacks have limited the widespread use of LDAC systems in civil/domestic applications (Bergero and Chiari, 2011).

Different liquid desiccant dehumidifiers that are able to overcome the droplets carryover problem have been designed and developed recently (Sullivan, 2011). One design uses an internally cooled/heated (isothermal) low flow rate flat-plate exchanger that is able to significantly reduce or eliminate the carryover of droplets by the low-speed air stream (Lowenstein et al., 2006; Mesquita et al., 2006; Andrusiak et al., 2010). Another design is the indirect-contact liquid-to-air energy exchanger, where the liquid desiccant and air stream are separated by semi-permeable membranes which eliminate the liquid desiccant carryover problem. The energy performance of using these membrane energy exchangers in a hybrid membrane LDAC system was studied by Bergero and Chiari (bergero and Chiari, 2010, 2011), and it was found that energy savings may exceed 60% in humid climates compared to a conventional AC system. However, the characteristics of the membrane LDAC systems have not been extensively studied.

The aim of this chapter is to analyze the characteristics of a membrane LDAC system that uses flat-plate liquid-to-air membrane energy exchangers (LAMEEs) to serve as the dehumidifier and regenerator (Erb et al., 2009; Vali et al., 2009; Hemingson et al., 2011; Akbari et al., 2012; Moghaddam et al., 2013a-e). The proposed system is modeled using TRNSYS (Kein, 2000; TRNSYS, 2010). The performance of the system is investigated under different climate conditions (i.e. outdoor temperature and relative humidity), design conditions (i.e. number of transfer units and solution heat exchanger effectiveness) and operating conditions (i.e. liquid desiccant flow rate and temperature of solution entering the regenerator/dehumidifier).

2.4 LDAC SYSTEM

2.4.1 LAMEE

In the proposed LDAC system, the dehumidifier and regenerator are liquid-to-air membrane energy exchangers (LAMEEs) with counter-flow configuration as shown in Figure 2.1. The specifications of the LAMEEs at design conditions are shown in Table 2.1.

The air and desiccant solution streams in the LAMEEs are separated by semi-permeable membrane (e.g. polyethylene, polypropylene) that allows water vapor transmission but

does not allow the transmission of any liquid water (Larson 2006; Larson et al., 2007). Therefore, no liquid desiccant droplets are entrained in the air streams due to the indirect-contact between air and liquid desiccant. Membrane properties have a significant role in the heat and mass transfer in the LAMEEs, especially for the mass transfer. Beriault (2011) conducted a comparison between several types of commercial membranes. It was found that commercial membranes significantly vary in their prices and properties (e.g. pore size, porosity, liquid penetration pressure, modulus of elasticity). A good membrane should be characterized by the following (Beriault, 2011; Namvar, 2012; Zhang et al., 2012b). (1) Low vapor diffusion resistance in order to increase the rate of moisture transfer. (2) High modulus of elasticity in order to reduce the deflections in the membrane, and consequently reduce the flow misdistribution that may occur in the flow channels. (3) High liquid penetration pressure, so that no desiccant solution leaks into the air channels. All these parameters were considered when selecting the permeable membrane that is used in the LAMEEs, and therefore the AY Tech. ePTFE laminate membrane was selected. Table 2.1 shows the properties of the AY Tech. ePTFE membrane.

It is worth mentioning that flow mal-distribution due to membrane bulging is a concern in LAMEEs. Bulging may lead to blockage of air channels and the degradation of the LAMEE's performance (Hemingson, 2010; Abdel-Salam et al., 2015b). The occurrence of flow mal-distribution depends on several factors such as: (a) modulus of elasticity of the membrane; (b) air and solution flow rates, and (c) thickness of channels. It is assumed in this thesis that the LAMEEs used don't encounter any flow-maldistribution.

The directions of heat and mass transfer are determined by the temperature and concentration of desiccant solution and the temperature and humidity ratio of air. For instance, in order to dehumidify a humid air stream, the equilibrium humidity ratio of desiccant solution should be lower than the humidity ratio of air in the dehumidifier, and vice versa in the regenerator in order to regenerate a dilute desiccant solution.

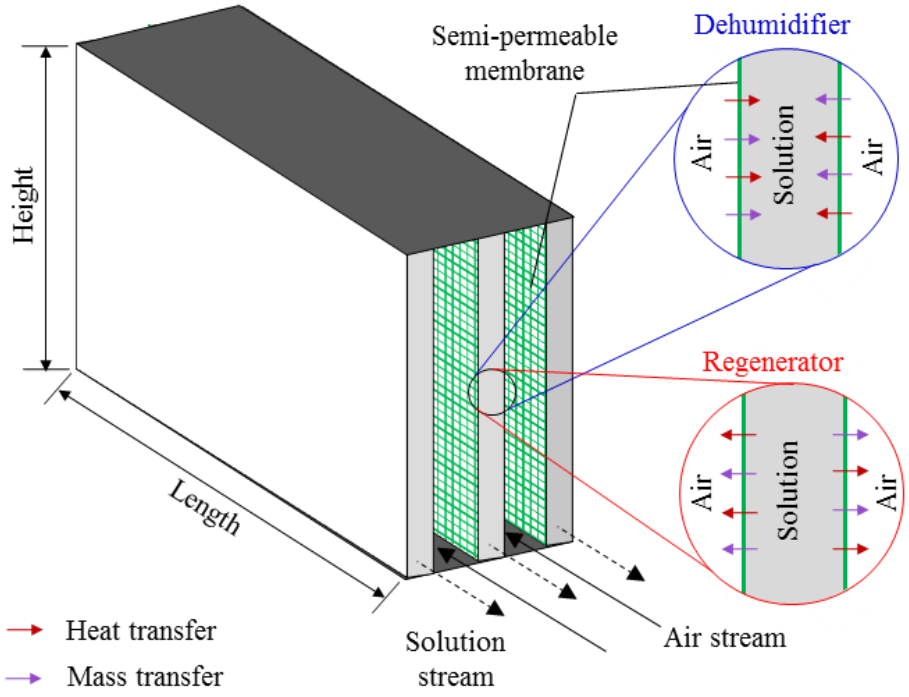

FIGURE 2.1. Schematic diagram of a liquid-to-air membrane energy exchanger (LAMEE). The membrane separates the air and liquid desiccant solution stream but allows heat and moisture transfer from air to solution in the dehumidifier and from solution to air in the regenerator.

TABLE 2.1. The LAMEEs specifications and the membrane properties.

Parameter	**Value**	**Unit**
LAMEE specifications		
• Height	1	m
• Length	2	m
• Number of solution channels	250	-
• Air channel thickness	6.35	mm
• Solution channel thickness	3.17	mm
Membrane properties		
• Type	AY Tech. ePTFE	-
• Thickness	0.54	mm
• Vapor diffusion resistance	97	s/m
• Modulus of elasticity	387	MPa
• Liquid penetration pressure	82	kPa
• Thermal conductivity	0.334	W/m·K

2.4.2 Liquid desiccant solution

Several liquid desiccant solutions that differ in thermodynamic properties and cost are available and can be used in the LAMEE. The most widely used liquid desiccants are lithium chloride (LiCl), magnesium chloride ($MgCl_2$), lithium bromide (LiBr), calcium chloride ($CaCl_2$) and triethylene glycol (TEG) (ASHRAE, 2008). In addition, liquid desiccant solutions could be mixed together to provide the desirable thermodynamic properties at economical cost.

Although some economical liquid desiccants such as $MgCl_2$ can be used in the LAMEE, this might lead to crystallization under some operating conditions. It is necessary to avoid crystallization risk as it may lead to several undesirable consequences as follows (Namvar et al., 2012; Afshin et al., 2010). (1) The reduction of heat and mass transfer surface area. (2) Mal-distribution of the fluid flow. (3) Blockage of the desiccant channels. (4) Membrane fouling and improper desiccant pumping (Charles and Johnson, 2008). Therefore, although LiCl is more expensive than $MgCl_2$ (Afshin et al., 2010), LiCl is selected to be used in the proposed LDAC system due to its lower crystallization risk and lower equilibrium humidity ratio under wide operating conditions.

2.4.3 Description of the system

A schematic diagram of the proposed membrane LDAC system is shown in Figure 2.2(a), and a conceptual schematic diagram for the processes taking place in the liquid desiccant loop is shown in Figure 2.2(b). The system consists of two air streams and three fluid loops. The air streams are the dehumidification and regeneration air streams, while the fluid loops are the chilling system, heating system and liquid desiccant loops.

The core loop of the proposed system is the liquid desiccant loop as it transfers moisture and heat between the supply air stream and the regeneration air stream using the following components: dehumidifier, heater, regenerator, solution-to-solution sensible heat exchanger and cooler as shown in Figure 2.2(a). Storage tanks can be used to increase the performance of LDAC systems by storing the diluted and concentrated desiccant solution (Keßling et al., 1998; Kessling et al., 1998), but they are not considered in this thesis.

In cooling and dehumidifying condition, the cold-concentrated solution (see state 1 in Figure 2.2(a)) enters the dehumidifier where it cools and dehumidifies the supply air stream, and becomes warm and diluted (state 2) as it leaves the dehumidifier. The warm-diluted solution is preheated to state 3 by the solution-to-solution sensible heat exchanger, using the hot-concentrated solution leaving the regenerator. Prior to entering the regenerator, the liquid desiccant is heated to the specified set point temperature (state 4) in the heater. The hot-diluted solution (state 4) passes through the regenerator in order to transfer its moisture to the regeneration air, and becomes more concentrated to be reused again in the dehumidifier. The hot-concentrated solution (state 5) leaving the regenerator is precooled to state 6 in the solution-to-solution sensible heat exchanger using the warm-diluted solution leaving the dehumidifier. Finally, the solution is cooled to the specified set point temperature (state 1) by the cooler. The solution coming out from the cooler is cold and concentrated, and is ready to enter the dehumidifier to repeat the cycle again.

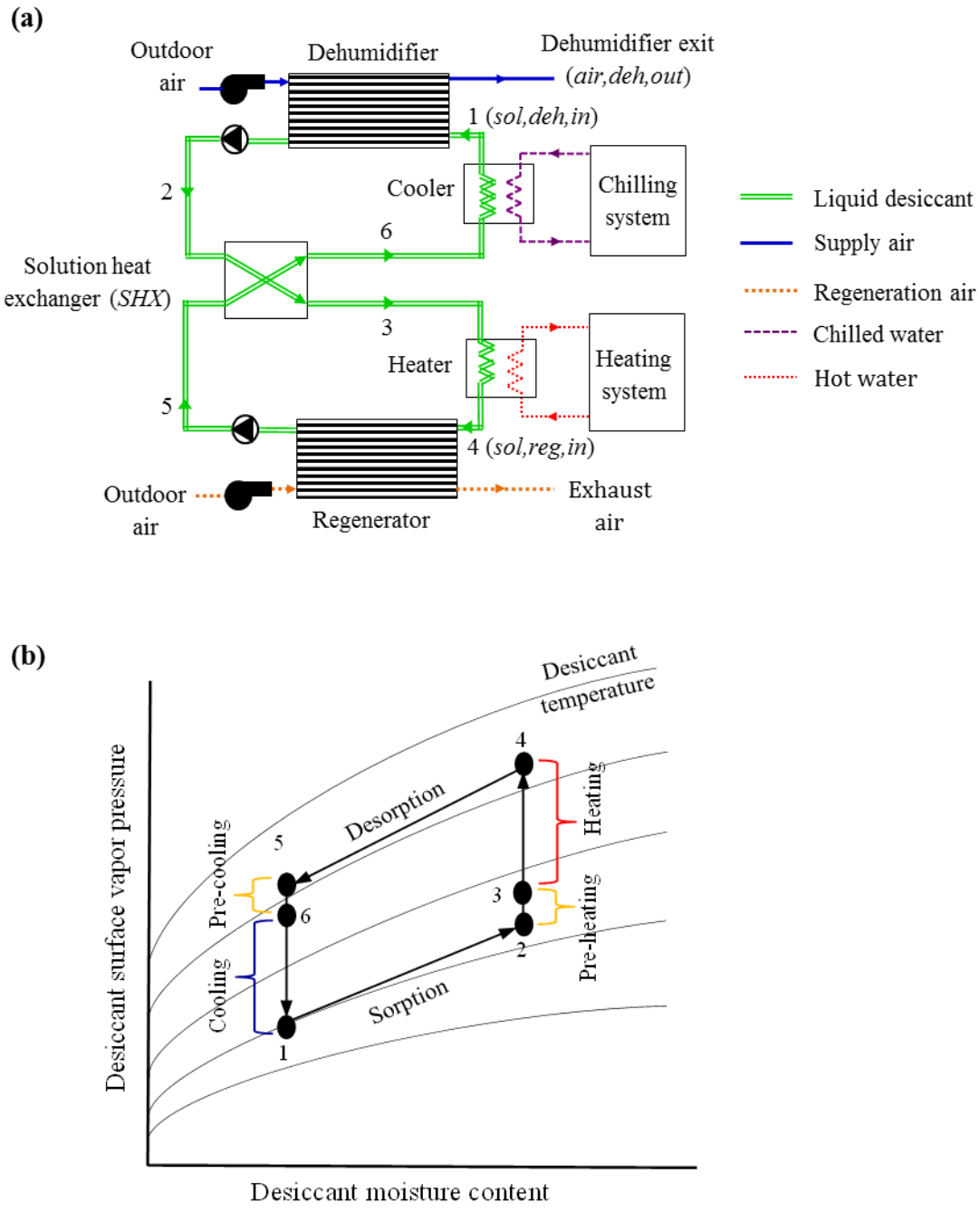

FIGURE 2.2. A schematic of the (a) proposed membrane LDAC system and (b) processes taking place in liquid desiccant loop.

2.5 SYSTEM SIMULATION

2.5.1 Simulation tool

The proposed system is simulated using the TRNSYS program. TRNSYS is widely used in thermal systems simulations due to the flexibility of its modular structure (TRNSYS, 2010). Thermal systems are simulated in TRNSYS by specifying the components that constitute the system and connecting them together. Components that are commonly used in thermal systems are available in the TRNSYS library, where the physical behavior of each component is described using algebraic/differential equations written in FORTRAN (Klein, 2000). TRNSYS also allows users to add new components that are not included in its library. In this study, custom components were created to simulate thermal performance of the LAMEE (dehumidifier/regenerator), chilling system, heating system and solution-to-solution sensible heat exchanger. The mathematical formulations of the created components are described in the next section.

2.5.2 Mathematical formulation

2.5.2.1 LAMEE

An analytical solution developed by Zhang (2011) is used in this paper to describe the steady-state performance of the counter-flow LAMEE. In Zhang's analytical model, the problem is solved in one-dimension. In addition, the axial dispersion of heat and mass, and heat and mass losses to the surroundings are negligible (Zhang, 2011). Since Zhang's analytical solution was initially developed to predict the steady-state heat and mass transfer in a hollow fiber membrane shell-and-tube energy exchanger with counter-flow configuration, a modification was implemented in order to be used in predicting the flat-plate LAMEE performance. The modification is that the overall heat and mass transfer coefficients are calculated based on the flat-plate LAMEE configuration as shown in equations (2.1) and (2.2), respectively, and substituted into Zhang's analytical correlations (Ge et al., 2013).

$$U=\left[\frac{1}{h_{c,sol}}+\frac{\delta}{k}+\frac{1}{h_{c,air}}\right]^{-1} \tag{2.1}$$

$$U_m=\left[\frac{1}{h_{m,air}}+\frac{\delta}{k_m}\right]^{-1} \tag{2.2}$$

where, U is the overall heat transfer coefficient ($W/m^2 \cdot K$), U_m is the overall mass transfer coefficient ($kg/m^2 \cdot s$), h_c is the convective heat transfer coefficient ($W/m^2 \cdot K$), δ is the thickness of the membrane (m), k is the thermal conductivity of the membrane ($W/m \cdot K$), h_m is the convective mass transfer coefficient ($kg/m^2 \cdot s$), and k_m is the permeability of the membrane ($kg/m \cdot s$). Subscripts air and sol refers to the air and solution, respectively.

In this study, the Nusselt number (Nu) is set constant at 8.24, because it is assumed that there are fully developed laminar flow and constant heat flux (Incropera and Dewitt, 2002). Therefore, the convective heat and mass transfer coefficients are calculated by the definitions in equations (2.3) and (2.4), respectively (Welty et al., 2001).

$$Nu = \frac{h_c D_h}{k_f} \tag{2.3}$$

$$h_m = \frac{h_c}{c_p} Le^{-\frac{2}{3}} \tag{2.4}$$

where, D_h is the hydraulic diameter of the flow channel (m) and it equals twice the channel spacing for flow between infinite parallel flat plates, k_f is the thermal conductivity of the fluid ($W/m \cdot K$), c_p is the specific heat capacity ($J/kg \cdot K$), and Le is Lewis number which is defined as the ratio between the thermal to mass diffusivities.

For the sake of simplicity, the moisture content absorbed/desorbed by the liquid desiccant in the LAMEE is neglected compared with the desiccant mass flow rate. Fumo and Goswami (2002) and Liu et al. (2006) have verified this assumption experimentally for liquid desiccant dehumidification applications and the solution concentration is assumed to be constant in the air dehumidification and solution regeneration processes (Incropera and Dewitt, 2002). The governing equations for heat and moisture conservation in the air and solution flows can be written as follows.

$$\frac{dT_{air}^*}{dx^*} = NTU(T_{sol}^* - T_{air}^*) \tag{2.5}$$

$$\frac{dT_{sol}^*}{dx^*} = \frac{NTU}{Cr^*}(T_{sol}^* - T_{air}^*) + \frac{H^*}{Cr^* c_{p,air}} \cdot \frac{dW_{air}^*}{dx^*} \tag{2.6}$$

$$\frac{dW_{air}^{*}}{dx^{*}} = NTU_m(W_{sol}^{*} - W_{air}^{*}) \tag{2.7}$$

$$\frac{dW_{sol}^{*}}{dx^{*}} = 2500\frac{E_T}{H^{*}} \cdot \frac{dT_{sol}^{*}}{dx^{*}} \tag{2.8}$$

where, NTU is the number of heat transfer units, NTU_m is the number of mass transfer units, Cr^* is the thermal capacity ratio between solution and air flows, and E_T is the slope of equilibrium humidity to temperature of solution (g/kg·K).

Several dimensionless parameters are used in normalizing the governing equations as follows.

$$T^{*} = \frac{T - T_{air,in}}{T_{sol,in} - T_{air,in}} \tag{2.9}$$

$$W^{*} = \frac{W - W_{air,in}}{W_{sol,in} - W_{air,in}} \tag{2.10}$$

$$x^{*} = \frac{x}{L} \tag{2.11}$$

$$H^{*} = 2500\frac{W_{sol,in} - W_{air,in}}{T_{sol,in} - WT_{air,in}} \tag{2.12}$$

where, T is the temperature (ºC), W is the humidity ratio (g/kg), L is the length of the LAMEE (m) and H^* is an operating condition factor which is defined as the ratio between the potential for mass transfer to that for heat transfer (Simonson and Besant, 1999a).

A flow chart for the analytical model is presented in Figure 2.3. It is worth mentioning that the results obtained from the modified analytical solution were validated against numerical and experimental results in previous studies, and they were found to be reliable for the LAMEE performance evaluation (Namvar et al., 2012; Ge et al., 2013).

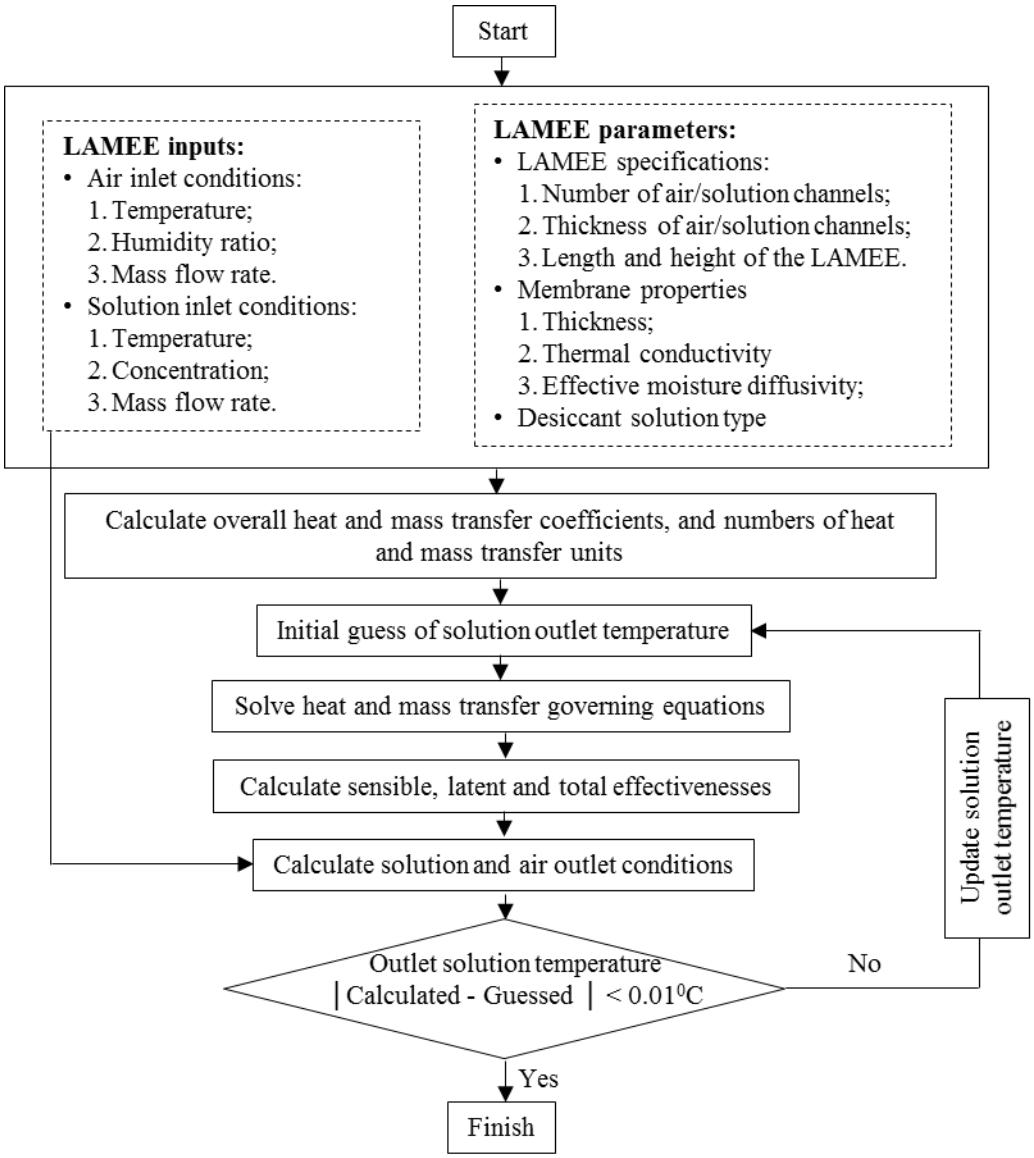

FIGURE 2.3. Flow chart of the analytical model used to evaluate the performance of the LAMEE.

2.5.2.2 Solution-to-solution sensible heat exchanger

The effectiveness of the solution-to-solution sensible heat exchanger (ε_{SHX}) is assumed to be constant in this study, and it is set to be 0.85. Therefore, the temperatures of the concentrated (T_6) and diluted (T_3) solutions leaving the sensible heat exchanger are calculated using equations (2.13) and (2.14), respectively.

$$\varepsilon_{SHX} = \frac{T_5 - T_6}{T_5 - T_2} \tag{2.13}$$

$$\varepsilon_{SHX} = \frac{T_3 - T_2}{T_5 - T_2} \tag{2.14}$$

where, as shown in Figure 2.2(a), subscripts 5 and 6 refer to the inlet and outlet of the hot liquid desiccant, respectively, while subscripts 2 and 3 refer to the inlet and outlet of the cold liquid desiccant, respectively.

2.5.2.3 Hydronic heating and cooling systems

The energy consumption rates of the air fans and solution pumps (P_p) are calculated using standard TRNSYS components. Custom TRNSYS components were created for the heating and cooling systems. The energy consumption rates by the heating and cooling systems are calculated as follows.

The temperature of the chilled water leaving the chilling system is assumed to be 3ºC higher than the evaporator set point temperature (T_{ev}), and the cooler is assumed to have a constant effectiveness equal to 0.85 (ASHRAE, 2008). Since the coefficient of performance of the chilling system ($COP_{chiller}$) is strongly dependent on T_{ev}, it is calculated at different T_{ev} using the correlation shown in equation (2.15), where the condenser temperature is assumed to be fixed at 45ºC (Zhang et al., 2005). The heat transfer rate from the solution to the chilled water (q_{cool}) is calculated using equation (2.16), while the energy consumption rate of the cooling system (P_{cool}) is calculated using equation (2.17).

$$COP_{chiller} = 0.0001T_{ev}^{\ 3} + 0.0016T_{ev}^{\ 2} + 0.0746T_{ev} + 2.637 \tag{2.15}$$

$$q_{cool} = \dot{m}_{sol} c_{p,sol} (T_6 - T_1) \tag{2.16}$$

$$P_{cool} = \frac{q_{cool}}{COP_{chiller}} \tag{2.17}$$

The heater is assumed to have a constant effectiveness equal to 0.85. A constant thermal efficiency (η_{th}) of 95% is assumed. This is because η_{th} for a condensing boiler varies between 93% and 97% when the inlet temperature changes from 30ºC to 45ºC (ASHRAE, 2008), where this is the range of change in the solution inlet temperature to the boiler in this study. The heat transfer rate from the hot water to the solution (q_{th}) is calculated using

equation (2.18), while the energy consumption rate of the heating system (P_{th}) is calculated using equation (2.19).

$$q_{th} = \dot{m}_{sol} c_{p,sol} (T_4 - T_3) \tag{2.18}$$

$$P_{th} = \frac{q_{th}}{\eta_{th}} \tag{2.19}$$

where, as shown in Figure 2.2(a), subscripts 3 and 4 refer to the liquid desiccant entering and leaving the heater, respectively, while subscripts 6 and 1 refer to the liquid desiccant entering and leaving the cooler, respectively.

2.6 PERFORMANCE INDICES

In this study, six performance indices are used to investigate the influences of the studied parameters on the proposed LDAC system performance. These indices are as follows:

2.6.1 Moisture removal rate (MRR, g/s)

Is defined as the mass flow rate of water vapor removed from the supply air stream by the LDAC system.

$$MRR = \dot{m}_{air} (W_{amb} - W_{air,deh,out}) \tag{2.20}$$

where, W is the humidity ratio (g/kg).

2.6.2 Sensible heat ratio (SHR)

Is defined as the ratio between the sensible to total (sensible and latent) energy removed from the supply air stream.

$$SHR = \frac{q_{sen}}{q_{sen} + q_{lat}} \tag{2.21}$$

where, q_{sen} and q_{lat} are the rate of sensible and latent energy removed from the supply air stream (kW), respectively.

2.6.3 Cooling capacity (CC, kW)

Is calculated from the enthalpy difference between the supply and outdoor air. It represents the overall cooling provided by the LDAC system.

$$CC = \dot{m}_{air}(h_{amb} - h_{air,deh,out}) \quad (2.22)$$

where, h is the enthalpy of the air stream (kJ/kg).

2.6.4 Coefficient of performance (COP)

Is defined as the ratio between the cooling capacity and the total primary energy consumption in the LDAC system.

$$COP = \frac{CC}{P_{th} + \frac{P_{cool} + P_p}{0.3}} \quad (2.23)$$

where, 0.3 is the assumed equivalent conversion coefficient of electric power and thermal energy because the average efficiency for an electric power plant is around 30% (US DOE, 2010).

2.6.5 Electrical coefficient of performance (ECOP)

Is defined as ratio between the cooling capacity to the electrical energy consumption in the LDAC system.

$$ECOP = \frac{CC}{P_{cool} + P_p} \quad (2.24)$$

2.6.6 Thermal coefficient of performance (TCOP)

Is defined as ratio between the cooling capacity to the thermal energy consumption in the LDAC system.

$$TCOP = \frac{CC}{P_{th}} \quad (2.25)$$

2.6.7 Mass and energy balances

It is necessary to check mass and energy balances for the LDAC system to ensure that the created TRNSYS model conserves both mass and energy. Equations (2.26) and (2.27) were satisfied under all operating conditions which ensure the conservation of mass and energy within the LDAC system.

$$\frac{\left|\dot{m}_{air,deh,in} W_{air,deh,in} - \dot{m}_{air,deh,out} W_{air,deh,out}\right| - \left|\dot{m}_{air,reg,in} W_{air,reg,in} - \dot{m}_{air,reg,out} W_{air,reg,out}\right|}{MRR} < 0.01 \tag{2.26}$$

$$\frac{\left|q_{deh} + q_{th} - q_{reg} - q_{cool}\right|}{CC} < 0.01 \tag{2.27}$$

where, q_{deh}, q_{th}, q_{reg} and q_{cool} are the rate of heat transfer to/from the solution in the dehumidifier, heater, regenerator and cooler, respectively. Subscripts deh and reg refer to the dehumidifier and regenerator, respectively, while subscripts in and out refer to the air/solution inlet and outlet, respectively, from the dehumidifier/regenerator.

2.7 RESULTS AND DISCUSSION

The influences of several key parameters on performance of the proposed system are presented in this section. As mentioned previously, the parameters considered are as follows: solution inlet temperatures to regenerator ($T_{sol,reg,in}$) and dehumidifier ($T_{sol,deh,in}$), solution-to-solution sensible heat exchanger effectiveness (ε_{SHX}), thermal capacity rate ratio between solution and air flows (Cr^*), number of heat transfer units (NTU), ambient air temperature (T_{amb}) and ambient air relative humidity (RH_{amb}). The Cr^* and NTU are defined as shown in equations (2.28) and (2.29), respectively.

$$NTU = Max\left\{\frac{UA}{C_{air}}, \frac{UA}{C_{sol}}\right\} \tag{2.28}$$

$$Cr^* = \frac{C_{sol}}{C_{air}} \tag{2.29}$$

where, C is the thermal capacity (W/K).

In each case, only one parameter is changed, while the other parameters are kept constant at the reference values. The reference value for each of the studied parameters and the range over which each parameter is varied are shown in Table 2.2. The reference values for the studied parameters were selected so that the condition of the air leaving the dehumidifier is at 8 g/kg and 20ºC when the outdoor air condition is 17.5 g/kg and 35ºC. This would be a typical demand for the supply air humidity ratio in several buildings and

climates, especially in dedicated outdoor air systems where the humidity ratio of supply air should be low enough to be able to meet the total (i.e. space, ventilation and infiltration) latent load within the building. Although the air leaves the dehumidifier at a relatively high temperature ($T_{air,deh,out}$=20ºC), the sensible load not met in the LDAC system could be removed using chilled ceilings or conventional cooling ways (e.g. direct-expansion and vapor compression systems) that would operate at higher evaporation temperature and therefore higher $COP_{chiller}$.

TABLE 2.2. The reference values and variation ranges of the studied parameters.

Parameter	Reference value	Minimum value	Maximum value	Increment
NTU	10	1	15	2
Cr^*	3	2	6	1
$T_{sol,reg,in}$ (ºC)	45	40	65	5
$T_{sol,deh,in}$ (ºC)	20	15	25	2
ε_{SHX}	0.85	0.1	0.9	0.2
T_{amb} (ºC)	35	24	40	4
RH_{amb} (%RH)	50	20	80	10
$\dot{m}_{air}$ (kg/s)	0.44	-	-	-

2.7.1 Influence of solution inlet temperature to the regenerator ($T_{sol,reg,in}$)

Figure 2.4 shows the influence of $T_{sol,reg,in}$ on performance of the LDAC system. As shown in Figure 2.4(a), $T_{sol,reg,in}$ has a larger effect on the humidity ratio ($W_{air,deh,out}$) of the air leaving the dehumidifier than on its temperature ($T_{air,deh,out}$). When $T_{sol,reg,in}$ rises from 40 to 65ºC, $W_{air,deh,out}$ reduces from 9.5 to 3.8 g/kg, while $T_{air,deh,out}$ increases slightly by 1ºC. Although the temperature of the solution entering the dehumidifier is kept constant ($T_{sol,deh,in}$ = 20ºC), the slight increase in the outlet air temperature (i.e. 1ºC) is due to the higher water vapor phase change energy, which is released during the dehumidification process, at higher $T_{sol,reg,in}$. In addition, Figure 2.4(b) shows that the sensible heat ratio (SHR) decreases from 0.42 to 0.28, and the moisture removal rate (MRR) increases from 3.5 to 6.2 g/s when $T_{sol,reg,in}$ increases from 40 to 65ºC. This large improvement in the dehumidification is due to the enhanced solution regeneration at higher $T_{sol,reg,in}$. The higher the $T_{sol,reg,in}$, the higher its vapor pressure, and consequently the higher the potential for moisture transfer from the solution to the regenerating air stream. As a result, the

concentration of the solution leaving the regenerator and dehumidifier increases with $T_{sol,reg,in}$ as shown in Figure 2.4(c), where the solution concentration (C_{sol}) is defined as follows.

$$C_{sol} = \frac{\text{mass of salt}}{\text{mass of salt} + \text{mass of water}} \tag{2.30}$$

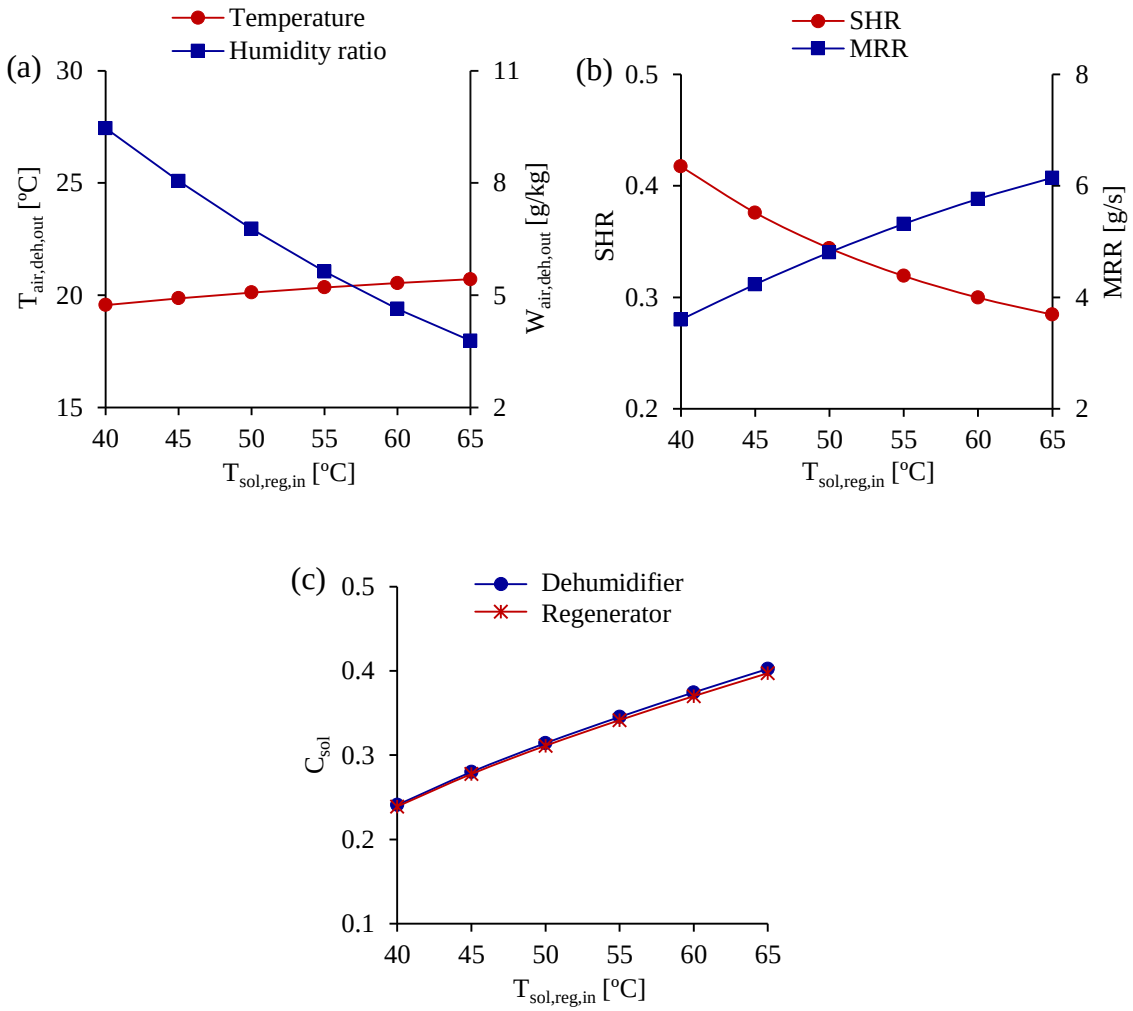

FIGURE 2.4. Influence of solution inlet temperature to the regenerator ($T_{sol,reg,in}$) on (a) outlet air state from the dehumidifier, (b) SHR and MRR of the dehumidifier and (c) concentration of the solution.

Table 2.3 shows the impact of $T_{sol,reg,in}$ on the CC and COPs of the LDAC system. When $T_{sol,reg,in}$ increases from 40 to 65ºC, the CC of the system increases by 36%, while the COP decreases by 17%. The COP reduction indicates that the achieved improvement in the CC

is lower than the additional energy required for operating the system at high $T_{sol,reg,in}$. Therefore, a proper control system should be installed in this and similar systems to achieve the required $T_{sol,reg,in}$, at which the LDAC system can provide the demanded dehumidification capacity with high COP. It is found that the ECOP increases by 13% and TCOP decreases by 50%, when $T_{sol,reg,in}$ increases from 40 to 65ºC. The increase in ECOP indicates that the achieved improvement in the CC of the system is larger than the additional electrical energy required for running the chilling system to cool the strong solution prior to entering the dehumidifier. On the contrary, the reduction in the TCOP indicates that the additional required thermal energy to heat the weak solution prior to entering the regenerator is larger than the improvement of the CC in the system.

TABLE 2.3. Influence of solution inlet temperature to the regenerator ($T_{sol,reg,in}$) on the performance of the system.

$T_{sol,reg,in}$ [ºC]	CC [kW]	COP	ECOP	TCOP
40	16.6	0.71	3.32	2.42
45	18.1	0.68	3.45	1.95
50	19.5	0.65	3.56	1.67
55	20.7	0.63	3.65	1.48
60	21.7	0.61	3.71	1.34
65	22.6	0.59	3.75	1.22

2.7.2 Influence of solution inlet temperature to the dehumidifier ($T_{sol,deh,in}$)

Figure 2.5 shows the influence of $T_{sol,deh,in}$ on performance of the LDAC system. As $T_{sol,deh,in}$ decreases, both the temperature ($T_{air,deh,out}$) and humidity ratio ($W_{air,deh,out}$) of the air leaving the dehumidifier decrease as shown in Figure 2.5(a). It is clear that $T_{air,deh,out}$ is more influenced by $T_{sol,deh,in}$, as it decreases by 56%, while $W_{air,deh,out}$ decreases by 44% in the studied range. Figure 2.5(b) shows that the MRR increases from 3.4 to 4.8 g/s and the SHR increases from 0.32 to 0.4 when $T_{sol,deh,in}$ decreases from 25 to 15ºC. The increase occurs in the SHR indicates that unlike the temperature of the solution entering the regenerator, the $T_{sol,deh,in}$ has larger influence on the supply air sensible cooling than on the dehumidification. The improvement in MRR is attributed to the reduction of vapor pressure of the solution passing through the dehumidifier, and therefore the increase of its potential to absorb more moisture from the air stream. Figure 2.5(c) shows that the concentration of

the solution leaving the dehumidifier/regenerator slightly decreases with the reduction of $T_{sol,deh,in}$.

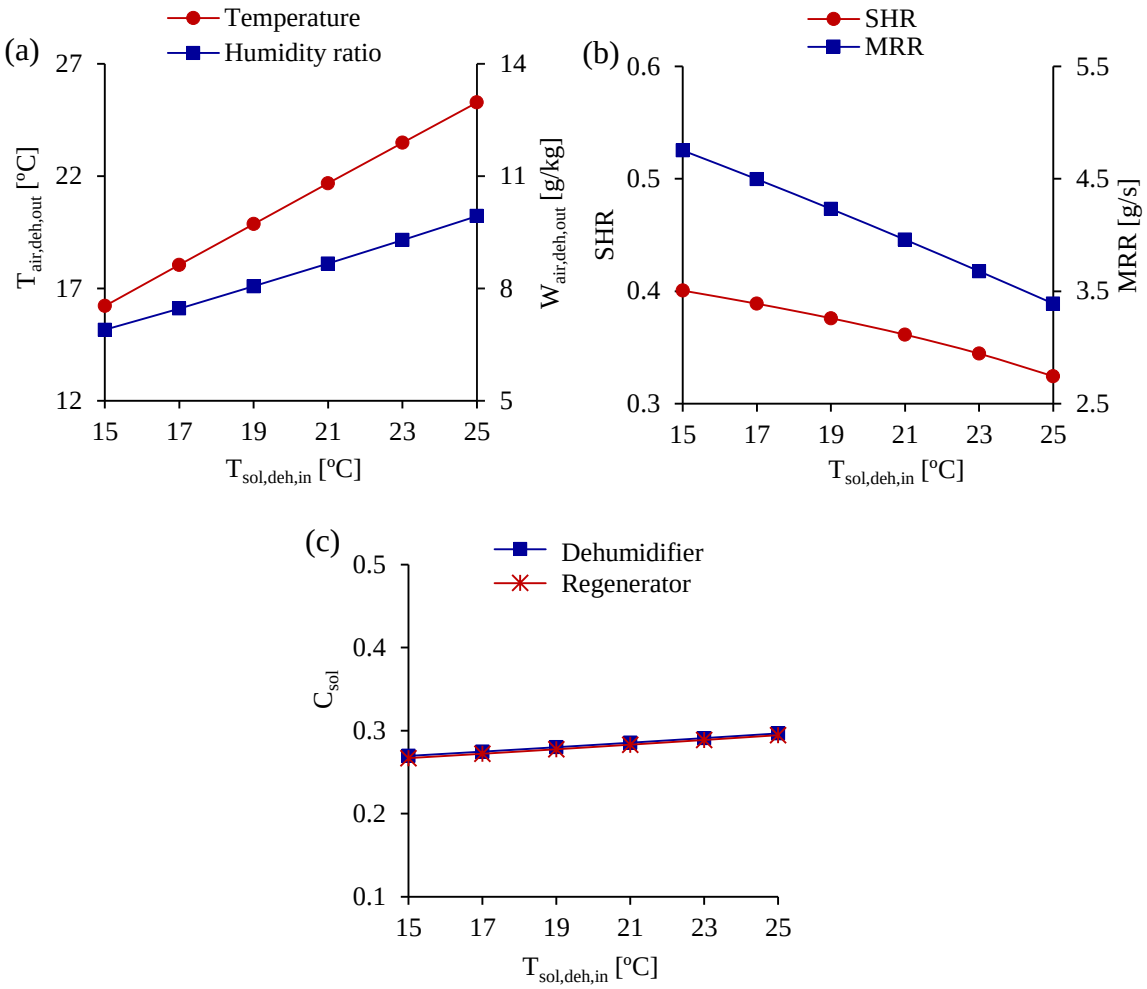

FIGURE 2.5. Influence of solution inlet temperature to the dehumidifier ($T_{sol,deh,in}$) on (a) outlet air state from the dehumidifier, (b) SHR and MRR of the dehumidifier and (c) concentration of the solution.

The CC and COPs of the LDAC system as $T_{sol,deh,in}$ varies from 15 to 25ºC are shown in Table 2.4. The CC and COP increase by 53% and 15%, respectively, when $T_{sol,deh,in}$ decreases from 25 to 15ºC. The ECOP increases by 9% when $T_{sol,deh,in}$ decreases from 25 to 19ºC, while it slightly varies when $T_{sol,deh,in}$ decreases beyond 19ºC due to the reduction in the $COP_{chiller}$ at low evaporation temperatures. The TCOP increases by 24% when $T_{sol,deh,in}$ decreases from 25 to 15ºC. This indicates that the improvement in the CC at lower

$T_{sol,deh,in}$ is larger than the increasing energy consumption for cooling and heating the solution before entering the dehumidifier and regenerator, respectively.

TABLE 2.4. Influence of solution inlet temperature to the dehumidifier ($T_{sol,deh,in}$) on the performance of the system.

$T_{sol,deh,in}$ [°C]	CC [kW]	COP	ECOP	TCOP
15	23.0	0.75	3.47	2.21
17	20.7	0.71	3.48	2.09
19	18.9	0.69	3.46	1.99
21	17.5	0.67	3.40	1.90
23	16.1	0.66	3.30	1.84
25	15.0	0.65	3.16	1.78

It can be concluded from Sections 2.7.1 and 2.7.2 that the outlet air states from the dehumidifier ($T_{air,deh,out}$ and $W_{air,deh,out}$) can be effectively controlled by regulating the set points of $T_{sol,deh,in}$ and $T_{sol,reg,in}$. However, if the set points are not accurately controlled simultaneously, this might result in over/under-dehumidifying the supply air stream, which will affect the energy efficiency of the LDAC system. Therefore, an efficient control system should be developed and employed in this and similar systems in order to adjust the solution temperatures to efficiently achieve the required cooling and dehumidifying capacities without causing un-necessary high thermal and electrical energy consumption.

2.7.3 Influence of solution-to-solution sensible heat exchanger effectiveness (ε_{SHX})

Varying ε_{SHX} does not affect the performance of the dehumidifier or regenerator. Although the CC, SHR and MRR of the system are not affected by the value of ε_{SHX}, it has an observable influence on the amount of thermal and electrical energy required for operating the system. In addition, ε_{SHX} has significant impact on the required capacities of the cooling and heating equipment, and hence the COPs of the system. Figure 2.6(a) shows that the COP, ECOP and TCOP increase by 23%, 14% and 38%, respectively, when ε_{SHX} =0.9 compared with the case without heat exchanger. Moreover, Figure 2.6(b) shows that the required capacity of the heating and cooling equipment reduces by 26% and 21%, respectively, when a sensible heat exchanger with ε_{SHX} =0.9 is added to the system

compared with the case where there is no heat exchanger. It is clear that installing a solution-to-solution sensible heat exchanger with high effectiveness leads to considerable savings in the capital and operating costs, and would therefore result in shorter payback periods. Therefore, a sensible heat exchanger for the heat recovery between concentrated and diluted solution flows is strongly recommended in this and similar systems.

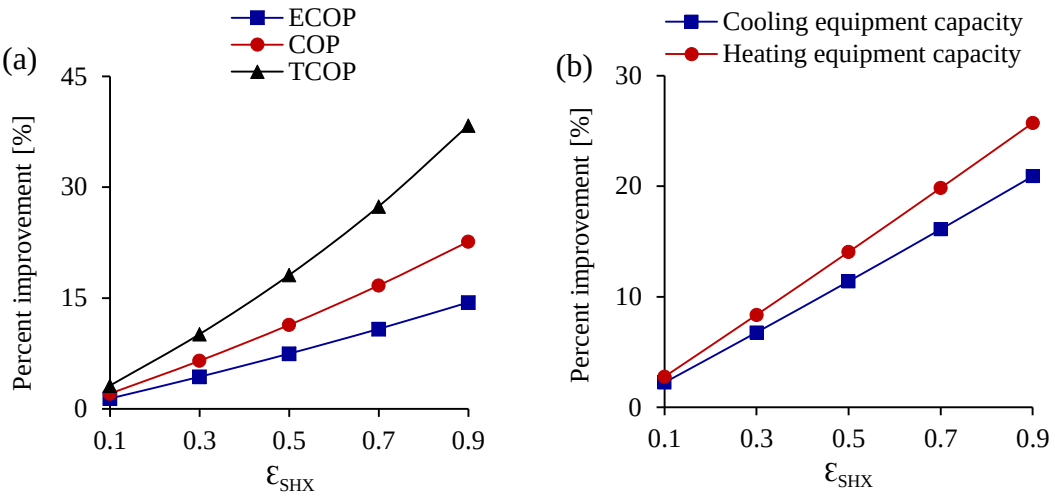

FIGURE 2.6. Influence of effectiveness of solution-to-solution sensible heat exchanger (ε_{SHX}) on (a) COP, ECOP and TCOP of the system, and (b) cooling and heating equipment capacities.

It is worth mentioning that when a solution-to-solution sensible heat exchanger is used in the LDAC system, an efficient control system should be installed because at some extreme operating conditions it is more beneficial to bypass the diluted and concentrated solution flows around the exchanger. For instance, if the temperature of the concentrated solution leaving the regenerator is lower than the temperature of the diluted solution leaving the dehumidifier, the heat exchanger would heat the concentrated solution instead of pre-cooling it and cool the diluted solution instead of pre-heating it. This would lead to an increase in the energy consumption and a decrease in the COPs of the system. Therefore, a solution-to-solution sensible heat exchanger should be efficiently controlled by detecting the inlet temperatures of concentrated and diluted solution flows as shown in Figure 2.7.

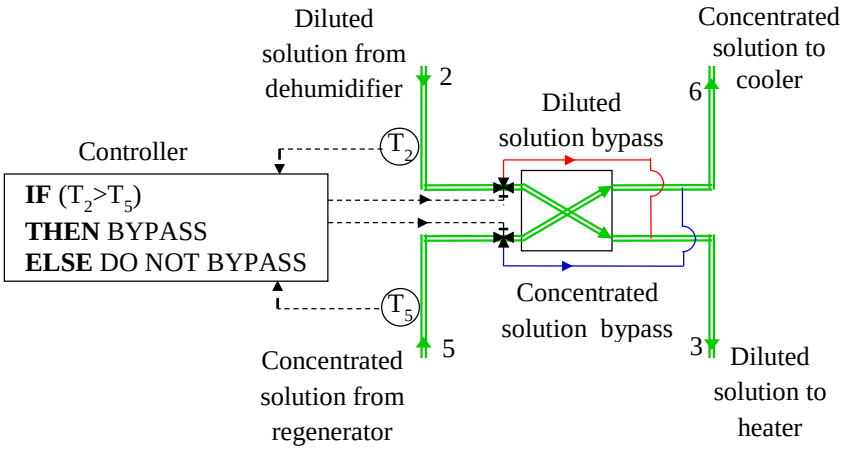

FIGURE 2.7. Control of solution-to-solution sensible heat exchanger.

2.7.4 Influence of thermal capacity rate ratio (Cr^*)

Although the desiccant flow rate is one of the predominant operating parameters for the performance of LDAC systems, there is no common optimum value that is applicable to different systems. This is because the optimum desiccant flow rate is determined by several factors, such as the heat and mass transfer coefficients that differ from one system to another and the outdoor air state. Thus, it should be determined for each LDAC system under different operating conditions. As equation (2.29) shows, Cr^* can be increased by either increasing the solution mass flow rate or reducing the air mass flow rate. Cr^* is varied in this study by changing the solution mass flow rate, while the air mass flow rate is kept constant in order to keep NTU constant (i.e. NTU=10).

The influence of Cr^* on performance of the LDAC system is shown in Figure 2.8. As shown in Figure 2.8(a), the humidity ratio of the air leaving the dehumidifier decreases from 10.5 to 7.2 g/kg as Cr^* increases from 2 to 4, while slight change is observed when Cr^* increases beyond 4. The humidity ratio and temperature of the outlet air from the dehumidifier decrease by 32% and 12%, respectively, as Cr^* increases from 2 to 4, while they decrease only by 7% and 3%, respectively, when Cr^* increases from 4 to 6. Figure 2.8(b) shows that the MRR increases by 48% when Cr^* increases from 2 to 4, while it increases by only 5% when Cr^* increases from 4 to 6. Since the potential for both heat and moisture transfer

increase simultaneously with Cr^*, the SHR does not change as much as the MRR, as the SHR decreases by 12% when Cr^* increases from 2 to 4, and only by 1% when Cr^* increases from 4 to 6. The achieved improvement with Cr^* is due to the considerable increase in the sensible, latent and total effectiveness of the LAMEEs (dehumidifier/regenerator) at high Cr^* [34]. In addition, when the desiccant flow rate increases, the solution thermal capacity and its capability of holding up more moisture increase as well.

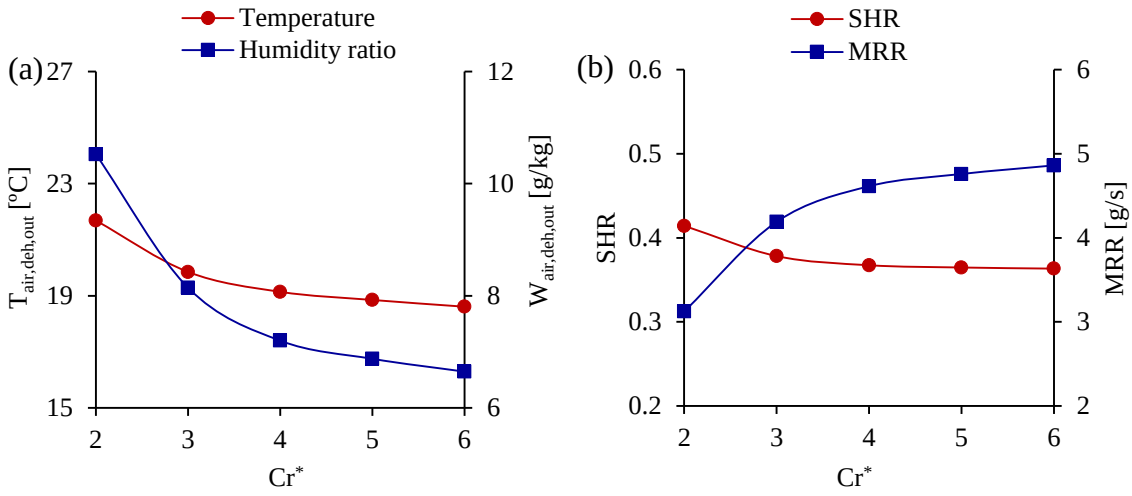

FIGURE 2.8. Influence of thermal capacity rate ratio (Cr^*) on (a) outlet air state from the dehumidifier and (b) SHR and MRR of the dehumidifier.

The changes in the CC and COPs of the LDAC system are shown in Table 2.5. The CC increases by 35% as Cr^* increases from 2 to 4 but it increases only slightly when Cr^* increases above 4. On the other hand, the COP, ECOP and TCOP increase over the entire range of Cr^*. This may be explained as follows: when Cr^* increases, the solution temperature experiences less change as the solution passes through the dehumidifier and regenerator due to the increase in its thermal capacity. Consequently, less electrical and thermal energy are consumed to condition the solution to the specified set points before entering the dehumidifier and regenerator. Therefore, although the CC does not significantly improve after Cr^*=4, the COP, ECOP and TCOP continue to increase with Cr^* due to the reduction in the energy required to operate the LDAC system at high Cr^*.

TABLE 2.5. Influence of thermal capacity rate ratio (Cr^*) on the performance of the system.

Cr^*	CC [kW]	COP	ECOP	TCOP
2	14.5	0.51	2.60	1.48
3	18.1	0.68	3.45	1.95
4	19.4	0.80	3.98	2.44
5	19.9	0.87	4.25	2.76
6	20.3	0.94	4.51	3.11

2.7.5 Influence of number of heat transfer units (NTU)

The NTU of the LAMEEs is one of the most important design parameters for the proposed LDAC system, as it has a strong impact on the performance (i.e. effectiveness) of the dehumidifier and regenerator that are considered as the core components for the proposed LDAC system. The NTU can be increased by either decreasing the air mass flow rate or increasing the LAMEE surface area, as seen from equation (2.28). Decreasing the air mass flow rate without decreasing the solution mass flow rate by the same ratio would lead to the increase of Cr*, as shown in equation (2.29). Therefore, the NTU is varied in this study by changing the LAMEE surface area, in order to keep Cr^* constant (i.e. $Cr^*=3$).

Figure 2.9(a) shows that when NTU increases from 1 to 10, the outlet air humidity ratio ($W_{air,deh,out}$) and temperature ($T_{air,deh,out}$) from the dehumidifier decreases from 14.2 to 8 g/kg and from 25.6 to 20ºC, respectively. It is clear that increasing NTU causes a considerable improvement in the performance of the system until NTU reaches 10, while raising NTU beyond 10 does not significantly improve the performance. As $W_{air,deh,out}$ and $T_{air,deh,out}$ decrease by 44% and 22%, respectively, when NTU increases from 1 to 10, while they only decrease by 4% and 1%, respectively, when NTU increases from 10 to 15. Figure 2.9(b) shows the same trends as it shows that when NTU increases from 1 to 10, the MRR increases from 1.5 to 4 g/s, and the SHR decreases from 0.5 to 0.38, while only slight improvement is achieved when NTU increases beyond 10.

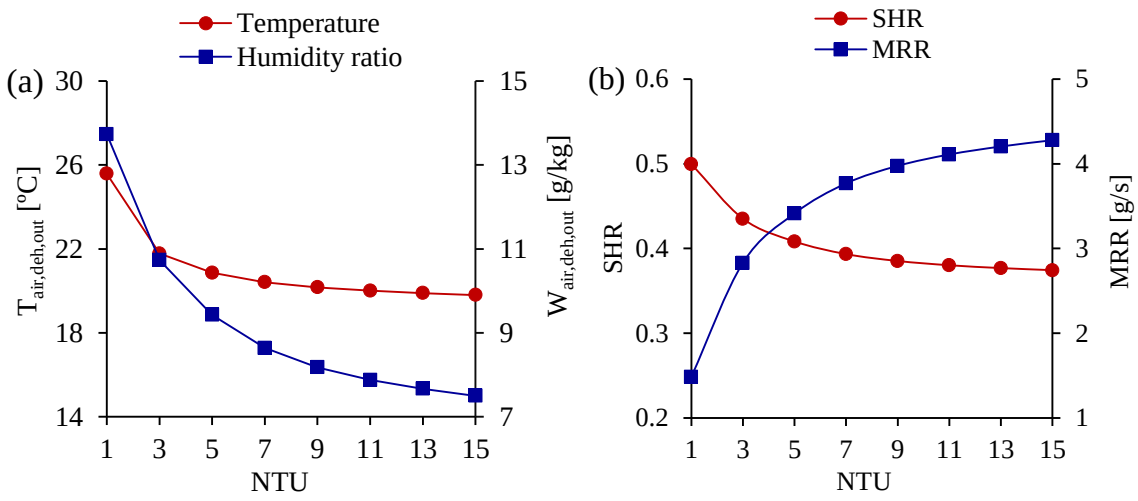

FIGURE 2.9. Influence of number of transfer units (NTU) on (a) outlet air state from the dehumidifier and (b) SHR and MRR of the dehumidifier.

Table 2.6 shows the variations of CC and COPs of the LDAC system with NTU. It is found that the CC and COP of the system increase from 8.8 to 18.1 kW and 0.43 to 0.68, respectively, when NTU increases from 1 to 10, while only slight improvement is achieved when NTU increases beyond 10. The trend at which ECOP and TCOP change depict the same point, as ECOP and TCOP increase by 70% and 23%, respectively when NTU increases from 1 to 10, while they only improve by less than 3% and 1%, respectively, when NTU increases from 10 to 15.

TABLE 2.6. Influence of number of transfer units (NTU) on the performance of the system.

NTU	CC [kW]	COP	ECOP	TCOP
1	8.8	0.43	2.04	1.58
3	14.1	0.57	2.91	1.81
5	16.1	0.61	3.17	1.85
7	17.2	0.64	3.33	1.87
9	17.9	0.67	3.41	1.93
11	18.3	0.69	3.49	1.97
13	18.6	0.69	3.52	1.97
15	18.8	0.69	3.55	1.97

The performance improvement of the system with NTU is expected, as the larger the NTU, the larger the surface area of the membrane that separates the air and solution streams in the dehumidifier/regenerator. This leads to a considerable increase in the sensible, latent and total effectiveness of the LAMEEs (dehumidifier/regenerator) (Namvar et al., 2012), and therefore an enhancement in the heat and mass transfer rates across the membrane. However, it should be noted that larger membranes surface areas will lead to higher capital cost. The results in Table 2.6 indicate that it is not beneficial to design LAMEEs with NTU larger than 10 in the proposed LDAC system because this leads to an increase in the capital costs of the system without achieving a considerable reduction in operating costs.

2.7.6 Influence of ambient air temperature (T_{amb})

With the increase of T_{amb} at a constant relative humidity, the humidity ratio of the ambient air also increases. Therefore, both the heat and mass transfer potential and the cooling and dehumidification loads increase due to the increase of ambient air temperature and humidity ratio. Figure 2.10(a) shows that the humidity ratio of the outlet air from the dehumidifier ($W_{air,deh,out}$) significantly increases with T_{amb} when $T_{sol,reg,in}$ and $T_{sol,deh,in}$ are kept constant at the reference values. Depending on the building and climate, it is expected that a supply humidity ratio of about 8 g/kg is achieved to remove the total latent load. Therefore, the LDAC system with the reference parameters may not meet the building latent loads when the ambient air conditions exceed 35ºC and 50% RH. However, as shown in Figure 2.10(b), $W_{air,deh,out}$ is significantly reduced when $T_{sol,reg,in}$ and $T_{sol,deh,in}$ are controlled simultaneously. As a result, an efficient control system should be installed in the system in order to control the solution temperature entering the dehumidifier and the regenerator according to the outdoor conditions and indoor cooling and dehumidification demanding. Figure 2.10(c) shows that the MRR increases linearly with T_{amb} due to the increase in mass transfer potential and the nearly constant effectiveness of the dehumidifier. However, since the heat transfer potential becomes larger than that for mass transfer as T_{amb} increases, the SHR increases.

As $W_{air,deh,out}$ and $T_{air,deh,out}$ increase with T_{amb}, the enthalpy difference between the ambient and air leaving the dehumidifier increase as well. This explains the enhancement that

occurs in the CC of the system, as shown in Table 2.7. The achieved improvement in the COPs of the system is attributed to the fact that the higher the T_{amb}, the higher the amount of heat and moisture transferred from the ambient air to the solution and the larger the amount of heat released from the air to the solution during the absorption process. Consequently, the thermal energy requirement for heating the solution prior to entering the regenerator is reduced with T_{amb}. This point coupled with the achieved increase in the CC of the system leads to the improvement of the COP, ECOP and TCOP.

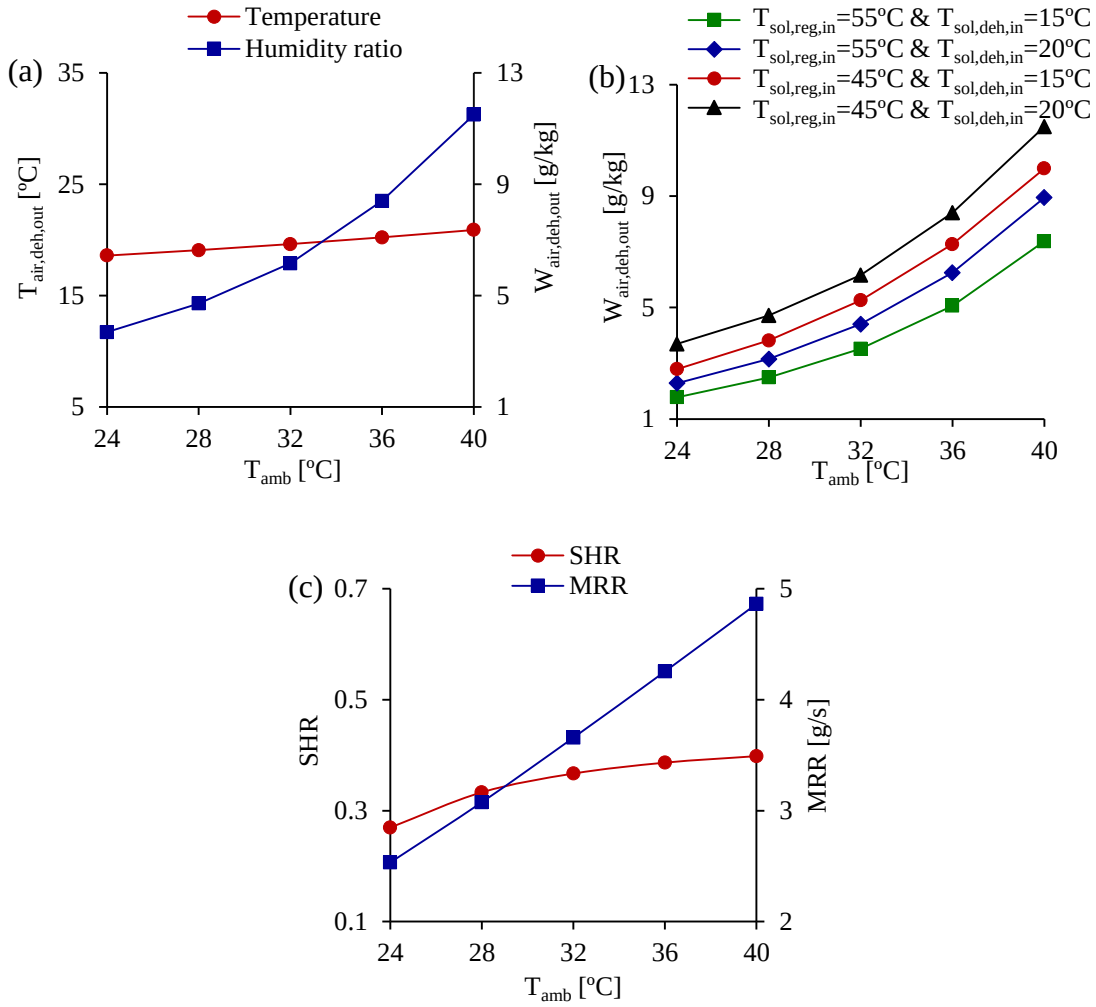

FIGURE 2.10. Influence of ambient air temperature (T_{amb}) on (a) outlet air state from the dehumidifier, (b) outlet air state from the dehumidifier at various solution temperatures and (c) SHR and MRR of the dehumidifier.

TABLE 2.7. Influence of ambient air temperature (T_{amb}) on the performance of the system.

T_{amb} [ºC]	CC [kW]	COP	ECOP	TCOP
24	9.0	0.35	2.08	0.80
28	12.1	0.46	2.57	1.14
32	15.2	0.57	3.02	1.55
36	18.4	0.68	3.46	2.01
40	21.6	0.79	3.80	2.56

2.7.7 Influence of ambient air relative humidity (RH_{amb})

The humidity ratio of the ambient air increases when the air relative humidity increases at constant temperature. This leads to an increase of the mass transfer potential, and therefore results in the increase in the amount of moisture removed by the system from the supply air stream. Figure 2.11(a) shows that $W_{air,deh,out}$ significantly increases with RH_{amb}. However, as shown in the previous section in Figure 2.10(b), $W_{air,deh,out}$ could be decreased significantly by controlling $T_{sol,reg,in}$ and $T_{sol,deh,in}$ simultaneously. Figure 2.11(b) shows that as RH_{amb} increases, SHR decreases and MRR increases due to the increase in mass transfer potential.

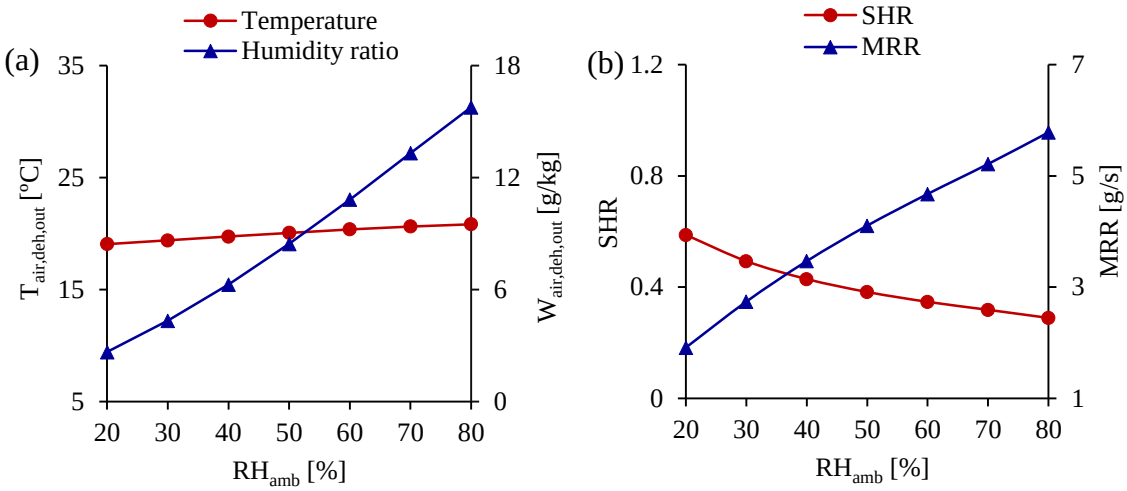

FIGURE 2.11. Influence of ambient air relative humidity (RH_{amb}) on (a) outlet air state from the dehumidifier and (b) SHR and MRR of the dehumidifier.

The CC and COPs of the system are shown in Table 2.8. As discussed in the previous section, the higher the ambient air humidity, the higher the CC of the system and the lower the thermal energy demand for heating the desiccant solution entering the regenerator. Therefore, the COP, ECOP and TCOP increase with RH_{amb}.

TABLE 2.8. Influence of ambient air relative humidity (RH_{amb}) on the performance of the system.

RH_{amb} [%]	CC [kW]	COP	ECOP	TCOP
20	12.6	0.55	2.63	1.77
30	14.7	0.60	2.95	1.83
40	16.5	0.64	3.22	1.89
50	18.1	0.68	3.45	1.95
60	19.5	0.71	3.65	2.01
70	20.9	0.74	3.84	2.06
80	22.7	0.79	4.10	2.15

2.8 CONCLUSION

In this chapter, the performance of a membrane LDAC system which uses two LAMEEs as the dehumidifier and regenerator is investigated under various climatic, design and operating conditions. It is found that the proposed LDAC system is more energy efficient (has higher COPs) in hot and humid climates. Results show that the dehumidification capacity of the system can be effectively controlled via regulating the temperatures of the liquid desiccant solution entering the regenerator and dehumidifier. The performance of the system significantly improves when NTU increases until NTU=10, while the performance improves only slightly when NTU is beyond this value. Also, increasing Cr^* is beneficial for the cooling capacity and COPs of the system, as they increase over the entire range of the tested Cr^*, especially when Cr^* increases from 2 to 4. It is found that the COP and SHR of the LDAC system are 0.68 and 0.38, respectively, at the reference condition. The proposed LDAC system can be more energy efficient if low-grade heat-sources (e.g. solar energy or waste heat) are available to cover a portion or the whole of the thermal energy required for solution regeneration, as this will lead to the increase of COP and TCOP, and the reduction of heating equipment capacity.

According to the results obtained in this study, it is recommended to set the solution inlet temperatures to the dehumidifier and regenerator at 15-20ºC and 45-55ºC, respectively, in order to achieve good performance for the proposed membrane LDAC system. The NTU and Cr^* are recommended to be within 5-10 and 3-5, respectively. A significant reduction in operating costs may be achieved during certain conditions (i.e. higher NTU), but it will be accompanied by an increase in the capital costs. Therefore, both the capital and the operating conditions have to be considered in selecting the optimal values for these parameters, and the payback period should be evaluated based on the actual application and operating condition.

CHAPTER 3

ANNUAL ENERGY MODELLING AND ECONOMICS OF A BASIC MEMBRANE LDAC SYSTEM

3.1 OVERVIEW

Recommended ranges for key operating and design parameters of a membrane LDAC system were presented in Chapter 2 under fixed conditions. To further investigate the feasibility of membrane LDAC (M-LDAC) systems in residential and commercial buildings, the annual energy performance of a basic configuration of a membrane LDAC system is simulated using TRNSYS and compared to a conventional air conditioning system. The thermal, economic and environmental performances are evaluated, and the influences of installing energy recovery ventilators (ERVs) in the M-LDAC system are evaluated under balanced/unbalanced operating conditions.

Results presented in this chapter fulfill part of the second objective of this thesis (i.e. to investigate the feasibility of several configurations for a membrane LDAC system), and more configurations are studied in Chapters 4 and 5 to completely address this objective. The manuscript used in this Chapter is published in Applied Energy.

Annual evaluation of energy, environmental and economic performances of a membrane liquid desiccant air conditioning system with/without ERV

(Applied Energy, 2014, Volume 116)

Ahmed H. Abdel-Salam, Carey J. Simonson

3.2 ABSTRACT

In this study, a membrane liquid desiccant air conditioning (M-LDAC) system is modeled using the TRNSYS building energy simulation software. Liquid-to-air membrane energy exchangers (LAMEEs) are used as a dehumidifier and regenerator in the proposed M-LDAC system to eliminate the carryover of desiccant droplets in supply and exhaust air streams, which may occur when direct-contact conditioners are used. A sensitivity study on the sensible, latent and total effectivenesses of the LAMEEs is performed under 36 operating and design conditions. The technical, environmental and economic performances of the proposed M-LDAC system are evaluated, and compared to those of a conventional air conditioning (CAC) system. The influences of installing an energy recovery ventilator (ERV) under balanced and unbalanced airflow rates conditions are investigated. Results show that the annual primary energy consumption and the life cycle cost (LCC) of the proposed M-LDAC system are 19% and 12% lower than that of the CAC system, and they reach 32% and 21% when an ERV, which operates under balanced airflow rates, is installed in the M-LDAC system.

3.3 INTRODUCTION

Air conditioning (AC) systems are installed in buildings to provide the occupants with healthy and productive environments. Considerable amount of energy is consumed in the operation of the widely used energy-inefficient conventional AC (CAC) systems, which lead to several environmental problems that are related to energy production such as air pollution, global warming and acid precipitation (Wang et al., 2010). Recent studies have shown that buildings are responsible for the consumption of around 40% of the primary energy consumption and the emission of nearly 33% of the greenhouse gases in the world (Perez-Lombard et al., 2008). All this has led to the development of a dilemma that consists of the following 3 interconnected issues: (1) energy efficiency of AC systems,

(2) environmental pollution and (3) indoor air quality (IAQ). This dilemma is believed to become even more crucial in the future due to the expected increase of the cooling degree days (CDD) in several climates, due to the climate change (Li et al., 2012). Therefore, scientists and engineers are trying to develop more efficient AC systems that are capable of achieving good IAQ with low energy consumption rates and air pollution emissions.

Among the evolving energy-efficient AC technologies are liquid desiccant air conditioning (LDAC) systems, which have showed promising performance during the past decades, and are believed to be a strong competitor with the widely used CAC systems. The following are the main advantages of LDAC systems:

(1) LDAC systems have the capability of efficiently controlling the indoor air humidity levels in applications that require efficient humidity control (Ge et al., 2011a).
(2) LDAC eliminates condensation on cooling coils which is prevalent in CAC systems, and thus prevents the growth of mold and bacteria (Xiao et al., 2011).
(3) The primary energy requirements of LDAC systems are lower than CAC systems, and thereby lower emissions are emitted to the environment when LDAC systems are used.
(4) The liquid desiccants, which are used in LDAC systems, can be regenerated at low temperatures in the range between 50ºC and 65ºC, and thus low-grade heat sources such as flat plate solar collectors and low-grade waste heat can cover the thermal energy requirements (Andrusiak et al., 2010).
(5) Liquid desiccants are capable of absorbing some pollutants from the supply air stream, which improves the IAQ within the conditioned space (Bergero and Chairi, 2011).

Recently, some studies have investigated the use of membrane energy exchangers as a dehumidifier and a regenerator, where some of them did not yield to acceptable results, while others have observed promising performance. For instance, Rattner et al. (2011) developed a mathematical model for a flat-plate membrane distillation device that can be used for liquid desiccant regeneration; unfortunately, the predicted performance of the regenerator was poor and a high regeneration temperature of up to 135ºC was required. On the other hand, Zhang (2011) conducted an experimental and theoretical study on the performance of a hollow fiber membrane energy exchanger, where the heat and mass

transfer performances of the investigated energy exchanger were found to be promising, for both air dehumidification and humidification applications. Bergero and Chiari (2010, 2011) investigated the performance of a hybrid LDAC system that uses membrane energy exchangers as the dehumidifier and regenerator, both experimentally and theoretically. They found that under fixed design and operating conditions, energy savings up to 60% could be achieved compared to a CAC system. Abdel-Salam et al. (2013a) performed a parametric study on a membrane LDAC (M-LDAC) system that uses membrane energy exchangers as the dehumidifier and regenerator, and it was concluded that the studied system is capable to cover the entire latent load for a wide range of practical applications, by regulating the thermal capacity ratio between solution and air streams (Cr^*), the number of heat transfer units (NTU), and the solution inlet temperatures to the dehumidifier and regenerator ($T_{sol,in,deh}$ and $T_{sol,in,reg}$).

Although some studies have been performed on the performance of LDAC systems that use membrane energy exchangers under fixed design and operating conditions, as mentioned previously, no available studies in the literature have evaluated the performance of these systems when installed in a building throughout the year. Thus, the present work extends the investigation of a previously studied M-LDAC system that uses liquid-to-air membrane energy exchangers (LAMEEs) as the dehumidifier and regenerator (Abdel-Salam et al., 2013a), by evaluating the annual performance of this system when installed in an office building located in a very hot and humid climate (Miami, Florida). The LAMEE used in the present work has been under research and development at the University of Saskatchewan during the last decade, where it has been studied experimentally and theoretically, and its performance was found to be promising for both air dehumidification and humidification applications (Erb et al., 2009; Abdel-Salam et al., 2014c). The proposed M-LDAC system will be modeled using the TRNSYS building energy simulation software (TRNSYS, 2010). The performance of the LAMEE will be first evaluated, when it is used as a dehumidifier and a regenerator, under different operating and design conditions. Then, the annual technical, environmental and economic performances of the proposed M-LDAC will be evaluated. The influence of installing an energy recovery ventilator (ERV) will be investigated, when it operates under balanced

and unbalanced airflow rates conditions. All the results obtained from the proposed system will be compared to those of a CAC system. Thus, in order to investigate the viability of the proposed M-LDAC system, the following four AC systems will be simulated in this study: (1) CAC system, (2) CAC system with ERV (CAC-ERV), (3) M -LDAC system and (4) M-LDAC system with ERV (M-LDAC-ERV).

3.4 SYSTEMS DESCRIPTION

3.4.1 Conventional air conditioning system (CAC)

In the CAC system (see Figure 3.1(a)), the outdoor air is mixed with a portion of the return air, and the mixed air passes over a cooling coil where it is cooled and dehumidified. Dehumidification can only occur if the air is cooled below its dew point temperature. Thus, if dehumidification is required, the supply air should be reheated using the heating coil in order to increase the supply air temperature and avoid thermal discomfort due to cold drafts.

3.4.2 Conventional air conditioning system with ERV (CAC-ERV)

The operating principle of the CAC-ERV system (see Figure 3.1(b)) is similar to the CAC system. The only difference is that in the CAC-ERV system, the outdoor air is preconditioned in an ERV, using the exhaust air from the building, before it is mixed with the return air.

It is expected that the sensible and latent effectivenesses of the ERV may vary under different outdoor conditions. However, Fauchoux et al. (2007) have found that negligible variations occur in the annual energy consumption and equipment sizes, when the sensible and latent effectivenesses of an ERV are set at constant values compared to when they are variable. Thus, it is assumed in this study that both the sensible and latent effectivenesses are maintained constant at 0.75. It is worth mentioning that ERVs are not beneficial at all operating conditions, and that sometimes it is more beneficial to bypass the outdoor air around them, depending on the thermodynamic conditions of both the return and fresh air streams (Fauchoux et al., 2007; Mumma, 2001; Rasouli et al., 2010). Several control methodologies have been proposed to control ERVs, where these strategies can be briefly

categorized as temperature-based (Fauchoux, 2007) and enthalpy-based (Mumma, 2001) control strategies. Rasouli et al. (2010) developed an efficient control methodology, which is a combination of the aforementioned control methodologies, in order to maximize the energy savings that would be achieved using an ERV. This control methodology is used to control the ERV in this study.

3.4.3 Membrane liquid desiccant air conditioning system (M-LDAC)

3.4.3.1. Air side

In the M-LDAC system (see Figure 3.2(a)), the outdoor air passes through a dehumidifier in order to be dehumidified to a condition that covers the entire latent load (i.e. space, ventilation and infiltration) within the building and a portion of the sensible load. The remaining sensible load is met by cooling the return air coming from the conditioned space as shown in Figure 3.2(a). The proposed M-LDAC system, which meets the sensible load by sensibly cooling the return air and the latent load by dehumidifying the ventilation air prior to mixing, has many advantages including:

(1) The cooling coil can operate at higher evaporating temperature than the cooling coil in the CAC system, which improves the coefficient of performance (COP).
(2) There is no condensation on the cooling coil which reduces the risk of mold growth and lower maintenance cost.
(3) The airflow rate through the LAMEE is limited to the ventilation airflow which means that the LAMEE is much smaller, and therefore reduces the capital costs.
(4) Control of the proposed system is expected to be better since the sensible coil and the dehumidifier LAMEE are sized to handle different airflows rather than having these exchangers sized to handle the same airflows.

3.4.3.2. Liquid desiccant side

The liquid desiccant leaves the dehumidifier shown in Figure 3.2(a) both warm and diluted, and thus needs to be regenerated before it can be used again to dehumidify the outdoor air. In order to be regenerated, the liquid desiccant must be heated prior entering the regenerator in order to increase its vapor pressure, which increases the potential of mass transfer from the liquid desiccant to the regeneration air. Thus, the warm and diluted liquid desiccant

leaving the dehumidifier is preheated in the solution sensible heat exchanger, and then heated in the solution heater to a specific set point (50ºC). After removing the required amount of moisture from the liquid desiccant in the regenerator through the desorption of moisture to the regeneration air, the hot and concentrated liquid desiccant leaving the regenerator must be cooled prior entering the dehumidifier in order to reduce its vapor pressure, which increases the potential of mass transfer from the humid outdoor air to the liquid desiccant. Therefore, the hot and concentrated liquid desiccant coming out from the regenerator is precooled in the solution sensible heat exchanger before it is cooled in the solution cooler to a specific set point (20ºC).

3.4.4. Membrane liquid desiccant air conditioning system with ERV (M-LDAC-ERV)

The operating principle of the M-LDAC-ERV system (see Figure 3.2(b)) is similar to the M-LDAC system. The only difference is the installation of an ERV in the M-LDAC-ERV system to precondition the outdoor air using the exhaust air from the conditioned space before it enters the dehumidifier. Since this leads to the reduction of the latent loads required to be covered by the dehumidifier, the set point temperatures of the solution cooler and heater are set at 23ºC and 45ºC, respectively, in the M-LDAC-ERV system. The used set point temperatures were selected based on the results presented in the previous chapter, so that the indoor air temperature and humidity ratio are kept nearly the same for the M-LDAC and M-LDAC-ERV systems within the recommended comfort ranges as will be presented in Section 8.2.1. Since lower latent loads are required to be met by the dehumidifier when an ERV is used, the set point temperatures of the liquid desiccant cooling and heating coils are increased and decreased, respectively, when the ERV is used. It is worth mentioning that the ON/OFF control methodology was adopted in this study, where the M-LDAC system is turned on if the indoor humidity ratio is above 9.3 g/kg, and the dry cooling coil is turned on if the indoor air temperature is above 24ºC. The ERV is controlled using the same control methodology mentioned in the previous section.

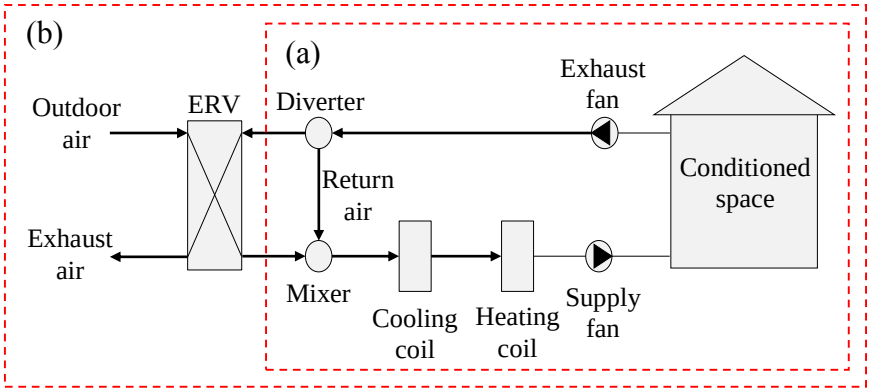

FIGURE 3.1. Schematic diagrams of the (a) CAC and (b) CAC-ERV systems.

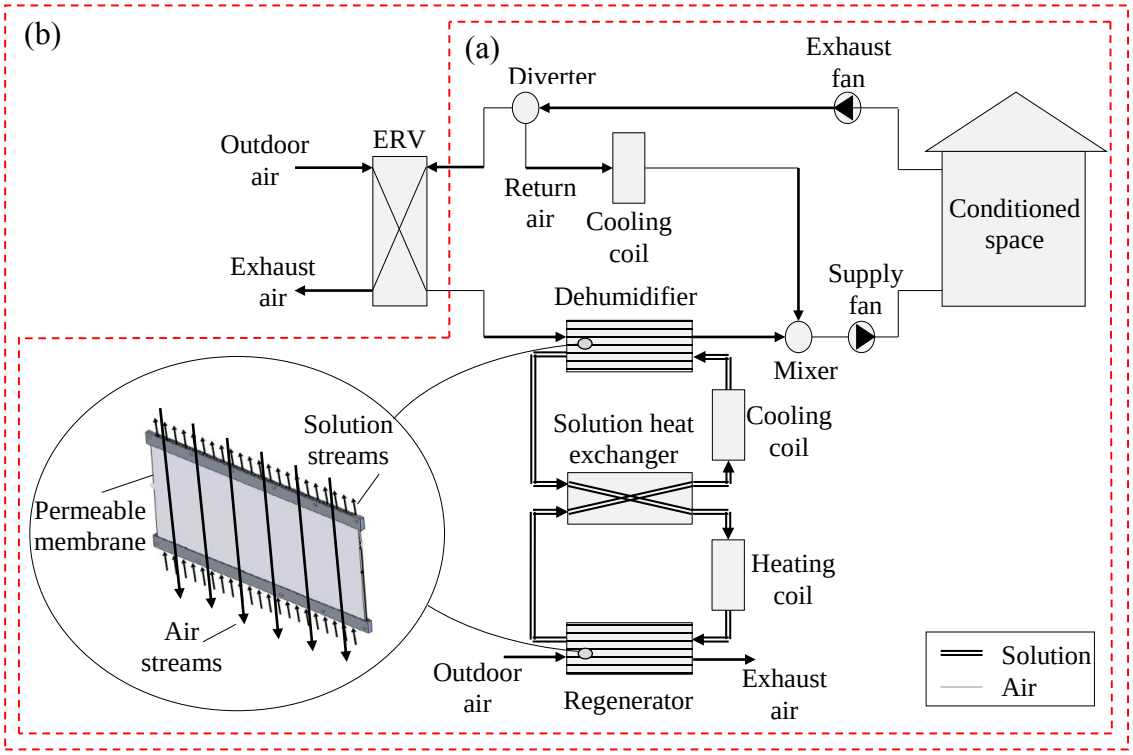

FIGURE 3.2. Schematic diagrams of the (a) M-LDAC and (b) M-LDAC-ERV systems.

3.5 BUILDING DESCRIPTION

The simulated building in this study is a small one-story office building, see Figure 3.3. It has a rectangular floor area of 511 m^2, with an aspect ratio of 1.5 and the main façade facing south. The floor to ceiling height is 3.1 m and the window-to-wall ratio is 0.21. This building is one of the 15 commercial buildings that were selected by the US Department of Energy (DOE), National Renewable Energy Laboratory (NREL), Pacific Northwest National Laboratory (PNNL) and Lawrence Berkeley National Laboratory (LBNL) to represent ~2/3 of the commercial buildings in the United States (Deru et al., 2011).

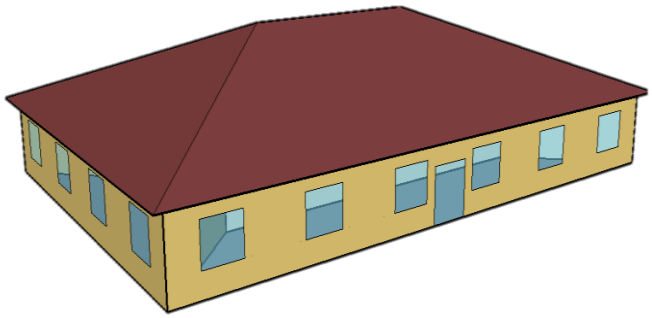

FIGURE 3.3. Schematic diagram of the one-story office building simulated in this study.

The building is simulated in this study as a single zone. The thermal envelope construction was developed with accordance to ANSI/ASHRAE/IESNA Standard 90.1-2004 (ASHRAE, 2004). A summary for the building specifications is given in Table 3.1. The U-factors of the exterior walls, roof and floor are 3.3, 0.36 and 1.8 W/(m^2.K), respectively. A window that has a U-factor and a solar heat gain coefficient (SHGC) of 5.2 W/(m^2.K) and 0.5, respectively, is used in this study, which is close from that recommended for office buildings located in climate zone 1A (ASHRAE, 2004). According to ANSI/ASHRAE Standard 62.1-2007 (ASHRAE, 2007), the occupant density and ventilation outdoor airflow rate are 5 people/100 m^2 and 10 L/s per person, respectively, for office buildings. This gives an outdoor ventilation airflow rate of 0.26 m^3/s (0.6 air change per hour).

The heat gain emitted from lighting is assumed to be 11 W/m^2 according to the building area method (ASHRAE, 2004), while the heat gain emitted by the equipment is assumed to be 10.8 W/m^2 (ASHRAE, 2009). The occupants are assumed to be seated and doing light work, and thus the sensible and latent heat gains produced are assumed to be 75 W each. The average air speed within the conditioned space is assumed to be 0.15 m/s according to ANSI/ASHRAE Standard 55-2004 (ASHRAE, 2004). The hourly schedules of the ventilation airflow rate, lighting, equipment and occupants with respect to the peak values are shown in Figure 3.4.

TABLE 3.1. Office building model specifications.

Parameter	Value	Unit
Aspect ratio of building[1]	1.5	
Average air speed within the space[4]	0.15	m/s
Equipment heat gain	10.8	W/m^2
Floor area[1]	511	m^2
Floor to ceiling height[1]	3.1	
Floor U-value[2]	1.8	W/(m^2.K)
Lighting heat gain	11	W/m^2
Occupant density[3]	5	people/100 m^2
Occupants latent heat gain[2]	75	W/person
Occupants sensible heat gain[2]	75	W/person
Roof U-value[2]	0.36	W/(m^2.K)
Total ventilation airflow rate	0.26	m^3/s
Ventilation airflow rate[3]	10	L/s/person
Wall U-value[2]	3.3	W/(m^2.K)
Window solar heat gain coefficient[2]	0.5	
Window to wall ratio[1]	21	%
Window U-value[2]	5.2	W/(m^2.K)

Sources: 1. Deru et al. (2011), 2. ANSI/ASHRAE Standard 90.1-2004, 3. ANSI/ASHRAE Standard 62.1-2007, 4. ANSI/ASHRAE Standard 55-2004.

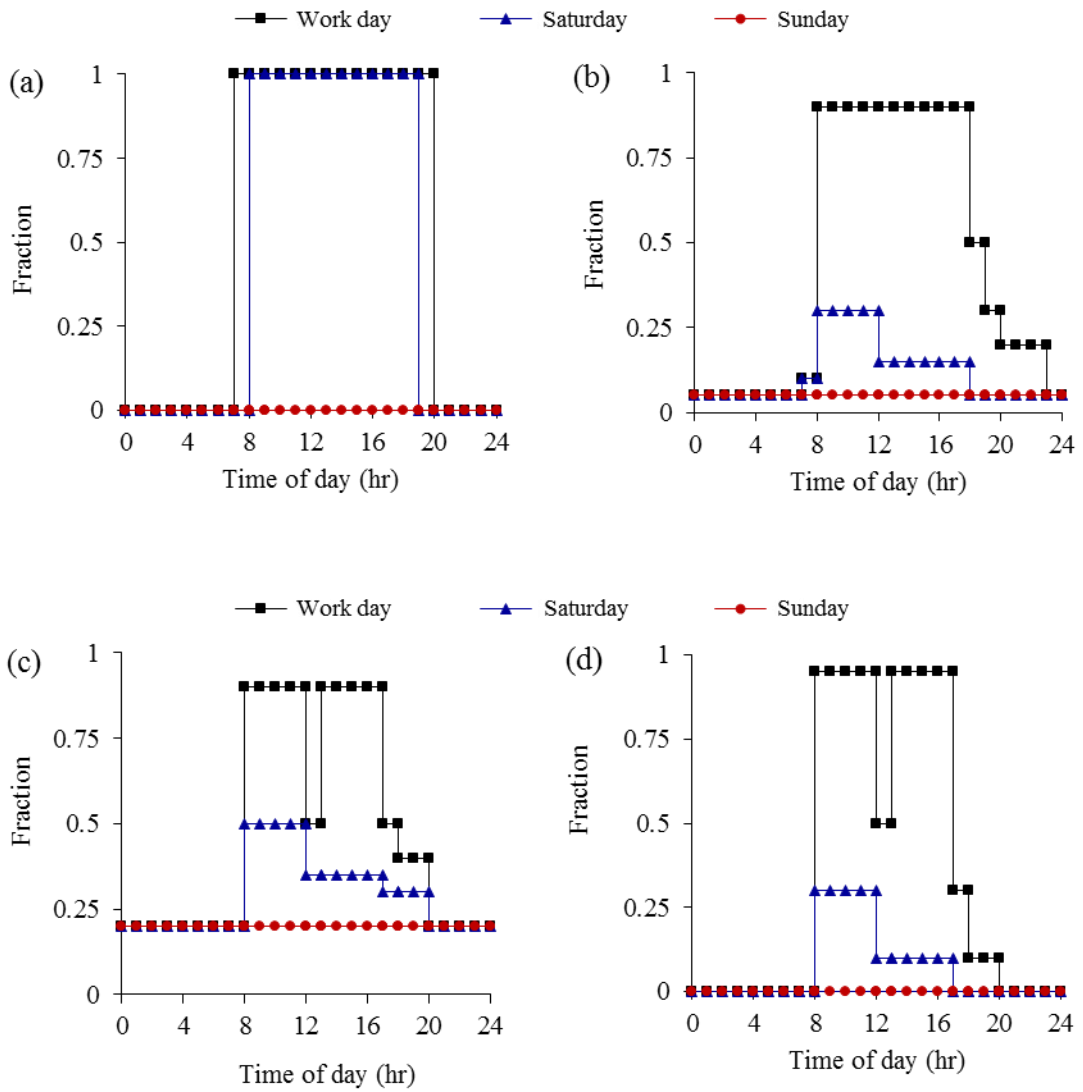

FIGURE 3.4. The hourly schedules of (a) ventilation airflow rate, (b) lighting, (c) equipment and (d) occupants, with respect to the peak values.

3.6 CLIMATIC CONDITIONS

ASHRAE classifies climate zones into several zones which range from 1 (i.e. very hot) to 8 (i.e. very cold) based on the temperature level, and from A (i.e. humid) to C (i.e. marine) based on the humidity level (ASHRAE, 2007). Figure 3.5 shows the classification of different climate zones in the United States, where it can be seen that Miami, Florida is classified as a climate zone 1A which represents a very hot-humid climate.

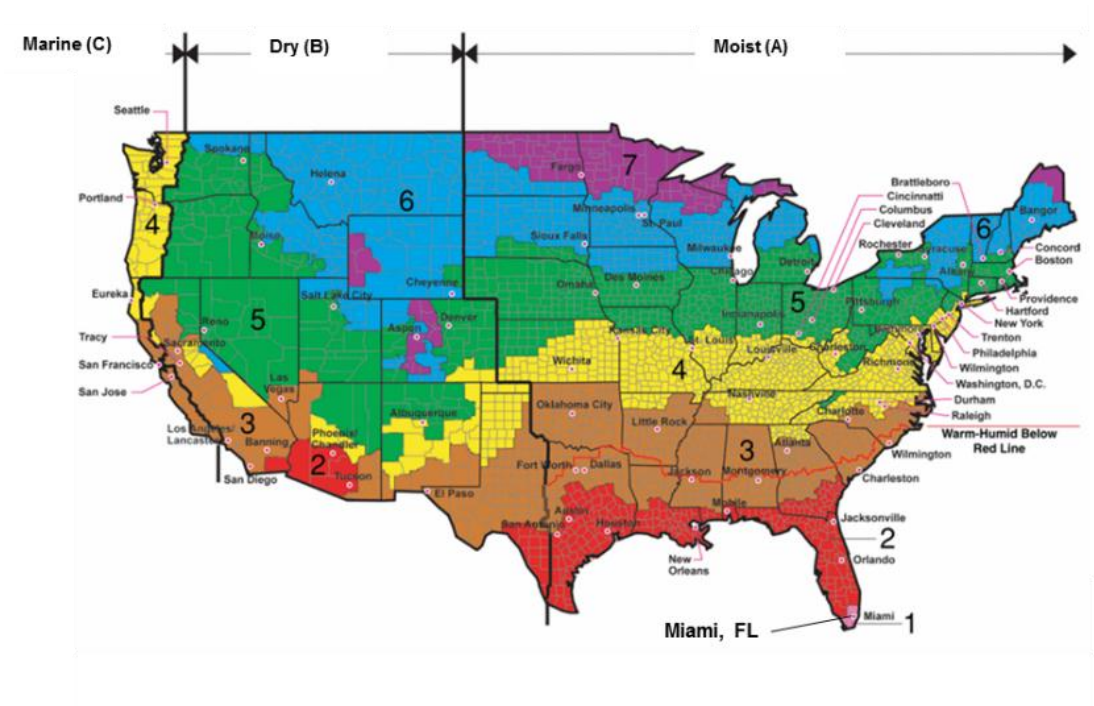

FIGURE 3.5. ASHRAE classification for different climate zones in the United States (Energy Modelling of Buildings, 2014).

The simulations are performed in Miami, Florida. A typical meteorological year (TMY2) weather data file is used in this study (TRNSYS, 2010). Figure 3.6 shows the annual hourly temperature, humidity ratio and total solar radiation in Miami according to the TMY2 weather data file used (TRNSYS, 2010). The cumulative outdoor air temperature and humidity ratio for Miami are shown in Figure 3.7. It is clear that cooling and dehumidification are required for nearly the entire year in Miami, and thus it is a suitable climate to investigate the performance of the liquid desiccant systems proposed in this study. Since the heating season is mild and short, the heating energy required in the winter season is not considered in this study, and the focus is only on the AC system.

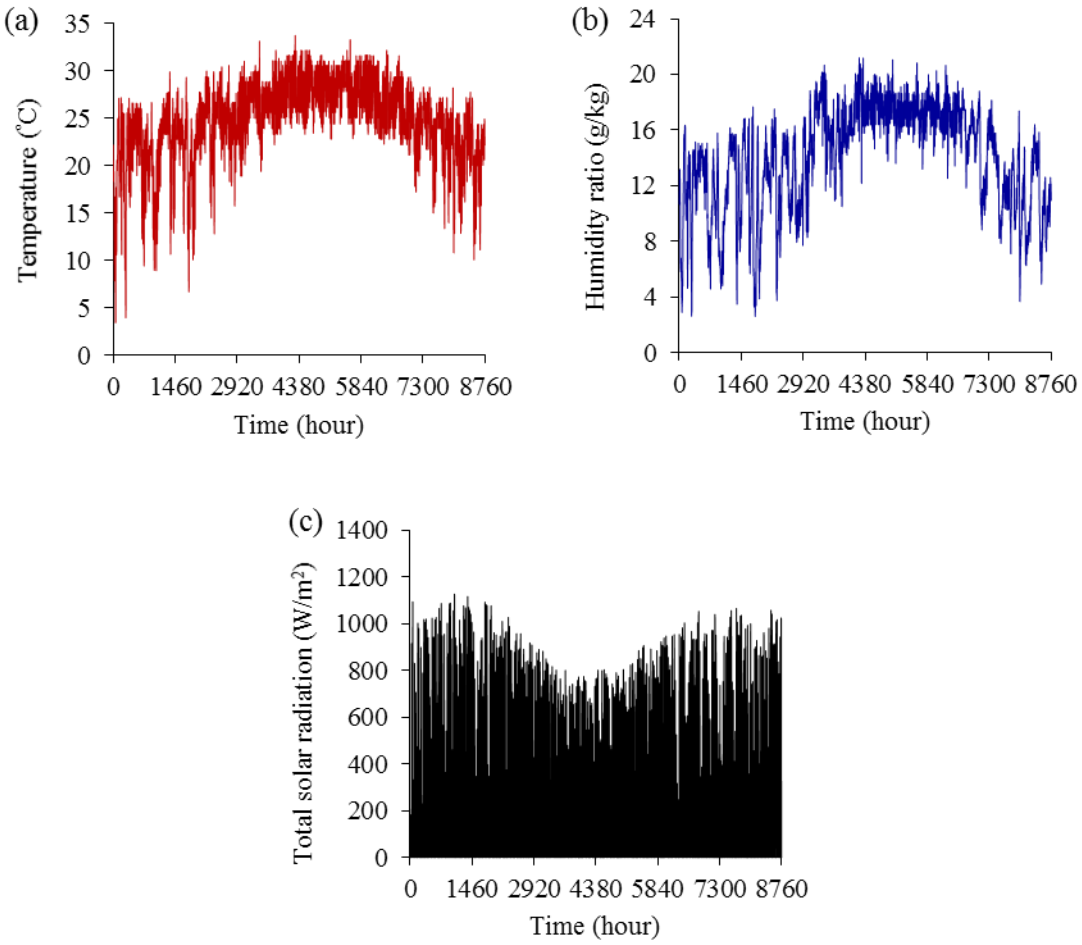

FIGURE 3.6. Annual hourly (a) total solar radiation, (b) humidity ratio and (c) temperature in Miami, Florida.

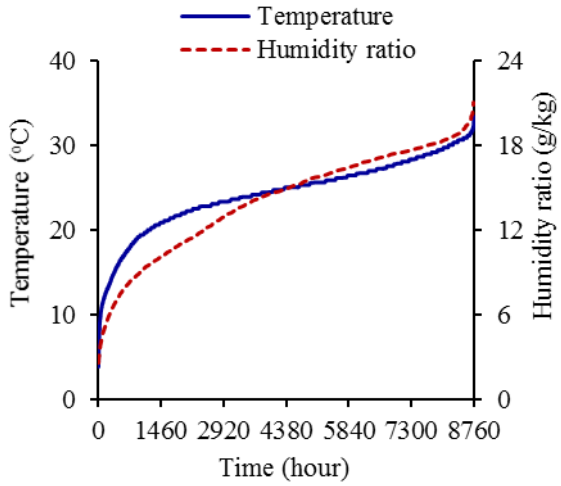

FIGURE 3.7. Annual cumulative outdoor air temperature and humidity for Miami, Florida.

3.7 LAMEE

Counter-flow LAMEEs are used as the dehumidifier and regenerator in the proposed M-LDAC system, as mentioned previously. The specifications of the used LAMEEs are presented in Figure 3.8. The length, width and height of the LAMEEs used in this study are 1m, 0.6m and 1.2 m, respectively. The air and desiccant solution flow rates in the LAMEEs are 0.33 and 0.34 kg/s, respectively. More details about the properties of the membrane and the analytical model used to model the LAMEE are presented in Chapter 2.

The size of the LAMEE is defined by the NTU, as shown in equation (2.28), and it should be specified before the manufacture of the LAMEE. The larger the NTU, the higher the effectiveness of the LAMEE, while the higher the capital costs; similarly, the larger Cr^*, the higher the effectiveness, while the higher the initial and pumping cost (Rasouli et al., 2011). Therefore, the NTU and Cr^* are chosen to be 7 and 3, respectively, in this study for both the dehumidifier and regenerator. The chosen values for NTU and Cr^* are based on results presented in the aforementioned chapter, where it is found that the NTU and Cr^* are recommended to be within 5 to10 and 2 to 4, respectively, in order to obtain high performance for the LAMEE whether it is operated under dehumidification or regeneration mode.

The hydrodynamic and thermal entry lengths for the LAMEEs in this study are 30% and 25% of the LAMEE's length. Since Nu is higher in the developing region than in the fully developed region (i.e. Nu=8.24) (Zhang et al., 2010b), the influence of using higher Nu than 8.24 on the effectivenesses of the LAMEEs is studied to investigate the applicability of this assumption. It is found that at constant air and solution flow rates, increasing the Nu by ~21% (from 8.24 to 10) leads to ~19% increase in the NTU of the LAMEE (from 7 to 8.36), while the maximum improvement in the effectiveness of the LAMEE does not exceed 3%. Thus, the airflow is assumed to be fully developed in the current study and Nu is taken as 8.24 (Incropera and Dewitt, 2002; Mahmud et al., 2010; Hemingson et al., 2011; Zhang and Niu, 2001; Ge et al., 2013a, 2013b).

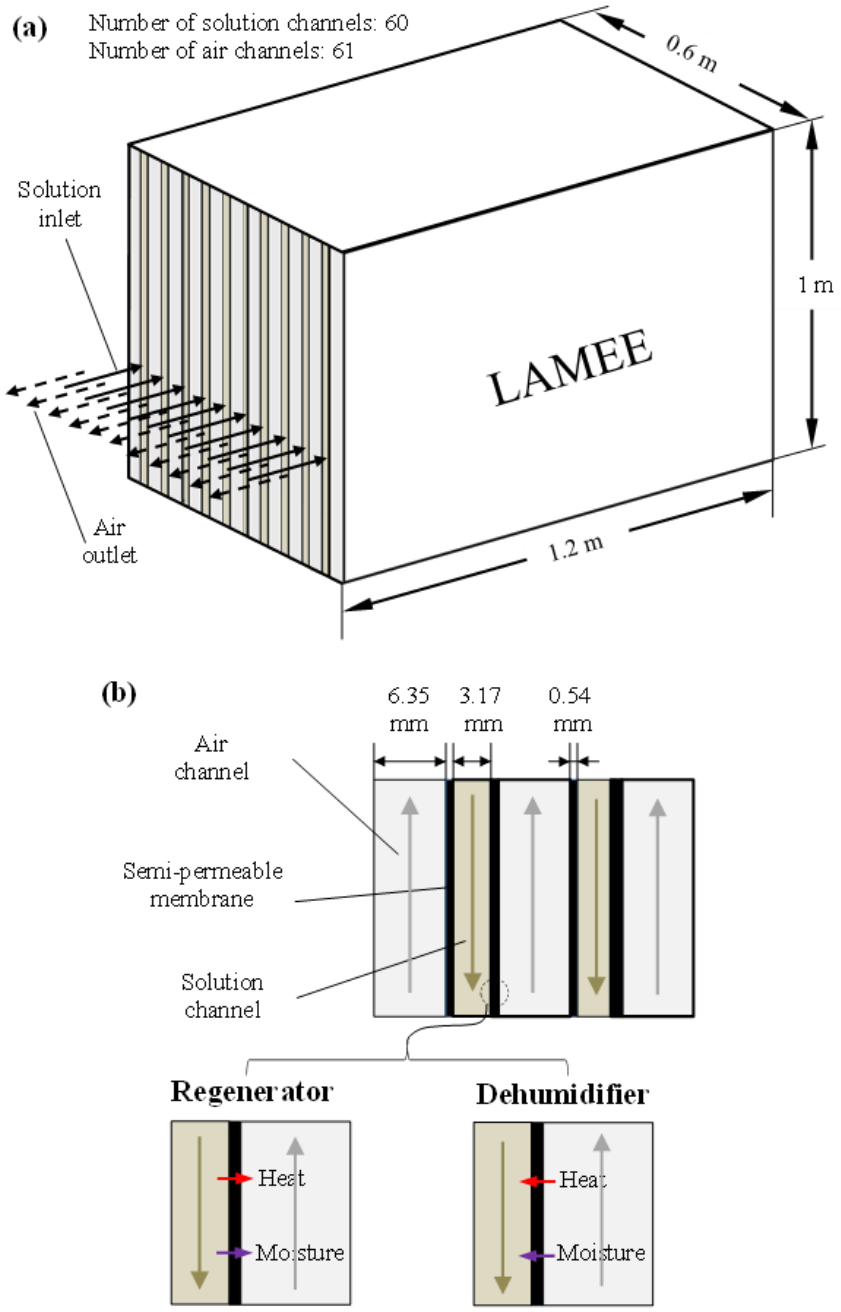

FIGURE 3.8. Schematics of the (a) LAMEE and (b) top view and direction of heat and mass transfer in the regenerator and dehumidifier LAMEEs.

3.8 SYSTEMS SIMULATION

The TRNSYS building energy simulation program is used to simulate the four AC systems investigated in this study. As previously mentioned in Section 2.5.1, the standard TRNSYS deck includes several built-in components that simulate the commonly used equipment in AC systems (TRNSYS, 2010). In addition, the Thermal Energy System Specialists (TESS) has developed several components for equipment that are not included in the standard TRNSYS deck. Table 3.2 lists the components that are used to model the AC systems investigated in this study.

TABLE 3.2. TRNSYS and TESS used components.

Type	Parameter	Type	Parameter	Type	Parameter
 Type56	Building model	 LAMEE	LAMEE's created component	 Type114	Pump
 Type15-6	TMY2 weather data	 Type667	Energy recovery ventilator	 Type112a	Fan
 Type77	Soil temperature	 Type699	Sensible heat exchanger	 Type11e	Diverter
 Type571	Infiltration airflow rate	 Type752g	Sensible and latent cooling coil	 Type11c	Mixer
 Type33e	Psychometric relations	 Type1246	Sensible cooling coil	 Macro	Macro
 Type65c	Output recorder	 Type659	Sensible heater	 Equation	ON/OFF controller

3.9 ANALYSIS

3.9.1 LAMEEs performance analysis

The LAMEEs (i.e. dehumidifier and regenerator) are the core components of the proposed M-LDAC system, and their performances significantly influence the performance of the M-LDAC system. The performance of the LAMEE is evaluated in this study by performing a sensitivity study for its sensible, latent and total effectivenesses under 36 design and operating conditions. The effectiveness is defined as the ratio between the actual to the maximum possible transfer rate. The sensible, latent and total effectivenesses define the

LAMEE's ability to transfer heat, moisture, and heat and moisture, respectively, and they are calculated using equations (3.1), (3.2) and (3.3), respectively (Simonson and Besant, 1999a; ASHRAE, 2008). The parameters investigated in the performed sensitivity study are as follows: (1) thermal capacity rate ratio between solution and airflows (Cr^*), (2) number of heat transfer units (NTU), (3) solution inlet temperature to regenerator ($T_{sol,reg,in}$), (4) solution inlet temperature to dehumidifier ($T_{sol,deh,in}$), (5) air inlet temperature to LAMEEs ($T_{air,in}$) and (6) air inlet relative humidity to LAMEEs ($RH_{air,in}$).

$$\varepsilon_{sen} = \frac{T_{air,in} - T_{air,out}}{T_{air,in} - T_{sol,in}} \tag{3.1}$$

$$\varepsilon_{lat} = \frac{W_{air,in} - W_{air,out}}{W_{air,in} - W_{sol,in}} \tag{3.2}$$

$$\varepsilon_{tot} = \frac{\varepsilon_{sen} + H^* \varepsilon_{lat}}{(1+H^*)} \tag{3.3}$$

where, T is the temperature (ºC), W is the humidity ratio (g/kg) and H^* is an operating condition factor developed by Simonson and Besant (1999a) which is defined as the ratio between the potential for mass transfer to that for heat transfer. Subscripts air, sol, in and out refer to the air, solution, inlet and outlet, respectively. Subscripts sen, lat, and tot refer to sensible, latent and total, respectively.

3.9.2 AC systems technical performance analysis

The technical performance of the four AC systems is investigated by evaluating the following: (1) the indoor air temperatures and relative humidities, (2) the capacities of the equipment, (3) the annual primary energy consumption and (4) the influence of the exhaust airflow rate ratio of the ERV, when it is used. The indoor air conditions and the capacities of the equipment are directly obtained from the developed TRNSYS models, while the primary energy consumption is calculated as follows. First, the energy (q) delivered to the air/solution streams by the heating equipment, cooling equipment, fans and pumps are calculated using the developed TRNSYS models. Then, the total primary energy consumptions of the CAC and CAC-ERV systems are calculated using equation (3.4), and the total primary energy consumptions of the M-LDAC and M-LDAC-ERV are calculated using equation (3.5).

$$E_{CAC/CAC\text{-}ERV}=\frac{q_{air,reheat}}{\eta_{boiler}}+\frac{1}{CF_{electrical\text{-}thermal}}\left\{\frac{q_{air,cool}}{COP_{air,chiller}}+\frac{q_{air,fans}}{\eta_{fans}\eta_{motor}}\right\} \quad (3.4)$$

$$E_{M\text{-}LDAC/M\text{-}LDAC\text{-}ERV}=\frac{1}{CF_{electrical\text{-}thermal}}\left\{\begin{array}{c}\frac{q_{sol,cool}}{COP_{sol,chiller}}+\frac{q_{air,cool}}{COP_{air,chiller}}+\frac{q_{sol,heat}}{COP_{sol,heatpump}}\\ +\frac{q_{air,fans}}{\eta_{fans}\eta_{motor}}+\frac{q_{sol,pumps}}{\eta_{pumps}\eta_{motor}}\end{array}\right\} \quad (3.5)$$

The supply and exhaust fans are assumed to be centrifugal-type HVAC fans that have efficiencies of 60%. The pressure drops in the supply and exhaust ducts are assumed to be 1250 Pa and 500 Pa, respectively (Fauchoux et al., 2007). The ERV is assumed to have a pressure drop of 200 Pa (Fauchoux et al., 2007), while the pressure drop caused by each of the LAMEEs is assumed to be 250 Pa (Moghaddam et al., 2013c). The cooling energy required to cool the air and solution streams in the four AC systems is assumed to be provided using direct expansion chillers. Since the COP for a given chiller increases with the evaporating temperature (Zhang et al., 2005; Niu et al., 2010)), the chillers used to cool the solution and air in the M-LDAC system are assumed to have COPs of 7 and 5.5, respectively (Niu et al., 2010). While, the chiller used to cool the air in the CAC system is assumed to have a lower COP of 4 (Niu et al., 2010), because it operates at relatively lower evaporating temperatures. The heating energy required for the solution regeneration is assumed to be provided using an electrical heat pump that has a COP of 5 (Niu et al., 2010), while a gas-fired boiler with efficiency (η) of 90% is assumed to provide the thermal energy required for reheating the overcooled air in the CAC system (Niu et al., 2010). The equivalent conversion coefficient of electric power and thermal energy ($CF_{electrical\text{-}thermal}$) is assumed to be 0.33, because over 75% of the electricity generated in Florida is obtained using natural gas and coal power plants that have efficiencies of 32.8% and 32%, respectively (Florida Public Service Commision, 2013; US DOE, 2010).

The exhaust airflow rate ratio of ERV ($R_{exhaust}$), given in equation (3.6), is defined as the ratio between the exhaust and supply airflow rates in the ERV. Several studies have been performed on ERVs, where balanced airflow conditions were assumed (Fauchoux, 2007; Mumma, 2001; Rasuoli et al., 2010). However, this might not be the case in practical applications especially for buildings that are located in hot and humid climates, where the

$R_{exhaust}$ is commonly less than unity in order to ensure that the building is pressurized. Pressurizing a conditioned space is important in hot and humid climates, to avoid the accumulation of moisture within the building envelope, which might lead to the degradation of the thermal resistance of the envelope, and the growth of mold and bacteria (Lstiburek, 1993). Although most of the results presented in this study are calculated based on a balanced airflow rates ($R_{exhaust} = 1$), the influence of unbalanced airflow conditions ($R_{exhaust} < 1$) on the annual primary energy consumption of the CAC-ERV and M-LDAC-ERV systems are evaluated in Section 3.10.2.4. The $R_{exhaust}$ is equivalent to the thermal capacity ratio (C^*) used for an air-to-air sensible heat exchangers, where $R_{exhaust}=1$ means that the air flows are balanced (i.e. $C^*=1$). From heat exchanger theory, it is known that effectiveness increases as C^* decreases (Incropera and Dewitt, 2002). However, both the sensible and latent effectivenesses of the ERV were kept constant at 0.75 under the different investigated $R_{exhaust}$ values in this study, for the sake of simplification. It is worth mentioning that the achieved saving in annual primary energy consumption due to the install of ERV is expected to decrease at lower $R_{exhaust}$, due to the reduction of the amount of heat recovery rate (HRR) and mass recovery rate (MRR) in the ERV at low exhaust airflow rate as given in equations (3.7) and (3.8), respectively.

$$R_{exhaust} = \frac{\dot{m}_{exhaust}}{\dot{m}_{fresh}} \tag{3.6}$$

$$HRR_{ERV} = \varepsilon_{sen} \cdot C_{min} \cdot \left(T_{exaust,in} - T_{fresh,in}\right) \tag{3.7}$$

$$MRR_{ERV} = \varepsilon_{lat} \cdot \dot{m}_{min} \cdot \left(W_{exaust,in} - W_{fresh,in}\right) \tag{3.8}$$

where, $\dot{m}$ is the air mass flow rate in kg/s, and subscripts exhaust and fresh refer to the exhaust and fresh airflow streams, respectively.

3.9.3 Environmental analysis

The air pollution emissions emitted as a result of the energy consumed in each of the four studied AC systems are calculated as shown in equation (3.9), which is developed by the authors. The air pollution emissions that are included in this study are carbon dioxide (CO_2), carbon monoxide (CO), sulfur oxides (SO_x), nitrous oxides (NO_x) and particulate matters (PM). Since the M-LDAC and M-LDAC-ERV systems are totally operated using electricity in this study, the air pollution emissions from these systems are calculated using

only the first term of equation (3.9). Although the CAC and CAC-ERV systems mainly depend on electricity to run the chillers and fans, a small amount of natural gas is still required to operate the gas-fired boiler that is used to reheat the overcooled supply air stream. Thus, for the CAC and CAC-ERV systems, the air pollution emissions resulted from electrical energy requirements are calculated using the first term of equation (3.9), while the second term of the equation is used to calculate the air pollution emissions resulted from the natural gas required for the gas-fired boiler.

$$F_i = \left(\sum \frac{\alpha_j \, \varphi_{i,j}}{\eta_j} \right) \cdot E_{electrical} + \varphi_{i,natural\ gas} \cdot E_{electrical} \tag{3.9}$$

where, α_j is the percent of electricity generated using a given type of power plant with respect to the total electricity generated in Florida, $\varphi_{i,j}$ is the amount of pollutant emitted from a given power plant in kg/GJ, η_j is the efficiency of the power plant, $E_{electrical}$ is the electrical energy requirements in GJ and $E_{natural\ gas}$ is the natural gas requirements in GJ. Subscripts i and j refers to the type of pollutant (i.e. CO_2, CO, SO_x, NO_x or PM) and the type of power plant (i.e. natural gas, coal or oil), respectively.

The natural gas, coal and oil power plants generate approximately 50.8%, 24.8% and 2.4%, respectively, of the electricity in Florida, while the rest (~22%) is generated using nuclear energy and other renewable sources (Florida Public Service Commision, 2013). Table 3.3 shows the amount of air pollution emissions from the different types of power plants (Yoshiyuli et al., 2010; Natural Gas Supply Association, 2013), the efficiency of each of these power plants (US DOE, 2010) and the percent of electricity that each type of power plants generates with respect to the total electricity generated in Florida (Florida Public Service Commision, 2013).

TABLE 3.3. Environmental emissions from different types of power plants Yoshiyuli et al., 2010; Natural Gas Supply Association, 2013), the percent of electricity generated in Florida using different types of power plants (Florida Public Service Commision, 2013) and the efficiency of different power plants (US DOE, 2010).

Parameter	Natural Gas	Coal	Oil
$\varphi_{CO2,j}$ (kg/GJ)	50.29	89.41	70.49
$\varphi_{CO,j}$ (kg/GJ)	0.017	0.089	0.014
$\varphi_{NOx,j}$ (kg/GJ)	0.039	0.196	0.192
$\varphi_{SOx,j}$ (kg/GJ)	0.0004	1.113	0.482
$\varphi_{PM,j}$ (kg/GJ)	0.003	1.179	0.036
α_j (%)	50.8	24.8	2.4
η_j (%)	32.8	32.0	37.8

3.9.4 Economic analysis

The initial cost (IC), operating cost (OC), life cycle cost (LCC) and payback period (PBP) of the investigated four AC systems are calculated to determine the feasibility of the proposed system from an economic point of view. The IC is the cost required to purchase and install the required equipment for each system (e.g. fans, heating and cooling equipment, ERVs, heat exchangers, LAMEEs). The OC is the cost required to operate the installed equipment. The LCC is the summation of the IC and OC throughout the life cycle of the AC system. The present value method is used, in this study, to calculate the LCC. In this method, all the anticipated future expenses are converted to the expected present value using a present worth factor (PWF) that can be calculated using equation (3.10) (Duffie and Beckman, 2006). The payback period (PBP) is the time needed for the cumulative energy savings due to a more efficient technology to cover the additional initial cost (IC) of the technology. The PBP for the CAC-ERV, M-LDAC and M-LDAC-ERV systems are evaluated in this study with respect to the CAC system as shown in equation (3.12). It is worth mentioning that the life cycle of the system (N) is assumed to be 15 years in this chapter (Li et al., 2010). According to Rushing et al. (Rushing et al., 2011), the interest rate (i) and discount rate (d) are nearly 4% and 3%, respectively, based on the expected escalation for Florida. The maintenance and demolition costs for the four AC systems are not included, and it is assumed that there are no residual values for the four investigated AC systems (Li et al., 2010).

$$PWF = \begin{cases} \frac{1}{d - i}\left[1 - \left(\frac{1+i}{1+d}\right)^{N}\right] & \text{if } (i \neq d) \\ \frac{N}{N+1} & \text{if } (i = d) \end{cases} \quad (3.10)$$

$$LCC = IC + PWF \cdot OC_{\text{first year}} \quad (3.11)$$

$$PBP = \frac{IC_{\text{system}} - IC_{CAC}}{OC_{\text{annual,CAC}} - OC_{\text{annual,system}}} \quad (3.12)$$

The current prices of the natural gas ($17.15/GJ) and electricity ($0.12/kWhr) in Florida were obtained from the US Energy Information Administration (EIA) website (US EIA, 2013).The IC of direct expansion chiller and heat pump is assumed to be $171/kW (Rasouli et al., 2011; Mossman, 2010). The centrifugal-type HVAC supply and exhaust fans are assumed to cost $851/($m^3$/s) (Rasouli et al., 2011; Mossman, 2010). The gas-fired boiler is assumed to cost $68.2/kW (Rasouli et al., 2011; Mossman, 2010). The costs of the ERV, LAMEEs and solution-to-solution sensible heat exchanger are estimated to be $6000/($m^3$/s) (Fauchoux et al., 2007), $7062/($m^3$/s) (Rasouli et al., 2011) and $350/$m^2$ (Arga, 2011), respectively.

3.10 RESULTS AND DISCUSSION

The four AC systems investigated in this study are evaluated from technical, environmental and economic points of views, as mentioned previously. This section is organized as follows. First, a sensitivity study for the sensible, latent and total effectivenesses of the LAMEE under different design and operating conditions is presented in Section 3.10.1, when LAMEE operates as a dehumidifier and regenerator. The technical performance of the four AC systems are presented in Section 3.10.2 which is divided in four sub-Sections as follows: the indoor air conditions during the occupied hours (Section 3.10.2.1), the capacities of used equipment (Section 3.10.2.2), the primary energy consumption (Section 3.10.2.3) and the influence of the exhaust airflow rate ratio of the ERV on the CAC-ERV and M-LDAC-ERV systems (Section 3.10.2.4). The environmental and economic performance evaluations are presented in Sections 3.10.3 and 3.10.4, respectively. A brief summary for the technical, economic and environmental

performances of the investigated systems is presented in Section 3.10.5, and recommendations for increasing the energy savings of the M-LDAC system are discussed in Section 3.10.6.

3.10.1 LAMEEs performance

The influences of the six investigated design and operating parameters, previously mentioned in Section 3.9.1, on the sensible, latent and total effectivenesses of the LAMEEs are evaluated in this Section when they are studied independently. Table 3.4 shows the reference value and variation range for each of the six studied parameters.

TABLE 3.4. Reference values and variation ranges of the studied parameters.

Parameter	Reference	Minimum	Maximum	Increment
NTU	10	1	15	2
Cr^*	3	2	6	1
$T_{sol,reg,in}$ (ºC)	45	40	65	5
$T_{sol,deh,in}$ (ºC)	20	15	25	2
$T_{air,in}$ (ºC)	35	24	36	4
$RH_{air,in}$ (%RH)	50	20	80	10

3.10.1.1 Influence of thermal capacity rate ratio between solution and airflows (Cr^*) and number of heat transfer units (NTU)

It is worth mentioning that Cr^* is varied by changing the solution mass flow rate, and the air mass flow rate is kept constant in order to keep NTU constant, while NTU is varied by changing the permeable membrane's surface area, in order to keep Cr^* constant.

As shown in Figure 3.9(a), the sensible, latent and total effectivenesses of the dehumidifier significantly increase with Cr^* until $Cr^* = 4$, while a slight improvement occurs when Cr^* increases beyond 4. The effectivenesses of the regenerator increase over the entire range of Cr^*, but as with the dehumidifier is larger between 2 and 4. The observed improvements in the effectivenesses of the dehumidifier and regenerator with Cr^* are attributed to the increase in the solution's ability to hold more heat and moisture at higher solution mass flow rates. Therefore, the solution experiences lower change in its temperature and consequently its vapor pressure as it passes through the LAMEEs, which leads to the

increase in the potential for both heat and mass transfer throughout the exchanger. Thus, the trend is similar to that for sensible heat exchangers and is expected (Incropera and Dewitt, 2002).

Figure 3.9(b) shows that the sensible, latent and total effectivenesses of the dehumidifier and regenerator significantly increase when NTU increases from 1 to 7, while slight improvement occurs when NTU increases beyond 7. The achieved improvement in the effectiveness with NTU is due to the increase in the membrane surface area, which increases the rate of both heat and mass transfer between the air and solution streams. The trend of effectiveness with NTU is as expected for sensible heat exchangers (Incropera and Dewitt, 2002).

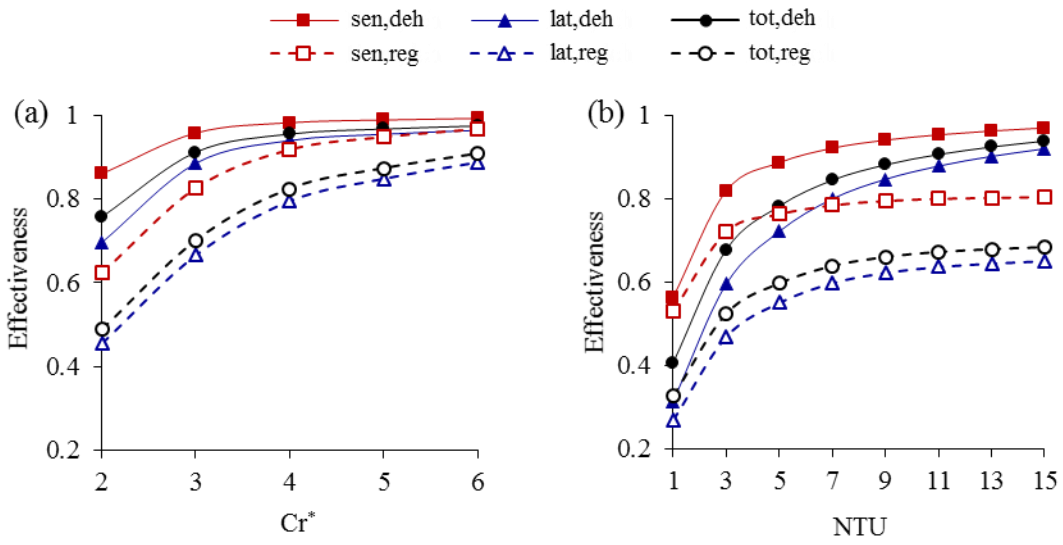

FIGURE 3.9. Influences of thermal capacity rate ratio between solution and airflows (Cr^*) and number of heat transfer units (NTU) on the effectivenesses of the (a) dehumidifier and (b) regenerator.

3.10.1.2 Influence of inlet solution temperature to dehumidifier ($T_{sol,deh,in}$) and regenerator ($T_{sol,reg,in}$)

Figure 3.10(a) shows that $T_{sol,deh,in}$ does not have a strong influence on the effectivenesses of the dehumidifier nor the regenerator. A slight change (~5%) occurs in the dehumidifier effectiveness as $T_{sol,deh,in}$ changes from 15ºC to 25ºC due to the fact that although reducing

$T_{sol,deh,in}$ results in a lower outlet air temperature and humidity ratio, the solution inlet temperature and equilibrium humidity ratio decreases in a similar manner, which leads to the simultaneous change of the denominator and numerator in equations (3.1), (3.2) and (3.3). Similar to the $T_{sol,deh,in}$, the $T_{sol,reg,in}$ does not have considerable impact on the effectivenesses of the dehumidifier as shown in Figure 3.10(b). While the sensible and latent effectivenesses of the regenerator increase and decrease, respectively, with increasing $T_{sol,reg,in}$. The observed increase in the sensible effectiveness of the regenerator with $T_{sol,reg,in}$ is due to the improvement in the potential for heat transfer at high $T_{sol,reg,in}$.

The reduction in the latent effectiveness of the regenerator when $T_{sol,reg,in}$ increases is believed to be attributed to the following. The slope of the desiccant solution concentration lines become steeper as the temperature increases, as can be seen from a psychometric chart, and thus increasing $T_{sol,reg,in}$ increases the potential for mass transfer. On the other hand, as more moisture transfer takes place, the temperature of the solution is reduced due to the release of more heat of phase change from the solution stream to the air stream, and thus the increase in actual moisture transfer increases by a lower rate than the maximum possible potential.

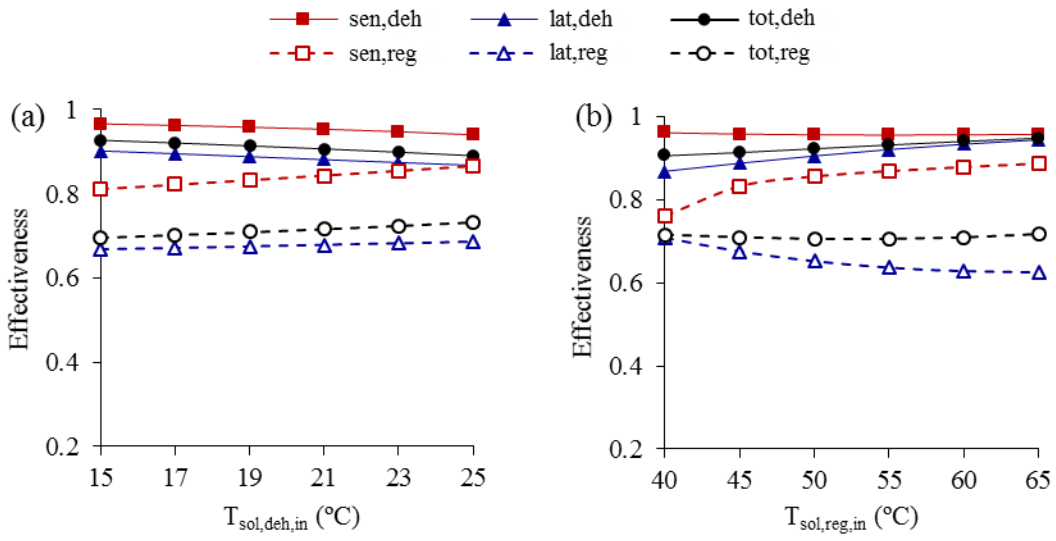

FIGURE 3.10. Influences of inlet solution temperature to the dehumidifier ($T_{sol,deh,in}$) and regenerator ($T_{sol,reg,in}$) on the effectivenesses of the (a) dehumidifier and (b) regenerator.

3.10.1.3 Influence of inlet air temperature ($T_{air,in}$) and relative humidity ($RH_{air,in}$)

The $T_{air,in}$ is found to have a more considerable impact on the effectivenesses of the regenerator than those of the dehumidifier, as shown in Figure 3.11(a). This can be related to the direction of heat and mass transfer in the LAMEEs. Also, it is observed that the effectivenesses of both the dehumidifier and regenerator improve when $T_{air,in}$ decreases. Similarly, Figure 3.11(b) shows that the effectivenesses of the regenerator are more influenced by the $RH_{air,in}$ than those of the dehumidifier, and that they improve when the $RH_{air,in}$ decreases.

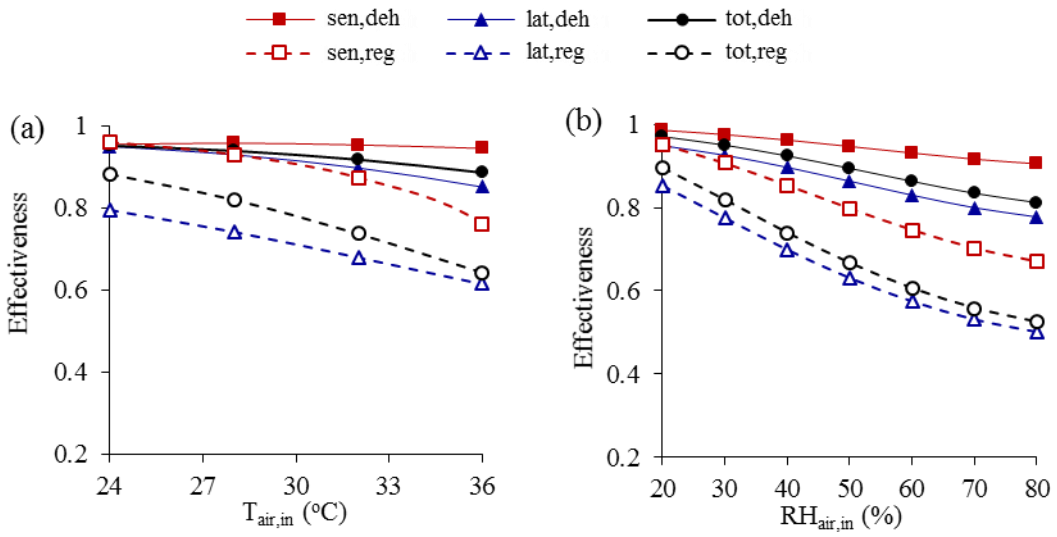

FIGURE 3.11. Influences of inlet air temperature ($T_{air,in}$) and relative humidity ($RH_{air,in}$) on the effectivenesses of the (a) dehumidifier and (b) regenerator.

In sum, the performed sensitivity study shows that the latent effectiveness of the LAMEE is always lower than its sensible effectiveness, whether the LAMEE is used as a regenerator or a dehumidifier. This is common in membrane energy exchangers due to the fact that the mass transfer resistance is usually higher than that of heat transfer (Zhang, 2011). In addition, it is found that the sensible and latent effectivenesses of the dehumidifier are always larger than those for the regenerator, which may be due to the following. The potential for mass transfer relative to heat transfer in the regenerator is larger than that for the dehumidifier (i.e. $H^*_{reg} \approx 3.5$ and $H^*_{deh} \approx 1.8$ at the reference values shown in Table 3.4), due to the steepness of the RH and concentration lines at higher operating temperatures on

a psychrometric chart. Thus, the energy of phase change that is released in the regenerator due to desorption is larger than that released in the dehumidifier due to absorption. The larger the released energy of phase change, the larger the change in air and solution temperatures and vapor pressures within the LAMEEs. Therefore, as the fluids flow through the LAMEE, the heat and mass transfer potential decreases at a faster pace in the regenerator than in the dehumidifier, which leads to the limitation of the regenerator effectiveness compared to that of the dehumidifier.

3.10.2 AC systems technical performance

3.10.2.1 Indoor air conditions

An attempt was made to obtain similar indoor air conditions for the four AC systems simulated in this study, in order to assure that the comparisons performed between the primary energy consumption, environmental emissions and economics are based on the same basis. It is worth mentioning that the focus of this study is on the AC system, while the heating system was overlooked for the sake of simplification, as previously mentioned. The indoor air temperature is maintained at 24±2ºC, 20±2ºC and <18ºC for 92%, 6% and 2% of the 3312 occupied hours, respectively, when the M-LDAC and M-LDAC-ERV systems are used, and for 86%, 11% and 3% of the 3312 occupied hours, respectively, when the CAC and CAC-ERV systems are used. Thus, the indoor air temperature is maintained within the recommended comfort zones during all over the year, except only for 2-3% of the occupied hours during the winter due to the absence of the heating system. The indoor relative humidities for the M-LDAC and M-LDAC-ERV systems are found to be maintained between 35 %RH and 65 %RH for 98% of the 3312 occupied hours. Similarly the indoor relative humidities for the CAC and CAC-ERV systems are found to be maintained between 35 %RH and 65 %RH for 96% of the 3312 occupied hours. It is clear that the indoor air temperatures and relative humidities are very close to each other for the four AC systems simulated in this study, which indicates that the comparison between the technical, environmental and economic performances of the AC systems is implemented under the same criteria.

3.10.2.2 Equipment capacities

Table 3.5 shows the capacities of the cooling and heating equipment used in each of the four AC systems. The capacity of the chilling system used for cooling the air in the CAC system is found to be 50 kW, and it is reduced to 24 kW (by 52%) when the M-LDAC system is used. This is because the entire latent load and a portion of the sensible load is covered in the M-LDAC system by the dehumidifier; thus, the chilling system used for cooling the air in the M-LDAC system is required to only cover the sensible load that is not met in the dehumidifier. However, an additional chilling system and heat pump that have capacities of 12 kW and 18 kW, respectively, are required to be installed in the M-LDAC system to cool and heat the solution prior entering the dehumidifier and regenerator, respectively.

It is found that installing an ERV has a significant impact on the capacities of the cooling and heating equipment for the systems studied. In the CAC-ERV system, the capacities of the chilling system and gas fired boiler are 28% and 14% lower than those installed in the CAC system, respectively. In the M-LDAC-ERV system, the capacities of the chilling system and heat pump used to condition the solution decrease by 25% and 22%, respectively, compared to the M-LDAC system. However, it is found that the capacity of the chilling system used to cool the air in the M-LDAC-ERV system slightly increases by 4% compared to the M-LDAC system.

TABLE 3.5. Capacities of the equipment used in the four AC systems

	CAC	M-LDAC	CAC-ERV	M-LDAC-ERV
Air chilling system (kW)	50	24	36	25
Solution chilling system (kW)	-	12	-	9
Solution heat pump (kW)	-	18	-	14
Gas fired boiler (kW)	7	-	6	-

3.10.2.3 Primary energy consumption

The primary energy consumptions for the four AC systems investigated in this study are presented in this section. Figure 3.12(a) shows the percent savings in monthly primary energy consumption for the CAC-ERV, M-LDAC and M-LDAC-ERV systems, compared

to the CAC system. Figure 3.12(b) shows the monthly primary energy consumptions for each of the four systems studied. As shown in Figure 3.12, the M-LDAC-ERV has the lowest monthly primary energy consumption throughout the year. Although the M-LDAC is found to be more energy efficient than the CAC system throughout the year, the CAC-ERV system is found to be as energy efficient as the M-LDAC system.

Figure 3.13 shows the annual primary energy consumption for all the investigated systems. The annual cooling, heating and fans primary energy consumption for the CAC system are 513 MJ/(m^2.year), 74 MJ/(m^2.year) and 124 MJ/(m^2.year), respectively, while they are 270 MJ/(m^2.year), 175 MJ/(m^2.year) and 131 MJ/(m^2.year), respectively, for the M-LDAC system. The M-LDAC system has a 47% lower cooling primary energy consumption than the CAC system, while the heating and fans primary energy consumption are 136% and 6% higher, respectively. The CAC-ERV reduces the cooling and heating primary energy consumption by 23% and 20%, respectively, compared to the CAC system. Also, the M-LDAC-ERV system reduces the cooling and heating primary energy consumption by 13% and 34%, respectively, compared to the M-LDAC system.

The total annual primary energy consumption for the CAC, M-LDAC, CAC-ERV and M-LDAC-ERV systems are 711 MJ/(m^2.year), 576 MJ/(m^2.year), 578 MJ/(m^2.year) and 485 MJ/(m^2.year), respectively. The percent energy savings in the annual primary energy consumption that the M-LDAC, CAC-ERV and M-LDAC-ERV systems achieve compared to the CAC system are 19%, 19% and 32%, respectively. It can be concluded from these results, that the CAC-ERV is as energy efficient as the M-LDAC system. Therefore, it is not recommended to use the M-LDAC system without an ERV, because the annual primary energy savings that would be achieved using this system can be achieved using the CAC-ERV system, which has lower initial costs. The installation of an ERV in the M-LDAC system is strongly recommended, because this significantly decreases the capacities of the solution cooling and heating systems, and increases the percent savings in the annual primary energy consumption.

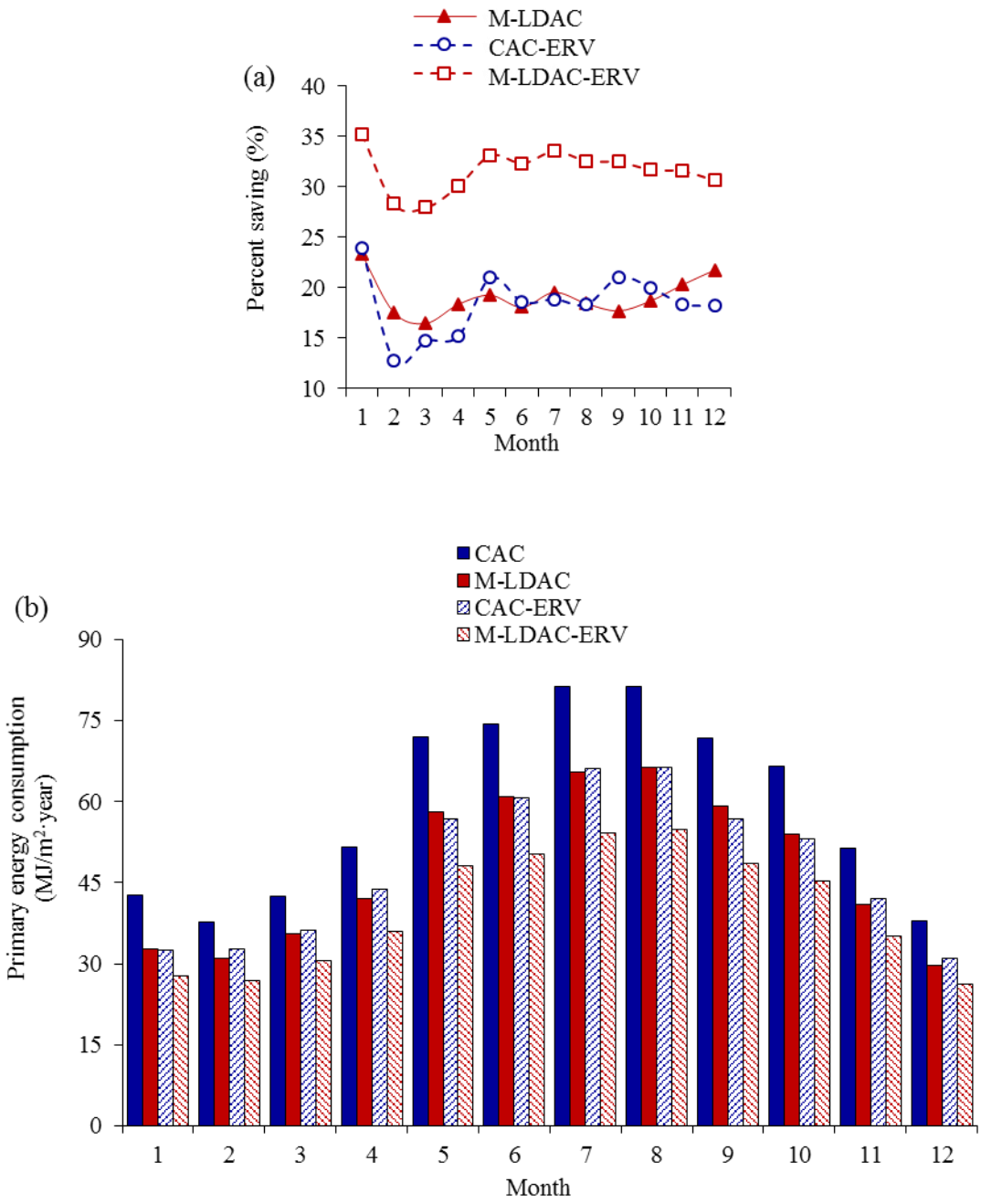

FIGURE 3.12. The monthly (a) percent saving in primary energy consumption and (b) primary energy consumption.

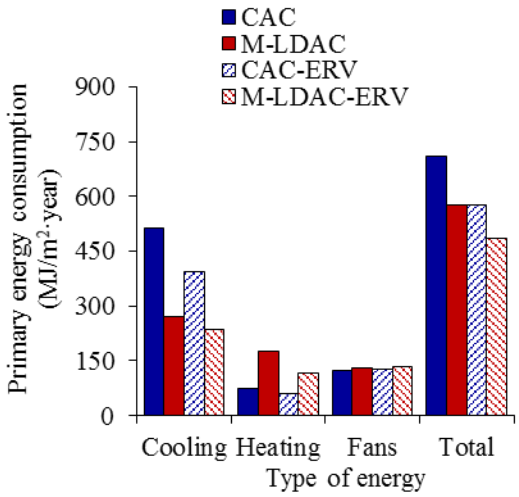

FIGURE 3.13. Annual primary energy consumption of the four AC systems.

3.10.2.4 Influence of exhaust airflow rate ratio ($R_{exhaust}$)

As mentioned previously, in the two systems that include an ERV (i.e. CAC-ERV and M-LDAC-ERV), the hot-humid outdoor air is cooled and dehumidified in the ERV using the exhaust air leaving the building. Thus, the flow rate of the exhaust air leaving the building has significant influence on the amount of energy that can be recovered in the ERV. The lower the exhaust airflow rate, the lower the heat and moisture that will be transferred from the hot-humid outdoor air to the exhaust air leaving the building as shown in equations (3.7) and (3.8), respectively. Consequently, the energy savings that can be achieved using the ERV decrease as the exhaust airflow rate decreases. It is worth mentioning that the two systems that do not include an ERV (i.e. CAC and M-LDAC) are not affected by the exhaust air flow rate, and therefore are not included in this section.

The percent increase in the annual primary energy consumption of the CAC-ERV and M-LDAC-ERV systems when they operate under unbalanced airflow rates condition ($R_{exhaust} < 1$), with respect to the balanced airflow rates condition ($R_{exhaust} = 1$) for each of them, are shown in Figure 3.14. For the CAC-ERV system, it is found that the annual primary energy consumption increases by nearly 3%, 5%, 8% and 11% when $R_{exhaust}$ is 0.9, 0.8, 0.7 and 0.6, respectively, compared to the case when $R_{exhaust} = 1$. The annual primary energy consumption for the M-LDAC-ERV system increases by nearly 2%, 3%, 5% and 6% when $R_{exhaust}$ is 0.9, 0.8, 0.7 and 0.6, respectively, compared to the case when

$R_{exhaust}$ = 1. It can be concluded that $R_{exhaust}$ has a significant influence on the annual primary energy consumption when ERVs are installed in hot and humid climates. In addition, it is found that $R_{exhaust}$ has larger influence on the CAC-ERV system than the M-LDAC-ERV system.

It is strongly recommended to seal the building during construction to reduce infiltration. Otherwise, the AC system has to be operated under highly unbalanced airflow rates (low $R_{exhaust}$) to avoid the growth of mold and bacteria that may result from the infiltration of hot and humid air through the envelope of the building.

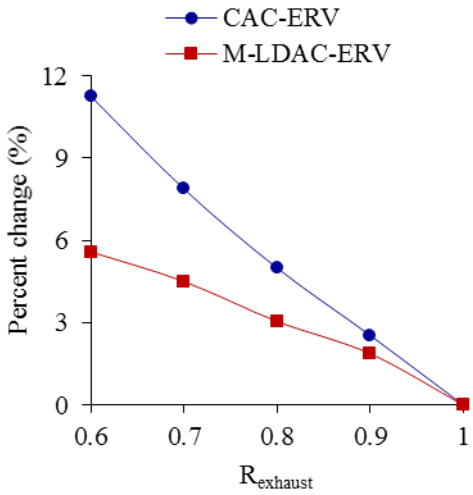

FIGURE 3.14. Influence of exhaust airflow rate ratio ($R_{exhaust}$) on annual primary energy consumption of the CAC-ERV and M-LDAC-ERV systems.

3.10.3 Environmental performance

The environmental performances of the four AC systems are evaluated in this section by calculating the following annual environmental emissions: CO_2, CO, NO_x, SO_x and PM. The environmental emissions resulted from an AC system mainly depend on the amount and type of the energy used to operate the system. Therefore, the annual environmental emissions from the four AC systems are found to follow, to a large extent, the trends of the annual primary energy consumption presented in the previous Section. The annual environmental emissions for each of the four AC systems are shown in Table 3.6.

TABLE 3.6. Annual environmental emissions for the four AC systems in Kg/year.

	CAC	M-LDAC	CAC-ERV	M-LDAC-ERV
F_{CO_2}	18,138	14,710	14,703	12,436
F_{CO}	11	9	9	8
F_{NO_x}	26	22	21	18
F_{SO_x}	96	87	78	73
F_{PM}	99	89	80	75

The percent reduction in the annual environmental emissions that the M-LDAC, CAC-ERV, M-LDAC-ERV systems achieve compared to the CAC system are shown in Figure 3.15. It is clear that the M-LDAC-ERV system achieves the largest percent reduction in the annual environmental emissions followed by the CAC-ERV system and then the M-LDAC system. Although the total annual primary energy consumptions of the CAC-ERV and M-LDAC systems are almost the same (see Figure 3.13), the annual environmental emissions of the M-LDAC system are found to be larger than those of the CAC-ERV system. This is because natural gas covers a portion of the energy requirements of the CAC-ERV system, while the M-LDAC system is totally operated using electricity.

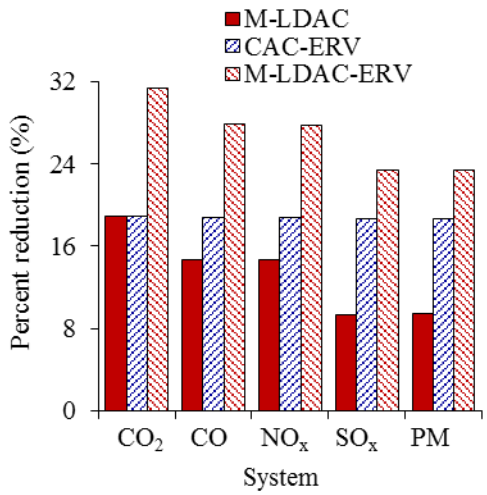

FIGURE 3.15. The percent reduction in annual environmental emissions that the M-LDAC, CAC-ERV and M-LDAC-ERV systems achieve compared to the CAC system.

3.10.4 Economic performance

In this section, the economics (i.e. IC, OC, LCC, and PBP) of the four AC systems are presented and discussed, in order to determine the economic feasibility of the proposed system. Table 3.7 shows the IC, OC, LCC, and PBP for each of the four AC systems investigated. Compared to the CAC system, the CAC-ERV decreases both the IC_{total} (from \$13,688 to \$12,538) and $OC_{first\ year}$ (from \$4,201/year to \$3,406/year) by 8% and 19%, respectively, which results in a 17% reduction in the LCC (from \$79,224 to \$65,673). Compared to the M-LDAC, the M-LDAC-ERV increases the IC_{total} (from \$19,638 to \$20,104) by 2% and decreases the $OC_{first\ year}$ (from \$3,208/year to \$2,701/year) by 16%. Thus, the LCC of the M-LDAC-ERV (\$62,240) system is 11% lower than that of the M-LDAC system (\$69,682). Since the CAC-ERV has lower IC and OC compared to the CAC system, its PBP (-1.4 years) is immediate. On the other hand, although both the M-LDAC and M-LDAC-ERV systems reduce the OC compared to the CAC system, they have higher IC. Thus, there will be a PBP for the M-LDAC and M-LDAC-ERV systems of 6 and 4.3 years, respectively.

TABLE 3.7. Initial costs (IC), operating costs (OC), life cycle cost (LCC), and payback period (PBP) for the four AC systems.

	CAC	**M-LDAC**	**CAC-ERV**	**M-LDAC-ERV**
Electiricty (kWhr/year)	29,824	26,960	24,284	22,696
Natural gas (GJ/year)	38	-	30	-
$OC_{electricity}$ (\$/year)	3,549	3,208	2,890	2,701
$OC_{natural\ gas}$ (\$/year)	652	-	516	-
$IC_{air\ chilling\ system}$ (\$)	9,670	4,642	6,962	4,835
$IC_{solution\ chilling\ system}$ (\$)	-	2,321	-	1,741
$IC_{solution\ heat\ pump}$ (\$)	-	3,481	-	2,708
$IC_{gas\ fired\ boiler}$ (\$)	478	-	410	-
IC_{fans} (\$)	3,540	4,000	3,540	4,000
$IC_{auxiliary\ heat\ exchangers}$ (\$)	-	1,750	-	1,750
IC_{ERV} (\$)	-	-	1,626	1,626
IC_{LAMEEs} (\$)	-	3,444	-	3,444
$OC_{first\ year}$ (\$/year)	4,201	3,208	3,406	2,701
IC_{total} (\$)	13,688	19,638	12,538	20,104
PBP (year)	-	6	-1.4	4.3
LCC (\$)	79,224	69,682	65,673	62,240

It can be concluded that installing an ERV improves the economics of both the CAC and M-LDAC systems, and that it has larger impact on the economics of the CAC system than the M-LDAC system. Therefore, it is strongly recommended to install an ERV in hot-humid climates whether a CAC or a M-LDAC system is used. The percent change in the IC_{total}, $OC_{first\ year}$ and LCC of the M-LDAC, CAC-ERV and M-LDAC-ERV systems with respect to the CAC system are presented in Figure 3.16. The percent reductions in the LCC of the M-LDAC, CAC-ERV and M-LDAC-ERV systems are 12%, 17% and 21%, respectively, compared to the CAC system. It is found that the CAC-ERV system is more economical than the M-LDAC system. While, it is found that the M-LDAC-ERV system has the lowest LCC among the investigated AC systems, and is 21% lower than the LCC of the CAC system.

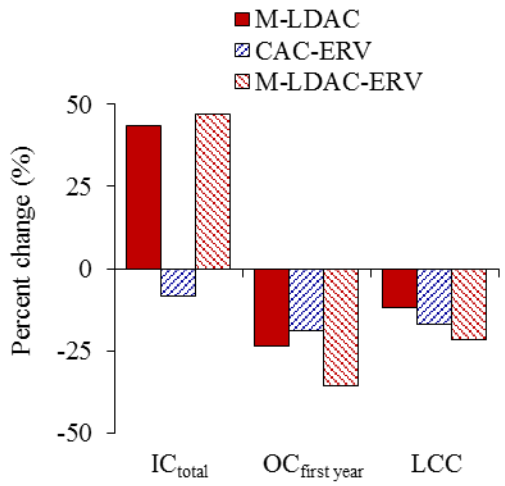

FIGURE 3.16. Percent change in annual IC_{total}, total $OC_{first\ year}$ and LCC of the M-LDAC, CAC-ERV and M-LDAC-ERV systems compared to the CAC system.

3.10.5 Summary

3.10.5.1 LAMEE effectivenesses

The performed sensitivity study on the sensible, latent and total effectivenesses shows that the number of heat transfer units (NTU), thermal capacity ratio between solution and air (Cr^*), air inlet temperature ($T_{air,in}$) and air inlet relative humidity ($RH_{air,in}$) have considerable influences on the effectivenesses of LAMEEs used in an LDAC system. The effectivenesses increase with NTU and Cr^*, and decrease with $T_{air,in}$ and $RH_{air,in}$. The

solution inlet temperatures to the dehumidifier ($T_{sol,deh,in}$) and the regenerator ($T_{sol,reg,in}$) have slight influences on the effectivenesses of the LAMEEs.

3.10.5.2 Annual primary energy consumption

The annual primary energy consumption decreases by 19% when the proposed M-LDAC system is used, compared to the CAC system. The percent savings in the annual primary energy consumption increases from 19% to 32% when an ERV, which operates under balanced airflow rates condition ($R_{exhaust} = 1$), is installed in the M-LDAC system (i.e. M-LDAC-ERV system). Also, it is found that installing an ERV that operates at $R_{exhaust} = 1$ in the CAC system (i.e. CAC-ERV system) decreases the annual primary energy consumption by 19%, compared to the CAC system. Therefore, the proposed M-LDAC system is not recommended to be installed without an ERV.

3.10.5.3 Exhaust airflow rate ratio ($R_{exhaust}$) of ERV

The energy consumption of the systems with an ERV (CAC-ERV and M-LDAC-ERV) increase considerably as the exhaust airflow rate ratio ($R_{exhaust}$) decreases. For example, the annual primary energy consumptions of the CAC-ERV and M-LDAC-ERV systems increase by 11% and 6%, respectively, when $R_{exhaust}$ decreases from 1 to 0.6. It is concluded that although $R_{exhaust}$ has large influence on both the CAC-ERV and M-LDAC-ERV systems, it has a more significant influence on the CAC-ERV system.

3.10.5.4 CO_2 emissions

The CO_2 annual emissions decrease by 19% when the proposed M-LDAC system is used, compared to the CAC system, and the percent reduction goes up to 31% when an ERV, which operates at $R_{exhaust} = 1$, is installed in the M-LDAC system.

3.10.5.5 Life cycle costs (LCC)

The LCC of the M-LDAC is found to be 12% percent lower than the LCC of the CAC system. When an ERV, which operates at $R_{exhaust} = 1$, is installed in the CAC system, the LCC is reduced by 17%. While it is found that when an ERV, which operates at $R_{exhaust}=1$,

is installed in the M-LDAC system, the LCC reduces by 21% compared to a CAC system without an ERV.

3.10.6 Keys for improvement

3.10.6.1 Type of liquid desiccant heating system

The type of liquid desiccant heating system plays a crucial role in the thermal, environmental and economic performances of any LDAC system. There are several ways to provide the thermal energy required for dilute desiccant regeneration such as: (i) natural gas boiler, (ii) electrical heat pump, (iii) solar thermal system with natural gas boiler backup, and (iv) solar thermal system with electrical heat pump backup. The thermal, economic and environmental performances of the M-LDAC system (with/without ERV) with each of the four aforementioned heating systems are evaluated in Chapter 4.

3.10.6.2 Simultaneous solution heating and cooling

More energy savings can be achieved using a heat pump to simultaneously cool and heat the concentrated and dilute desiccant solutions, respectively. This will reduce/eliminate the thermal energy required for the regeneration of the dilute desiccant solution, and consequently increase the energy savings achieved using the M-LDAC system. If the solution is to be simultaneously heated and cooled using the same heat pump, the loads of the four major components (i.e. dehumidifier, regenerator, condenser and evaporator) should be carefully matched (Niu et al., 2012). In addition, an efficient control system should be adopted. The annual performance of a heat-pump M-LDAC system is investigated in Chapter 5, the fundamentals of capacity matching in heat-pump LDAC systems are defined in Chapter 6, and a novel strategy for optimal-control of heat-pump LDAC systems is presented in Chapter 7.

3.11 CONCLUSION

In this chapter, the TRNSYS building energy simulation program is used to investigate a membrane liquid desiccant air conditioning (M-LDAC) system that has liquid-to-air membrane energy exchangers (LAMEEs) as the dehumidifier and regenerator. The influence of six operating and design parameters are investigated on the sensible, latent and

total effectivenesses of the LAMEEs, and it is found that the number of heat transfer units (NTU), thermal capacity ratio between solution and air (Cr^*) and air inlet temperature ($T_{air,in}$) and relative humidity ($RH_{air,in}$) are the most influential parameters on the effectivenesses of the LAMEEs. The annual primary energy consumption of the four different systems operating in Miami, Florida (ordered from lowest to higher) are: (1) M-LDAC-ERV system (485 MJ/(m^2.year)), (2) M-LDAC system (576 MJ/(m^2.year)), (3)CAC-ERV system (578 MJ/(m^2.year)), (4) CAC system (711 MJ/(m^2.year)). The initial costs (IC) of the M-LDAC ($19,638) and M-LDAC-ERV ($20,104) systems are higher than the CAC ($13,688) and CAC-ERV ($12,538) systems. The life cycle cost (LCC) of the CAC-ERV system ($65,673) is lower than the M-LDAC system ($69,682), while the M-LDAC-ERV system is found to be the most economic system with a LCC of $62,240. In addition, the CO_2 annual emissions of the CAC-ERV (14.7 ton/year), M-LDAC (14.7 ton/year) and M-LDAC-ERV (12.4 ton/year) systems are lower than the CAC system (18.1 ton/year).

In conclusion, the simulations results in this chapter have shown that the M-LDAC system is a promising system from technical, environmental and economic points of views. The results show that the performance of M-LDAC systems can be improved by adding an energy recovery ventilator, a solar thermal system or a heat pump to M-LDAC system. It is recommended that more research be conducted on LDAC systems that use novel conditioners, which prevent the carryover of desiccant droplets by air streams, to enhance the application of these energy efficient LDAC systems in residential and commercial buildings.

CHAPTER 4

ANNUAL ENERGY MODELLING AND ECONOMICS OF A SOLAR MEMBRANE LDAC SYSTEM

4.1 OVERVIEW

The energy performance of the basic membrane LDAC system studied in Chapter 3 showed that considerable energy savings can be achieved compared to a conventional air conditioning system. In addition, it was found that the solution heating energy requirements represent a considerable portion of the total energy requirements. Thus, the feasibility of integrating a solar thermal system with the membrane LDAC is investigated in this chapter. Several solar thermal systems are modelled when they are installed in membrane LDAC systems. Each of the solar systems studied was optimized based on the life cycle costs of the whole solar LDAC system, and guidelines for the sizing and design of solar LDAC systems are presented.

The manuscript used in this Chapter is published in Solar Energy. A Post-Doctoral Fellow "Dr. Gaoming Ge" has contributed to this manuscript by proof reading it. As the lead author of the paper, I conducted the research, analyzed the results, wrote the manuscript, incorporated co-authors comments and addressed the reviewers' comments.

Thermo-Economic Performance of a Solar Membrane Liquid Desiccant Air Conditioning System

(Solar Energy, 2014, Volume 102)

Ahmed H. Abdel-Salam, Gaoming Ge, Carey J. Simonson

4.2 ABSTRACT

A solar membrane liquid desiccant air conditioning (S-M-LDAC) system is proposed and investigated in this study. Liquid-to-air membrane energy exchangers (LAMEEs) are used for humid air dehumidification and dilute desiccant solution regeneration in the S-M-LDAC system. This eliminates the problem of desiccant droplets carry over in supply and exhaust air streams, which limits the wide use of conventional direct-contact liquid desiccant air conditioning systems in commercial/residential applications. Eight systems configurations, which mainly differ in the heating and air systems, are simulated using the TRNSYS building energy simulation software. Four heating systems are investigated as follows: (i) natural gas boiler, (ii) electrical heat pump, (iii) solar thermal system (STS) with natural gas boiler backup, and (iv) STS with electrical heat pump backup. Two air systems are studied - one with and one without an energy recovery ventilator. Parametric studies are performed to study the influences of the collector area and storage volume of hot water tank relative to collector area on the annual solar fraction, annual collector efficiency and life cycle cost. The size of the STS is optimized to give the lowest life cycle cost, and then the economic and environmental performances are evaluated for the systems studied by calculating the initial cost, annual operating cost, life cycle cost, payback period and annual CO_2 emissions. Results show that using a STS to cover the thermal energy required to regenerate the dilute desiccant solution significantly improves the economic and environmental performances of the systems studied, with more significant reductions when a natural gas boiler is used as the backup heating system and there is no energy recovery ventilator.

4.3 INTRODUCTION

Solar thermal cooling systems are promising technologies compared to conventional cooling systems, especially in applications that are located in hot and humid climates and

require efficient temperature and humidity control. The use of solar thermal cooling systems reduces the burning of fossil fuels (Kim et al., 2012) and the emission of greenhouse gases (Mendes et al., 1998). In general, solar thermal cooling systems are classified into open cycles, closed cycles and thermo-mechanical systems, where open cycles are characterized by their ability to be operated using low-grade heat sources (Hwang et al., 2008). Open cycles are classified into solid desiccant air conditioning (SDAC) and liquid desiccant air conditioning (LDAC) systems, where LDAC systems are characterized by several advantages, compared to SDAC systems, as follows. (i) Solid desiccants release heat to process air during dehumidification process, while liquid desiccants can simultaneously cool and dehumidify the process air. (ii) Liquid desiccants have greater capacities to hold moisture than solid desiccants (ASHRAE, 2009). (iii) LDAC systems require low regenerating temperatures in the range of 40-70ºC, while SDAC systems require high regenerating temperatures in the range of 60-115ºC (Katejanekarn and Kumar, 2008); consequently, LDAC systems can be efficiently operated using low grade heat sources such as flat-plate solar collectors (Gommed et al., 2004). (iv) LDAC systems can be coupled with concentrated liquid desiccant storage systems, which allow more flexible timing of the regeneration (Keßling et al., 1998). (v) The air conditioning and solution regeneration functions can be physically separated in LDAC systems because liquid desiccants can be conveniently piped between exchangers located in different places (Sullivan et al., 2011).

The core components of any LDAC system are the dehumidifier, which is used to remove moisture from humid air, and the regenerator, which is used to regenerate dilute desiccant solution. Several dehumidifiers and regenerators designs were proposed in the last decades (Dai and Zhang, 2004; Gommed and Grossman, 2007; Katejanekarn et al., 2009; Alosaimy and Hamed, 2011; Davies, 2005; Lychnos and Davies, 2012; Li and Yang, 2008; Audah et al. 2011; Alizadeh, 2008; Li and Zhang, 2009; Cheng and Zhang, 2013a, 2013b); the widely used among available designs are the packed beds, parallel-plates and spray chambers (Mesquita 2007).

The relative coincidence between peak solar radiation and peak cooling and latent heat loads makes solar energy a suitable choice for regeneration of the dilute desiccant solution in LDAC systems (Andrusiak et al., 2010). Löf (1955) initiated one of the earliest efforts in the investigation of solar LDAC systems. Since the 1950's, several methods have been in use to harness solar energy in the regeneration of the dilute desiccant solution. One method is the solar collector/regenerator (C/R), where the dilute desiccant solution is brought into direct contact with air and directly regenerated in a solar collector (Katejanekarn et al., 2009; Alosaimy and Hamed, 2011; Davies, 2005; Lychnos and Davies, 2012; Yutong and Hongxing, 2008). In other methods, the dilute desiccant solution is either heated using hot water collected from solar collectors (Audah et al., 2011; Alizadeh, 2008; Gommed and Grossman, 2007; Crofoot and Harrison, 2012; Andrusiak et al., 2010), or heated directly in a solar collector (Li and Zhang, 2009; Cheng et al., 2013) and then regenerated in a separate regenerator.

In all the aforementioned dehumidifier/regenerator designs, air and solution streams are in direct contact. This may lead to the carryover of desiccant droplets in supply and exhaust air streams, which may lead to the degradation of indoor air quality in conditioned space and the corrosion of downstream ducting and equipment. The desiccant droplets carryover in air streams can be eliminated by replacing direct-contact liquid desiccant devices with liquid-to-air membrane energy exchangers (LAMEEs), as previously discussed in Chapters 2 and 3.

The main objective of the current study is to investigate the feasibility of a solar membrane LDAC (S-M-LDAC) system, which uses flat-plate LAMEEs as the dehumidifier and regenerator. To this aim, four desiccant solution heating systems configurations are studied as follows: natural gas (NG) boiler, electrical heat pump (HP), solar thermal system (STS) with a NG boiler backup, and STS with an electrical HP backup. Parametric studies are performed in order to evaluate the annual solar fraction (SF_{annual}), annual collector efficiency ($\eta_{c,annual}$) and life cycle cost (LCC), which are used to optimize the collector area (A_c) and the volume of hot water storage tank (V_t). The annual thermal, economic and environmental performances for each of the systems studied are evaluated with/without an

energy recovery ventilator (ERV). To meet the objectives of this study, totally eight systems configurations are modeled in a very hot and humid climate (Miami, Florida) using the TRNSYS building energy simulation software.

4.4 DESCRIPTION OF HVAC SYSTEMS

In total, eight systems configurations are investigated in this study in order to evaluate the feasibility of the proposed solar membrane liquid desiccant air conditioning (S-M-LDAC) system. As shown in Figure 4.1, the same membrane liquid desiccant air conditioning system (M-LDAC) is used in the eight systems configurations, while the differences between the different configurations are in the liquid desiccant heating system and the energy recovery ventilator (ERV). Four liquid desiccant heating systems are studied: natural gas (NG) boiler, electrical heat pump (HP), solar thermal system (STS) with NG boiler backup, and STS system with electrical HP backup. These 4 systems are studied with and without an ERV. Table 4.1 shows the acronyms, and type of heating and air systems for each of the eight systems' configurations investigated in this study.

4.4.1 Air-side

As shown in Figure 4.1, when an ERV is installed in an all-air HVAC system, the outdoor hot and humid air is preconditioned using the air leaving the conditioned space. It is assumed that the ERV is operated under balanced supply and exhaust air flow rates, and with sensible and latent effectivenesses of 75%. The entire latent load and a portion of the sensible load of the building (including space, ventilation and infiltration air loads) are covered by the dehumidifier, which dehumidifies the ventilation air leaving the ERV, or the ventilation air from outdoors if no ERV is used. A part of the return air from the conditioned space passes through the sensible-only cooling coil, which covers sensible load not met by the dehumidifier. Then, the cooled return air leaving the cooling coil is mixed with the dry ventilation air leaving the dehumidifier before being supplied to the conditioned space. The sensible-only cooling coil operates at a higher evaporating temperature, and consequently at higher COP, than wet cooling coils used in conventional air-conditioning (CAC) systems. Thus, it is assumed that the COP of the chilling plant for the sensible-only cooling coil is 5.5, which is higher than the COP of 4 that is commonly

used for wet cooling coils in CAC systems (Niu et al., 2010). The efficiencies of the supply and exhaust fans are assumed to be 60%. The pressure drops across the supply and exhaust sides are assumed to be 1250 Pa and 500 Pa, respectively, and the ERV is assumed to cause additional 200 Pa pressure drop (Fauchoux et al., 2007).

4.4.2 Liquid desiccant air conditioning system

The cool and concentrated desiccant solution, which is used to meet the entire latent load of the conditioned space, leaves the dehumidifier both warm and dilute. The dilute desiccant solution has to be regenerated in order to be reused to dehumidify the hot and humid ventilation air. The desiccant solution regeneration is performed by increasing its temperature to a level that makes its vapor pressure higher than that of the regeneration air. Thus, the desiccant solution is preheated in the solution-to-solution sensible heat exchanger before being heated to a specific set point temperature in the heating coil (45ºC when ERV is used and 50ºC when ERV is not used). The hot and dilute desiccant solution leaving the heating coil enters the regenerator, where it is concentrated using the regeneration air (i.e. outdoor air in this study). Although the desiccant solution coming out from the regenerator is concentrated, its temperature still high. The concentrated desiccant solution has to be cooled before entering the dehumidifier, in order to decrease its vapor pressure and be able to absorb moisture from the humid ventilation air stream. Therefore, it is precooled in the solution-to-solution sensible heat exchanger and then cooled by a dry cooling coil to a specific set point (23ºC when ERV is used and 20ºC when ERV is not used). It is assumed that the chilling plant for the dry cooling coil used to cool desiccant solution operates at a COP of 7 (Niu et al., 2010), due to the high evaporating temperature in the chilling plant.

4.4.3 Liquid desiccant heating systems

As mentioned previously, several types of heating systems are investigated in this study. It is assumed that the efficiency of the NG boiler is 90%, and the COP of the electrical HP is 5 (Niu et al., 2010). The performance of flat plate solar collector is evaluated in this study based on the steady-state quadratic efficiency curve collector model as shown in equation (4.1). The optical efficiency parameter of the collector (a_0) is 0.78, while the thermal losses parameters (a_1 and a_2) are 3.87 W/(m^2·K) and 0.012 W/(m^2·K), respectively

(La et al., 2011). The water mass flow rate in the collector is kept at 40 kg/(hr·m^2), which lies in the practical range (36-72 kg/(hr·m^2)) recommended by ASHRAE (Kim et al., 2012). The incidence angle modifier is set constant at 0.1. The collector faces south, and its slope angle is 25.7^o N (latitude of Miami), which is recommended to maximize solar gain when the STS is operated year round (Elminir et al., 2006). The thermal storage tank is vertical with an aspect ratio of 4:1, and it includes 15 fully mixed nodes to account for the thermal stratification within the storage tank. The overall thermal loss coefficient of the walls is assumed to be 0.7 W/(m^2·K), which lies in the range (0.5-0.9) recommended by Syed et al. (2005).

$$\eta_c = a_0 - a_1 \frac{\Delta T}{I_T} - a_2 \frac{(\Delta T)^2}{I_T} \tag{4.1}$$

where, I_T is the total solar radiation on a tilted surface (W/m^2).

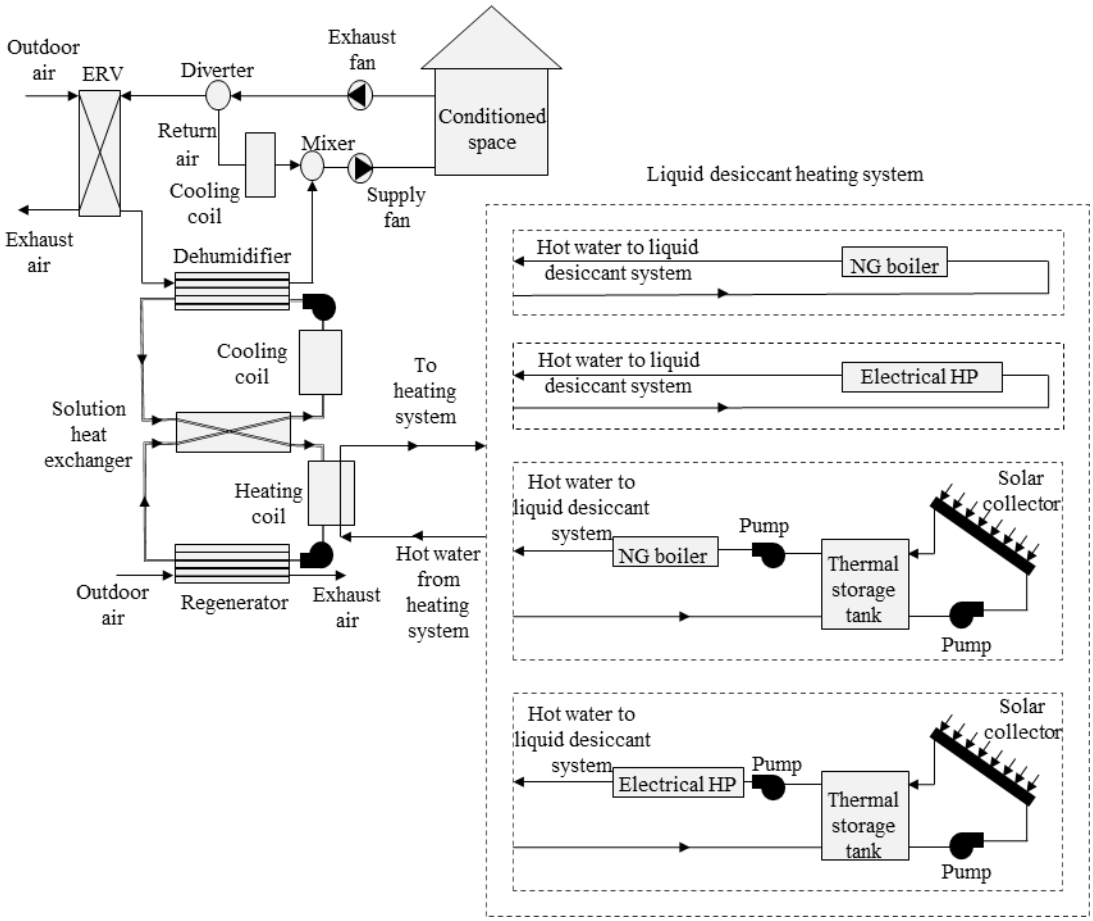

FIGURE 4.1. Schematic diagram for the M-LDAC systems studied.

TABLE 4.1. Acronyms used for the eight membrane LDAC systems studied in this chapter based on the type of air and heating system installed in each of them.

Acronym	Membrane LDAC system specification				
	Heating system			Air system	
	NG boiler	Electrical HP	STS	ERV	Without ERV
M-LDAC-NG	▪				▪
M-LDAC-ERV-NG	▪			▪	
S-M-LDAC-NG	▪		▪		▪
S-M-LDAC-ERV-NG	▪		▪	▪	
M-LDAC-HP		▪			▪
M-LDAC-ERV-HP		▪		▪	
S-M-LDAC-HP		▪	▪		▪
S-M-LDAC-ERV-HP		▪	▪	▪	

4.4.4 Conventional air conditioning systems

In addition to the eight M-LDAC systems investigated in this study, a conventional air conditioning (CAC) system and a CAC system with ERV (CAC-ERV) are included, in order to compare the performances of the eight systems configurations studied against them. In the CAC and CAC-ERV systems, since the direct supply of the overcooled air stream leaving the cooling coil to the conditioned space may cause thermal discomfort for the occupants (Qi et al., 2012; Abdel-Salam et al., 2013d), a NG boiler is installed in order to reheat the overcooled air stream before being delivered to the conditioned space. More details about the CAC and CAC-ERV systems are presented in Chapter 3.

4.5 WEATHER AND BUILDING DESCRIPTIONS

The proposed systems are simulated in a small one-story office building located in Miami, Florida (very hot and humid). Detailed information about the climatic conditions and building specifications is presented in Chapter 3.

4.6 MODELING APPROACH

The systems configurations investigated in this study are simulated using the TRNSYS building energy simulation software (TRNSYS, 2010a). As previously discussed in Chapters 2 and 3, a new TRNSYS component was developed for the LAMEE and the

standard TRNSYS and TESS Types are used to model the other equipment required to simulate the systems investigated (e.g. cooling and heating coils, fans, pumps, solar collectors, storage tank, ERV). Figure 4.2 shows the data flow between the TRNSYS and TESS Types which are used to simulate the S-M-LDAC-ERV system. Similar TRNSYS models were developed to simulate the other systems configurations investigated in this study.

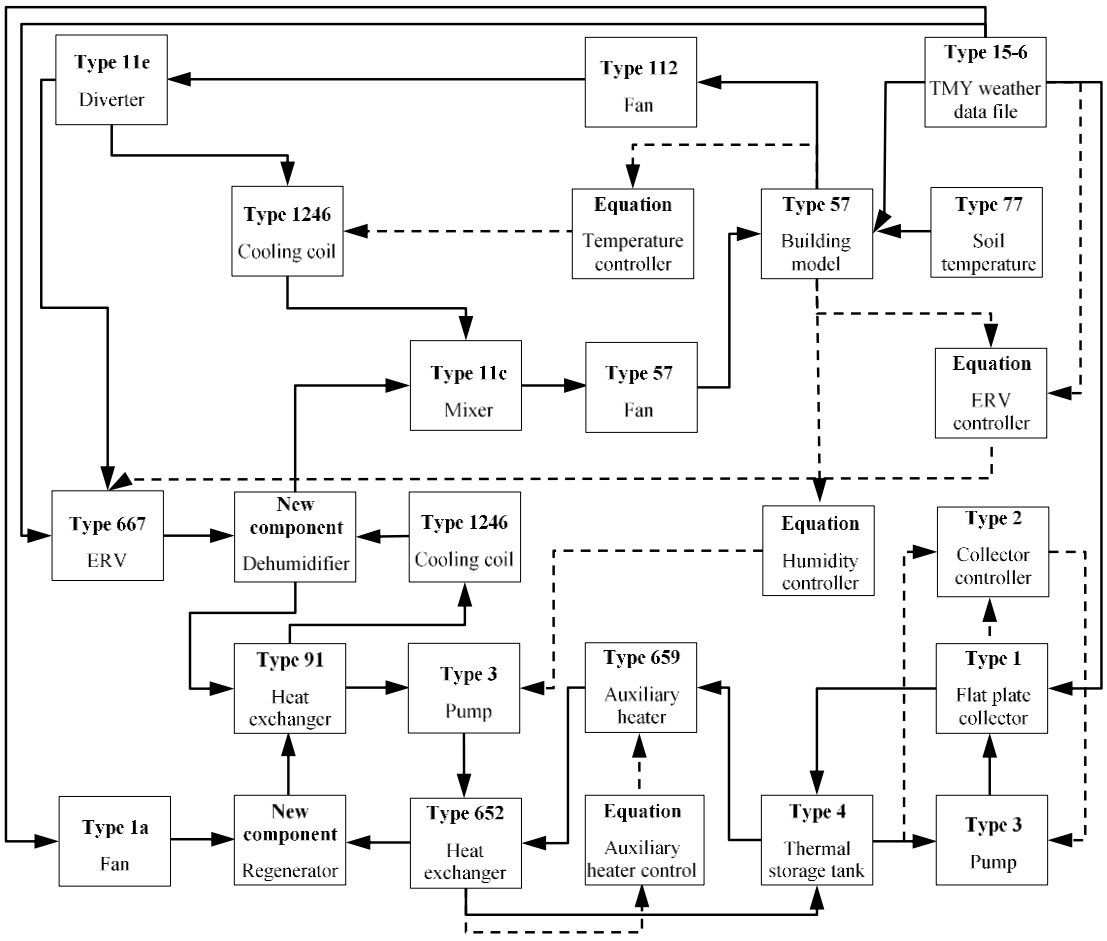

FIGURE 4.2. Block diagram of the TRNSYS model developed for the S-M-LDAC-ERV system.

4.7 PERFORMANCE INDICES

The performance indices that are used to evaluate the thermal, economic and environmental performances of the systems studied are presented in this Section. The thermal performance of the solar thermal system (STS) is evaluated in terms of the annual solar fraction (SF_{annual}) and annual collector efficiency ($\eta_{c,annual}$). The life cycle cost (LCC) and payback period (PBP) are used to evaluate the economic performance, and the amount of annual CO_2 emissions (F_{CO2}) is used as an indication to the environmental impact.

4.7.1 Annual solar fraction

The annual solar fraction (SF_{annual}) is defined as the ratio between the annual thermal energy transferred from the storage tank to desiccant solution and the total annual thermal energy required for desiccant solution regeneration.

$$SF_{annual} = \frac{q_{thermal,solution,solar}}{q_{thermal,solution,solar}} \tag{4.2}$$

4.7.2 Annual collector efficiency

The annual collector efficiency ($\eta_{c,annual}$) is defined as the ratio between the useful thermal energy captured by solar collectors and the total incident solar radiation.

$$\eta_{c,annual} = \frac{q_{c,useful}}{A_c \sum I_T} \tag{4.3}$$

4.7.3 Economic and environmental performance indices

Detailed information about the life cycle cost, payback period and annual CO_2 emissions is presented in Chapter 3. The economic parameters (i.e. prices of natural gas and electricity in Florida, initial costs of installed equipment, life cycle of system, expected interest and discount rates in Florida) that are used to calculate the PWF and LCC are given in Table 4.2.

TABLE 4.2. The economic parameters used to evaluate the LCC of systems studied.

Component	Value	Unit
Life cycle of system[1,2]	15	years
Interest rate[3]	4	%
Discount rate[3]	3	%
Energy costs		
• Natural gas price[4]	17.15	$/GJ
• Electricity price[4]	0.12	$/kWhr
Initial costs		
• Solar collector[5]	110	$/m^2
• Electrical heat pump[1,6]	171	$/kW
• Centrifugal-type HVAC fan[1,6]	851	$/(m^3/s)
• Natural gas boiler[1,6]	68.2	$/kW
• Energy recovery ventilator[2]	6000	$/(m^3/s)
• LAMEE[1]	7062	$/(m^3/s)
• Solution heat exchanger[7]	350	$/m^2
• Storage tank[8]	811.2	$/m^3
• Pumps[9]	881*Wp$^{0.4}$	$/kW

Sources: 1. Rasoui et al. (2011), 2. Fauchoux et al. (2007), 3. Rushing et al., (2011), 4. US Energy Information Administration (2013), 5. Alibaba Group (2014), 6. RSMeans (2010), 7. Agra (2011), 8. Al-Alili et al. (2012), 9. Gebreslassie et al. (2009).

4.8 RESULTS AND DISCUSSION

The design of a thermal system begins with estimating the loads required to be covered, in order to determine the capacity of the equipment. Then, the type of equipment is to be selected based on its availability and other important factors (i.e. initial cost and energy efficiency, etc.). Performing economic and environmental assessments for several scenarios is necessary in order to assist the selection from different available technologies/options.

The methodology followed to design and investigate the systems studied in the current paper is as follows. The sizes of heating and cooling equipment were first estimated for the M-LDAC and M-LDAC-ERV systems (see Figure 4.3), so that they cover the dehumidification and sensible cooling loads during all the occupied hours. Electrical heat pumps were selected to cover the air and solution cooling loads, while different

technologies including solar thermal system (STS) were investigated to cover the solution heating loads. It is worth mentioning that a STS should be properly sized (i.e. collector area (A_c) and volume of hot water storage tank (V_t)) in order to optimize the life cycle cost (LCC) of the whole system. Thus, the thermal performances of the STSs used in the M-LDAC and M-LDAC-ERV systems were first evaluated in terms of investigating the influence of the A_c and V_t on the solar fraction (SF) and collector efficiency (η_c) (see Figures 4.4 and 4.5). This was followed by optimizing the A_c and V_t based on the LCC for each of the four systems which use STS (see Figure 4.6). Eventually, economic and environmental comparisons between all the systems configurations studied were performed (see Figures 4.7 and 4.8).

4.8.1 Monthly cooling and heating energy demands

The monthly cooling and heating energy demands for the M-LDAC and M-LDAC-ERV systems are shown in Figure 4.3. The M-LDAC-ERV system requires less cooling and heating energy than the M-LDAC system. This is because when the hot-humid ventilation air is preconditioned by the ERV, its temperature and humidity ratio decrease, which means that less cooling and heating energy are required to condition the desiccant solution prior entering the dehumidifier and regenerator, respectively, and less cooling energy is needed to cover the sensible load of the air that is not met by the dehumidifier. As given in Table 4.3, the capacity of the air dry cooling coil, solution cooling coil and solution heating coil are 24 kW, 12 kW and 18 kW, respectively, for the M-LDAC system, while they are 25kW, 9 kW and 14 kW, respectively, for the M-LDAC-ERV system. Since the thermal energy requirements for the M-LDAC system are higher than the M-LDAC-ERV system, it is expected that the use of solar energy to heat the desiccant solution prior entering the regenerator will lead to more significant energy savings in the M-LDAC system, compared to the M-LDAC-ERV system.

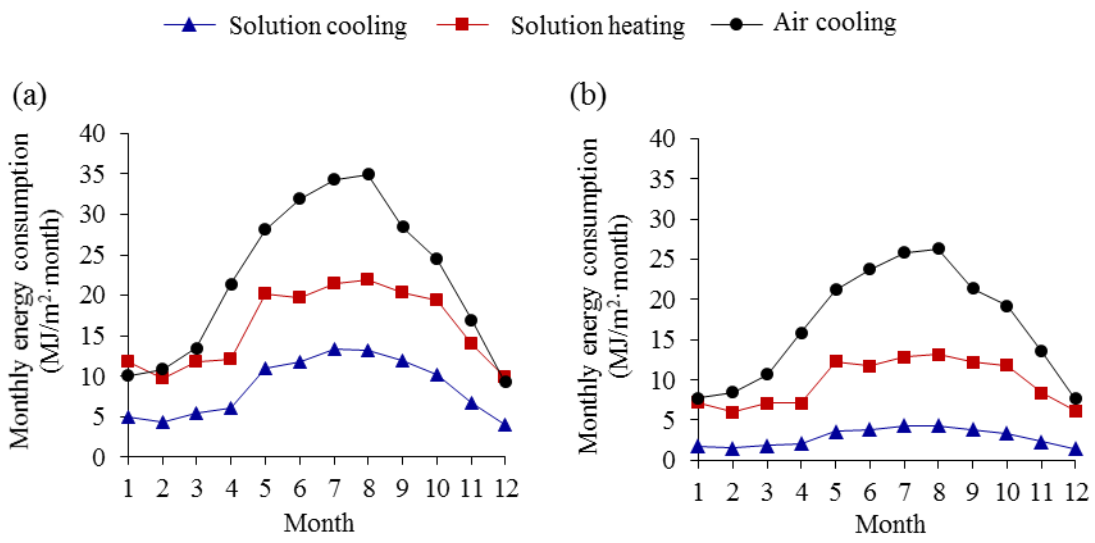

FIGURE 4.3. Annual monthly cooling and heating energy requirements for the (a) M-LDAC and (b) M-LDAC-ERV systems

TABLE 4.3. Capacities of cooling and heating equipment used in the M-LDAC and M-LDAC-ERV systems in kW.

System	Air cooling coil	Solution cooling coil	Solution heating coil
M-LDAC	24	12	18
M-LDAC-ERV	25	9	14

4.8.2 Influences of collector area and storage volume relative to collector area

The collector area (A_c) and storage volume relative to collector area (V_t) have significant influences on both the thermal and economic performances of the solar thermal system (STS). In this section, a parametric study is conducted to evaluate these influences on the annual solar fraction (SF_{annual}), annual collector efficiency ($\eta_{c,annual}$) and life cycle cost (LCC). A wide range of A_c and V_t are investigated, as the A_c is varied from 5 m^2 to 100 m^2 and the V_t is varied from 10 L/m^2 to 100 L/m^2, respectively. In addition, two different thermal energy demands and load temperatures are included in the parametric study, which represent the M-LDAC and M-LDAC-ERV systems.

4.8.2.1 Annual solar fraction

The SF_{annual} of the S-M-LDAC and S-M-LDAC-ERV systems are shown in Figure 4.4. The SF_{annual} increases with A_c, where the improvement is significant at low A_c and it gradually decreases at large A_c. The influence of V_t on the SF_{annual} of the S-M-LDAC system is found to be negligible at $A_c \leq 20$ m^2 and gradually increases as A_c increases above 20 m^2. Similarly, the influence of V_t on the SF_{annual} of the S-M-LDAC-ERV system is found to be only observable at $A_c > 30$ m^2. The improvement that occurs in the SF_{annual} with the increase in V_t is found to be larger at low V_t than at large values, similar to the A_c. Although increasing V_t increases the heat losses from the tank, the rate of energy that is supplied to the solution flow increases as well. The resulting improvement in SF_{annual} shows that the amount of thermal energy that is captured by the STS and delivered to the solution flow at large V_t is higher than the heat losses. Figure 4.4 shows that the trends in SF_{annual} are similar for the cases with and without ERV. However, the SF_{annual} values are higher with the ERV because the required heating energy is lower. For instance, the SF_{annual} of the S-M-LDAC system at A_c of 10 m^2 and 20 m^2 are 21% and 36%, respectively, while they are 28% and 43%, respectively, for the S-M-LDAC-ERV system.

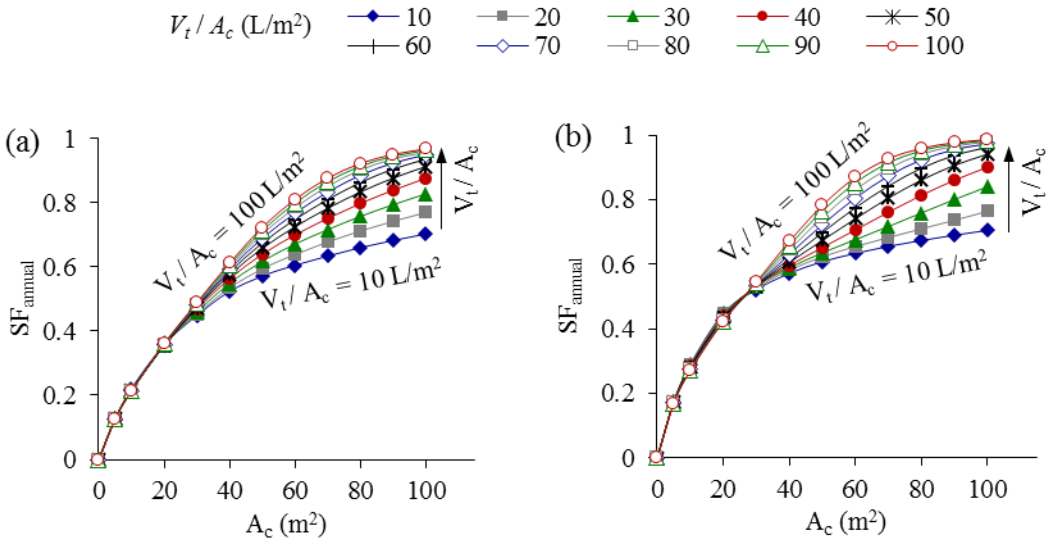

FIGURE 4.4. Influence of collector area (A_c) and storage volume relative to collector area (V_t) on annual solar fraction (SF_{annual}) of the (a) S-M-LDAC and (b) S-M-LDAC-ERV systems.

It is worth mentioning that the improvement of SF_{annual} with A_c is due to the increase in the amount of solar energy that can be collected when A_c increases, and consequently a larger portion of the load is covered at larger A_c which increases the SF_{annual}. The increase in SF_{annual} with V_t is attributed to the fact that the larger the storage volume, the large the thermal stratification in the tank and the larger the amount of solar energy that can be stored in the tank and delivered to the load. It is worth mentioning that the trends obtained for the variation of SF_{annual} with A_c and V_t are in accordance with previous studies performed on similar solar thermal systems (Molero-Villar et al., 2012; Kim et al., 2012; Assilzadeh et al., 2005; Chung et al., 1998).

4.8.2.2 Annual collector efficiency

Figure 4.5 presents $\eta_{c,annual}$ for the S-M-LDAC and S-M-LDAC-ERV systems. It can be seen that A_c and V_t have opposite influences on $\eta_{c,annual}$. It is found that increasing V_t increases $\eta_{c,annual}$, where when V_t increases from 10 L/m^2 to 100 L/m^2, the $\eta_{c,annual}$ increases by 21-26% for both the S-M-LDAC and S-M-LDAC-ERV systems, at any fixed A_c. Similar to what was observed in SF_{annual}, larger improvements occur in $\eta_{c,annual}$ with V_t at low V_t values than at high values. On the other hand, increasing A_c decreases the $\eta_{c,annual}$, as it is found that when A_c increases from 10 m^2 to 100 m^2, the $\eta_{c,annual}$ decreases by 12-15% for both the S-M-LDAC and S-M-LDAC-ERV systems, at any fixed V_t. It is clear that the trends and magnitudes of $\eta_{c,annual}$ are almost the same for both the S-M-LDAC and S-M-LDAC-ERV systems, with slightly different magnitudes due to the different thermal energy demands and load temperature for the two systems.

The observed improvement in $\eta_{c,annual}$ with increasing V_t is attributed to the fact that the larger the V_t, at a fixed A_c, the larger the thermal stratification in the storage tank, and therefore the lower the water temperature at the collector inlet. This leads to the increase in the amount of solar energy that can be captured by the water as it flows through the collector, and consequently improves $\eta_{c,annual}$. While the decrease of $\eta_{c,annual}$ with A_c is because increasing A_c, at a fixed V_t, increases the water temperature in the storage tank, which increases the water temperature at the collector inlet. Therefore, the amount of solar

energy that can be captured by the water as it flows through the collector decreases, which decreases $\eta_{c,annual}$.

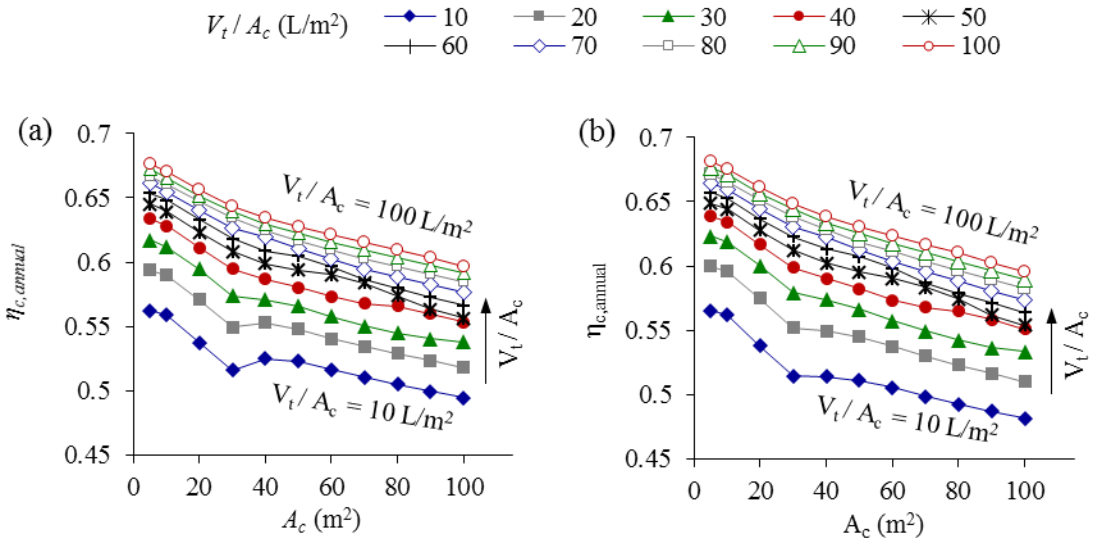

FIGURE 4.5. Influence of collector area (A_c) and storage volume relative to collector area (V_t) on annual collector efficiency ($\eta_{c,annual}$) of the (a) S-M-LDAC and (b) S-M-LDAC-ERV systems.

4.8.2.3 Life cycle cost (LCC)

As shown in Figure 4.4, the larger the A_c and V_t, the larger the SF_{annual}; this means that lower auxiliary heating will be required, which decreases the OC_{annual}. On the other hand, the larger the size of the STS, the higher the initial (IC); thus, the optimum size of the STS from an economic point of view is the size that achieves higher savings in the annual operating costs (OC_{annual}) and lower increase in the IC. The influences of A_c and V_t on the LCC are presented in this section in order to identify the most economic STS size for each of the systems configurations investigated. As mentioned previously, two different backup heating systems are used (i.e. electrical HP and NG boiler). This besides the two different thermal energy demands and load temperatures (i.e. which represent the M-LDAC and M-LDAC-ERV systems) results in four systems configurations as follows: (i) S-M-LDAC-HP, (ii) S-M-LDAC-ERV-HP, (iii) S-M-LDAC-NG, and (iv) S-M-LDAC-ERV-NG.

Figure 4.6 shows the influences of A_c and V_t on the LCC for each of the four systems configurations investigated in this section. In general, the LCC decreases with A_c, at any fixed V_t, until it reaches a global minimum and any further increase in A_c beyond this minimum point leads to an increase in the LCC. This is due to the increase of the IC of the STS in a way that exceeds the achieved savings in OC_{annual}. On the other hand, it is found that there is no general trend for the influence of V_t on the LCC that is applicable to all the systems studied. It is worth mentioning that although the magnitude of the LCC of a STS with A_c and V_t may vary from one system to another, the general trends obtained for the LCC in the current study are in accordance with previous studies (Kim et al., 2012; Assilzadeh et al., 2005; Chung et al., 1998; Florides et al., 2002a, 2002b).

From an economic point of view, the optimum size of STS is the size that leads to the global minimum LCC, where the SF_{annual} does not have to be at the highest possible achievable value. Table 4.4 shows the STS size that achieves the global minimum LCC for each of the four systems configurations studied in this Section. It is found that when an electrical HP is used as the backup heating system, the size of the STS does not have considerable effect on the LCC, see Figures 4.6(c) and 4.6(d). This is because the electrical HP is an energy efficient source of thermal energy, especially when it operates in hot climates such as Miami. On the other hand, significant savings are possible from the STS when a NG boiler is used as the backup heating system, see Figures 4.6(a) and 4.6(b). This is attributed to the low efficiency and high OC_{annual} of the NG boiler, which makes the STS a better choice of supplying thermal energy.

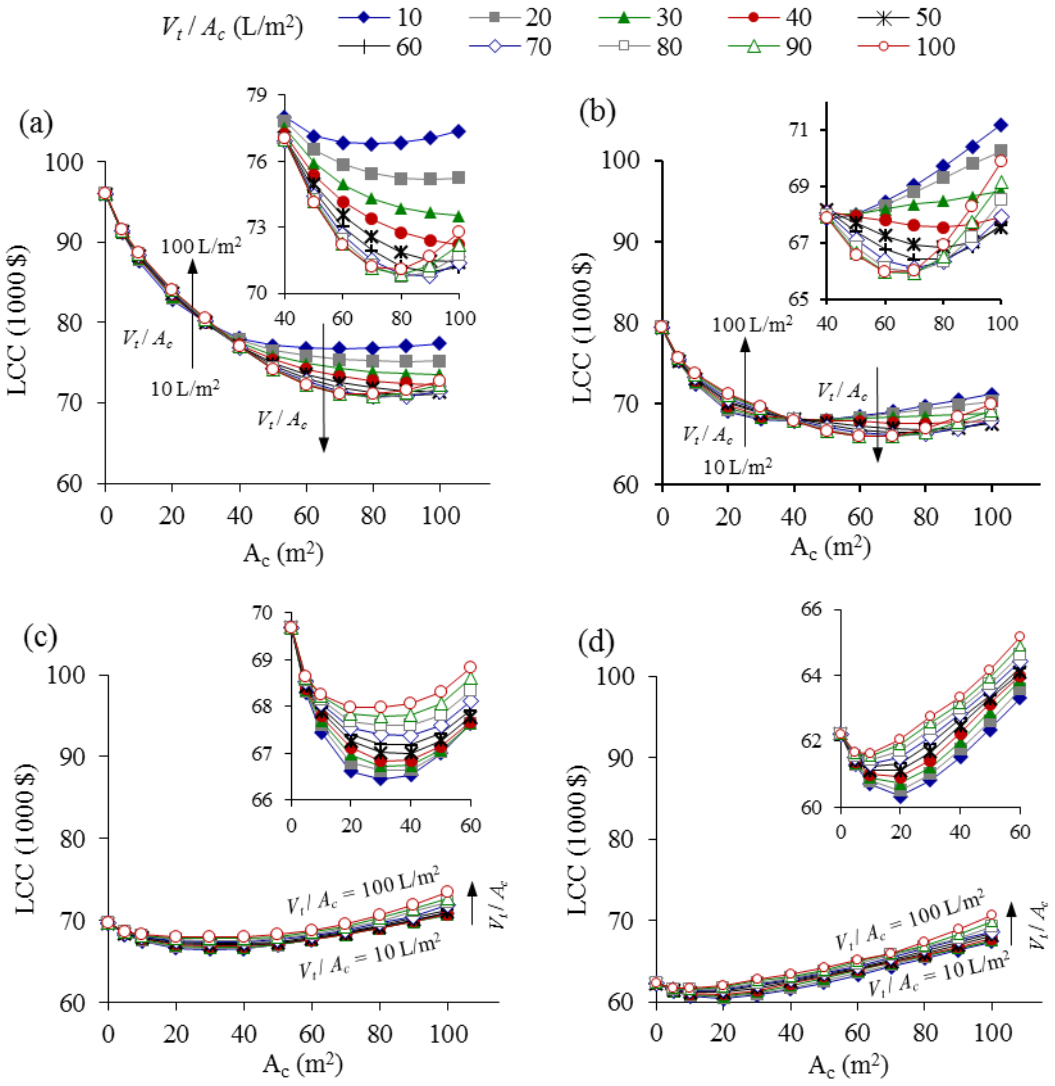

FIGURE 4.6. Influence of collector area (A_c) and storage volume relative to collector area (V_t) on life cycle cost (LCC) of the (a) S-M-LDAC-NG, (b) S-M-LDAC-ERV-NG, (c) S-M-LDAC-HP and (d) S-M-LDAC-ERV-HP systems.

TABLE 4.4. The optimum STS sizes and global minimum LCC the studied systems.

System	A_c (m²)	V_t (L/m²) [L]	LCC ($)
S-M-LDAC-NG	80	80 [6400]	69,954
S-M-LDAC-ERV-NG	70	90 [6300]	66,627
S-M-LDAC-HP	30	10 [300]	66,754
S-M-LDAC-ERV-HP	20	10 [200]	60,544

4.8.3 Economic and environmental feasibility

The optimum economic sizes, given in Table 4.4, are used in this Section for the systems configurations that include STSs. Figure 4.7 shows the economic and environmental performances indices for all the systems configurations studied, and a breakdown analysis for the IC and OC_{annual} are shown in Figure 4.8. Results show that all the systems studied have lower LCCs than the CAC system (i.e. without ERV), except the M-LDAC-NG and M-LDAC-ERV-NG systems. While, it is found that the CAC-ERV system has the third lowest LCC after the S-M-LDAC-ERV-HP and M-LDAC-ERV-HP systems. The F_{CO2} of the CAC system is found to be higher than all the systems studied, except the M-LDAC-NG system. The CAC-ERV system is found to be more environmental friendly than the CAC and M-LDAC-NG systems, while it results in higher F_{CO2} than the other systems studied. A more detailed analysis for the influence of using a STS to heat the dilute desiccant solution prior entering the regenerator in the systems studied is presented in Section 4.8.2 in order to provide useful information for designers and engineers when designing LDAC systems in general, and the heating system required for dilute desiccant solution regeneration in specific.

4.8.3.1 M-LDAC-NG versus S-M-LDAC-NG

As shown in Figure 4.8, the IC ($17,386) and OC_{annual} ($5,040/year) of the M-LDAC-NG system are 27% and 20%, respectively, higher than those of the CAC system. This results that the LCC ($96,005) of the M-LDAC-NG is 21% higher than that of the CAC system. There is no PBP for the M-LDAC-NG system in this case because both its IC and OC_{annual} are higher than those of the CAC system.

When a STS is integrated with the M-LDAC-NG system, the IC and OC_{annual} become $32,809 and $2,381/year, respectively; thus, the LCC of the S-M-LDAC-NG ($69,954) becomes lower than the LCCs of the M-LDAC-NG and CAC systems by 27% and 12%, respectively. The PBP for the S-M-LDAC-NG system is 10.5 years instead of no payback if the M-LDAC-NG is used. Figure 4.7 shows that the F_{CO2} of the M-LDAC-NG (18.6 tons/year) and S-M-LDAC-NG (11.1 tons/year) systems are 3% higher and 39% lower, respectively, than the F_{CO2} of the CAC system (18.1 tons/year).

It is clear that if the backup heating system is a NG boiler, a STS should be integrated with the M-LDAC-NG. Otherwise, the IC, OC_{annual}, LCC and F_{CO2} of the M-LDAC-NG will be higher than those of the CAC system, which is in agreement with the findings of Qi et al. (2012).

4.8.3.2 M-LDAC-ERV-NG versus S-M-LDAC-ERV-NG

The OC_{annual} of the M-LDAC-ERV-NG system ($3,915/year) is found to be 7% and 22% lower than the OC_{annual} of the CAC and M-LDAC-NG systems, respectively. However, the IC of the M-LDAC-ERV-NG system ($18,353) is 34% higher than that of the CAC system; thus, this results in a LCC for the M-LDAC-ERV-NG system ($79,432), which is almost equal to that of the CAC system (79,224 $). The PBP for the M-LDAC-ERV-NG is expected to be 16.3 years.

The integration of a STS with the M-LDAC-ERV-NG system makes it more economic. Although the IC of the S-M-LDAC-ERV-NG system ($31,390) is 129% higher than that of the CAC system, its OC_{annual} ($2,259/year) is 46% lower. This leads to the reduction of the LCC of the S-M-LDAC-ERV-NG system ($66,627) by 16% compared to the CAC system, with a PBP of 9.1 years which is lower than the 10.5 years obtained for the S-M-LDAC-NG system. The F_{CO2} of the M-LDAC-ERV-NG and S-M-LDAC-ERV-NG systems are found to be 18% and 45%, respectively, lower than that of the CAC system.

Similar to the M-LDAC-NG system, the M-LDAC-ERV-NG system is not economically viable (i.e. with respect to the CAC and CAC-ERV systems) if no STS is used to provide a large portion of the thermal energy requirements, and therefore integrating a STS with this system is necessary in order to be economically feasible.

4.8.3.3 M-LDAC-HP versus S-M-LDAC-HP

Figure 4.8 shows that the OC_{annual} of the M-LDAC-HP system ($3,208/year) is 24% lower than that of the CAC system, while its IC ($19,637) is 43% higher. The LCC of the M-LDAC-HP system ($69,682) is 12% lower than that of the CAC system, and its PBP is 6 years. It is found that the LCC decreases to $66,754 when the S-M-LDAC-HP system is

used, while the PBP increases to 6.8 years due to the additional costs of the STS. It can be seen from Figure 4.8 that the percent reduction in the OC_{annual} when a STS is used with the M-LDAC-HP system is not significant, unlike the case for the M-LDAC-NG and M-LDAC-ERV-NG systems. This is attributed to the high thermal efficiency of the electrical HP, which is assumed to be nearly 1.6 (Niu et al., 2010), compared to that of the NG boiler, which is assumed to be 0.9. The F_{CO2} of the M-LDAC system with an electrical HP is found to be lower than that of the CAC whether a STS is used or not, unlike the case when a NG boiler is used and ERV is not installed. As, the F_{CO2} of the M-LDAC-HP (14.7 ton/year) and S-M-LDAC-HP (12.7 ton/year) systems are 19% and 30%, respectively, lower than the CAC system.

4.8.3.4 M-LDAC-ERV-HP versus S-M-LDAC-ERV-HP

The IC of the M-LDAC-ERV-HP system ($20,104) is 47% higher than that of the CAC system; however, its OC_{annual} ($2,701/year) is 36% lower. This leads to a lower LCC for the M-LDAC-ERV-HP system by 21% compared to the CAC system. Among all the studied scenarios, this scenario is found to be the least affected by the integration of a STS. As, the integration of a STS with the M-LDAC-ERV-HP system reduces its LCC by only 3%. This attributed to the high thermal efficiency of the electrical HP, as mentioned previously, besides the low thermal energy demand and load temperature due to the installation of an ERV.

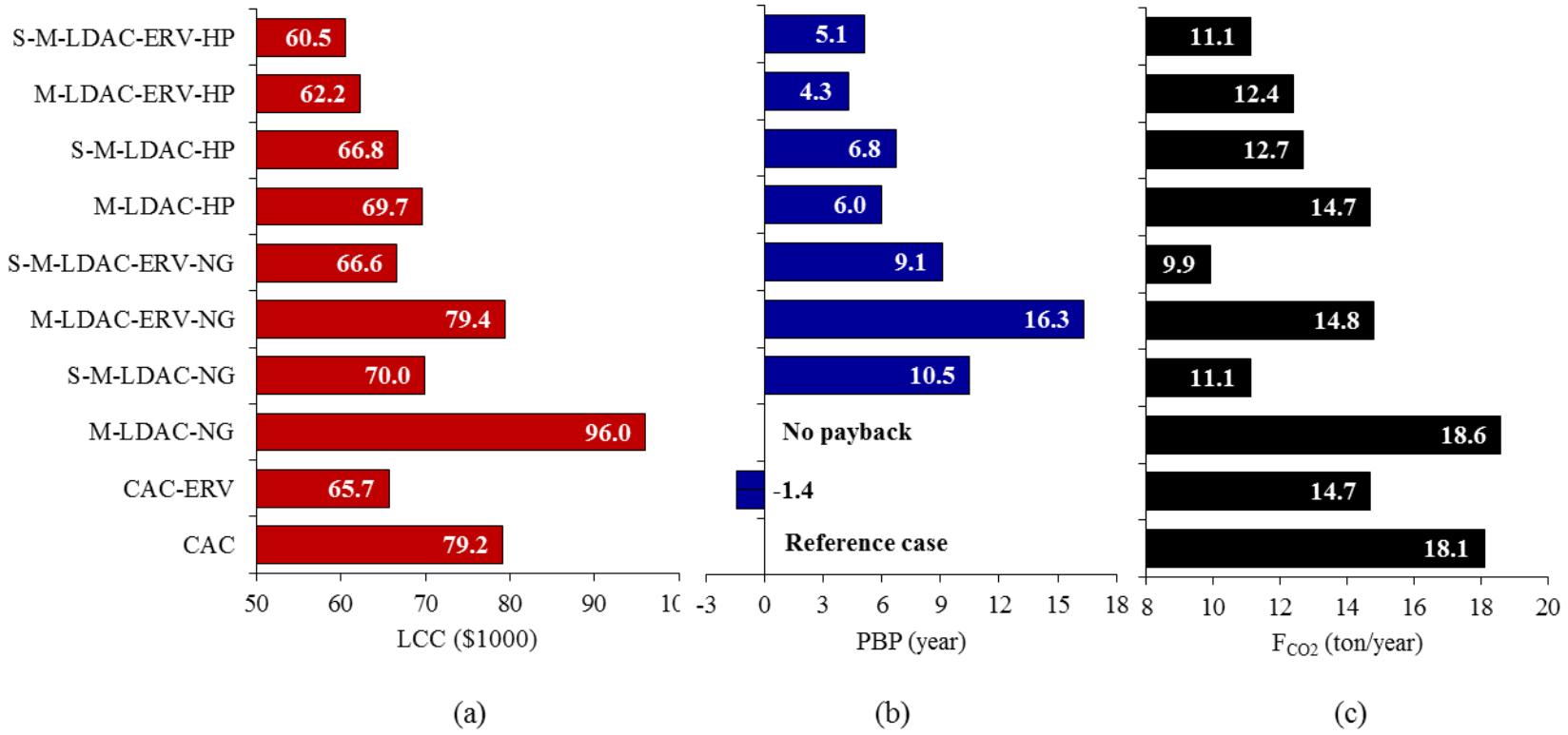

FIGURE 4.7. The life cycle cost (LCC), payback period (PBP), and annual CO_2 emissions (F_{CO2}) of the M-LDAC and CAC systems.

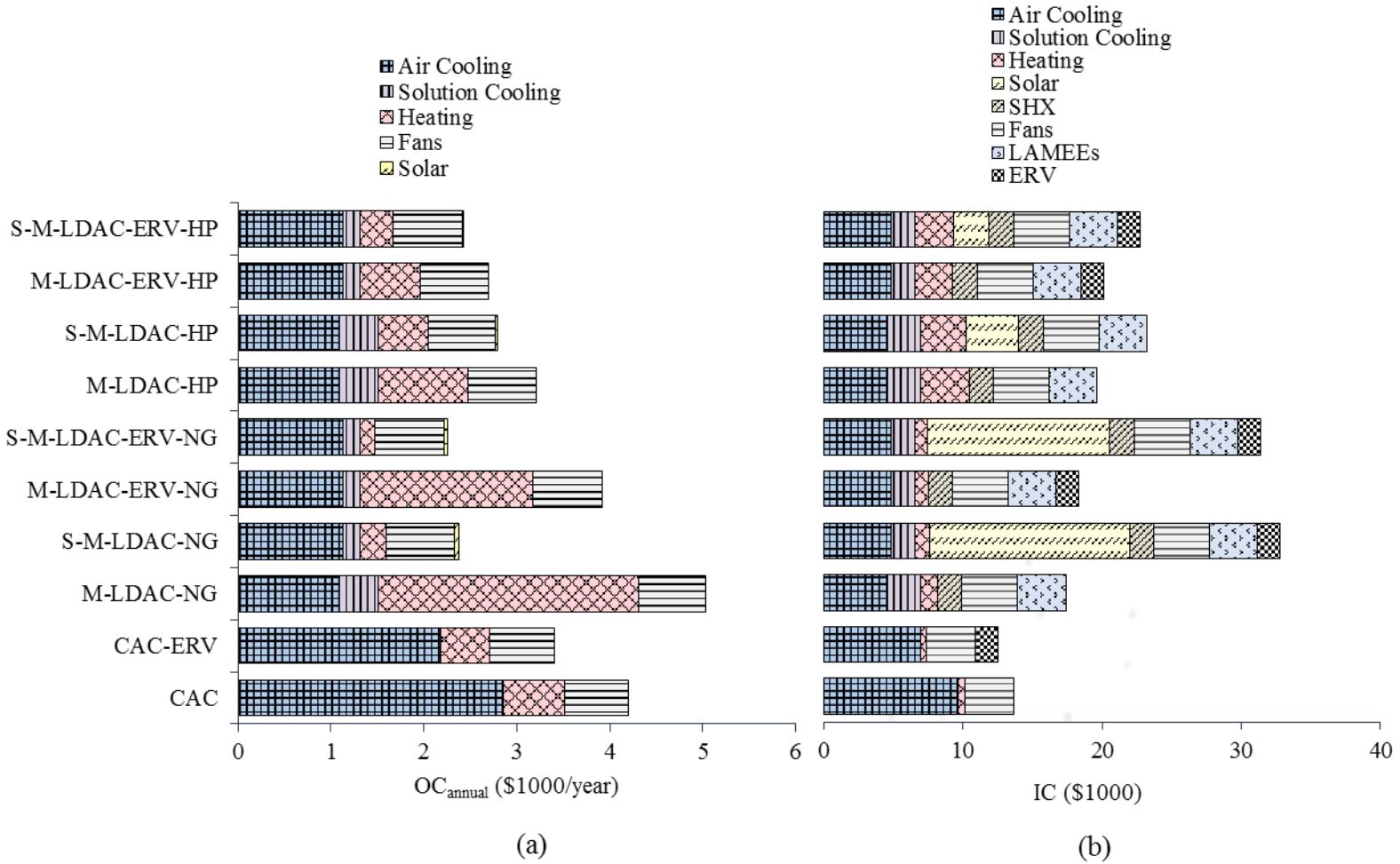

FIGURE 4.8. Breakdown analysis of the (a) annual operating cost (OC_{annual}) and (b) initial cost (IC) of the M-LDAC and CAC systems.

4.8.4 Summary

It is found that increasing the V_t improves both the SF_{annual} and $\eta_{c,annual}$ by different rates. For instance, when the V_t increases from 10 L/m^2 to 100 L/m^2, the $\eta_{c,annual}$ improves by nearly 22% at any fixed A_c, which shows that the improvement in the $\eta_{c,annual}$ with V_t is not strongly dependent on the A_c. On the other hand, the improvement occurs in the SF_{annual} with the V_t is found to be strongly dependent on the A_c. For instance, when the V_t increases from 10 L/m^2 to 100 L/m^2, the SF_{annual} of the S-M-LDAC system only increases from 45% to 49% (by 9%) at A_c = 30 m^2, while it increases from 70% to 97% (by 39%) at A_c = 100 m^2. It is found that increasing the A_c leads to a significant increase in the SF_{annual}, while it decreases the $\eta_{c,annual}$. For instance, at V_t = 50 L/m^2, the SF_{annual} of the S-M-LDAC system increases from 13% to 91% (by 600%) when the A_c increases from 5 m^2 to 100 m^2, while the $\eta_{c,annual}$ only decreases from 64% to 56% (by 13%). It is clear that the rate of improvement in the SF_{annual} is much larger than the reduction that occurs in the $\eta_{c,annual}$; therefore, increase the A_c has a favorable influence on the overall performance of the STS.

The significance of the A_c and V_t influences on the LCC are found to be strongly dependent on the: (i) type of backup heating system, (ii) thermal energy demand, (iii) load temperature and (iv) V_t if A_c is under investigation and vice versa. Larger reductions occur in the LCC due to the installation of a STS when the backup heating system is a NG boiler, compared to the cases when an electrical HP is used. Also, larger reductions in the LCC are achieved due to the installation of a STS when no ERV is used compared to the cases when ERV is installed in the system, regardless the type of backup heating system. The LCC and PBP of the M-LDAC-NG decrease from $96,005 and no payback to $69,954 and 10.5 years, respectively, when a STS is used. Similarly, the use of a STS has reduced the LCC and PBP of the M-LDAC-ERV-NG from $79,432 and 16.3 years to $66,627 and 9.1 years, respectively. Although similar results with lower magnitudes are observed for the LCCs when the STS is installed in the M-LDAC-HP and M-LDAC-ERV-HP systems, the PBPs for these systems are increased due to the increase in the IC. For instance, the LCC of the M-LDAC-HP has decreased by 4.2% (from $69,682 to $66,754) when a STS is used, while its PBP has increased by 13.3% (from 6 years to 6.8 years). Similarly, the LCC of the M-LDAC-ERV-HP has decreased by 3.2% (from $62,200 to $60,500) due to the integration

of a STS, while its PBP has increased by 21% (from 4.3 years to 5.2 years). The use of a STS has led to the reduction of F_{CO2} in all the systems configurations investigated, with more considerable reductions when a NG boiler is used as the backup heating system.

It is worth mentioning that the energy and economic performances of the proposed systems may vary from one hot humid location to another. The influences of several operating and design parameters on the performance of the M-LDAC system were investigated in a previous study (Abdel-Salam et al., 2013a). A wide range of outdoor air conditions were covered, which ranged from 24ºC and 9.3 g/kg up to 35ºC and 28.9 g/kg. It was concluded that the higher the outdoor air temperature and humidity, the higher the electrical, thermal and total coefficients of performance of the M-LDAC system. In addition, the thermal and economic feasibilities of solar thermal systems are expected to increase in sunny climates, where higher solar gains can be achieved. Thus, the weather data for different locations are recommended to be considered prior applying the results obtained in the current study to another location.

Moreover, there are advantages and disadvantages for the proposed LAMEEs when compared with traditional packed bed exchangers. The semi-permeable membrane used to eliminate the liquid carryover in the air streams would increase the heat and moisture transfer resistances and the initial cost as well. The added fractions in the total resistances are very dependent on the properties of the membrane and operating conditions (Ge et al., 2014b). On the other hand, the membrane applied in the LAMEE can keep uniform flow distribution in air and solution channels and reduce the mal-distribution of solution and air flows in the energy exchanger compared with packed bed exchangers. Also, the pressure drop in the packed bed is generally higher than that of LAMEE (Gandhidasan, 2002; Moghaddam et al., 2013c), which means higher operating costs for the fans to deliver the air flow in the air conditioning system.

4.9 CONCLUSION

In this study, the thermal, economic and environmental performances of the proposed solar membrane liquid desiccant air conditioning (S-M-LDAC) system, which use liquid-to-air membrane energy exchangers (LAMEE) as a dehumidifier and a regenerator, are investigated. Eight systems configurations are simulated using TRNSYS, and compared against a conventional air conditioning systems with and without energy recovery ventilator. It is found that the use of a solar thermal system (STS) to provide the thermal energy required for the regeneration of the dilute desiccant solution increases the initial costs but decreases the annual operating costs, compared to the non-solar systems. The life cycle cost is always lower with the STS than with no solar; however, the payback period is not always shorter when a STS is used. The payback period is shorter for the STS with natural gas boiler backup but longer for the STS with electrical heat pump backup, compared to the same systems without solar. The annual CO_2 emissions are found to be always lower when a STS is used.

In conclusion, it is not recommended to use a natural gas boiler in the membrane liquid desiccant air conditioning system with/without energy recovery ventilator if there is no STS used because this will lead to higher initial and operating costs, and consequently to higher life cycle cost than the conventional air conditioning system. If an electrical heat pump is to be used, which is strongly recommended due to its high thermal efficiency especially in hot climates, the integration of a relatively small STS will still lead to reductions in the life cycle cost; however, this will be accompanied with an increase in the payback period. The conventional air conditioning system with an energy recovery ventilator is strongly recommended to be considered if the choice is based on the economics, as its life cycle cost is found to be competitive. While, if the environmental performance of the system is to be considered, all the S-M-LDAC configurations will produce lower annual CO_2 emissions than the conventional air condition system either with or without an energy recovery ventilator.

CHAPTER 5

ANNUAL ENERGY MODELLING AND ECONOMICS OF A HEAT-PUMP MEMBRANE LDAC SYSTEM

5.1 OVERVIEW

All the membrane LDAC systems studied in Chapters 3 and 4 use heat pumps to cover the solution cooling loads, and use another solution heating equipment such as gas boiler, solar thermal or heating heat pump to cover the solution heating loads. A more compact configuration for the membrane LDAC system is studied in this chapter, where the evaporator and condenser of the same heat pump are used to cover the solution cooling and heating loads, respectively. The annual energy performance of this system is simulated using TRNSYS. The economics of the system is compared to the economics of all the systems studied in Chapters 3 and 4, in order to identify the most promising configuration for a membrane LDAC system.

The manuscript used in this Chapter is published in the Proceedings of esim 2014 (IBPSA-Canada's 8th Biennial Conference). A Post-Doctoral Fellow "Dr. Gaoming Ge" has contributed to this manuscript by reviewing the manuscript and providing technical advice. As the lead author of the paper, I conducted the research, analyzed the results, wrote the manuscript, incorporated co-authors comments and addressed the reviewers' comments.

TRNSYS Modelling of a Hybrid Membrane Liquid Desiccant Air Conditioning System

(In Proceedings of esim 2014: IBPSA-Canada's 8th Biennial Conference, 2014)

Ahmed H. Abdel-Salam, Gaoming Ge, Carey. J. Simonson

5.2 ABSTRACT

The attention to liquid desiccant air conditioning (LDAC) systems is increasing worldwide. This is mainly due to the ability of these systems to efficiently maintain indoor air humidity within acceptable ranges in energy efficient way compared to conventional air conditioning systems. LDAC systems still under R&D in order to reduce/eliminate common drawbacks, such as the carryover of desiccant droplets in air streams, and to develop novel configurations which aim to achieve higher energy efficiency. To address these, two improvements are implemented on a LDAC system in this chapter. First, liquid-to-air membrane energy exchangers (LAMEEs) are used as the dehumidifier and regenerator, in order to avoid the carryover of desiccant droplets in air streams. Second, the desiccant solution heating and cooling energy requirements are simultaneously provided using a hybrid liquid desiccant heat pump (LDHP). The proposed hybrid membrane LDAC (H-M-LDAC) system is annually simulated using TRNSYS when installed in an office building located in Miami, FL. Results show that the COPs of the return air heat pump (RAHP), LDHP and H-M-LDAC system vary under different operating conditions with an approximate average annual values of 4.5, 7.8 and 1, respectively.

5.3 INTRODUCTION

In liquid desiccant air conditioning (LDAC) systems, the desiccant solution should be regenerated after it absorbs the moisture from humid air. Liquid desiccant regeneration is achieved by heating the desiccant solution up to 45ºC-65ºC in order to increase its vapor pressure, and then transferring the moisture from the desiccant solution to the regeneration air, which could be either exhaust air from the building or ambient air. Since considerable amount of heating is consumed in the regeneration of dilute desiccant solution, many studies have investigated the potential of integrating LDAC systems with solar thermal systems (Abdel-Salam et al. 2013; Crofoot and Harrison 2012; Li et al. 2010; Gommed and

Grossman 2007; Davies 2005). The results of solar LDAC systems were promising from energy consumption point of view. However, the achieved energy savings using solar LDAC systems are accompanied with higher initial costs (Abdel-Salam et al. 2013). In addition, a heat pump may be still needed in a solar LDAC system in order to cool the desiccant solution before it removes the moisture from the humid air. Some researchers have investigated the potential of using the heat rejected from the solution cooling heat pump in order to cover the heating requirements of dilute desiccant solution, and this was found to improve the coefficient of performance (COP) of the system Thus, a hybrid liquid desiccant heat pump (LDHP) will be used in this chapter in order to simultaneously provide the solution heating and cooling requirements.

In the current chapter, a hybrid M-LDAC (H-M-LDAC) system will be annually simulated, for the first time in the scientific literature, using the TRNSYS building energy simulation software. The proposed H-M-LDAC system is characterized by two advanced modifications, compared to conventional LDAC systems as follows. (1) LAMEEs are used in the H-M-LDAC systems as dehumidifier and regenerator, which eliminate the desiccant droplets carry over problem. (2) Only one liquid desiccant heat pump (LDHP) is used in the H-M-LDAC system to simultaneously cover the heating and cooling requirements of the dilute and concentrate solution streams, respectively. The H-M-LDAC system's economics is compared to the economics of all the systems studied in Chapters 3 and 4, in order to identify the most promising configuration for a membrane LDAC system.

5.4 SYSTEM DESCRIPTION

A schematic diagram for the proposed H-M-LDAC system is presented in Figure 5.1. The hot-humid outdoor air passes through the dehumidifier, where the entire latent load and a portion of the sensible load are covered. The return air is sensibly cooled as it passes through the evaporator of the return air heat pump (RAHP), in order to cover any additional sensible load not covered by the dehumidifier. The dehumidified fresh air is mixed with the sensibly cooled return air, and then the mix is supplied to the conditioned space. More details about the operating principles of the system are presented in Section 3.4.3.

As can be seen from Figure 5.1, the LDHP can be operated in two modes, as it is operated so that either the condenser typically matches with the solution heating requirements (Case A), or the evaporator load typically matches with the solution cooling requirements (Case B). In Case A, the evaporator load is higher than the solution cooling requirements, and thus an auxiliary evaporator is used to cover the evaporator load. In Case B, the condenser load is higher than the solution heating requirements, and thus an auxiliary condenser is used to cover the condenser load. More details about each operating condition are presented in Section 5.5.3.

The H-M-LDAC system is controlled in the current chapter using an ON/OFF control methodology, and it operates at one of three operating modes as follows.

- Sensible Mode ($Mode_{sensible}$): This operating mode occurs when the indoor humidity ratio is $\leq$ 9.3 g/kg and the indoor air temperature is > 24ºC. In this case, only the RAHP is in operation in order to cool the indoor air down to the set point temperature.
- Latent Mode ($Mode_{latent}$): This operating mode occurs when the indoor air temperature is $\leq$ 24ºC and the indoor air humidity ratio is > 9.3 g/kg. In this case, only the LDHP is in operation in order to dehumidify the indoor air down to the set point humidity ratio.
- Total Mode ($Mode_{total}$): This operating mode occurs when the indoor air temperature is > 24ºC and the indoor air humidity ratio is > 9.3 g/kg. In this case, both the LDHP and RAHP are in operation in order to cool and dehumidify the indoor air down to the set point temperature and humidity ratio.

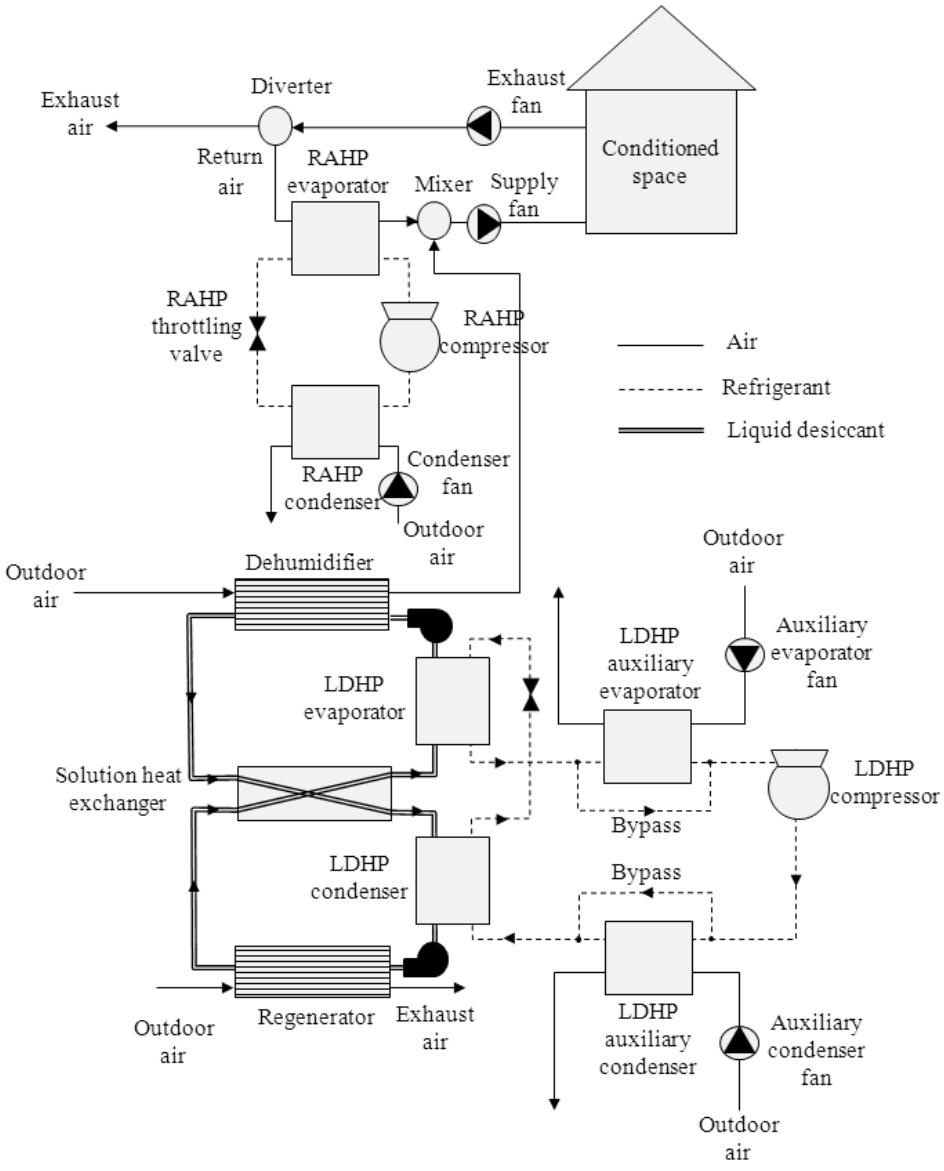

FIGURE 5.1. Schematic diagram for the H-M-LDAC system.

5.5 MODELLING APPROACH

The H-M-LDAC system proposed in the current chapter is annually simulated using the TRNSYS building energy software. The H-M-LDAC system is modelled for a small office building located in Miami, FL. Detailed information about the climatic conditions and building specifications is presented in Chapter 3. The modelling approach followed in this chapter to evaluate the performance of the H-M-LADC system is presented in the following three sections.

5.5.1 LAMEE

The dehumidifier and regenerator are flat-plate liquid-to-air membrane energy exchangers (LAMEEs), as mentioned previously. More information about the analytical model of the LAMEE is presented in Chapter 2, and the specifications of the LAMEE used in this chapter are presented in Chapter 3.

5.5.2 Return air heat pump (RAHP)

The effectiveness of the evaporator/condenser ($\varepsilon_{cond/evap}$) is calculated using the effectiveness-NTU method, equation (5.1), where the $NTU_{cond/evap}$ is assumed to be 2 (Tu et al., 2014). The evaporating temperature (T_{evap}) is calculated as shown in equation (5.3) after determining the operating conditions of the return air stream ($\dot{m}_{air}$, $T_{evap,in}$, $T_{evap,out}$). The condenser used in the RAHP is air cooled, and the condensing temperature (T_{cond}) is assumed to be 10ºC higher than the ambient air temperature (i.e. ΔT_{cond}=10ºC). After calculating the evaporating and condensing temperatures, the compressor power (P_{comp}) is calculated, equation (5.5), where the theoretical efficiency (η_{th}) of the RAHP is assumed to be 55% (Tu et al., 2014). In order to present a complete evaluation for the performance of the RAHP, the fan power ($P_{fan,cond}$) required to circulate the ambient air in the air-cooled condenser is calculated, equation (5.6), where the pressure drop in the condenser (ΔPr_{cond}) is assumed to be 375 Pa and the efficiency of the fan is assumed to be 60%. The COP of the RAHP (COP_{RAHP}) is then calculated, equation (5.7), where the power of both the compressor and condenser's fan are included.

$$\varepsilon_{evap/cond} = 1 - e^{-NTU_{evap/cond}} \tag{5.1}$$

$$q_{evap} = \dot{m}_{air,evap}\, c_{p,air}\, (T_{air,evap,in} - T_{air,evap,out}) \tag{5.2}$$

$$T_{evap} = T_{air,evap,in} - \frac{q_{evap}}{\varepsilon_{evap}\, \dot{m}_{air,evap}\, c_{p,air}} \tag{5.3}$$

$$T_{cond} = T_{amb} + 10 \tag{5.4}$$

$$P_{comp} = \frac{q_{evap}}{\eta_{th}\, \frac{273.15+T_{evap}}{T_{cond} - T_{evap}}} \tag{5.5}$$

$$P_{fan,cond} = \frac{q_{cond}\, \Delta Pr_{air,cond}}{\varepsilon_{cond}\, c_{p,air}\, (T_{cond} - T_{air,cond,in})\, \eta_{fan}\, \rho_{air}} \tag{5.6}$$

$$COP_{RAHP} = \frac{q_{evap}}{W_{fan,cond} + W_{comp}} \tag{5.7}$$

5.5.3 Liquid desiccant heat pump (LDHP)

Unlike the RAHP which only provides cooling for the return air stream, the LDHP provides simultaneous heating and cooling for the dilute and concentrate solution streams, respectively. The capacities of the condenser and evaporator of the LDHP have to be efficiently matched with the cooling and heating solution loads, respectively, in order to avoid either the overheating of dilute solution stream or the overcooling of concentrate solution stream. For this reason, the heat ratio for the LDHP (HR_{LDHP}) is defined in order to show the relation between the thermal loads of the condenser and evaporator of the LDHP, and the heating and cooling energy required by solution streams. The HR_{LDHP} is defined as follows.

$$HR_{LDHP} = \frac{\frac{q_{sol,cool}}{q_{sol,heat}}}{\frac{q_{evap}}{q_{cond}}} \tag{5.8}$$

where, $q_{sol,cool}$ and $q_{sol,heat}$ are the cooling and heating energy requirements of the desiccant solution, respectively, q_{evap} is the evaporator load, and q_{cond} is the condenser load. In order to assure that the LDHP is operating at the proper operating mode, the HR_{LDHP} is checked at every time step. A flow chart which shows how the operating mode of the LDHP is determined at every time step is presented in Figure 5.2.

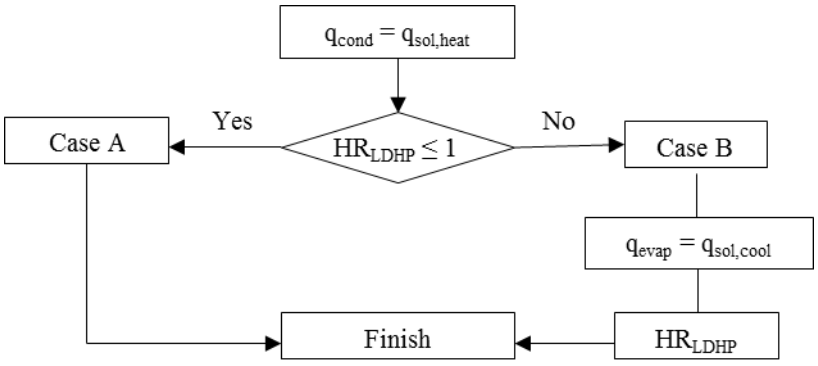

FIGURE 5.2. Flow chart of the operating modes of the LDHP.

The next two sections show how the COP_{LDHP} is evaluated at each operating mode (i.e. Case A or Case B) for the LDHP.

Case A:

If $HR_{LDHP} \leq 1$, the condenser load matches the solution heating requirements and the evaporator provides larger cooling energy than that required for the concentrate solution cooling. Thus, an auxiliary evaporator is used in order to reject the additional cooling energy. The required evaporator and condenser loads are calculated using the operating conditions of the concentrate and dilute solution streams, equations (5.9) and (5.10). The evaporating temperature is then calculated using equation (5.11), in order to assure that the evaporating temperature does not exceed the ambient air temperature at any operating condition when the air-cooled auxiliary evaporator is used. The condensing temperature is then calculated, equation (5.12), followed by the power of the compressor, equation (5.13). The amount of cooling energy which should be rejected from the auxiliary evaporator is calculated as shown in equation (5.14), and the fan power required to circulate the ambient air through the auxiliary evaporator is calculated using equation (5.15).

$$q_{evap,sol} = \dot{m}_{sol,evap}\, c_{p,sol}\, (T_{sol,evap,in} - T_{sol,evap,out}) \tag{5.9}$$

$$q_{cond} = \dot{m}_{sol,cond}\, c_{p,sol}\, (T_{sol,cond,in} - T_{sol,cond,out}) \tag{5.10}$$

$$T_{evap} = \text{Min}\left\{ T_{sol,evap,in} - \frac{q_{evap,sol}}{\varepsilon_{evap}\, \dot{m}_{sol,evap}\, c_{p,sol}},\ T_{amb}-10 \right\} \tag{5.11}$$

$$T_{cond} = T_{sol,cond,in} + \frac{q_{cond}}{\varepsilon_{cond}\, \dot{m}_{sol,cond}\, c_{p,sol}} \tag{5.12}$$

$$P_{comp} = \frac{q_{cond}}{\eta_{th}\, \dfrac{273.15+T_{cond}}{T_{cond} - T_{evap}}} \tag{5.13}$$

$$q_{evap,aux} = \left| q_{cond} - P_{comp} - q_{evap,sol} \right| \tag{5.14}$$

$$P_{fan,evap,aux} = \frac{q_{evap,aux}\, \Delta Pr_{air,evap,aux}}{\varepsilon_{evap,aux}\, c_{p,air}\, (T_{amb} - T_{eavp})\, \eta_{fan}\, \rho_{air}} \tag{5.15}$$

Case B:

If $HR_{LDHP} > 1$, the heat pump loads will not be matched with the solution heating and cooling requirements under the aforementioned operating condition (i.e. condenser meets the solution heating load). Thus, the LDHP is operated so that the evaporator load matches with the solution cooling requirements and an additional condenser will be used in order to meet the condensation requirements in the LDHP. The condensing and evaporating temperatures are calculated using equations (5.12) and (5.16), respectively. The power of the compressor is then calculated, equation (5.17), and the fan power required to circulate the ambient air in the secondary condenser is evaluated, equation (5.19).

$$T_{evap} = T_{sol,evap,in} - \frac{q_{evap}}{\varepsilon_{evap}\, \dot{m}_{sol,evap}\, c_{p,sol}} \tag{5.16}$$

$$P_{comp} = \frac{q_{evap}}{\eta_{th}\, \frac{273.15+T_{evap}}{T_{cond}-T_{evap}}} \tag{5.17}$$

$$q_{cond,aux} = \left| q_{evap} - P_{comp} - q_{cond,sol} \right| \tag{5.18}$$

$$P_{fan,cond,aux} = \frac{q_{cond,aux}\, \Delta Pr_{air,cond,aux}}{\varepsilon_{cond,aux}\, c_{p,air}\, (T_{cond} - T_{amb})\, \eta_{fan}\, \rho_{air}} \tag{5.19}$$

Eventually, the COP of the LDHP (COP_{LDHP}) is calculated as follows.

$$COP_{LDHP} = \frac{q_{sol,cool} + q_{sol,heat}}{P_{fan,aux,evap/cond} + P_{comp,LDHP}} \tag{5.20}$$

5.6 PERFORMANCE INDICES

The performance of the H-M-LDAC system is evaluated using the following indices. (1) The annual COP_{RAHP}, which is calculated as shown in equation (5.7). (2) The annual HR_{LDHP} and COP_{LDHP} which are calculated as shown in equations (5.8) and (5.20), respectively. (3) The annual COP of the H-M-LDAC system ($COP_{H\text{-}M\text{-}LDAC}$), which is calculated as follows.

$$COP_{H\text{-}M\text{-}LDAC} = \frac{q_{air}}{\left(\frac{P_{comp,LDHP} + P_{comp,RAHP} + P_{fans}}{0.33} \right)} \tag{5.21}$$

where, q_{air} is the total (sensible and latent) cooling load of the supply air stream, and W_{fans} includes the fans power for the supply and exhaust ducts, the air-cooled condenser of the RAHP, the auxiliary condenser/evapoarator of the LDHP. It is worth mentioning that the electrical-thermal conversion coefficient is assumed to be 0.33 in the current chapter.

5.7 RESULTS AND DISCUSSION

5.7.1 Annual performance of LDHP and RAHP

The annual hourly temperature lifts for the RAHP and LDHP are shown in Figure 5.3. The temperature lift for the LDHP ($T_{lift,LDHP}$) is found to be higher than that for the RAHP ($T_{lift,RAHP}$) year round. This is because although the evaporating temperature for the LDHP (~17ºC) is higher than that for the RAHP (~13ºC), the condensing temperature for the LDHP is significantly higher than the RAHP. This is because the LDHP simultaneously covers the heating and cooling requirements of the desiccant solution, which means that the LDHP is operated at high condensing temperatures in order to heat the diluted desiccant up to 50ºC before being supplied to the regenerator. In addition, it can be seen from Figure 5.3 that unlike the $T_{lift,RAHP}$ which fluctuates depending on the ambient conditions, the $T_{lift,LDHP}$ is almost constant during all operating conditions. The fluctuation of the $T_{lift,RAHP}$ is because the condenser of the RAHP is air cooled, which means that the condensing temperature depends on the ambient air temperature. On the other hand, the evaporating and condensing temperatures of the LDHP are mainly determined based on the desiccant solution set points which are maintained constant, as previously mentioned, except for the startup of the system and the few cool operating hours where the evaporating temperature is determined based on the ambient temperature as shown in equation (5.11).

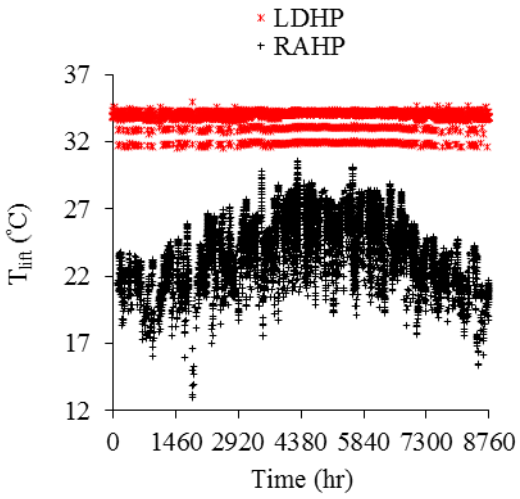

FIGURE 5.3. The annual hourly temperature lifts for the RAHP and LDHP.

Figure 5.4 shows the annual hourly values and the frequency of occurrence for the COP_{LDHP} and COP_{RAHP}. Although $T_{lift,RAHP}$ is lower than $T_{lift,LDHP}$, it is found that the COP_{LDHP} is higher than the COP_{RAHP}. The COP_{RAHP} lies in the range of 3.8-6.8, while the COP_{LDHP} lies in the range of 4.2-10.6. This is expected due to the fact that the LDHP provides simultaneous heating and cooling for the desiccant solution, which means that the LDHP is operated in a more energy efficient manner compared to the RAHP which provides only cooling for the return air. It is found that the ambient air conditions have an opposite influence on the COP_{LDHP} compared with the COP_{RAHP}, as can be seen from Figure 5.4(a). The COP_{RAHP} is found to decrease during the hot summer months, and improves during the mild winter months. This is expected for the RAHP, as the higher the ambient air temperature the higher the condensing temperature, which decreases the COP_{RAHP}. On the other hand, the COP_{LDHP} is found to have an opposite trend, where it improves during the hot summer months and decreases during the mild winter months.

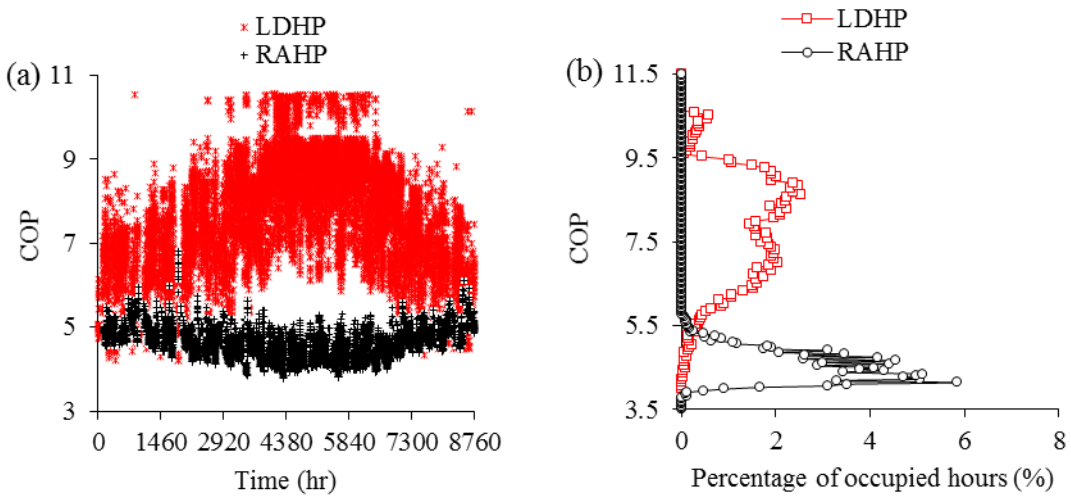

FIGURE 5.4. The (a) annual hourly values and (b) frequency of occurrence for the COP_{LDHP} and COP_{RAHP}.

As previously discussed, there are two operating modes for the LDHP (Case A and Case B). It is necessary to track the operating mode of the LDHP in order to assure that the heating and cooling requirements of the desiccant solution are efficiently matched with the condenser and evaporator loads of the LDHP at different operating condition. As can be seen from Figure 5.5, it is found that the LDHP operates at Case A operating mode for 95% of the operating hours, and operates at Case B for 5% of the operating hours. In Case A, the solution cooling requirements range from 30% to 100% of the evaporator load, depending on the operating conditions, with an average value of 77%. While in Case B, the condenser load ranges from 100% to 130% of the solution heating requirements, depending on the operating conditions, with an average value of 106%. It is worth mentioning that this shows a potential for improving the COP_{LDHP} by using the available cooling energy when the LDHP operates at Case A to provide a portion of the sensible cooling required for the return air. This is expected to cause an observable improvement in the energy efficiency of the LDHP, and consequently in the energy efficiency of the H-M-LDAC system. This point is recommended to be investigated in detail in future work.

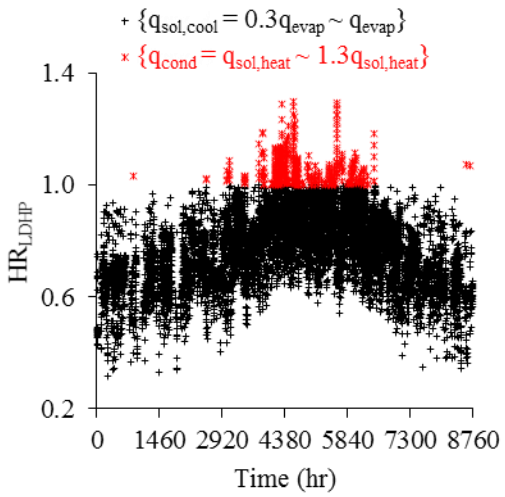

FIGURE 5.5. The hourly annual heat ratio between the solution heating and cooling requirements, and the evaporator and condenser loads of the LDHP (HR_{LDHP}).

5.7.2 Annual performance of H-M-LDAC system

After evaluating the performance of the LDHP and RAHP, the performance of the whole system is analyzed in the current section. Figure 5.6 shows the annual hourly values and frequency of occurrence for the COP of the H-M-LDAC system ($COP_{H\text{-}M\text{-}LDAC}$). It is found that the $COP_{H\text{-}M\text{-}LDAC}$ is not maintained within specific range year around. The H-M-LDAC system operates for approximately 15%, 21% and 63% of the operating hours at $Mode_{sensible}$, $Mode_{latent}$ and $Mode_{total}$, respectively. It is clear from Figure 5.6 that the operating mode has a significant impact on the $COP_{H\text{-}M\text{-}LDAC}$, where the $COP_{H\text{-}M\text{-}LDAC}$ is the lowest during $Mode_{latent}$ and the highest during $Mode_{sensible}$.

Since the $COP_{H\text{-}M\text{-}LDAC}$ is dependent on both the outdoor air conditions, and the cooling and dehumidification requirements of the conditioned space, the $COP_{H\text{-}M\text{-}LDAC}$ is plotted versus the cooling load in order to have a better understanding of the performance of the H-M-LDAC system, see Figure 5.7. It can be seen that the $COP_{H\text{-}M\text{-}LDAC}$ is strongly correlated with the cooling load when the H-M-LDAC system operates at either $Mode_{latent}$ or $Mode_{total}$, with larger slope during $Mode_{total}$ compared with $Mode_{latent}$. It can be seen that the $COP_{H\text{-}M\text{-}LDAC}$ is high during $Mode_{sensible}$ which is believed to be due to the following. The H-M-LDAC system is controlled using an ON/OFF control methodology, as previously mentioned. During $Mode_{sensible}$, the LDHP is turned off; however, the desiccant

solution stream might still cool and dehumidify the fresh air stream for a few time steps, depending on the operating conditions, but at lower capacity due to the quick variations that would occur in the dilute and concentrate desiccant solution streams when the LDHP is turned off. Thus, although there is no energy consumed by the LDHP during $Mode_{sensible}$, the desiccant cycle causes a cooling effect for the fresh air stream, which when added to the sensible cooling caused by the RAHP will result in high $COP_{H\text{-}M\text{-}LDAC}$.

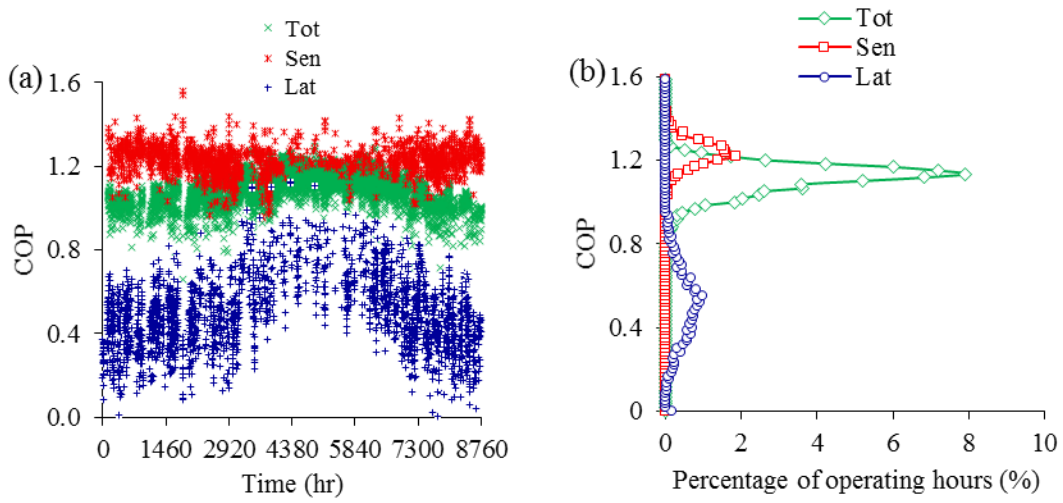

FIGURE 5.6. The (a) annual hourly values and (b) frequency of occurrence for the $COP_{H\text{-}M\text{-}LDAC}$.

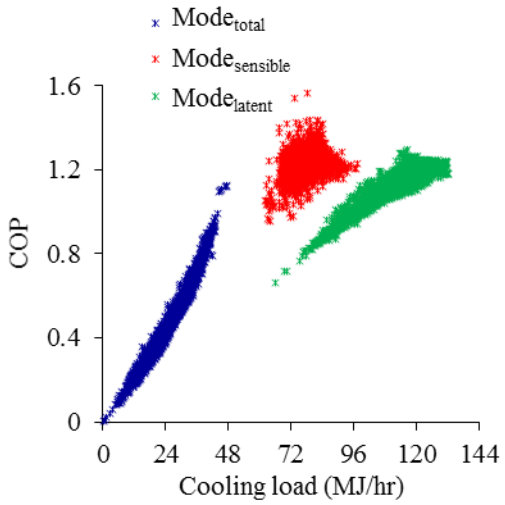

FIGURE 5.7. The annual hourly $COP_{H\text{-}M\text{-}LDAC}$ versus the annual hourly cooling loads.

5.7.3 Sensitivity analysis of LDHP and RAHP parameters

In this section, the influences of the $NTU_{cond/evap}$, $\Delta Pr_{cond/evap}$, η_{th} and ΔT_{cond} on the $COP_{H\text{-}M\text{-}LDAC}$ are evaluated. Each of the investigated parameters is varied by up to ±20% of its base value in ±5% intervals, and the equivalent percent change in the $COP_{H\text{-}M\text{-}LDAC}$ is evaluated. Figure 5.8 shows the variation of the $COP_{H\text{-}M\text{-}LDAC}$ due to the different variations performed in the $NTU_{cond/evap}$, $\Delta Pr_{cond/evap}$, η_{th} and ΔT_{cond}. It is found that ΔT_{cond} has the lowest influence on the $COP_{H\text{-}M\text{-}LDAC}$, while η_{th} has the largest influence.

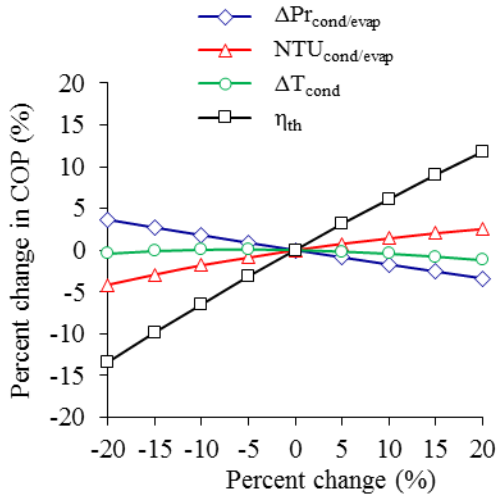

FIGURE 5.8. The influence of the $NTU_{cond/evap}$, $\Delta P_{cond/evap}$, η_{th} and ΔT_{cond} on the $COP_{H\text{-}M\text{-}LDAC}$.

5.7.4 Comparison between life cycle costs of different M-LDAC systems configurations

A schematic diagram which summarizes the M-LDAC systems configurations studied in this and previous chapters is presented in Figure 5.9. The solution cooling load was provided in all the M-LDAC systems studied by a cooling heat pump, while the heating load was provided by either: (i) a heating heat pump, (ii) a gas boiler, (iii) a solar thermal system with heating heat pump backup, (iv) a solar thermal system with gas boiler back up, or (v) sol-to-sol heat pump (i.e. the condensing heat of the solution cooling heat pump). Each of the five M-LDAC configurations was studied with and without an energy recovery ventilator (ERV) installed in the air system. In total, 10 configurations of M-LDAC systems

were investigated and compared with a conventional AC system with and without ERV. Detailed descriptions for the conventional AC and M-LDAC systems studied are presented in Chapters 3 and 4.

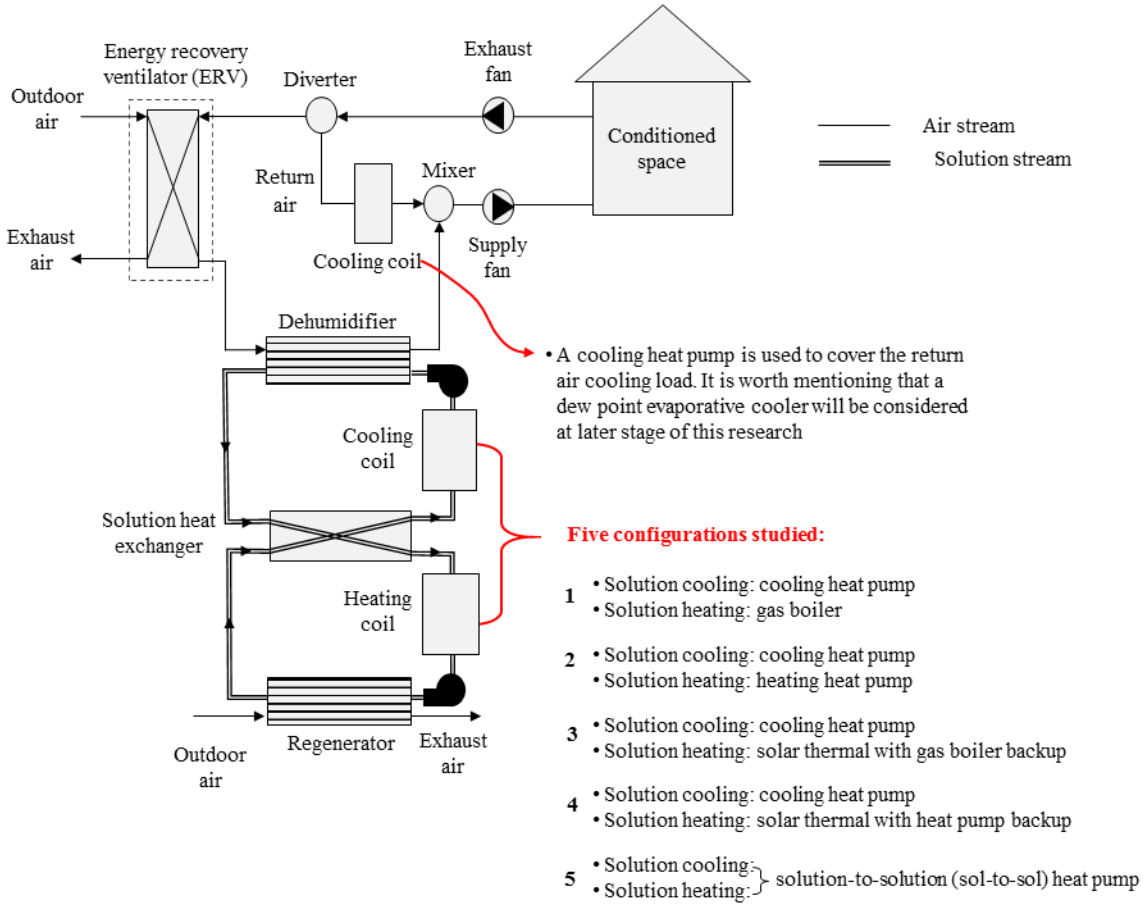

FIGURE 5.9. Schematic diagram summarizes the M-LDAC systems studied in Chapters 3, 4 and 5.

Figure 5.10 shows the life cycle costs of the M-LDAC systems studied according to the type of solution heating equipment. It is concluded that not all the configurations of M-LDAC systems are more energy efficient and economic than the conventional AC system, unlike what may be expected. In addition, the sol-to-sol heat-pump M-LDAC system is found to be the most promising configuration among the configurations studied. It is worth mentioning that some problems, related to capacity matching, were identified in the sol-to-sol heat-pump M-LDAC system. It is believed that if these problems could be solved out,

the performance of the sol-to-sol heat-pump M-LDAC system will be even more promising as will be presented in the next chapters.

Two heat pumps are used in all the configurations presented in Figure 5.9 to separately cover the solution and air cooling loads. This enables the operation of the system at either the sensible or latent modes as previously discussed in Section 5.4. It is expected that there might be some merits for using one heat pump to simultaneaously cover the air and solution cooling loads, and thus this will be studied in Chapters 6 and 7.

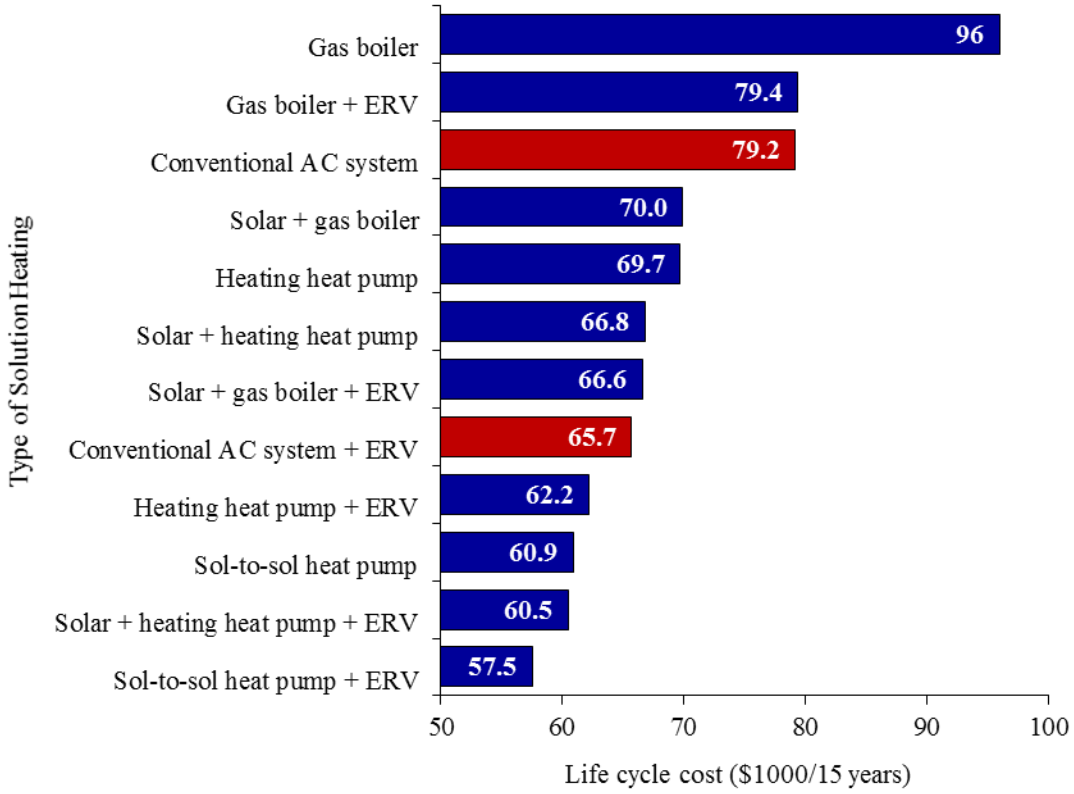

FIGURE 5.10. Life cycle costs of the M-LDAC systems studied in Chapters 3, 4 and 5.

5.8 CONCLUSION

The annual COP of a hybrid membrane liquid desiccant air conditioning (H-M-LDAC) system was evaluated in this chapter using the TRNSYS building energy simulation software for a small office building located in Miami, FL. The main advantages of the

proposed H-M-LDAC system are: (1) the elimination of the desiccant droplets carryover problem through the use of liquid-to-air membrane energy exchangers (LAMEEs) as the dehumidifier and regenerator, and (2) the simultaneous heating and cooling of the desiccant solution using a hybrid liquid desiccant heat pump (LDHP).

It is found that the annual hourly COP of the LDHP ranges between 4.2 and 10.6, with an annual average value of 7.8. The annual hourly COP of the return air heat pump (RAHP) ranges between 3.8 and 6.8, with an annual average value of 4.5. A new matching index was defined for the hybrid LDHP in this chapter, where it was found that there is auxiliary cooling energy which is provided by the LDHP for 95% of the operating hours, This is promising, because considerable reductions is expected to be achieved in the return air cooling requirements if the auxiliary cooling energy provided by the LDHP is used to precool the return air before it enters the RAHP. Based on the evaluated COPs for the RAHP and LDHP, the average annual thermal COP of the H-M-LDAC system is found to be 1. The COP of the H-M-LDAC system is found to be strongly influenced by the cooling loads and the mode of operation of the system. The influence of four heat pump parameters was investigated on the COP of the H-M-LDAC system, where the theoretical efficiency of the heat pump is found to be the most influential parameter.

The life cycle cost of the H-M-LDAC system is found to be the lowest among all the systems studied in Chapter 3 and 4, and thus it is recommended that future research focus on this system. In specific, more research is needed to be conducted on capacity matching and optimal-control strategies in heat-pump LDAC systems.

CHAPTER 6

FUNDAMENTALS OF CAPACITY MATCHING IN HEAT-PUMP LDAC SYSTEMS

6.1 OVERVIEW

It was concluded from Chapter 5 that the heat-pump LDAC system has the best energy and economic performances, compared to the other configurations studied in Chapters 3 and 4. Meanwhile, it was found that there is no clear understanding for how capacity matching can be achieved in a heat-pump LDAC system. Thus, the third objective of this thesis is to define the fundamentals of capacity matching in heat-pump LDAC systems.

In this chapter, different configurations that were used in previous heat-pump LDAC systems to achieve capacity matching are reviewed and categorized. The dimensionless capacity-matching index that is proposed in Chapter 5 (the heat ratio of the liquid desiccant heat pump) is modified and used to quantify the degree of capacity matching in a heat-pump LDAC system. A novel configuration for a heat-pump membrane LDAC system is proposed to eliminate the failure of achieving capacity matching under any operating condition. The capacity matching in this novel configuration is investigated by conducting a parametric study to evaluate the influences of the key design and operating parameters.

The manuscript in this chapter is published in the International Journal of Refrigeration.

Capacity matching in heat-pump membrane liquid desiccant air conditioning systems

(International Journal of Refrigeration, 2014, Volume 48)

Ahmed H. Abdel-Salam, Carey J. Simonson

6.2 ABSTRACT

Two improvements for liquid desiccant air conditioning (LDAC) systems are recently gaining much attention. First, one heat pump is used to simultaneously cover the solution heating and cooling loads, instead of using separate cooling and heating equipment. Second, liquid-to-air membrane energy exchangers (LAMEEs) are being investigated for use as the dehumidifier and regenerator to eliminate the carryover of desiccant droplets by the air streams. These two improvements are combined in the current work in a heat-pump membrane LDAC (H-M-LDAC) system. The focus of this paper is on matching the capacities of the heat pump evaporator and condenser to meet the solution cooling and heating needs. A comprehensive review is presented and a novel capacity matching index (CMI) is proposed. A parametric study and sensitivity analysis are performed to quantify the influences of six key design and operating parameters on the CMI and coefficient of performance (COP) of the H-M-LDAC system.

6.3 INTRODUCTION

Many research projects have been performed on LDAC technologies during the last few decades, and the focuses of these projects can be briefly divided as follows (Lowenstein, 2008). (1) Several studies focus on heat and mass transfer in the dehumidifiers and regenerators (e.g. packed beds (Bassuoni, 2011), solar regenerators (Peng and Zhang, 2011), membrane exchangers (Ge et al., 2014a; Abdel-Salam et al., 2014a), and falling-film exchangers (Mesquita, 2007)). (2) Other studies focus on the properties of pure and mixed liquid desiccant solutions (e.g. LiCl and $CaCl_2$ (Conde, 2004; Ahmed et al., 1997), and the crystallization limits of desiccant solutions (Afshin, 2010)). (3) The third focus area is on the LDAC system as a whole considering different equipment and systems configurations to heat and cool the liquid desiccant (e.g. solar thermal and/or electric heat pump (Crofoot and Harrison, 2012; Abdel-Salam et al., 2014b), solar thermal and direct/indirect evaporative cooling (Kim et al., 2013), combined heat and power (Nayak et

al., 2009), concentrated solution storage tanks (Kessling et al., 1998)). In order to foster the wide spread of LDAC systems in residential and commercial applications, some concerns still need to be addressed. There are two specific topics which have received much attention in recent years, and will be addressed in the current study:

- Desiccant droplets carryover in air streams;
- Capacity matching in heat-pump LDAC systems.

The desiccant droplets carryover in air streams can be eliminated by replacing direct-contact liquid desiccant devices with liquid-to-air membrane energy exchangers (LAMEEs), as previously discussed in Chapters 2 and 3. Using the condenser and evaporator of a heat pump to simultaneously provide solution heating and cooling energy requirements has proven to be both economic and energy efficient, as presented in Chapter 5. In heat-pump LDAC systems, the capacities of the condenser (q_{cond}) and evaporator (q_{evap}) should be equal to the required solution heating ($q_{sol,heat}$) and cooling loads ($q_{sol,cool}$), respectively. This has led to researchers adding auxiliary condensers/heaters/coolers in heat-pump LDAC systems. Although capacity matching in heat-pump LDAC systems impacts the capital costs and energy performances of these systems, it has not been fully investigated in the scientific literature (Niu et al., 2012).

The main objectives of this chapter are to: (i) review the literature of heat-pump LDAC systems focusing on capacity matching, (ii) investigate the influences of key design and operating parameters on the performance and capacity matching in a heat-pump membrane LDAC (H-M-LDAC) system, and (iii) identify key controllable parameters in achieving capacity matching. The chapter is organized as follows. Previous studies on heat-pump LDAC systems are reviewed and discussed in Section 6.4. The specifications and modeling of the H-M-LDAC system are presented in Section 6.5. In Section 6.6, a novel capacity matching index (CMI) is proposed. Important results are presented and discussed in Section 6.7, which includes a parametric study and sensitivity analysis for six design and operating parameters as follows: ambient air temperature (T_{amb}) and humidity ratio (W_{amb}), solution inlet temperature to dehumidifier ($T_{sol,deh,in}$) and regenerator ($T_{sol,reg,in}$), number of heat transfer units (NTU) and solution-to-air heat capacity ratio (Cr^{*}).

6.4 REVIEW OF CAPACITY MATCHING IN VAPOR COMPRESSION HEAT-PUMP LDAC SYSTEMS

It is found that previous studies on heat-pump LDAC systems can be categorized into three categories, based on the relation between q_{evap}, $q_{sol,cool}$, q_{cond} and $q_{sol,heat}$, as follows.

(1) In the first category, q_{evap} matches $q_{sol,cool}$, while q_{cond} is lower than $q_{sol,heat}$ (Yadav, 1995). Thus, an auxiliary heater is installed after the condenser to provide supplemental heating energy required for the regeneration of dilute desiccant solution.

(2) Similar to the first category, q_{evap} and $q_{sol,cool}$ are matched in this category, while q_{cond} exceeds $q_{sol,heat}$ (Zhang and Zhang, 2014; Niu et al., 2012; Zhang et al., 2012a; Zhang et al., 2010a; Li et al., 2005). It is found that two systems configurations were previously used to achieve capacity matching under this category.

(2.a) The most common configuration uses an auxiliary condenser after the primary condenser of the heat pump (Li et al., 2005; Zhang et al., 2010a; Niu et al., 2012; Zhang et al., 2012a). In this configuration, the heat transfer rate from the refrigerant to the dilute solution stream is controlled to meet the heat transfer rate required to regenerate the dilute solution, and the extra condensing heat is rejected using the auxiliary condenser. The auxiliary condenser can be either air or water cooled, where it was firstly introduced by Zhang et al. (2012) that using a water cooled auxiliary condenser is more energy efficient than an air cooled auxiliary condenser.

(2.b) In another system configuration studied by Zhang and Zhang (2014), the capacity matching is achieved by transferring all the heating capacity of condenser to the dilute solution. Then, the concentrated solution leaving the regenerator is cooled using an auxiliary cooler to a level which achieves capacity matching in the system.

(3) In the third category, q_{evap} and q_{cond} match $q_{sol,cool}$ and $q_{sol,heat}$, respectively. Thus, no auxiliary equipment is required to be installed in this case (Begero and Chiara, 2010,2011,2013; Zhao et al., 2011; Yamaguchi et al., 2011; Zhang et al., 2013a). There is no information mentioned about capacity matching in the studies in this category and therefore, it is not clear whether capacity matching exists under design conditions or all operating conditions of the LDAC system. It is believed that more research is required to be conducted on this configuration in order to ensure that the required air conditioning

loads are met and capacity matching is achieved under a wide range of operating conditions.

The design and operating conditions of a heat-pump LDAC system are believed to have considerable impacts on the capacity matching between the heat pump and solution energy requirements. However, there is only one study on this topic in the scientific literature by Niu et al. (2012), which focused on control methods to achieve the capacity matching by regulating the compressor rotational speed, solution flow rate, and air flow rate through an auxiliary condenser. According to the review presented in this section, four parameters (q_{evap}, $q_{sol,cool}$, q_{cond} and $q_{sol,heat}$) should be clearly identified and regulated to achieve capacity matching in heat-pump LDAC systems. A novel index related to these four parameters (i.e. CMI) is proposed in this paper, and is used to quantify the capacity matching in the proposed H-M-LDAC system under wide ranges of the six design and operating parameters previously mentioned in Section 6.3 (i.e. T_{amb}, W_{amb}, $T_{sol,deh,in}$, $T_{sol,reg,in}$, NTU, Cr^{*}).

6.5 SYSTEM DESCRIPTION AND MODELING

6.5.1 System description

A schematic diagram for the H-M-LDAC system is presented in Figure 6.1, and the specifications of the core equipment used in the system are given in Table 6.1.

Two flat-plate LAMEEs are used in the H-M-LDAC system as the dehumidifier and regenerator. In order to decrease $q_{sol,cool}$ and $q_{sol,heat}$, a solution-to-solution heat exchanger is installed to precool and preheat the solution streams leaving the regenerator and dehumidifier, respectively. It was found in a previous study that the use of a solution-to-solution heat exchanger reduces $q_{sol,cool}$ and $q_{sol,heat}$ by up to 26% in a membrane LDAC system, depending on the design and operating conditions (Abdel-Salam et al., 2013).

As previously mentioned, one heat pump is used in the H-M-LDAC system to simultaneously cover $q_{sol,cool}$ and $q_{sol,heat}$ in this study. The heat pump is equipped with an auxiliary condenser and an auxiliary evaporator. Although the use of an auxiliary

condenser to achieve capacity matching was presented in previous studies (Li et al., 2005; Zhang et al., 2010a; Niu et al., 2012; Zhang et al., 2012a), the use of an auxiliary evaporator is proposed for the first time in the current work. It is worth mentioning that the auxiliary evaporator is installed in order to enable the investigation of wide ranges of design and operating conditions.

The required solution cooling/heating energy requirements and operating temperatures under the different operating conditions are provided by regulating the refrigerant flow rate and the condensing and evaporating temperatures in the heat pump. The capacity matching is achieved by regulating the air flow rate through the auxiliary condenser/evaporator. The H-M-LDAC system operates under one of three operating modes as follows.

- Auxiliary evaporator mode:

$$q_{cond} = q_{sol,heat} \,\&\, q_{evap} > q_{sol,cool} \tag{6.1}$$

$$q_{aux,evap} = q_{evap} - q_{sol,cool} \tag{6.2}$$

- Auxiliary condenser mode:

$$q_{evap} = q_{sol,cool} \,\&\, q_{cond} > q_{sol,heat} \tag{6.3}$$

$$q_{aux,cond} = q_{cond} - q_{sol,heat} \tag{6.4}$$

- Matched capacity mode:

$$q_{cond} = q_{sol,heat} \,\&\, q_{evap} = q_{sol,cool} \tag{6.5}$$

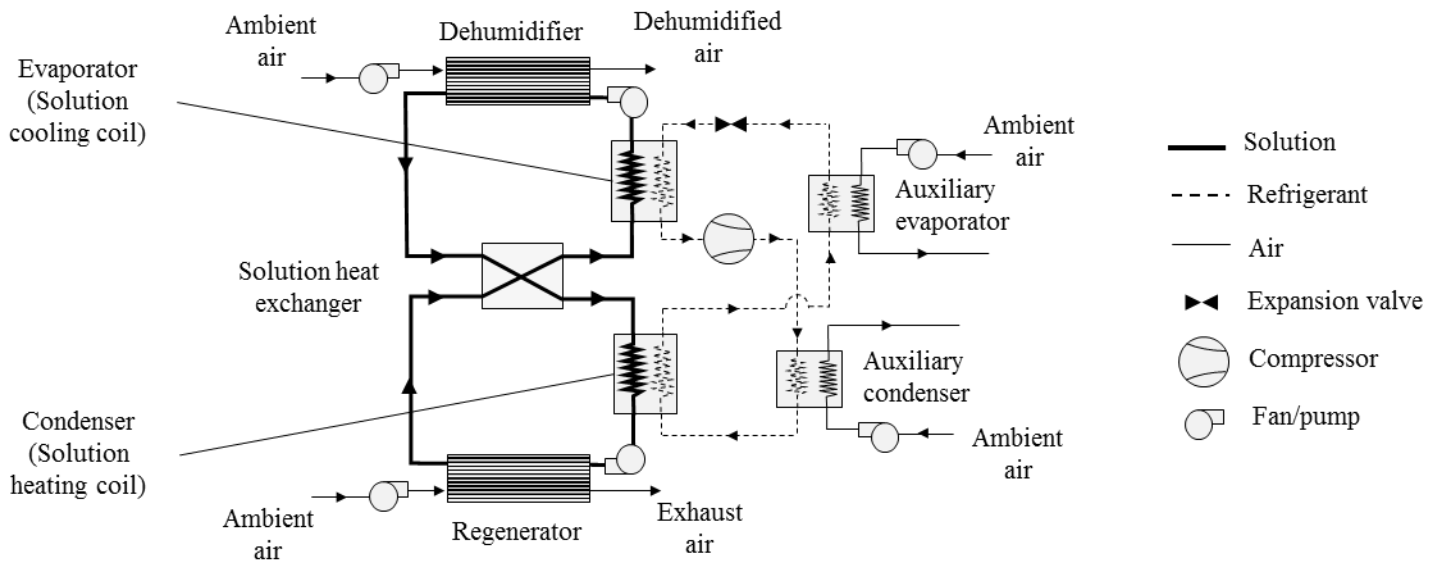

FIGURE 6.1. A schematic diagram of the heat-pump-membrane LDAC (H-M-LDAC) system.

TABLE 6.1. Specifications of the LAMEEs, semi-permeable membrane, and vapor compression heat pumps.

Parameter		Value
LAMEE	LAMEE height (m)	0.8
	LAMEE length (m)	1.06
	Air channel thickness (mm)	6.35
	Solution channel thickness (mm)	3.17
	Air pressure drop (Pa)	250
	Desiccant solution	Lithium Chloride
Membrane	Type	AY Tech. ePTFE
	Thickness (mm)	0.54
	Vapour diffusion resistance (s/m)	97
	Thermal conductivity (W/(m·K))	0.33
	Modulus of elasticity (MPa)	387
	Liquid penetration pressure (kPa)	>82
	Pore size (μm)	0.3
	Porosity (%)	85
	Tortuosity	1.56
	Membrane polymer	Polytetrafluoroethylene
Heat pump	Volumetric efficiency (%)	85
	Motor efficiency (%)	80
	Isontropic efficiency (%)	75
	Subcooling (ºC)	1
	Superheating (ºC)	2
	NTU of evaporator/condenser	2
	Air pressure drop (Pa)	375
	Refrigerant	R134a
Effectiveness of solution-to-solution heat exchanger		0.85

6.5.2 System modeling

The performance of the membrane liquid desiccant system is simulated using TRNSYS program (TRNSYS, 2010). A TRNSYS model which was developed for the system, where the LAMEE's performance is evaluated based on the analytical solution presented in Chapter 2. The performance of the heat pump is evaluated using CYCLE_D program, which was developed by the National Institute of Standards and Technology (NIST) for modeling vapor compression refrigeration systems (Brown et al., 2012). The thermodynamic properties of refrigerants are obtained in CYCLE_D from the library of REFPROP (Lemmon et al., 2010).

The performances of the evaporator and condenser of the heat pump are evaluated using the *effectiveness-NTU* method (Jin and Spliter, 2002; Karlsson and Fahlen, 2007). The refrigerant temperature during the two-phase zone is used in the thermodynamic relations between the solution and refrigerant loads (Lee and Kam, 2014). In order to check the applicability of this simplification, the ratios between the rate of heat transfer from/to the refrigerant at different zones of evaporator/condenser and total rate of heat transfer are calculated under several operating and design conditions investigated in this study. It is found that the rates of heat transfer from refrigerant in the superheated, two-phase and subcooled zones of the condenser with respect to the total condenser load are approximately 7%, 92% and 1%, respectively. In the evaporator, the rates of heat transfer to refrigerant in the two-phase and subcooled zones with respect to the total evaporator load are around 97% and 3%, respectively. This indicates that the aforementioned assumption can be used without causing significant influence on the obtained results (Jin and Spliter, 2002; Karlsson and Fahlen, 2007; Lee and Kam, 2014). It should be mentioned that a limitation in the program used to evaluate the performance of the heat pump is that a constant isentropic efficiency has to be assumed. Since the isentropic efficiency is expected to vary in a practical application under different operating conditions, the influence of the variation in isentropic efficiency on the performance of the heat-pump membrane LDAC system is recommended to be included in future research.

6.6 NOVEL CAPACITY MATCHING INDEX

The capacity matching can be achieved in the H-M-LDAC system under any operating condition by controlling the air flow rate in the auxiliary condenser/evaporator, as previously mentioned. However, this might lead to large $q_{aux,cond}$ or $q_{aux,evap}$ at some operating conditions and low system energy efficiency. A novel capacity matching index (CMI) is proposed in the current study to quantify the capacity matching in the H-M-LDAC system. The CMI depends on the ratio between $q_{sol,heat}$ and $q_{sol,cool}$ as well as the ratio between q_{cond} and q_{evap}, and it can be calculated by equation (6.6). It is worth mentioning that the CMI is defined based on the heat ratio defined in Chapter 5.

$$CMI = \frac{q_{sol,heat}}{q_{cond}} \times \frac{q_{evap}}{q_{sol,cool}} \tag{6.6}$$

Depending on design and operating conditions, the CMI may be lower than, equal to, or greater than the unity. The three operating modes of the H-M-LDAC system, previously mentioned in Section 6.5.1, can be determined based on the CMI as follows.

- CMI > 1: The heat pump produces excessive cooling which leads to the auxiliary evaporator mode (i.e. $q_{cond} = q_{sol,heat} \,\&\, q_{evap} > q_{sol,cool}$).
- CMI < 1: The heat pump produces excessive heating which leads to the auxiliary condenser mode (i.e. $q_{evap} = q_{sol,cool} \,\&\, q_{cond} > q_{sol,heat}$).
- CMI = 1: The heat pump produces both the correct amount of heating and cooling which leads to the matched capacity mode (i.e. $q_{cond} = q_{sol,heat} \,\&\, q_{evap} = q_{sol,cool}$).

6.7 RESULTS AND DISCUSSION

The performance of the H-M-LDAC system is first evaluated in this section under reference conditions, and then a parametric study and a sensitivity analysis are presented. Table 6.2 shows the reference value and variation range for each of the six design and operating parameters studied. It is worth mentioning that in the parametric study, only one parameter is varied while the other parameters are kept constant at the listed reference values.

TABLE 6.2. Reference values and variation ranges of the operating and design parameters used in the parametric study.

Parameter	Reference	Min	Max	Increment
$T_{sol,deh,in}$ (ºC)	20	14	26	2
$T_{sol,reg,in}$ (ºC)	50	41	59	3
T_{amb} (ºC)	35	26	41	3
W_{amb} (g/kg)	17.5	10	25	2.5
NTU	5	1	13	2
Cr*	4	2	6	1
$\dot{m}_{air}$ (kg/s)	0.31	-	-	-

6.7.1 Performance under reference operating conditions

Figure 6.2 shows the operating conditions of the H-M-LDAC system at the reference operating conditions given in Table 6.2. The ambient air is cooled and dehumidified as it passes through the dehumidifier, where it enters at AHRI summer conditions (i.e. 35ºC and 17.5 g/kg) (AHRI, 2005), and leaves at 21ºC and 8 g/kg. The solution stream leaves the dehumidifier at higher temperature and slightly lower concentration than it entered. The solution is then heated to 50ºC before it enters the regenerator where the moisture gained during the air dehumidification can be transferred to the regeneration air. The concentrated solution leaving the regenerator is cooled down to 20ºC before it enters the dehumidifier to decrease its water vapor pressure below that of the air required to be dehumidified.

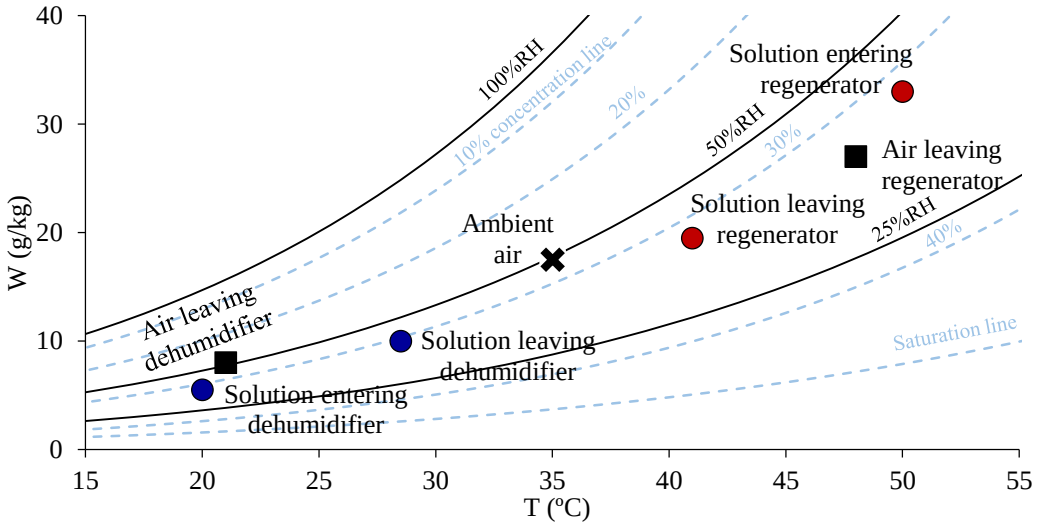

FIGURE 6.2. A schematic diagram of the operating conditions of H-M-LDAC system at reference conditions.

It is found that $q_{sol,heat}$ (12.6 kW) and $q_{sol,cool}$ (12.7 kW) are nearly equal. It is worth mentioning that $q_{sol,heat}$ and $q_{sol,cool}$ change from one design and operating condition to another, as will be presented in the next sections. Since q_{cond} is always larger than q_{evap} in any heat pump, the CMI is found to be 0.83 at the reference conditions. This indicates that the system operates at the auxiliary condenser mode, and 17% of q_{cond} needs to be rejected to ambient air using the auxiliary condenser. The coefficients of performance of the heat pump ($COP_{heat\ pump}$) and the system (COP_{system}) are calculated as shown in equations (6.7) and (6.8), respectively. The $COP_{heat\ pump}$ and COP_{system} are found to be 8.7 and 3.5, respectively, for these operating conditions.

$$COP_{heatpump} = \frac{q_{sol,heat} + q_{sol,cool}}{P_{comp}} \tag{6.7}$$

$$COP_{system} = \frac{\dot{m}_{air,deh}\,\Delta h_{air,deh}}{P_{comp} + P_{fans}} \tag{6.8}$$

where, P_{comp} and P_{fans} are the energy consumption rates of the compressor and air fans, respectively, $\dot{m}_{air,deh}$ is the air mass flow rate through the dehumidifier, and $\Delta h_{air,deh}$ is the change in the enthalpy of process air stream across the dehumidifier. It is worth mentioning that the energy consumption rate of the solution pump is negligible and thus it was not considered in equation (6.8).

The CMI and COP_{system} change under various design and operating conditions. A parametric study followed by a sensitivity study are presented in the next two sections to identify key parameters that significantly impact CMI and COP_{system}.

6.7.2 Parametric study

6.7.2.1 Solution inlet temperatures to dehumidifier and regenerator

The solution inlet temperatures to the dehumidifier ($T_{sol,deh,in}$) and regenerator ($T_{sol,reg,in}$) are key parameters to control the performance of LDAC systems. The cooling capacity and moisture removal rate of the proposed system are calculated as shown in equations (6.9) and (6.10), respectively, where both the cooling capacity and moisture removal rate increase as $T_{sol,reg,in}$ increases or $T_{sol,deh,in}$ decreases (see Table 6.3).

$$\text{Cooling capacity} = \dot{m}_{air,deh}\,\Delta h_{air,deh} \tag{6.9}$$

$$\text{Moisture removal rate} = \dot{m}_{air,deh} \Delta W_{air,deh} \quad (6.10)$$

TABLE 6.3. Influences of inlet solution temperatures to dehumidifier ($T_{sol,deh,in}$) and regenerator ($T_{sol,reg,in}$) on the moisture removal rate, cooling capacity and $COP_{heat\ pump}$.

$T_{sol,deh,in}$ (ºC)	Moisture removal rate (kg/hr)	Cooling capacity (kW)	$COP_{heat\ pump}$
26	8.9	8.7	11.9
24	9.6	9.8	10.9
22	10.2	10.8	9.7
20	10.7	11.8	8.7
18	11.3	12.8	7.8
16	11.8	13.8	7.1
14	12.3	14.7	6.5
$T_{sol,reg,in}$ (ºC)	**Moisture removal rate (kg/hr)**	**Cooling capacity (kW)**	**$COP_{heat\ pump}$**
59	12.8	13.2	6.7
56	12.2	12.8	7.3
53	11.5	12.3	7.9
50	10.7	11.8	8.7
47	9.9	11.2	9.5
44	9.0	10.6	10.5
41	8.1	10.0	11.6

Figure 6.3(a) shows that both $q_{sol,cool}$ and $q_{sol,heat}$ decrease nearly linearly as $T_{sol,deh,in}$ increases. Since the slopes of $q_{sol,cool}$ and $q_{sol,heat}$ vs $T_{sol,deh,in}$ are different, the lines will intersect at some point. In this case, the intersection occurs at about 19.5ºC. Figure 6.3(b) shows that $q_{sol,heat}$ and $q_{sol,cool}$ increase as $T_{sol,reg,in}$ increases, with $q_{sol,heat}$ having a larger slope. This indicates that $T_{sol,deh,in}$ has larger effect on $q_{sol,cool}$ than $q_{sol,heat}$, and while $T_{sol,reg,in}$ has a larger effect on $q_{sol,heat}$ than on $q_{sol,cool}$. It is found that $q_{sol,heat}$ becomes larger than $q_{sol,cool}$ when either $T_{sol,deh,in}$ or $T_{sol,reg,in}$ increases above specific values. As a result, CMI becomes close to the unity with the increase of either $T_{sol,deh,in}$ or $T_{sol,reg,in}$, as shown in Figures 6.3(c) and 6.3(d). The H-M-LDAC system is found to be operated at the auxiliary condenser mode (i.e. CMI < 1) under almost all the range of $T_{sol,deh,in}$ and $T_{sol,reg,in}$ studied. This means that at the reference conditions given in Table 6.2, the capacity matching can be achieved under wide range of $T_{sol,deh,in}$ and $T_{sol,reg,in}$ with only an auxiliary condenser (no

auxiliary evaporator needed). On the other hand, the auxiliary evaporator would be required when $T_{sol,deh,in}$ and $T_{sol,reg,in}$ are high.

Figures 6.3(c) and 6.3(d) show that COP_{system} decreases with either the decrease of $T_{sol,deh,in}$ or the increase of $T_{sol,reg,in}$. The decrease in COP_{system} when $T_{sol,deh,in}$ decreases can be explained as follows. The heat pump operates at higher temperature lift with the decrease of $T_{sol,deh,in}$, and thus $COP_{heat\ pump}$ decreases as given in Table 6.3. In addition, it can be seen from Figure 6.3(c) that the CMI considerably decreases below the unity with the reduction of $T_{sol,deh,in}$. This indicates that, besides the decrease of $COP_{heat\ pump}$, more energy will be consumed at low $T_{sol,deh,in}$ to reject the extra condensing heat. On the other hand, Figure 6.3(d) shows that although CMI becomes closer to the unity with the increase of $T_{sol,reg,in}$, it is accompanied with the decrease of COP_{system}. The main reason is that the increase of $T_{sol,reg,in}$ results in less improvement in the cooling capacity of the H-M-LDAC system compared to the decrease of $T_{sol,deh,in}$. The small increase in cooling capacity with increasing $T_{sol,reg,in}$ is only attributed to the improvement in the moisture removal rate due to the increase of solution concentration at dehumidifier inlet. In addition, $COP_{heat\ pump}$ decreases considerably with the increase of $T_{sol,reg,in}$, as given in Table 6.2, due to the increase of temperature lift. Thus, although the capacity matching improves with the increase of $T_{sol,reg,in}$, the energy required to operate the system increases at higher rate, which results in the decrease of COP_{system}.

In summary, the higher the $T_{sol,deh,in}$ and $T_{sol,reg,in}$, the closer CMI to the unity, which means that the capacity matching in the H-M-LDAC system improves. On the other hand, the COP_{system} improves only as $T_{sol,deh,in}$ increases, while the COP decreases with the increase of $T_{sol,reg,in}$. It can be concluded that, in addition to their ability to control the moisture removal rate, $T_{sol,deh,in}$ and $T_{sol,reg,in}$ are key parameters to achieve more efficient capacity matching in the H-M-LDAC system. Moreover, if the moisture removal rate and capacity matching need to be controlled by regulating $T_{sol,deh,in}$ and $T_{sol,reg,in}$, both of $T_{sol,deh,in}$ and $T_{sol,reg,in}$ should be simultaneously controlled to avoid the reduction of COP_{system}.

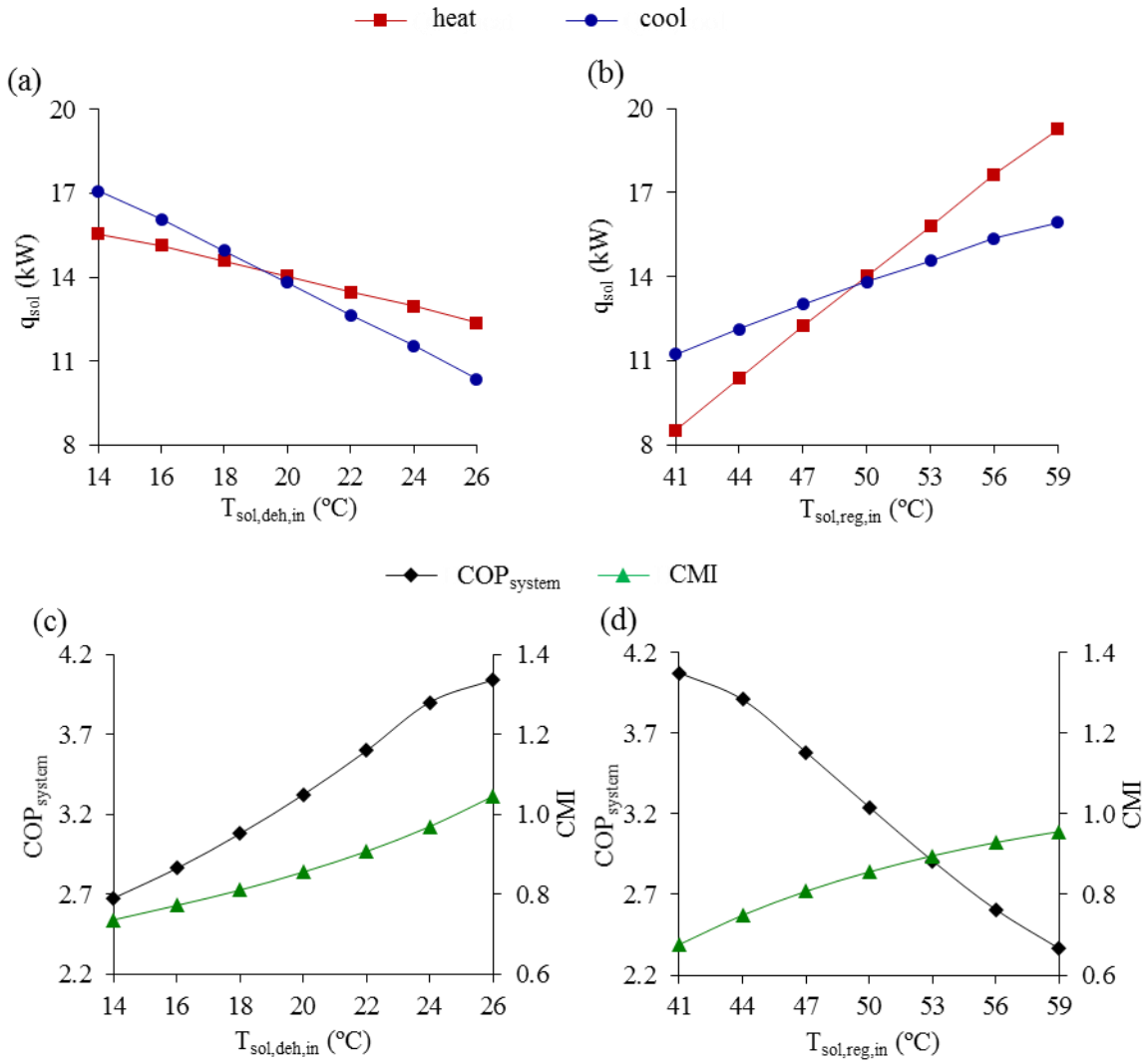

FIGURE 6.3. Influences of solution inlet temperatures to dehumidifier ($T_{sol,deh,in}$) and regenerator ($T_{sol,reg,in}$) on solution heating/cooling load (q_{sol}), capacity matching index (CMI) and coefficient of performance of H-M-LDAC system (COP_{system}).

6.7.2.2 Ambient air temperature and humidity ratio

The influences of ambient air temperature (T_{amb}) and humidity ratio (W_{amb}) on the moisture removal rate and cooling capacity of the H-M-LDAC system are presented in Table 6.4. It is clear that T_{amb} does not have considerable influence on the moisture removal rate, while the cooling capacity increases with increasing T_{amb}. On the other hand, the increase of W_{amb} increases both the moisture removal and cooling capacity.

TABLE 6.4. Influences of ambient air temperature (T_{amb}) and humidity ratio (W_{amb}) on the moisture removal rate, cooling capacity and $COP_{heat\ pump}$.

T_{amb} (°C)	Moisture removal rate (kg/hr)	Cooling capacity (kW)	$COP_{heat\ pump}$
41	10.7	13.6	7.6
38	10.7	12.7	8.1
35	10.7	11.8	8.7
32	10.8	10.9	9.4
29	10.8	10.0	8.9
26	10.8	9.1	8.4
W_{amb} (g/kg)	**Moisture removal rate (kg/hr)**	**Cooling capacity (kW)**	**$COP_{heat\ pump}$**
25.0	14.3	14.1	8.4
22.5	13.2	13.4	8.5
20.0	12.0	12.6	8.6
17.5	10.7	11.8	8.7
15.0	9.4	10.9	8.7
12.5	8.0	10.0	8.8
10.0	6.5	9.0	8.9

Figure 6.4(a) shows that increasing T_{amb} results in the increase of $q_{sol,cool}$ and the decrease of $q_{sol,heat}$. This is attributed to the increase of temperatures of the solution streams leaving the dehumidifier and regenerator with the increase of T_{amb}, and consequently the increase of the solution temperatures at the inlets of the cooling and heating coils. Unlike $T_{sol,deh,in}$ and $T_{sol,reg,in}$, it is found that the increase of T_{amb} beyond a specific value results that $q_{sol,cool}$ becomes larger than $q_{sol,heat}$. The increase of W_{amb}, on the other hand, increases $q_{sol,heat}$ and $q_{sol,cool}$ by similar rates, as shown in Figure 6.4(b). The increase of $q_{sol,heat}$ and $q_{sol,cool}$ when W_{amb} increases is attributed to the following. More heat of phase change is released when W_{amb} increases due to the increase of the moisture removal rate. Thus, the inlet solution temperature to the cooling and heating coils increases and decreases, respectively, with the increase of W_{amb}.

Figures 6.4(c) and 6.4(d) show that T_{amb} has significant influence on the CMI, while W_{amb} has negligible effect. This is attributed to the aforementioned influences of T_{amb} and W_{amb} on $q_{sol,cool}$ and $q_{sol,heat}$. As can be seen from Figure 6.4(c), the heat pump should be equipped with an auxiliary evaporator in order to achieve the capacity matching at low T_{amb} (i.e. T_{amb}

<32ºC). For example at T_{amb} = 26ºC, the CMI is 1.26 which means that q_{evap} exceeds $q_{sol,cool}$ by 26%. It is worth mentioning that the extra q_{evap} could be used to cool the airstream after the dehumidifier.

Although the cooling achieved by the system increases when T_{amb} increases, Figure 6.4(c) shows that the increase of T_{amb} results in a significant increase in COP_{system} only until a specific value, and any further increase in T_{amb} results in the reduction of COP_{system}. This is because the operating mode of the H-M-LDAC system changes from the auxiliary evaporator mode to the auxiliary condenser mode when T_{amb} exceeds 32ºC. Thus, the energy consumed by the heat pump decreases with the increase of T_{amb} until 32ºC due to the decrease of $q_{sol,heat}$, while it increases when T_{amb} exceeds 32ºC due to the increase of $q_{sol,cool}$. In addition, it is found that although CMI significantly changes over the entire range of T_{amb} studied, the COP_{system} is more influenced when T_{amb} is below 32ºC. This is because the H-M-LDAC system operates at the auxiliary evaporator mode at low T_{amb}, which means that high airflow rates are required in the auxiliary evaporator because the difference between T_{amb} and evaporating temperature is small.

Unlike the variation of COP_{system} with T_{amb}, it is found that COP_{system} increases over the entire range of increasing W_{amb}. Although the energy required to operate the heat pump increases when W_{amb} increases, the increase of COP_{system} indicates that the cooling capacity of the system increases at a higher rate than the energy consumed to operate the system. It is worth mentioning that if a specific air humidity ratio is required to be supplied to the conditioned space, this will require the regulation of the solution operating temperatures which will lead to the change of CMI and COP_{system}.

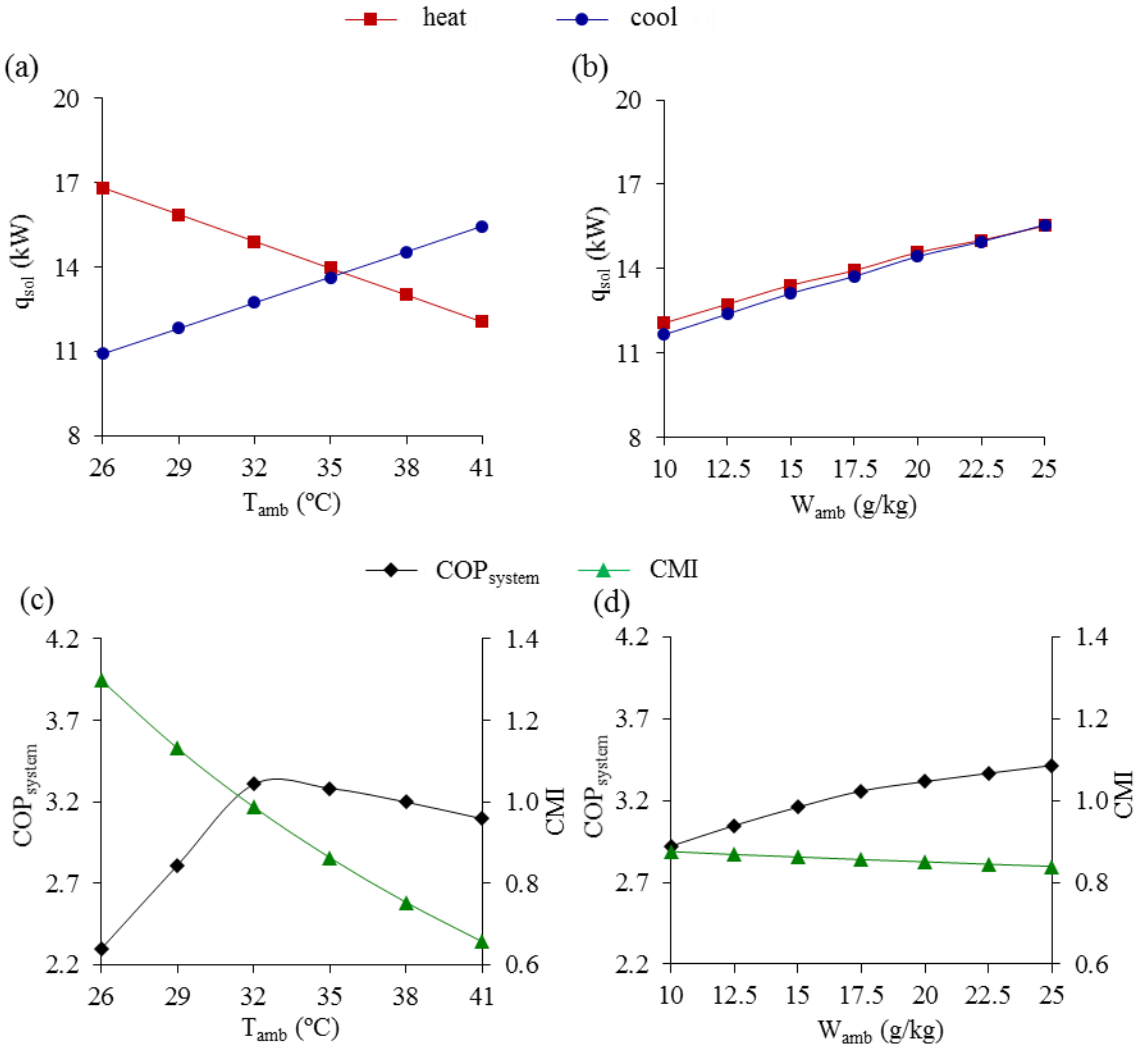

FIGURE 6.4. Influences of ambient air temperature (T_{amb}) and humidity ratio (W_{amb}) on solution heating/cooling load (q_{sol}), capacity matching index (CMI) and coefficient of performance of H-M-LDAC system (COP_{system}).

6.7.2.3 Number of heat transfer units and solution-to-air heat capacity ratio

The number of heat transfer units (NTU) and solution-to-air heat capacity ratio (Cr^*) have significant effects on the performance of the system, and they are defined as shown in equations (2.28) and (2.29), respectively. There are critical values for NTU and Cr^* that when exceeded, the rates of improvement in the performance significantly decrease, as can be seen from Table 6.5. It is worth mentioning that the air mass flow rate is kept constant at 0.31 kg/s at different values of NTU and Cr^*. The NTU is increased by increasing the

number of air and solution channels (i.e., by decreasing the face velocity of the LAMEE), and Cr^* is increased by increasing the solution mass flow rate.

TABLE 6.5. Influences of number of heat transfer units (NTU) and solution-to-air heat capacity ratio (Cr^*) on the moisture removal rate, cooling capacity and $COP_{heat\ pump}$.

NTU	Moisture removal rate (kg/hr)	Cooling capacity (kW)	$COP_{heat\ pump}$
1	4.4	5.7	8.9
3	8.7	10.0	8.5
5	10.7	11.8	8.4
7	11.9	12.8	8.4
9	12.6	13.3	8.3
11	13.0	13.7	8.3
13	13.3	13.9	8.3
Cr^*	**Moisture removal rate (kg/hr)**	**Cooling capacity (kW)**	**$COP_{heat\ pump}$**
2	8.1	9.2	8.1
3	9.9	11.0	8.5
4	10.7	11.8	8.7
5	11.1	12.2	8.8
6	11.4	12.4	9

Figure 6.5(a) shows that $q_{sol,heat}$ and $q_{sol,cool}$ increase by decreasing slopes with the increase of NTU. This is due to the rate at which the effectiveness of the dehumidifier and regenerator increase by when NTU increases (Ge et al, 2014a). On the other hand, Figure 6.5(b) shows that $q_{sol,heat}$ and $q_{sol,cool}$ increase over the entire range of Cr^* studied, which is attributed to the increase of the solution mass flow rate. It is found that the CMI only slightly changes over the entire ranges of NTU and Cr^* studied, as shown in Figures 6.5(c) and 6.5(d). The insignificant impact of NTU and Cr^* on CMI is due to the increase of $q_{sol,heat}$ and $q_{sol,cool}$ by almost the same rates, and the operation of the heat pump at nearly constant temperature lifts under the entire ranges of NTU and Cr^* studied.

Figures 6.5(c) and 6.5(d) show that NTU and Cr^* have opposite effects on COP_{system}. The COP_{system} significantly increases when NTU increases from 1 to 3, while increasing NTU results in slight improvement in COP_{system} in the range of 3 to 13. On the other hand, the increase of Cr^* results in the decrease of COP_{system}, which is attributed to the increase of

cooling capacity with Cr^* at lower rate than $q_{sol,cool}$ and $q_{sol,heat}$. It is worth mentioning that besides the reduction of COP_{system} at high Cr^*, it is not practically desirable to operate the LAMEE at high Cr^*. This is in order to avoid the deflection of membranes, which may lead to flow maldistribution and the degradation of the LAMEE's performance.

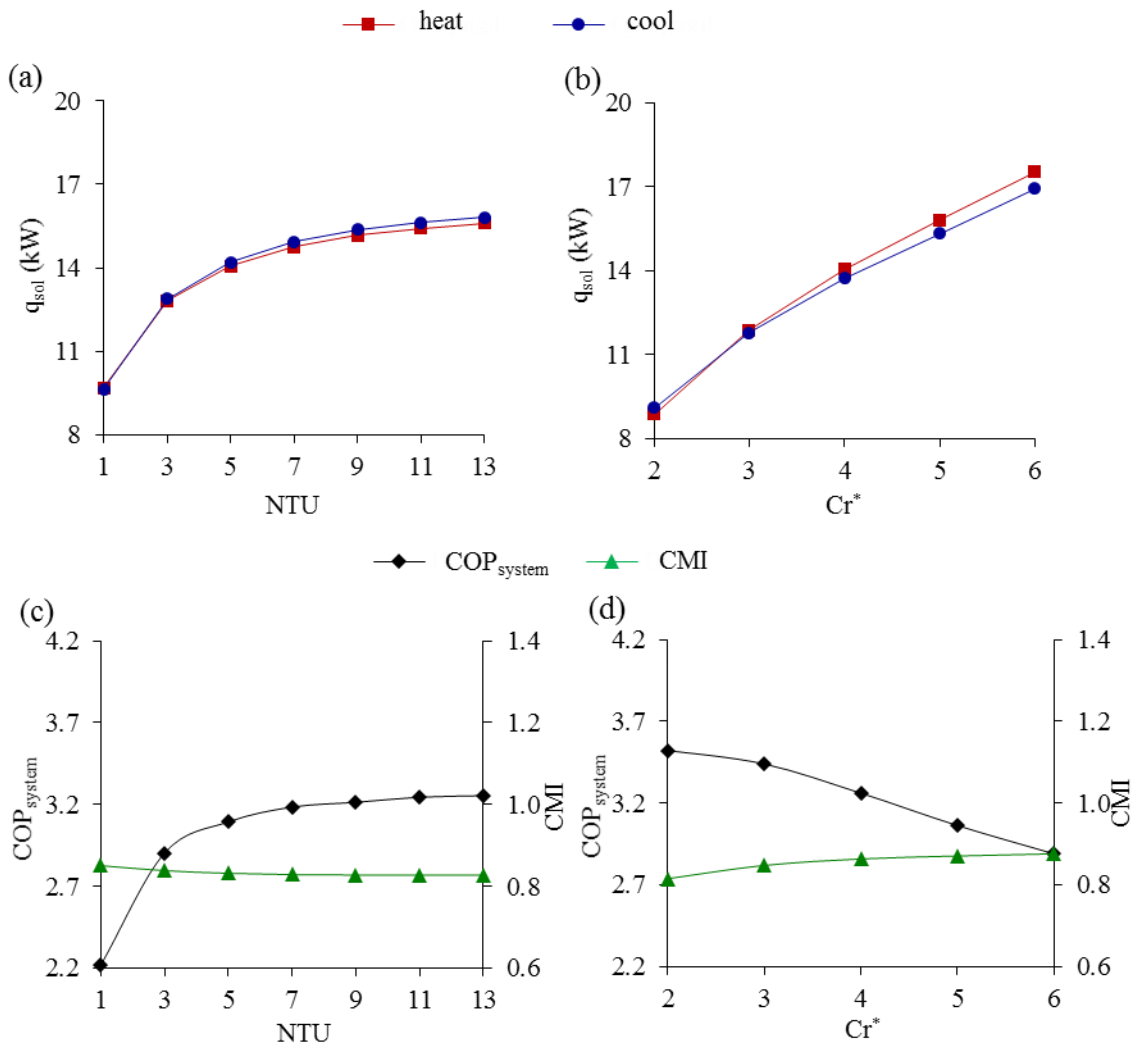

FIGURE 6.5. Influences of number of heat transfer units (NTU) and solution-to-air heat capacity ratio (Cr^*) on solution heating/cooling load (q_{sol}), capacity matching index (CMI) and coefficient of performance of H-M-LDAC system (COP_{system}).

It can be concluded that although NTU and Cr^* do not have significant influences on the capacity matching in the proposed H-M-LDAC system, they are key parameters for the moisture removal rate and COP_{system}. Thus, proper values should be selected for these

parameters during the design phase of the system. It should be considered that unlike the Cr^* which can be changed during the operation of the system by regulating the solution mass flow rate, it will not be possible to change the NTU without affecting the fresh airflow rate once the system is installed without performing major modifications.

6.7.3 Sensitivity analysis

A sensitivity analysis is presented in Figure 6.6 to show the sensitivity of the moisture removal rate, COP_{system} and CMI to the six design and operating parameters studied. The percent change in the studied parameters is limited by their minimum and maximum practical values, and thus the maximum percent changes induced in the studied parameters are different.

Figure 6.6 shows that the moisture removal rate and COP_{system} are influenced by the six parameters studied, except that T_{amb} has almost no impact on the moisture removal rate as previously mentioned. The CMI is only significantly influenced by T_{amb}, $T_{sol,reg,in}$ and $T_{sol,deh,in}$. It can be seen from Figure 6.6 that $T_{sol,reg,in}$ and $T_{sol,deh,in}$ have opposite effects on the moisture removal rate, while they change the CMI in the same direction. Thus, it can be depicted that $T_{sol,deh,in}$ and $T_{sol,reg,in}$ can be regulated to achieve simultaneous control over the moisture removal rate and capacity matching.

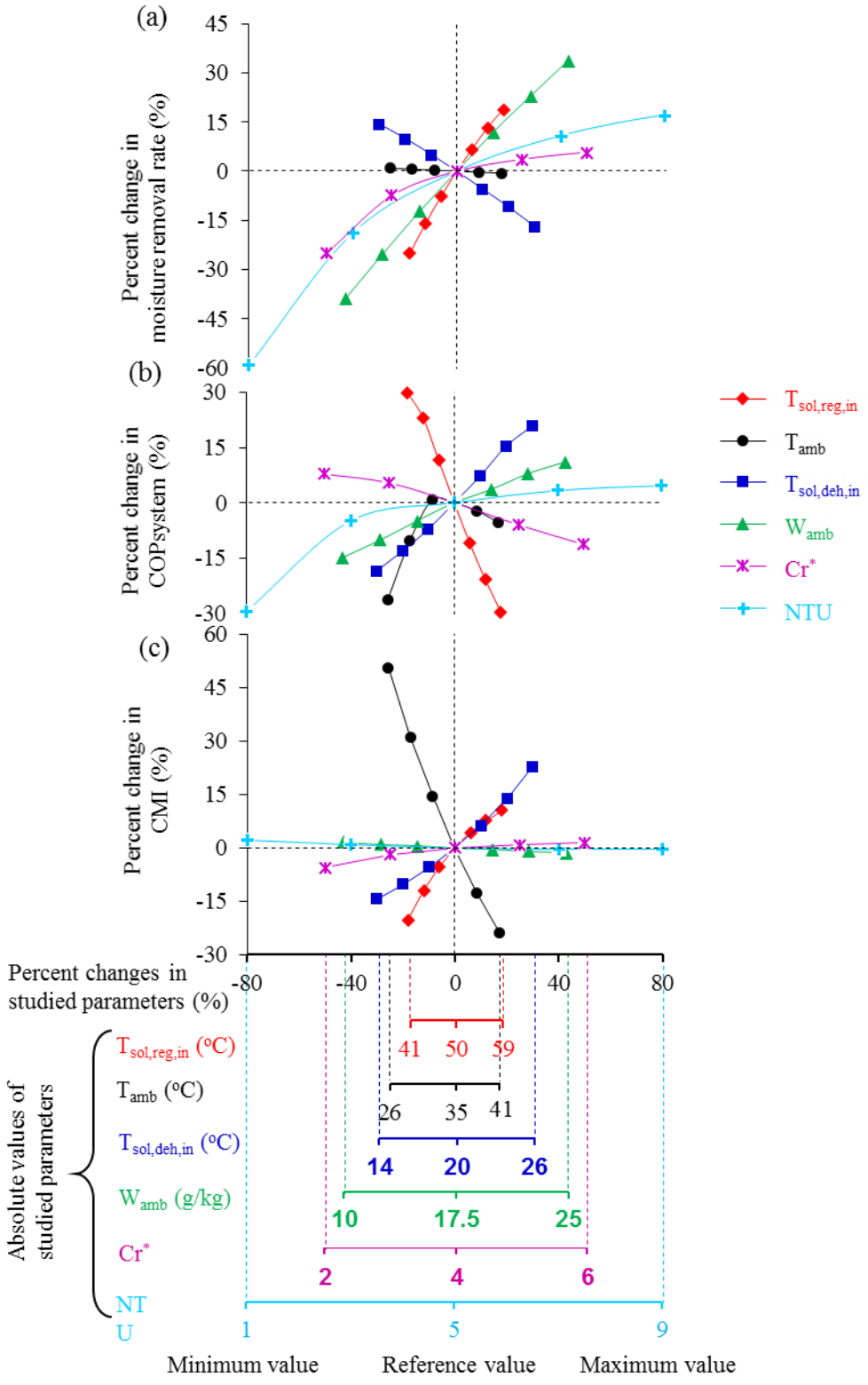

FIGURE 6.6. Sensitivity analysis of influence of the six parameters studied on the (a) moisture removal rate, (b) coefficient of performance of system (COP_{system}), and (c) capacity matching index (CMI).

6.8 RECOMMENDED TOPICS FOR FUTURE WORK

The results presented in Section 6.7 show that capacity matching in heat-pump LDAC systems is a technical issue under several operating conditions. Thus, it is recommended for future studies to explore novel techniques to achieve capacity matching in heat-pump LDAC systems such as:

(1) The use of a smaller size for the regenerator than the dehumidifier (i.e. $NTU_{regenerator} < NTU_{dehumidifier}$) is expected to result in the operation of a heat-pump LDAC system at conditions where the capacity matching index (CMI) is closer to unity than a heat-pump LDAC system with the same size for the dehumidifier and regenerator (i.e. $NTU_{regenerator} = NTU_{dehumidifier}$). This is because a higher inlet solution temperature to the regenerator ($T_{sol,reg,in}$) would be required when $NTU_{regenerator}$ is lower than $NTU_{dehumidifier}$ compared to the case when the sizes of the dehumidifier and regenerator are the same, in order to compensate the reduction in the effectiveness of the regenerator. It is worth mentioning that although the increase of $T_{sol,reg,in}$ will result in increasing the solution heating load, the solution cooling load will simultaneously increase. This is because the solution inlet temperature to the cooling coil will be higher as a result of the increase of the outlet solution temperature from the regenerator. Thus, future studies are recommended to consider the influence of the ratio between $NTU_{regenerator}$ and $NTU_{dehumidifier}$ on the COP of the system as it is expected to vary simultaneously with the CMI.

(2) The use of a concentrated desiccant solution storage tank could function as the auxiliary condenser or auxiliary evaporator to achieve capacity matching in a heat-pump LDAC system. If the heat-pump LDAC system is required to be operated at the auxiliary-condenser mode, the flow rate of the solution stream entering the regenerator could be regulated to remove all the condensing heat from the heat pump, and thus no auxiliary condenser would be needed. The solution stream leaving the regenerator should then be divided into two streams (i.e. $Cr^*_{regenerator} \neq Cr^*_{dehumidifier}$) to be directed to the dehumidifier and the solution storage tank. If the heat-pump LDAC system is required to be operated at the auxiliary-evaporator mode, the solution storage tank could be used as a source of either an auxiliary heat or a concentrated solution. Thus, the capacity of the evaporator could be matched with the solution cooling load and no auxiliary evaporator would be needed.

6.9 CONCLUSION

The capacity matching and performance of a heat-pump membrane liquid desiccant air conditioning (H-M-LDAC) system are investigated in this paper. A novel capacity matching index (CMI) is proposed and used to quantify the capacity matching in the H-M-LDAC system. The influences of six design and operating parameters on the capacity matching and performance of the proposed system are studied. The studied parameters are as follows: the ambient air temperature (T_{amb}) and humidity ratio (W_{amb}), the inlet temperatures of solution to dehumidifier ($T_{sol,deh,in}$) and regenerator ($T_{sol,reg,in}$), the number of heat transfer units (NTU), and the solution to air heat capacity ratio (Cr^*).

It is found that in addition to the commonly used auxiliary condenser (CMI<1), an auxiliary evaporator (CMI>1) may be necessary to achieve capacity matching at low T_{amb}, depending on design/operating conditions. Moreover, it is possible to eliminate the need for both the auxiliary evaporator and auxiliary condenser, and still achieve capacity matching at some design/operating conditions. The moisture removal rate and coefficient of performance of the system (COP_{system}) are considerably influenced by the six parameters studied by different rates, except for T_{amb} which has negligible influence on the moisture removal rate. The CMI is strongly influenced only by T_{amb}, $T_{sol,deh,in}$ and $T_{sol,reg,in}$, and it is not significantly affected by W_{amb}, NTU and Cr^*.

Although NTU and Cr^* do not have considerable direct influences on the CMI, these two parameters are key parameters for the moisture removal rate of the system. This means that they, indirectly, affect the CMI because the values of $T_{sol,deh,in}$ and $T_{sol,reg,in}$ required to dehumidify the air to a specific humidity ratio vary accordingly with NTU and Cr^*. Thus, all these four parameters (i.e. NTU, Cr^*, $T_{sol,deh,in}$ and $T_{sol,reg,in}$) should be considered during the design and operation of heat-pump LDAC systems to improve the CMI and COP_{system} at different climatic conditions (i.e. T_{amb} and W_{amb}).

CHAPTER 7

NOVEL STRATEGIES FOR OPTIMAL-CONTROL OF LDAC SYSTEMS

7.1. OVERVIEW

It was found in Chapter 6 that the inlet solution temperatures to the dehumidifier and regenerator are the key controllable parameters to control the humidity ratio of the air leaving the dehumidifier. In addition, it was found that the COP of the system is significantly influenced by these inlet temperatures. The fourth objective of this thesis is to develop novel strategies for optimal-control of LDAC systems, based on the findings presented in Chapter 6.

The main concept of the control strategies developed and presented in this chapter to address the fourth objective of the thesis is that there are infinite combinations of solution inlet temperatures to the regenerator and dehumidifier that can be used to meet a specific latent load. The influences of the proposed control strategies on the performances of the main components of a heat-pump membrane LDAC system, as well as the performance of the whole system, are presented and discussed in detail. Although the proposed strategies are applied in this thesis on a heat-pump membrane LDAC system, it can be useful in controlling other types of LDAC systems with different heating and cooling equipment.

The manuscript presented in this chapter was submitted in May 2015 to the International Journal of Refrigeration.

A Novel Control Strategy for A Heat-Pump Membrane Liquid Desiccant Air Conditioning System

(Submitted to the International Journal of Refrigeration in May 2015)

Ahmed H. Abdel-Salam, Carey J. Simonson

7.2. ABSTRACT

Heat-pump liquid desiccant air conditioning (heat-pump LDAC) systems can efficiently control indoor air humidity and provide healthy environments for occupants. Although several studies have been recently conducted on heat-pump LDAC systems, no information is available in the scientific literature about the control of these systems. A novel control strategy for heat-pump LDAC systems is developed and presented in this paper. The applicability of the proposed control strategy is demonstrated in this study on a heat-pump membrane LDAC system, which uses two liquid-to-air membrane energy exchangers (LAMEEs) as the dehumidifier and regenerator. Results show that the simultaneous regulation of solution inlet temperatures to the dehumidifier ($T_{sol,deh,in}$) and regenerator ($T_{sol,reg,in}$) enables the control of the system to meet the entire latent loads and to achieve one of the following additional objectives: (1) meet the entire sensible loads, (2) optimize the coefficient of performance of the system (COP_{system}), or (3) achieve capacity matching. At ambient air conditions of 35ºC and 12.5 g/kg, it is found that an improvement of up to 126% (i.e. from 1.9 to 4.3) can be achieved in the COP_{system} when it is operated under the right combination of $T_{sol,deh,in}$ and $T_{sol,reg,in}$.

7.3. INTRODUCTION

The use of a heat pump to simultaneously cover the solution heating and cooling loads is a promising way to increase the compactness and energy efficiency of LDAC systems, as discussed in Chapters 5 and 6. It is found from the comprehensive literature review presented in Chapter 6 that although several studies have been performed on heat-pump LDAC systems, no studies in the scientific literature have proposed control strategies for heat-pump LDAC systems yet, and thus this will be the focus of this paper.

The main objective of this chapter is to develop and present a novel control strategy for heat-pump LDAC systems. The control strategy is applied in this study on a heat-pump membrane LDAC system, which uses two LAMEEs as the dehumidifier and regenerator, and uses a heat pump to cover the solution heating ($q_{sol,heat}$) and cooling ($q_{sol,cool}$) loads. The proposed control strategy is based on controlling the performance of a heat-pump LDAC system by regulating its solution inlet temperatures to the dehumidifier ($T_{sol,deh,in}$) and regenerator ($T_{sol,deh,in}$). It is worth mentioning that although the proposed control strategy is investigated in this paper when applied on a heat-pump membrane LDAC system, it can be useful in controlling all types of LDAC systems, even when different heating and cooling sources are used.

7.4. SYSTEM DESCRIPTION AND MODELLING

The control strategies proposed in this chapter are applied on the system presented in Figure 6.1. Detailed information about the description and modelling of the system are presented in Section 6.5.

7.5. NOVEL CONTROL STRATEGY

A novel control strategy is developed and presented in this chapter for heat-pump LDAC systems. The main concept of this control strategy is that there are infinite combinations of solution inlet temperatures to the regenerator ($T_{sol,reg,in}$) and dehumidifier ($T_{sol,deh,in}$) that can be used to meet a specific latent load. Figure 7.1 shows a psychrometric chart which illustrates the main concept of the proposed control strategy. At ambient air condition of 35ºC and 12.5 g/kg, it can be seen that ambient air can be dehumidified to 7 g/kg using different combinations of $T_{sol,reg,in}$ and $T_{sol,deh,in}$. The alphabetical letters a, b, c, d, and e used in Figure 7.1 indicate the required combination of $T_{sol,reg,in}$ and $T_{sol,deh,in}$ to dehumidify the ambient air from 12.5 g/kg to 7 g/kg. As $T_{sol,deh,in}$ changes, the solution inlet concentration to the dehumidifier ($C_{sol,deh,in}$) should be regulated accordingly in order to reach the vapor pressure required for the solution stream entering the dehumidifier to achieve the required air dehumidification. The $C_{sol,deh,in}$ is controlled by regulating $T_{sol,reg,in}$, where at a constant $T_{sol,deh,in}$, the higher the $T_{sol,reg,in}$ the larger the $C_{sol,deh,in}$ and vice versa.

The solution heating ($q_{sol,heat}$) and cooling ($q_{sol,cool}$) loads vary according to the used combination of $T_{sol,reg,in}$ and $T_{sol,deh,in}$. Thus, $T_{sol,reg,in}$ and $T_{sol,deh,in}$ can be adjusted in order to reach a $q_{sol,heat}$ and $q_{sol,cool}$ which match the capacities of the condenser (q_{cond}) and evaporator (q_{cond}) of the heat pump, respectively. Also, $T_{sol,reg,in}$ and $T_{sol,deh,in}$ can be regulated to control the temperature of the air leaving the dehumidifier, which enables the simultaneous control over latent and sensible loads. Moreover, the COP of a heat-pump LDAC system (COP_{system}) can be optimized through the simultaneous regulation of $T_{sol,reg,in}$ and $T_{sol,deh,in}$. In summary, the main concept of the control strategy proposed in this study is that $T_{sol,reg,in}$ and $T_{sol,deh,in}$ can be simultaneously regulated to enable the control of a heat-pump LDAC system at one of three operating modes as follows:

- To cover the entire latent load and to optimize the COP_{system}.
- To cover the entire latent and sensible loads.
- To cover the entire latent load and to match $q_{sol,heat}$ and $q_{sol,cool}$ with q_{cond} and q_{evap}, respectively.

The control flow charts required to operate a heat-pump LDAC system under one of the aforementioned three operating modes are presented in Figure 7.2. It can be seen that only two initial guesses (i.e. $T_{sol,deh,in}$ and $T_{sol,reg,in}$) are required for any of the three control flow charts. In the three control flow charts presented, the desired operating condition is achieved as follows. First, $T_{sol,deh,in}$ and $T_{sol,reg,in}$ are regulated until the desired humidity ratio of air leaving the dehumidifier ($W_{air,deh,out}$) is reached. Then, $T_{sol,deh,in}$ and $T_{sol,reg,in}$ are further regulated according to the desired operating mode.

It is worth mentioning that $T_{sol,deh,in}$ and $T_{sol,reg,in}$ are controlled in this paper by regulating the refrigerant flow rate, and the condensing and evaporating pressures. This is expected to be implemented in a practical application by having an advanced simultaneous control for the compressor speed and an electronic expansion valve. Meanwhile, if no advanced control technology is available for a given heat pump, the results and concepts of the control strategy presented in this paper would still be beneficial for designers to identify the solution temperatures required to control sensible and latent loads or which achieve the optimal COP_{system} under the targeted range of operating conditions.

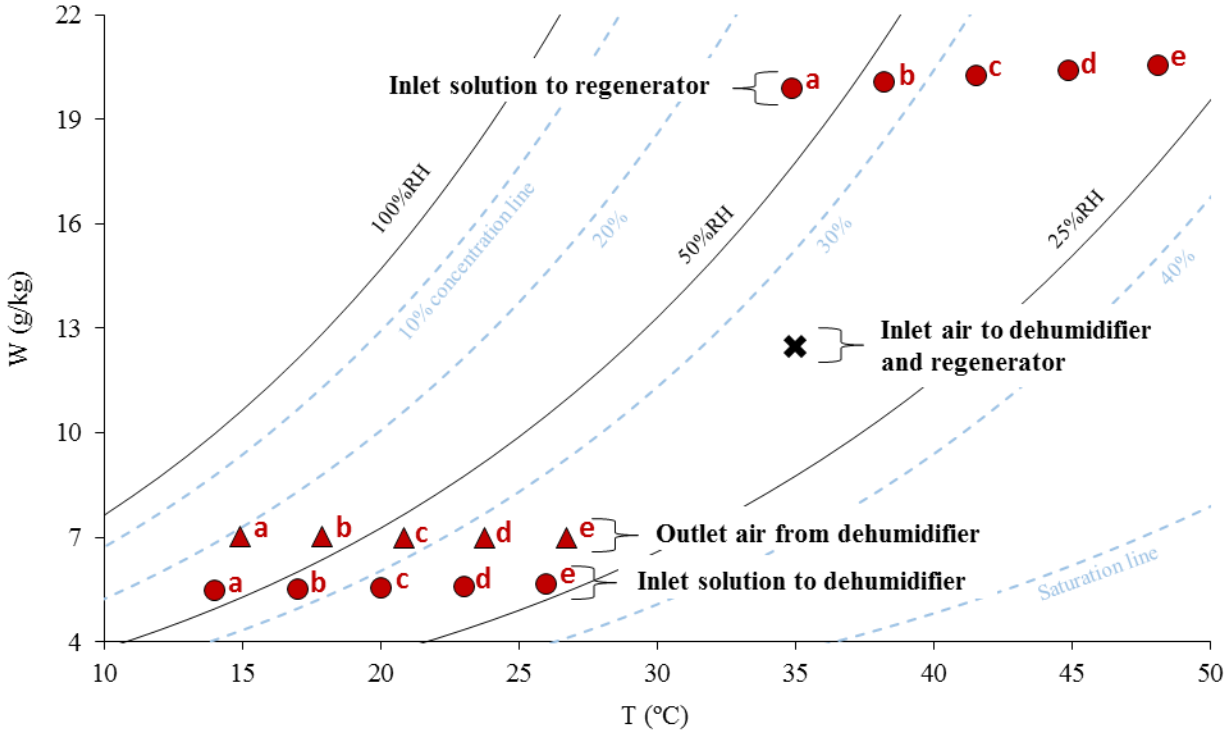

FIGURE 7.1. Example of different combinations of solution inlet temperatures to the dehumidifier ($T_{sol,deh,in}$) and regenerator ($T_{sol,reg,in}$) used to dehumidify an ambient air stream to a constant humidity ratio of 7 g/kg.

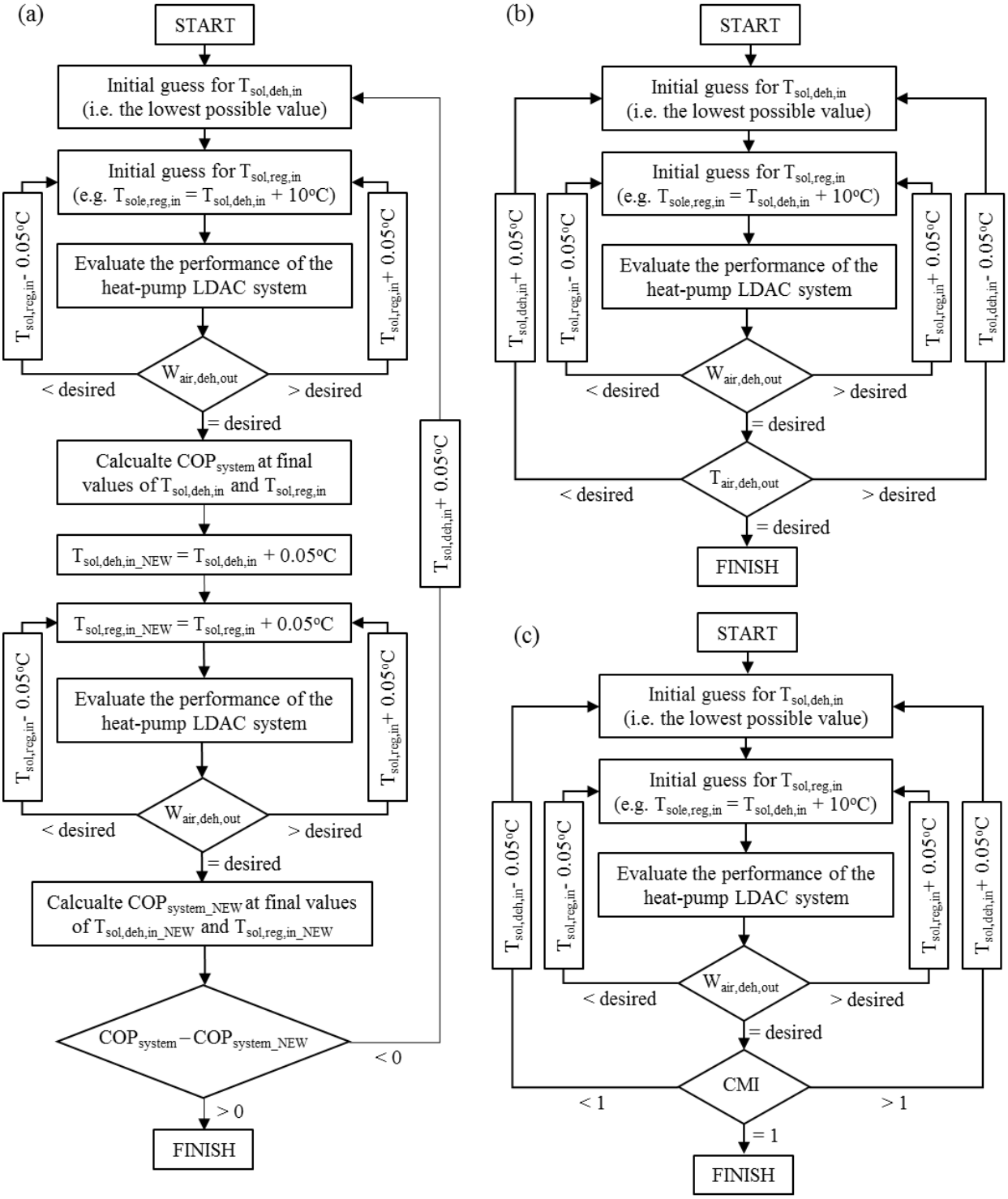

FIGURE 7.2. Control flow charts to control a heat-pump LDAC system to: (a) cover latent load and optimize COP_{system}, (b) cover latent and sensible loads, and (c) cover latent load and achieve capacity matching without auxiliary equipment.

7.6. RESULTS AND DISCUSSIONS

The novel control strategy proposed in this paper for heat-pump LDAC systems is first presented under ambient air temperature (T_{amb}) equals 35ºC and ambient air humidity ratio (W_{amb}) ranges between 12.5 g/kg and 20 g/kg at 2.5 g/kg increments. Then, the influences of several key operating/design parameters on COP_{system} are presented in a parametric study section, where the parameters investigated are as follows: (1) the humidity ratio set point; (2) the isentropic efficiency; (3) the type of refrigerant; (4) NTU_{deh}; (5) NTU_{reg}; (6) NTU_{evap}, and (7) NTU_{cond}.

The humidity ratio of the air leaving the dehumidifier ($W_{air,deh,out}$) is maintained constant at 7 g/kg under all operating conditions presented in this paper, except for when the influence of humidity ratio set point is investigated in Section 7.6.2.1. The outdoor air temperature leaving the dehumidifier ($T_{air,deh,out}$) changes according to the solution inlet temperature to the dehumidifier ($T_{sol,deh,in}$).

7.6.1. Detailed performance under different ambient air humidity ratios

The main objective of this section is to present a detailed thermodynamic analysis for the performance of equipment used in the heat-pump membrane LDAC system, in order to provide a clear illustration for how any of the three control scenarios proposed in Figure 7.2 can be achieved and what would be its implications on the thermodynamic performance of the system. Figure 7.3 shows a summary for the air and solution inlet conditions investigated in this section, and the performance of the heat-pump membrane LDAC system at these conditions is presented in the following sub-sections.

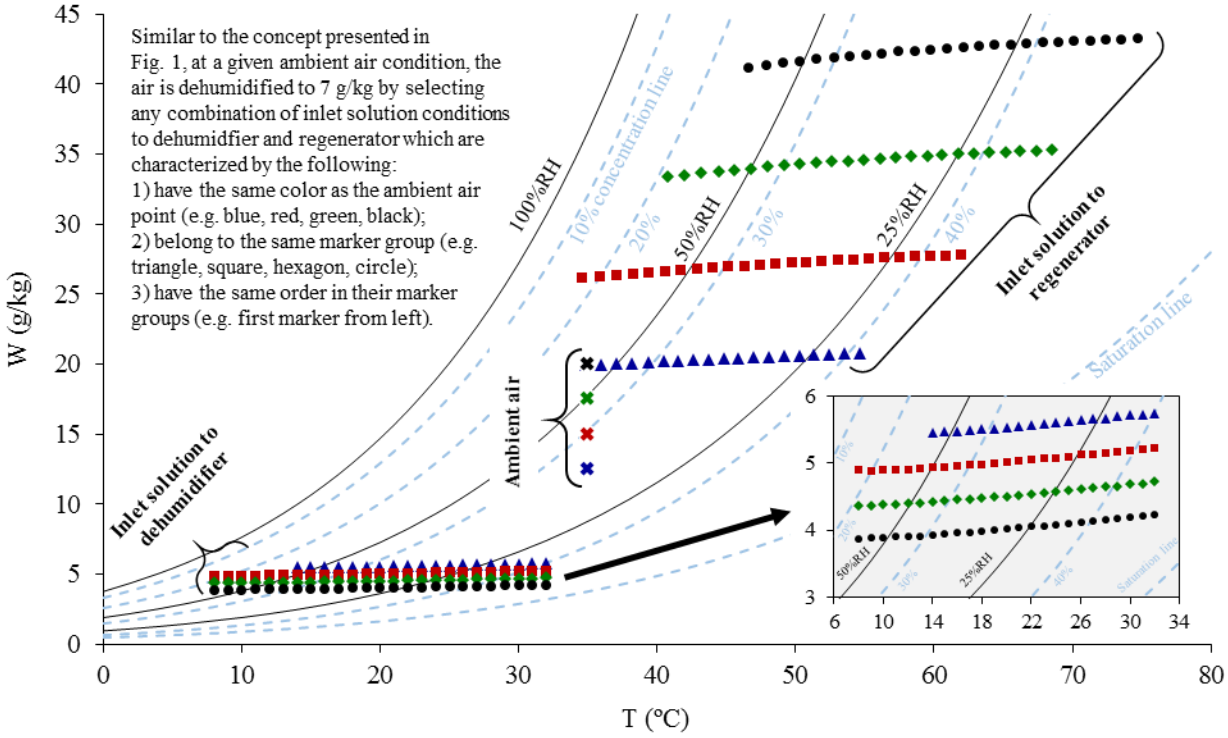

FIGURE 7.3. A summary for the air and solution operating conditions investigated in Section 7.6.1.

7.6.1.1. Desiccant solution

Figure 7.4 shows $T_{sol,reg,in}$ and $C_{sol,deh,in}$ required at different $T_{sol,deh,in}$ and W_{amb} in order to maintain $W_{air,deh,out}$ = 7 g/kg. At a constant $T_{sol,deh,in}$, $T_{sol,reg,in}$ should be increased as W_{amb} increases in order to increase $C_{sol,deh,in}$. The increase of $C_{sol,deh,in}$ with W_{amb} is necessary in order to reduce the vapor pressure of the solution stream entering the dehumidifier, and thus increase the solution ability to absorb more moisture in order to dehumidify the ambient air to 7 g/kg. Similarly, the increase of $T_{sol,deh,in}$ at a constant W_{amb} necessitates higher $T_{sol,reg,in}$ in order to increase $C_{sol,deh,in}$. In this case, the increase of $C_{sol,deh,in}$ is required to maintain the vapor pressure nearly constant with the increase of $T_{sol,deh,in}$, as the solution vapor pressure increases if $T_{sol,deh,in}$ is increased at a constant $C_{sol,deh,in}$.

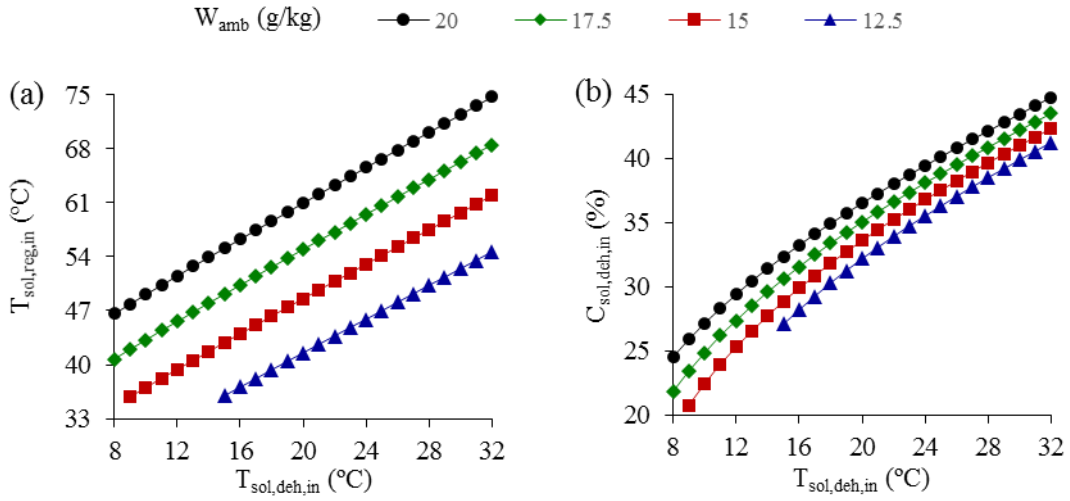

FIGURE 7.4. (a) Solution inlet temperature to regenerator ($T_{sol,reg,in}$) and (b) solution inlet concentration to dehumidifier ($C_{sol,deh,in}$), required at different solution inlet temperatures to dehumidifier ($T_{sol,deh,in}$) and ambient air humidity ratios (W_{amb}) to dehumidify ambient air to 7 g/kg.

Figure 7.5 shows $q_{sol,heat}$, $q_{sol,cool}$, and the ratio between $q_{sol,heat}$ and $q_{sol,cool}$ at different $T_{sol,deh,in}$. The ratio between $q_{sol,heat}$ and $q_{sol,cool}$ is lower than the unity at low $T_{sol,deh,in}$, while it exceeds the unity when $T_{sol,deh,in}$ exceeds a specific value depending on W_{amb}. At a constant $T_{sol,deh,in}$, the ratio between $q_{sol,heat}$ and $q_{sol,cool}$ increases with the increase of W_{amb}. Similarly, at a constant W_{amb}, the ratio between $q_{sol,heat}$ and $q_{sol,cool}$ increases with the

increase of $T_{sol,deh,in}$. It is worth mentioning that the ratio between $q_{sol,heat}$ and $q_{sol,cool}$ plays a significant role in achieving capacity matching in heat-pump LDAC systems.

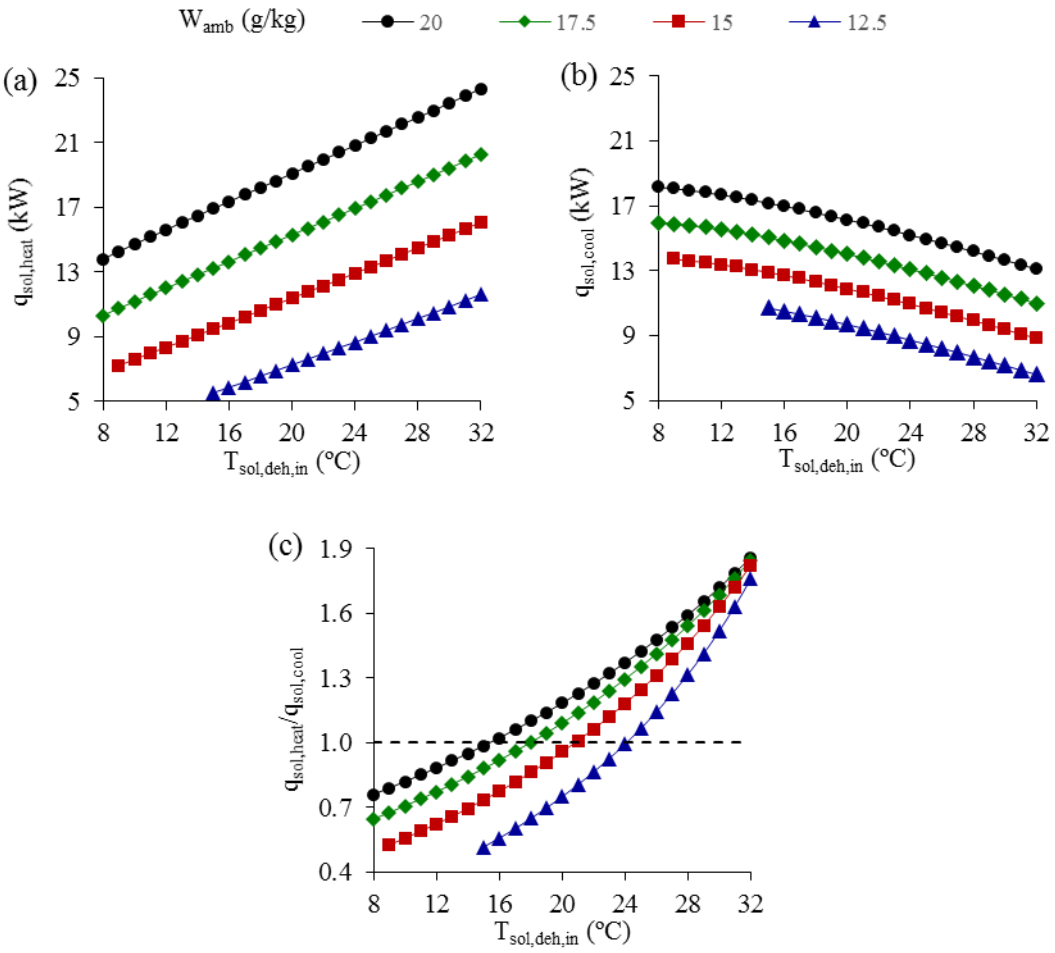

FIGURE 7.5. (a) Solution heating load ($q_{sol,heat}$), (b) solution cooling load ($q_{sol,cool}$), and (c) $q_{sol,heat}/q_{sol,cool}$ at different solution inlet temperatures to dehumidifier ($T_{sol,deh,in}$) and ambient air humidity ratios (W_{amb}).

7.6.1.2. Process air

Figure 7.6(a) shows that W_{amb} has almost negligible influence on $T_{air,deh,out}$; on the other hand, $T_{air,deh,out}$ is strongly influenced by $T_{sol,deh,in}$. If the LDAC system is expected to meet both the building's sensible and latent loads without using an auxiliary sensible cooling equipment, $T_{sol,deh,in}$ will be determined based on the value of $T_{air.deh.out}$ required to meet the entire sensible load and $T_{sol,reg,out}$ will be simultaneously regulated to ensure that the entire latent load is met. The control flow chart for this operating mode is presented in

Figure 7.2(b). While, if the objective of the LDAC system is required to meet the entire latent load and only a portion of the sensible load as may be expected in some LDAC installations, the best choice for $T_{sol,deh,in}$ is to be determined based on another control objective (i.e. optimum COP or capacity matching) as will be discussed later in association with Figure 7.10.

Figure 7.6(b) shows that the cooling capacity of the heat-pump membrane LDAC system significantly increases with the increase of W_{amb}, while it considerably decreases when $T_{sol,deh,in}$ increases. The moisture removal rate of the heat-pump membrane LDAC system increases with the increase of W_{amb}, while it is not influenced by $T_{sol,deh,in}$ as given in Table 7.1. This is because $W_{air,deh,out}$ is maintained constant at 7 g/kg when $T_{sol,deh,in}$ is varied at a constant W_{amb} by regulating $T_{sol,reg,in}$ accordingly.

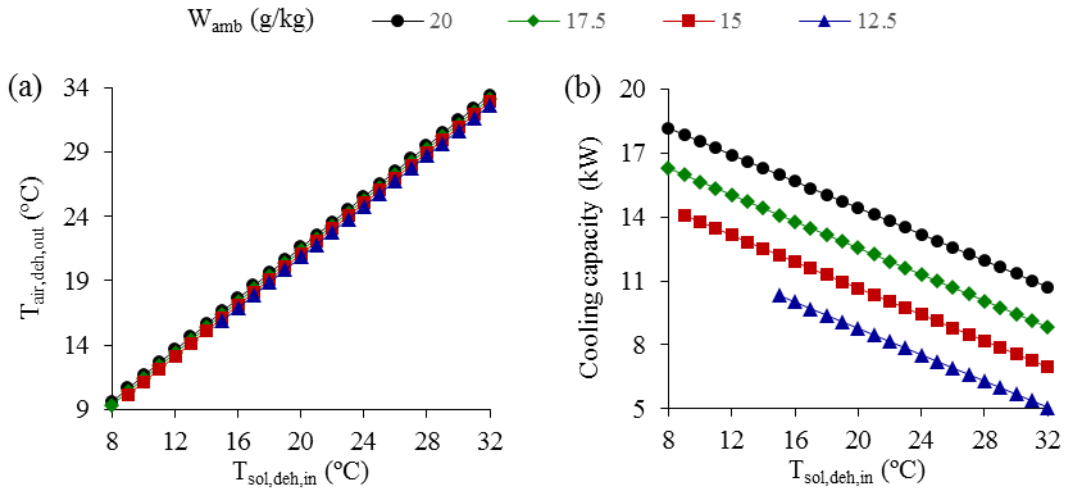

FIGURE 7.6. (a) Temperature of air leaving dehumidifier ($T_{air,deh,out}$) and (b) cooling capacity of the dehumidifier at different solution inlet temperatures to dehumidifier ($T_{sol,deh,in}$) and ambient air humidity ratios (W_{amb}).

TABLE 7.1. Moisture removal rate of the heat-pump membrane LDAC system in g/s at different solution inlet temperature to dehumidifier ($T_{sol,deh,in}$) and ambient humidity ratios (W_{amb}).

W_{amb} (g/kg)	$T_{sol,deh,in}$ (°C) [8, 9,…, 31, 32]
12.5	1.7
15.0	2.5
17.5	3.3
20.0	4.1

7.6.1.3. Heat pump

Figure 7.7 shows the variation in capacities of condenser (q_{cond}) and evaporator (q_{evap}) of the heat pump at different W_{amb} and $T_{sol,deh,in}$. Over the entire range of $T_{sol,deh,in}$ investigated at a constant W_{amb}, it is found that there are global minimum values for q_{cond} and q_{evap}. These global minimums occur when the q_{cond} and q_{evap} match $q_{sol,heat}$ and $q_{sol,cool}$, respectively, without the need for neither the auxiliary condenser nor the auxiliary evaporator. It can be seen from Figures 7.7(a) and 7.7(b) that $T_{sol,deh,in}$ which achieves the global minimums in q_{cond} and q_{evap} increases with the decrease of W_{amb} (e.g. from 22ºC at 20 g/kg to 26ºC at 12.5 g/kg). When the heat-pump membrane LDAC system operates at a $T_{sol,deh,in}$ lower than the value which results in the global minimum q_{cond} and q_{evap}, the system will be operating at the auxiliary condenser mode, while the system operates at the auxiliary evaporator mode when $T_{sol,deh,in}$ exceeds the value which results in the global minimum point.

Unlike the ratio between $q_{sol,heat}$ and $q_{sol,cool}$ which can be lower than, equal to, or greater than the unity as shown in Figure 7.5(c), the heat ratio for the heat pump (i.e. the ratio between q_{cond} and q_{evap}) must be greater than the unity. Figure 7.7(c) shows that the heat ratio of the heat pump slightly increases with the increase of $T_{sol,deh,in}$. The COP of the heat pump ($COP_{heat\ pump}$) is presented in Figure 7.7(d), where it can be seen that there is a global maximum for the $COP_{heat\ pump}$ at each W_{amb} studied. The global maximums in the $COP_{heat\ pump}$ are equivalent to the global minimums in q_{cond} and q_{evap}. The $COP_{heat\ pump}$ decreases when $T_{sol,deh,in}$ decreases below or increases above the value which leads to the global maximum $COP_{heat\ pump}$ at a given W_{amb}. This is because not all the heating and cooling energy produced by the heat pump are utilized by the solution.

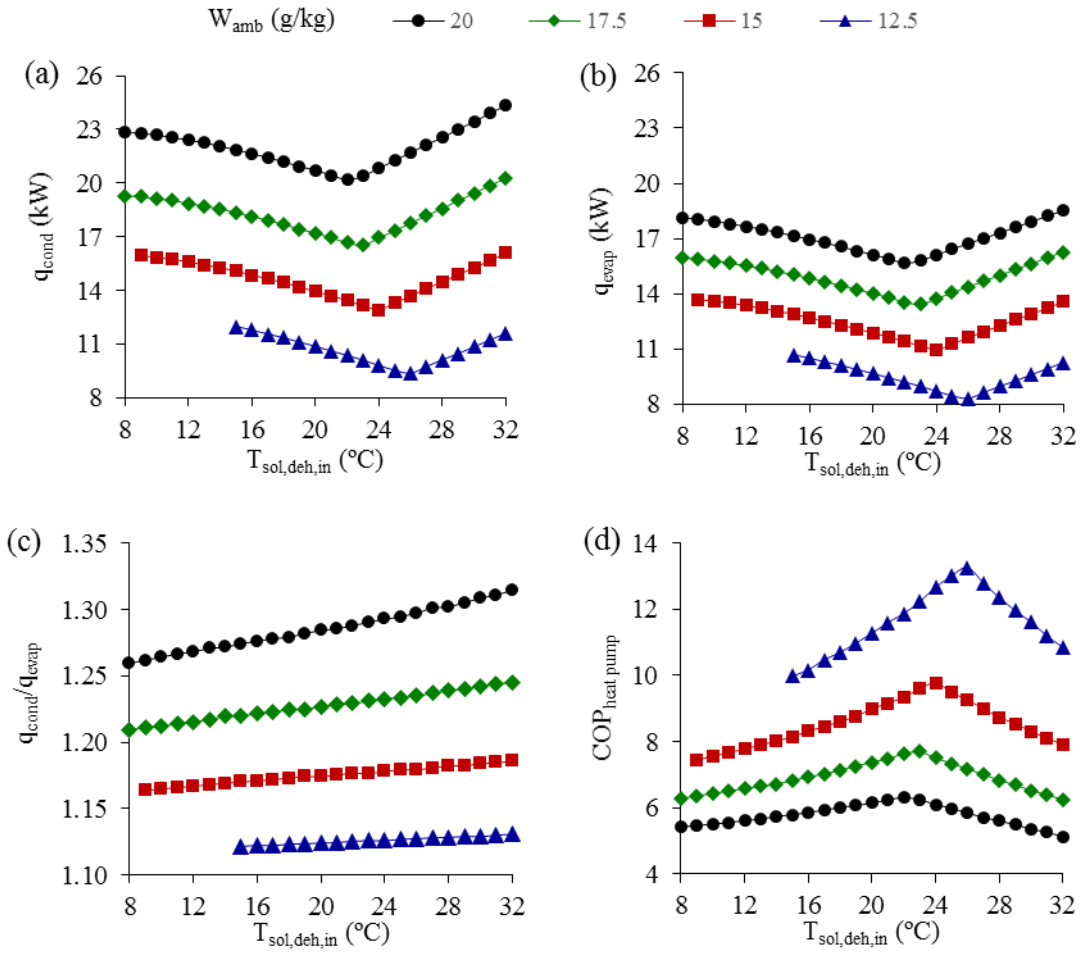

FIGURE 7.7. (a) Capacities of condenser (q_{cond}), (b) capacity of evaporator (q_{evap}), (c) heat ratio of the heat pump (q_{cond}/q_{evap}), and (d) COP of the heat pump ($COP_{heat\ pump}$) at different solution inlet temperatures to dehumidifier ($T_{sol,deh,in}$) and ambient air humidity ratios (W_{amb}).

7.6.1.4. LAMEEs

The sensible effectiveness is defined as the ratio between the actual and maximum rates of sensible heat transfer between the air and solution streams. While, the latent effectiveness is defined as the ratio between the actual and maximum rates of latent heat transfer between the air and solution streams, and the total effectiveness is defined as the ratio between the actual and maximum rates of total heat transfer between the air and solution streams. The sensible, latent and total effectivenesses are calculated as given in equations (3.1), (3.2) and (3.3), respectively.

The sensible and latent effectivenesses of the dehumidifier and regenerator LAMEEs are presented in Figure 7.8. The sensible effectivenesses of the dehumidifier and regenerator considerably decreases and increases, respectively, with the increase of $T_{sol,deh,in}$. At a given $T_{sol,deh,in}$, the sensible effectiveness of the dehumidifier decreases with the increase of W_{amb}, with more significant reductions at large $T_{sol,deh,in}$ as shown in Figure 7.8(a). While, the sensible effectiveness of the regenerator decreases with the increase of W_{amb} only when $T_{sol,deh,in}$ is greater than a specific value, and increases with W_{amb} when $T_{sol,deh,in}$ is lower than that value which can be seen from Figure 7.8(b). Since all the data points presented in this study were calculated at T_{amb} = 35ºC, then the closer either $T_{sol,deh,in}$ or $T_{sol,deh,in}$ to 35ºC, the smaller the potential for heat transfer and thus the sensible effectiveness decreases.

Figures 7.8(c) and 7.8(d) show that the latent effectivenesses for the dehumidifier and regenerator only slightly increases and decreases, respectively, with the increase of $T_{sol,deh,in}$ compared to the significant changes occur in the sensible effectivenesses. This is because at a given W_{amb}, the vapor pressures of solution streams entering the dehumidifier and regenerator only slightly varied with the increase of $T_{sol,deh,in}$. The potential between mass and heat transfer in LAMEEs can be defined using an operating parameter (H^*), equation (2.12), which was developed by Simonson and Besant (1999a). As can be seen from Figures 7.9(a) and 7.9(b), the trends observed for the H^* is inversely proportional with the sensible effectiveness.

The effectiveness of the LAMEE is strongly dependent on the number of heat transfer units (NTU), and the solution-to-air heat capacity ratio (Cr^*). The NTUs for the LAMEEs used as the dehumidifier and regenerator in this study are kept constant at 5. Although the air and solution mass flow rates are kept constant at 0.31 kg/s and 0.43 kg/s, respectively, it is found that the Cr^* varies between 3.6 and 4.5 over the entire range of operating conditions studied as presented in Figure 7.9 (c). The variation in the Cr^* is due to the change in the specific heat of desiccant solution with its temperature and concentration (Conde, 2004). It is worth mentioning that the effectiveness is significantly dependent on the Cr^* until Cr^* = 3-4 (Abdel-Salam and Simonson, 2014b; Ge et al., 2014a), while any further increase in the Cr^* beyond this range does not lead to significant influence on the effectiveness.

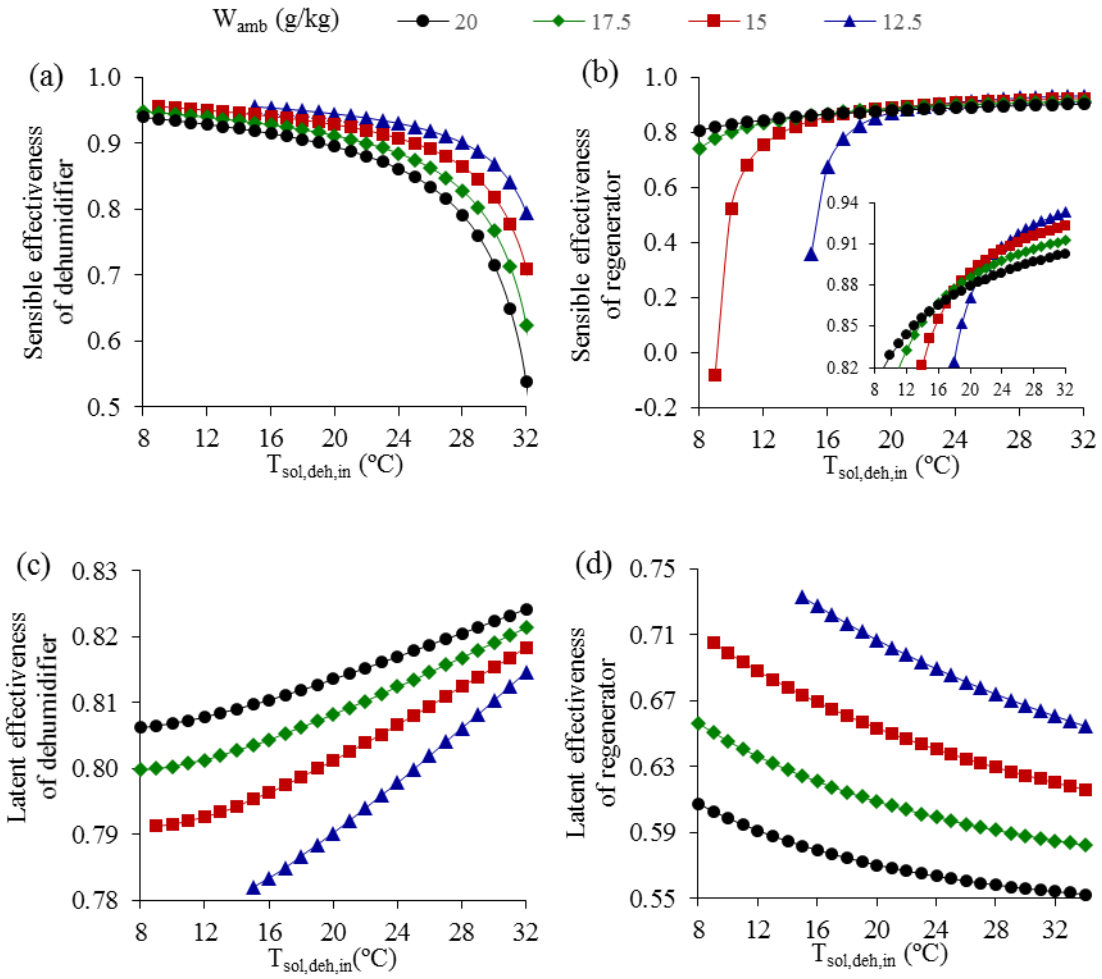

FIGURE 7.8. Sensible effectivenesses of (a) dehumidifier and (b) regenerator, and latent effectivenesses of (c) dehumidifier and (d) regenerator at different solution inlet temperatures to dehumidifier ($T_{sol,deh,in}$) and ambient air humidity ratios (W_{amb}).

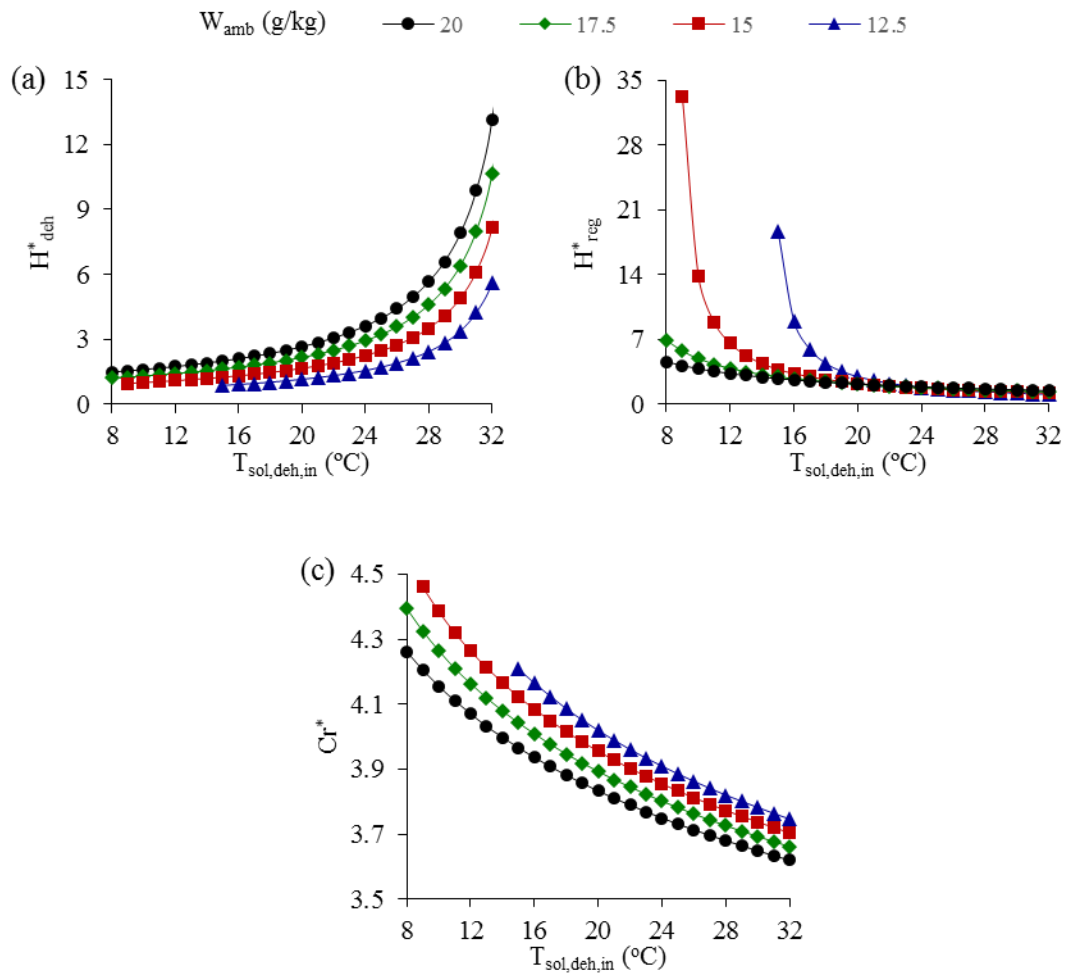

FIGURE 7.9. (a) Operating parameter of dehumidifier (H^*_{deh}), and (b) operating parameter of regenerator (H^*_{reg}), and (c) solution-to-air heat capacity ratio (Cr^*) at different solution inlet temperatures to dehumidifier ($T_{sol,deh,in}$) and ambient air humidity ratios (W_{amb}).

7.6.1.5. Coefficient of performance and capacity matching

The coefficient of performance (COP) is defined as the ratio between the useful thermal output from an air conditioning equipment/system and the electrical energy required for operation. The COP of the heat-pump membrane LDAC system (COP_{system}) and the heat pump ($COP_{heat\ pump}$) are defined in Section 6.7.1. A novel capacity matching index (CMI) is introduced in Section 6.6 to identify the operating mode of a heat-pump LDAC system (i.e. auxiliary evaporator, auxiliary condenser, or matched capacity). The CMI is defined as the ratio between $q_{sol,heat}$ and q_{cond}, multiplied by the ratio between q_{evap} and $q_{sol,cool}$.

The COP of the heat-pump membrane LDAC system (COP_{system}) and the capacity matching index (CMI) are presented in Figure 7.10. It can be seen from Figure 7.10(a) that at a constant $W_{amb,}$ the heat-pump membrane LDAC system can deliver $W_{air,deh,out}$ = 7 g/kg at a wide range of COP_{system} depending on the combination of $T_{sol,deh,in}$ and $T_{sol,reg,in}$ used. At W_{amb} = 12.5 g/kg, a maximum COP_{system} around 4.3 is achieved when $T_{sol,deh,in}$ is close from 24ºC, while the COP_{system} decreases when $T_{sol,deh,in}$ either decreases below or increases above 24ºC. At W_{amb} = 15 g/kg, it is found that COP_{system} close to the maximum achievable value (i.e. 3.5) can be achieved at a wider range of $T_{sol,deh,in}$ compared to W_{amb} = 12.5 g/kg. For instance at W_{amb} = 15 g/kg, the COP_{system} lies in the range between 3.4 and 3.5 when $T_{sol,deh,in}$ is between 16ºC and 24ºC.

Unlike both low and moderate W_{amb} (i.e. 12.5 g/kg and 15 g/kg), it is found that at W_{amb} = 17.5 g/kg and 20 g/kg, the COP_{system} continues to increase with the decrease of $T_{sol,deh,in}$, and as a result low $T_{air,deh,out}$ can be achieved at maximum COP_{system}. For instance, the highest COP_{system} at W_{amb} = 17.5 g/kg and 20 g/kg are 3.1 and 2.7, respectively, and they occur at $T_{sol,deh,in}$ = 10ºC and 8ºC, respectively. Thus, it can be concluded that the higher the W_{amb}, the lower the $T_{air,deh,out}$ can be achieved while maximizing the COP_{system}. In addition, it is found that the COP_{system} decreases with the increase of W_{amb}, which is attributed to the reduction in the $COP_{heat\ pump}$ with the increase of W_{amb}.

Figure 7.10(b) shows that for W_{amb} = 12.5 g/kg, 15 g/kg, 17.5 g/kg and 20 g/kg, the maximum COP_{system} occur at CMI = 0.88, 0.7, 0.58 and 0.6, respectively. Thus, the maximum COP_{system} at a given W_{amb} does not always occur when the capacity matching is achieved without using any auxiliary equipment (i.e. CMI = 1). It is concluded that the use of an auxiliary evaporator to achieve capacity matching is energy inefficient under all the operating conditions studied, as the COP_{system} degrades under the auxiliary-evaporating mode (i.e. CMI > 1). In addition to the degradation of the COP_{system}, the air leaves the dehumidifier at higher temperatures under the auxiliary-evaporating mode which leads to the reduction of the cooling capacity. On the other hand, the operation of heat-pump LDAC systems under the auxiliary-condensing mode (i.e. CMI < 1) at high W_{amb} results in higher cooling capacity and COP_{system} compared to the matched-capacity mode (i.e. CMI = 1).

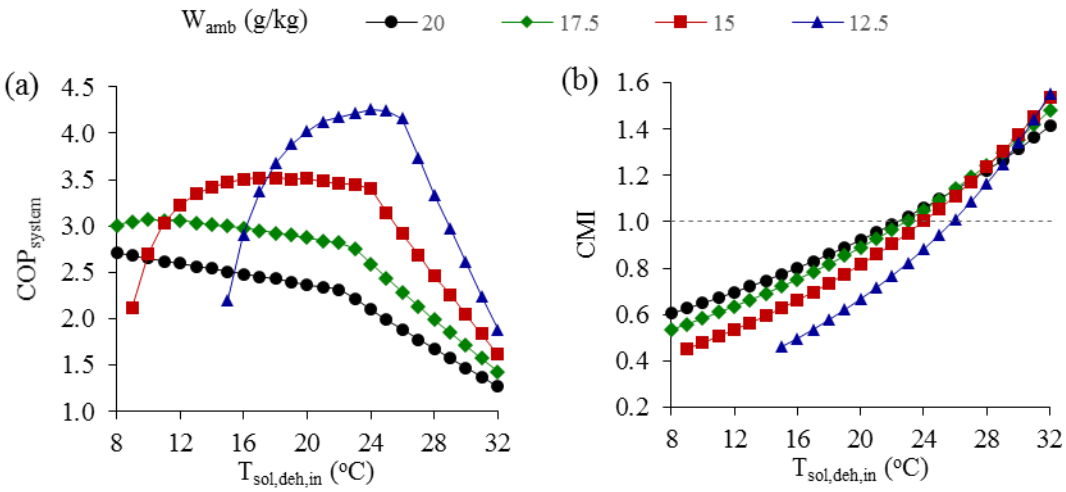

FIGURE 7.10. (a) Coefficient of performance of the H-M-LDAC system (COP_{system}), and (b) capacity matching index (CMI) at different solution inlet temperatures to dehumidifier ($T_{sol,deh,in}$) and ambient air humidity ratios (W_{amb}).

7.6.2. Parametric Study

In practice, the designer has to evaluate different scenarios for the performance of the used equipment such as the following. (1) Different values can be selected for the NTUs of the dehumidifier, regenerator, evaporator and condenser. (2) The performance of a heat pump varies according to its isentropic efficiency and the thermodynamics properties of the used refrigerant. (3) Different supply air conditions would be required to be delivered to the conditioned space depending on the space sensible and latent loads. The objective of this section is to investigate the performance of the heat-pump membrane LDAC system under various design and operating conditions.

The system is operated following the same methodology used in the aforementioned sections, which is controlling the latent load of the system using different combinations of $T_{sol,deh,in}$ and $T_{sol,reg,in}$ in order to achieve any of the three scenarios presented in Figure 7.2. Except for the parametric study which shows the influence of humidity ratio set point (i.e. Figure 7.11(a)), the humidity ratio set point is kept at 7 g/kg for the rest of parametric studies and the outdoor air conditions are kept constant at 35ºC and 12.5 g/kg. Seven key design and operating parameters are considered in this section as follows: (1) the humidity

ratio set point; (2) the isentropic efficiency; (3) the type of refrigerant; (4) NTU_{deh}; (5) NTU_{reg}; (6) NTU_{evap}, and (7) NTU_{cond}.

The NTUs are changed in this section by increasing the surface areas of the exchangers, while the air flow rates are maintained constant. No information is presented about the CMI in this section; however, the matched-capacity mode can be identified in Figures 7.11 and 7.12 at the points at which the slope of COP_{system} experiences a steep change, and the left and right of these points are the auxiliary-condenser and auxiliary-evaporator modes, respectively.

7.6.2.1. Humidity ratio set point

Figure 7.11(a) shows the influence of the humidity ratio set point on the COP_{system}. It is worth mentioning that although the temperature of the air stream leaving the dehumidifier is not presented in this section, it is expected to be around 1-2ºC higher than $T_{sol,deh,in}$ as previously presented in Figure 7.6(a). Thus, it can be seen from Figure 7.11(a) that wide range of supply air temperatures and humidity ratios can be achieved by simultaneously controlling $T_{sol,deh,in}$ and $T_{sol,reg,in}$ for a LDAC system. This shows that the control strategy proposed in Figure 7.2(b) can be used to control a heat-pump LDAC system to cover both sensible and latent loads without installing an auxiliary sensible cooling equipment. Since the variation of the humidity ratio set point at a constant $T_{sol,deh,in}$ mainly changes the latent load of the process air with no significant change in the sensible load, the COP_{system} follows similar trends to Figure 7.10(a). In general, it can be concluded from Figure 7.11(a) that the higher the humidity ratio set points, the higher the optimal COP_{system}. However, at low values of $T_{sol,deh,in}$, COP_{system} decreases as the supply humidity ratio increases.

7.6.2.2. Isentropic efficiency

Figure 7.11(b) shows that the influence of isentropic efficiency on COP_{system} becomes more significant at the operating conditions which are close from the matched-capacity mode than at the auxiliary-condenser and auxiliary-evaporator modes. This is because at either the auxiliary-condenser or auxiliary-evaporator modes, the energy consumed by auxiliary fans will have a strong contribution to the energy consumption of the system. On the other

hand, at operating conditions close from the matched-capacity mode, the energy required to operate the system will mainly depend on the compressor and thus any variation in the isentropic efficiency will have a more significant impact on the energy efficiency of the system.

7.6.2.3. Type of refrigerant

Figure 7.11(c) shows the influences of 17 types of refrigerants on the COP_{system}. It is worth mentioning that although some refrigerants result in higher COP_{system} than others, the environmental impacts of a refrigerant should be considered in addition to its thermodynamic properties. For instance, it can be seen from Figure 7.11(c) that R22 results in higher COP_{system} than R407C, while R22 is required to be phased out due to several environmental concerns and thus R407C is a better choice (EPA, 2015). A review article about the selection of refrigerants based on their thermodynamic and physical properties was conducted by Sarbu (2014); in addition, a thermodynamic analysis of refrigerants and the performance limits of vapor compression cycle based on the type of refrigerants are presented in Domanski et al. (2014).

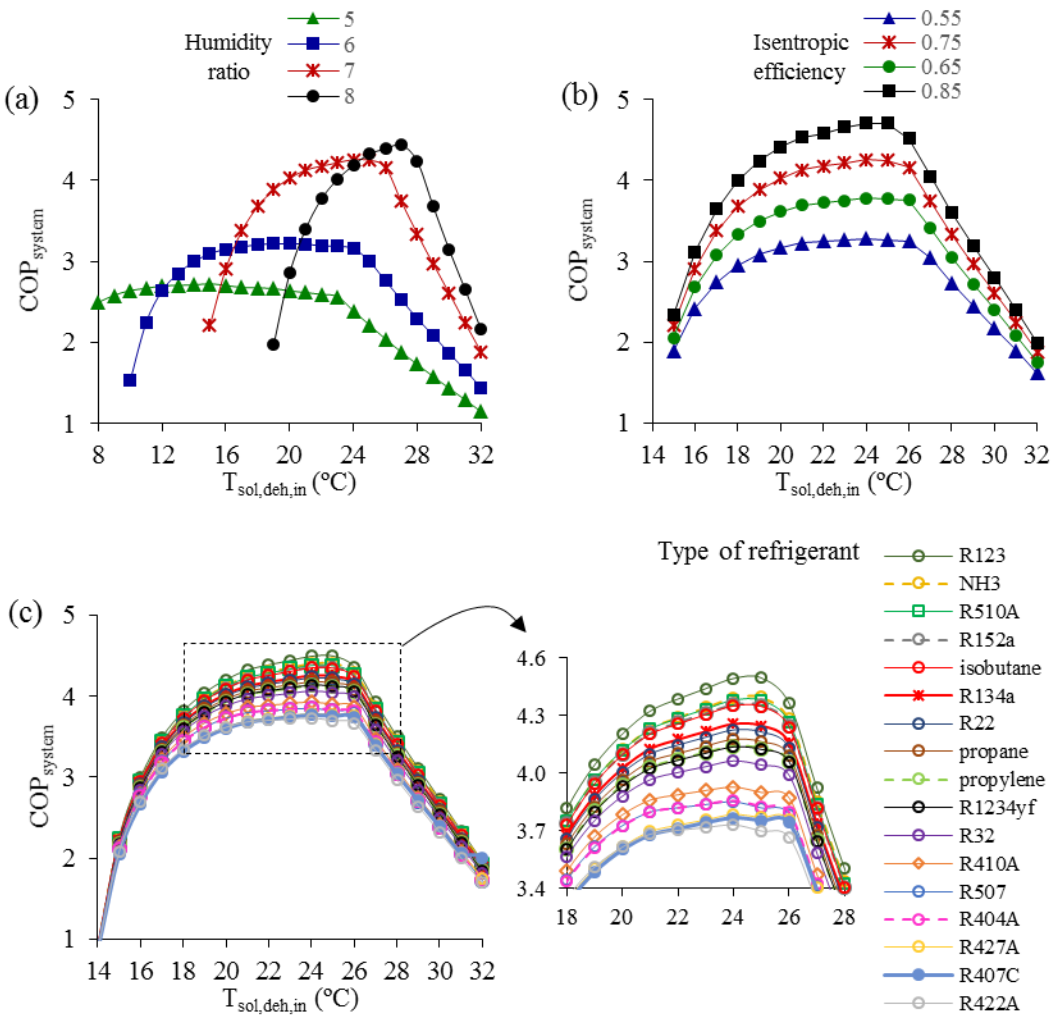

FIGURE 7.11. The influences of the NTUs of dehumidifier, regenerator, condenser and evaporator on the COP_{system} under balanced (i.e. $NTU_{deh}=NTU_{reg}$, $NTU_{evap}=NTU_{cond}$) and unbalanced (i.e. $NTU_{deh} \neq NTU_{reg}$, $NTU_{evap} \neq NTU_{cond}$) conditions.

7.6.2.4. Balanced NTU_{deh} and NTU_{reg}

Figure 7.12(a) shows that the higher NTU_{deh} and NTU_{reg}, the higher the optimal COP_{system}. However, at low values of $T_{sol,deh,in}$, COP_{system} decreases as NTU_{deh} and NTU_{reg} increase. This is attributed to the change in the effectivenesses of the dehumidifier and regenerator, which result in the change of outlet solution temperatures, and consequently the energy demand of the compressor and auxiliary fans. For instance, although higher compressor work is required at low NTUs compared to higher NTUs, lower auxiliary work is required at low NTUs because lower airflow rates are needed in the auxiliary condenser due to the larger difference between the condensing and ambient air temperatures. It can be concluded

from the results presented in Figure 7.12(a) that increasing NTU_{deh} and NTU_{reg} does not always result in high COP_{system}. For example, if the LDAC system is required to meet both the sensible and latent loads and operate at $T_{sol,deh,in}$ = 18ºC, the use of high or low NTUs for the dehumidifier and regenerator results in lower COP_{system} compared to if intermediate NTUs are to be used. This is strongly recommended to be considered by LDAC designers while sizing the equipment used in a given LDAC system.

7.6.2.5. Unbalanced NTU_{deh} and NTU_{reg}

Another possible scenario that can be considered by a LDAC designer is to select unbalanced NTUs for the dehumidifier and regenerator, as presented in Figure 7.12(b). It is found that, under almost all operating conditions, the scenario with balanced NTUs (i.e. NTU_{deh} = NTU_{reg} = 5) results in the highest COP_{system}, followed by the scenario at which NTU_{deh} is larger than NTU_{reg}. This is because the process of interest in a heat-pump LDAC system is the cooling and dehumidification that take place in the dehumidifier, while the remaining processes are required to deliver a specific solution inlet conditions for the dehumidifier. Thus, designing a heat-pump LDAC system with high NTU_{deh} results in low energy requirements to operate the remaining equipment in the system. It is worth mentioning that at $T_{sol,deh,in}$ < 16ºC, higher COP_{system} is achieved when NTU_{reg} is larger than NTU_{deh} compared to the other two scenarios (i.e. NTU_{deh} = NTU_{reg}, NTU_{deh} > NTU_{reg}). This is attributed to aforementioned explanation associated with Figure 7.12(a).

7.6.2.6. Balanced NTU_{evap} and NTU_{cond}

Figure 7.12(c) presents the influence of the NTUs of the evaporator (NTU_{evap}) and condenser (NTU_{cond}) used in the heat pump on COP_{system}. At majority of operating conditions, it is found that COP_{system} increases with the increase of NTU_{evap} and NTU_{cond}. This is expected because the effectiveness of the evaporator/condenser increases with the increase of its NTU, which results in the increase of evaporating temperature and the reduction of the condensing temperature, and thus the improve of the energy efficiency of the heat pump due a lower temperature lift. However, it is found that at $T_{sol,deh,in}$ < 16ºC the lower the NTU_{evap} and NTU_{cond}, the higher the COP_{system}. This is because lower air flow rates are required in the auxiliary condenser in the case of low NTU due to its high

condensing temperature, and consequently lower auxiliary work is consumed by the auxiliary fans.

7.6.2.7. Unbalanced NTU_{evap} and NTU_{cond}

Figure 7.12(d) shows the influences of using unbalanced NTUs for the evaporator and condenser; it can be seen that balanced NTUs achieve higher COP_{system} for almost all operating conditions than the other two scenarios studied. The higher COP_{system} for the scenario at which $NTU_{evap} > NTU_{cond}$ at $T_{sol,deh,in} < 16^{o}C$ is attributed to the low auxiliary-condenser energy consumption at this case due to its high condensing temperature.

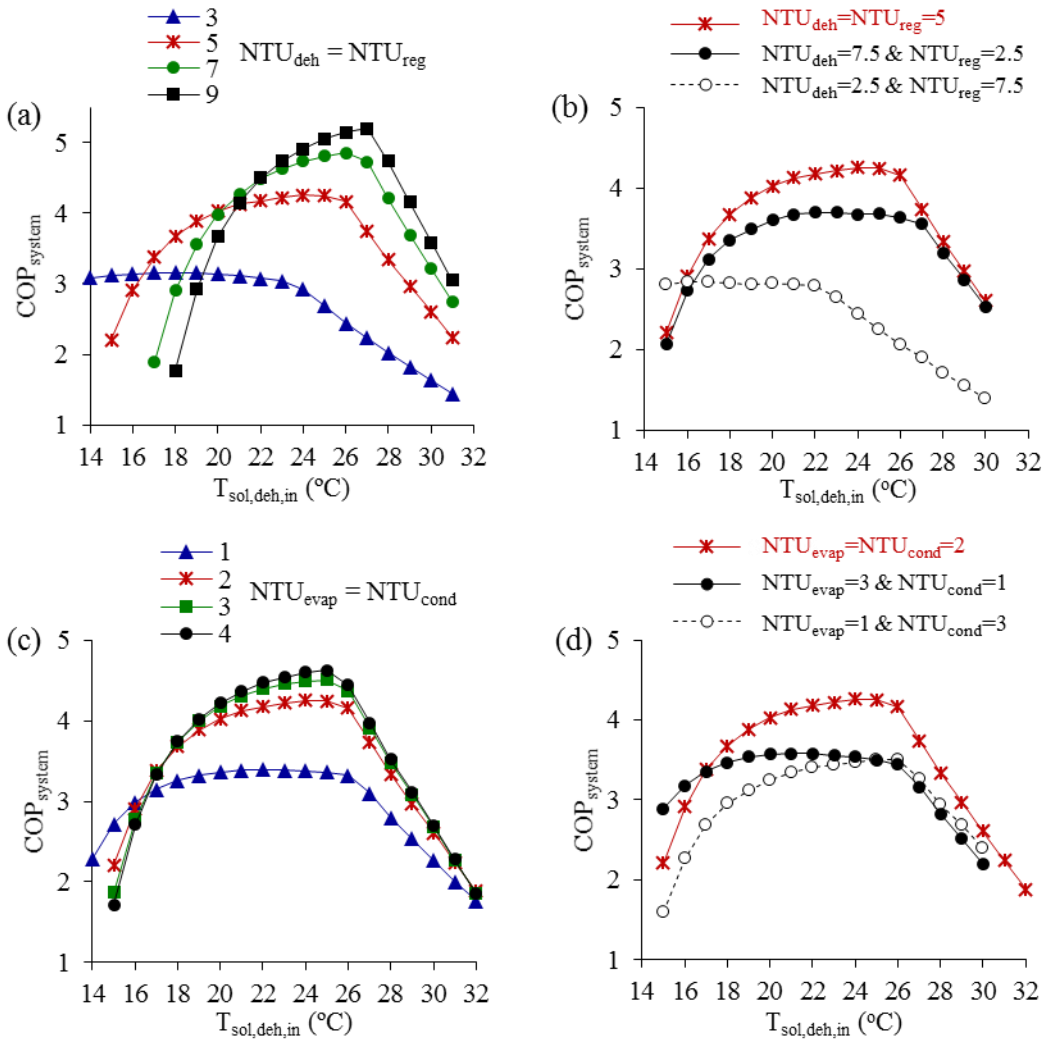

FIGURE 7.12. The influences of the NTUs of dehumidifier, regenerator, condenser and evaporator on the COP_{system} under balanced (i.e. $NTU_{deh}=NTU_{reg}$, $NTU_{evap}=NTU_{cond}$) and unbalanced (i.e. $NTU_{deh} \neq NTU_{reg}$, $NTU_{evap} \neq NTU_{cond}$) conditions.

It can be seen from Figures 7.11 and 7.12 that a membrane heat-pump LDAC system can be operated at high COP up to 4.5 depending on the design and operating conditions. A study by Rhodes et al. (2012) showed that the mean COP for 3818 air conditioning systems installed in Austin, TX is 2.9 with a standard deviation of 0.5. This shows that considerable energy savings can be achieved using the membrane heat-pump LDAC system proposed in this study.

7.7. RECOMMENDED TOPICS FOR FUTURE WORK

- In many LDAC installations, latent loads are covered by the liquid desiccant cycle and an auxiliary sensible cooling equipment is usually used to cover sensible loads. It is demonstrated in this paper that the liquid desiccant cycle of a heat-pump LDAC system can be controlled to simultaneously cover latent and sensible loads, without an auxiliary sensible cooling equipment. This is believed to be useful to all LDAC applications, especially in applications which require 100% fresh air such as hospitals and educational facilities. However, using a LDAC system to only condition the fresh air in a dedicated outdoor air system results in a smaller LDAC system (Abdel-Salam and Simonson, 2014b). Although the entire space latent loads can be covered by the LDAC system, an auxiliary sensible cooling equipment might still be required to remove additional sensible loads from the return air before mixing it with the fresh air. It is recommended for future studies to extend the control strategies presented in this paper on different LDAC configurations which include auxiliary sensible cooling equipment.

- The proposed control strategies can be extended to be applied to LDAC systems which use different types of heating (e.g. solar thermal, gas boiler) and cooling (e.g. direct/indirect/dew point evaporative cooling) equipment. The concepts presented in this paper can be followed in order to identify the required solution inlet temperatures to the dehumidifiers and regenerators, which are expected to result in higher COP.

7.8. CONCLUSION

A novel control strategy for heat-pump LDAC systems is developed in this study, and is applied on a heat-pump membrane LDAC system, which uses two liquid-to-air membrane

energy exchangers (LAMEEs) as the dehumidifier and regenerator. The proposed control strategy enables the operation of a heat-pump LDAC system under one of three operating modes as follows: (1) to cover latent loads and optimize the COP of the system (COP_{system}), (2) to cover latent loads and achieve capacity matching, or (3) to cover latent and sensible loads. Results show that the simultaneous control of solution inlet temperatures to the dehumidifier ($T_{sol,deh,in}$) and regenerator ($T_{sol,reg,in}$) enables the control of the heat-pump membrane LDAC system under any of the three aforementioned operating modes. The performances of the main components of the heat-pump membrane LDAC system, as well as the performance of the whole system, are presented and discussed in detail in the paper. A parametric study was conducted to investigate the influences of seven key design/operating parameters. Based on the results presented, the following conclusions can be made:

- At a constant latent load, the sensible effectivenesses of the dehumidifier and regenerator LAMEEs significantly change under different combinations of $T_{sol,deh,in}$ and $T_{sol,reg,in}$, while the latent effectivenesses are slightly affected.
- The peak values for the sensible and latent effectivenesses for the dehumidifier and regenerator LAMEEs are achieved under either the auxiliary-evaporator mode or the auxiliary-condenser mode.
- The optimal COP_{system} is achieved when the system operates under the auxiliary-condenser mode.
- The operation of a heat-pump LDAC system under the auxiliary-evaporator mode leads to a significant degradation in the COP_{system}.
- It is more energy efficient to meet both sensible and latent loads at high ambient humidity ratio, or at low humidity ratio set point.
- Higher COP_{system} can be achieved when the dehumidifier and regenerator, and the evaporator and condenser, operate under balanced rather than unbalanced NTUs.
- The type of refrigerant is crucial for the overall performance of the system. Among 17 types of refrigerant investigated, R123 and NH_3 achieve the highest COP_{system}.

CHAPTER 8

IMPORTANCE OF TRANSIENTS IN EVALUATING THE PERFORMANCE OF A LDAC SYSTEM

8.1 OVERVIEW

A majority of the LDAC system research in the literature and all the research in the previous chapters of this thesis have been based on steady-state models. However, no clear quantification is available in the literature for the influence of transients in evaluating the performance of a LDAC system. Thus, the fifth objective of this thesis is to evaluate the importance of transients in evaluating the performance of LDAC systems.

A data set obtained from a field test on a solar LDAC system is analyzed in this chapter to address the fifth objective of the thesis. A direct comparison of the transient and quasi-steady performance of the LDAC system is conducted. Results show that a steady-state model can reliably predict the performance of a LDAC system with acceptable uncertainty. In addition to evaluating the importance of transients on LDAC systems, other findings are obtained from the field test and presented in this chapter as follows. (1) The influences of environmental conditions on the quasi-steady heat and mass transfer performance. (2) Transient daily profiles for the solar LDAC system. (3) A new method to quantify the quasi-steady performance of a LDAC system from transient field data.

The manuscript presented in this chapter is submitted to the ASME Journal of Solar Energy Engineering in June 2015. Mr. Chris McNevin, Ms. Lisa Crofoot and Dr. Stephen Harrison have contributed to this manuscript by conducting the field test and collecting the data at Queen's University in Kingston, ON. In addition, Mr. Chris McNevin contributed to writing Section 8.5 of this chapter. My contributions to the manuscript are analyzing the data, developing the novel methods proposed, writing the paper, and incorporating co-authors' review comments.

A field study of a solar liquid desiccant air conditioning system: Quasi-steady and transient performance

(Submitted to the ASME Journal of Solar Energy Engineering in June 2015)

Ahmed H. Abdel-Salam, Chris McNevin, Lisa Crofoot,
Stephen J. Harrison, Carey J. Simonson

8.2 ABSTRACT

The field performance of a low-flow internally-cooled/heated solar liquid desiccant air conditioning (LDAC) system is investigated in this paper. The performance (sensible and latent heat transfer rates, coefficient of performance (COP) and uncertainties) of the LDAC system is quantified with and without solar thermal collectors. The COP increases by up to 270% when solar collectors provide heat to regenerate the desiccant rather than a gas boiler. A major contribution of this work is a direct comparison of the transient and quasi-steady performance of the LDAC system. This paper is the first to quantify the importance of transients and shows that, for the environmental and operating conditions in this paper, transients can be neglected when estimating the energy consumption of the LDAC system. Neglecting transients changes the total cooling energy transfer and the primary energy consumption during a test day by less than 10%. Another major contribution of this work is the development and verification of a new method that quantifies (with acceptable uncertainties) the quasi-steady performance of a LDAC system from transient field data using average data.

8.3 INTRODUCTION

Solar liquid desiccant air conditioning (LDAC) systems are promising technologies for air dehumidification (Katejanekarn et al., 2009; Liu et al., 2009a; Pineda and Diaz, 2011; Niu et al., 2012; Enteria et al., 2013; Dai et al., 2001; Gommed and Grossman, 2007; Katejanekarn and Kumar, 2008; Mohammad et al., 2013; Mei and Dai, 2008; Misha et al., 2012). Recently, several LDAC technologies have transformed from prototype systems for research and development to commercial systems available in the global market (AILR; Trane; Advantix). Previous studies have shown several advantages for LDAC systems compared to other air conditioning technologies such as conventional air conditioning and

solid desiccant dehumidification systems as previously discussed in Section 4.3. However, there are still some concerns about LDAC systems that should be solved before the technology can be safely and effectively adopted in residential and commercial buildings.

Among the major concerns of LDAC systems is the carryover of desiccant droplets into supply and exhaust air streams. One technology is to use liquid-to-air membrane energy exchangers (LAMEEs), as presented in the aforementioned chapters. Another technology, which is the focus of this chapter, is to use a low-flow internally-cooled/heated energy exchanger as the dehumidifier/regenerator (Lowenstein, 1994; Zhang et al., 2013b; Liu et al., 2009b; Yin et al., 2008, 2010; Bansal et al., 2011; Lowenstein et al., 2006; Ali et al., 2003; Qi et al., 2013, 2014; Mesquita et al., 2006; Mesquita, 2007; Jones, 2008; Crofoot and Harrison, 2012; Crofoot, 2012; Andrusiak and Harrison, 2009a, 2009b; Andrusiak et al., 2010; Crofoot et al., 2014; Salimizad e tal., 2014; McNevin and Harrison, 2014)

The low-flow internally-cooled/heated design was first developed by AIL Research Inc. in US Patent 6,745,826 B2 (Lowenstein, 1994). In this design, the desiccant solution flow rate is reduced by a factor of 20 to 30 compared to conventional conditioners, which eliminates desiccant droplets carryover. Unlike conventional conditioners designs that can operate either adiabatically or internally cooled/heated, the low-flow design must be internally cooled/heated because of the low thermal capacity rate of desiccant solution. The low flow rate (capacity rate) of the desiccant solution leads to a rapid change in the temperature of the desiccant solution as it flow through the exchanger, and consequently to the degradation of the mass transfer if the dehumidifier/regenerator is not internally cooled/heated. Several studies have been conducted on low-flow internally cooled/heated energy exchangers (Zhang et al., 2013b; Liu et al., 2009b; Yin et al., 2008, 2010; Bansal et al., 2011), where they were found to have more promising performances compared to adiabatic energy exchangers (Yin and Zhang, 2010; Bansal et al., 2011). It was found that a low-flow dehumidifier performs better with a parallel-flow configuration, while the performance of a low-flow regenerator was higher with a counter-flow configuration (Ali et al., 2003). The performance of a low-flow dehumidifier/regenerator was found to

improve with the increase of the wetted area, and decrease with the increase of the film thickness (Qi et al., 2013, 2014).

Manufacturers usually conduct field tests for new air conditioning systems before these systems are being commercialized in order to ensure the durability of the systems and their ability to cover cooling loads under wide range of operating conditions (AILR, Trane, Advantix). Several field tests have been conducted by researchers for LDAC systems (Katejanekarn et al., 2009; Gommed and Grossman, 2007; Lowenstein et al., 2006; Jones, 2008; Crofoot and Harrison, 2012; Crofoot, 2012; Crofoot et al., 2014). During these tests, LDAC systems were operated for several days and the transient performances of the systems were reported under wide ranges of environmental conditions (e.g. hot-dry, hot-humid and cool-humid climates). The focus of field tests presented in previous studies was on reporting transient daily performances, while quasi-steady performances were overlooked. It is believed that a more comprehensive approach should be followed in analyzing data obtained from field tests in order to maximize the benefit from collected data, and to be able to evaluate both transient and quasi-steady performances as will be presented in this paper.

The low-flow internally-cooled/heated solar LDAC system under investigation in this chapter was studied in previous studies by AIL Research Inc. (Lowentein et al., 2006) and the Solar Calorimetry Laboratory at Queen's University (Mesquita et al., 2006; Mesquita, 2007; Jones, 2008; Crofoot and Harrison, 2012; Crofoot, 2012; Andrusiak and Harrison, 2009a, 2009b; Andrusiak et al., 2010; Crofoot et al., 2014; Salimizad e tal., 2014; McNevin and Harrison, 2014), and its performance was found to be promising. The system was originally installed and instrumented at test site located in Kingston ON Canada (Jones, 2008) with support from Natural Resources Canada (NRCan) as part of Canada's contribution to IEA Task 38 (IEA). Originally driven by a natural gas boiler, the system was later modified to augment the boiler output with solar thermal energy (Crofoot, 2012). A TRNSYS model has been developed by Crofoot (2012) for the solar LDAC system to predict its performance, and the simulation results were found to be of acceptable accuracy

compared to the experimental results. The system has been under study and refinement since its first installation.

For the current chapter, measured data collected from a field test for the solar LDAC system (Crofoot et al., 2014) is further analyzed and discussed in order to: (1) investigate the influences of ambient air conditions on the quasi-steady performance of the system; (2) quantify the improvement in the COP of the LDAC system when it is integrated with a 95 m^2 evacuated-tube solar thermal array compared to if a gas boiler is used; (3) evaluate the transient performance of the system; (4) compare between the quasi-steady and transient performances of the system, and (5) develop and verify a new method to quantify the quasi-steady-state performance of a LDAC system using averaging for transient field data.

8.4 GENERAL SYSTEM DESCRIPTION

A schematic diagram of the solar LDAC system studied in this paper is presented in Figure 8.1. Six fluid streams/loops are used in the system as follows: process air stream, regeneration air stream, cooling water loop, heating water loop, dehumidifier solution loop and regenerator solution loop. Figure 8.2 shows conceptual schematics for the direction of heat and mass transfer within the low-flow internally-cooled/heated dehumidifier/regenerator used in the solar LDAC system.

8.4.1 Process air dehumidification

As shown in Figures 8.1 and 8.2(a), the process air enters the dehumidifier to be dehumidified using a concentrated desiccant solution stream. The solution flow rate is kept low in the dehumidifier to avoid the carryover of desiccant droplets in the process air stream, as previously mentioned. As the desiccant solution absorbs moisture from the air stream, heat is released and the temperature of the solution increases. Cooling water flows through the dehumidifier to remove the phase change energy and cool the solution stream, which increases the potential for mass transfer from the process air to the solution in the dehumidifier. An evaporative cooling tower is used to cool the cooling water prior entering the dehumidifier, and thus the cooling water inlet temperature to the dehumidifier is

strongly dependent on ambient air conditions. Depending on the inlet temperature of the water, the process air may be heated or cooled as it flows through the dehumidifier.

8.4.2 Dilute solution regeneration

The dilute desiccant solution leaving the dehumidifier is collected in the solution sump, as shown in Figure 8.1. Cooler solution is drawn from the solution sump and passes through a solution-to-solution heat exchanger to be preheated prior entering the regenerator, using the concentrated-hot solution leaving the regenerator. The dilute-hot solution enters the regenerator, where it is regenerated by the regeneration air and heating water as shown in Figure 8.2(b). The heating water, which comes from either a gas boiler or a solar thermal system, passes through the regenerator to increase the potential for mass transfer from the solution to the regeneration air. The concentrated-hot desiccant solution leaving the regenerator is precooled in the solution-to-solution heat exchanger before it enters the solution sump.

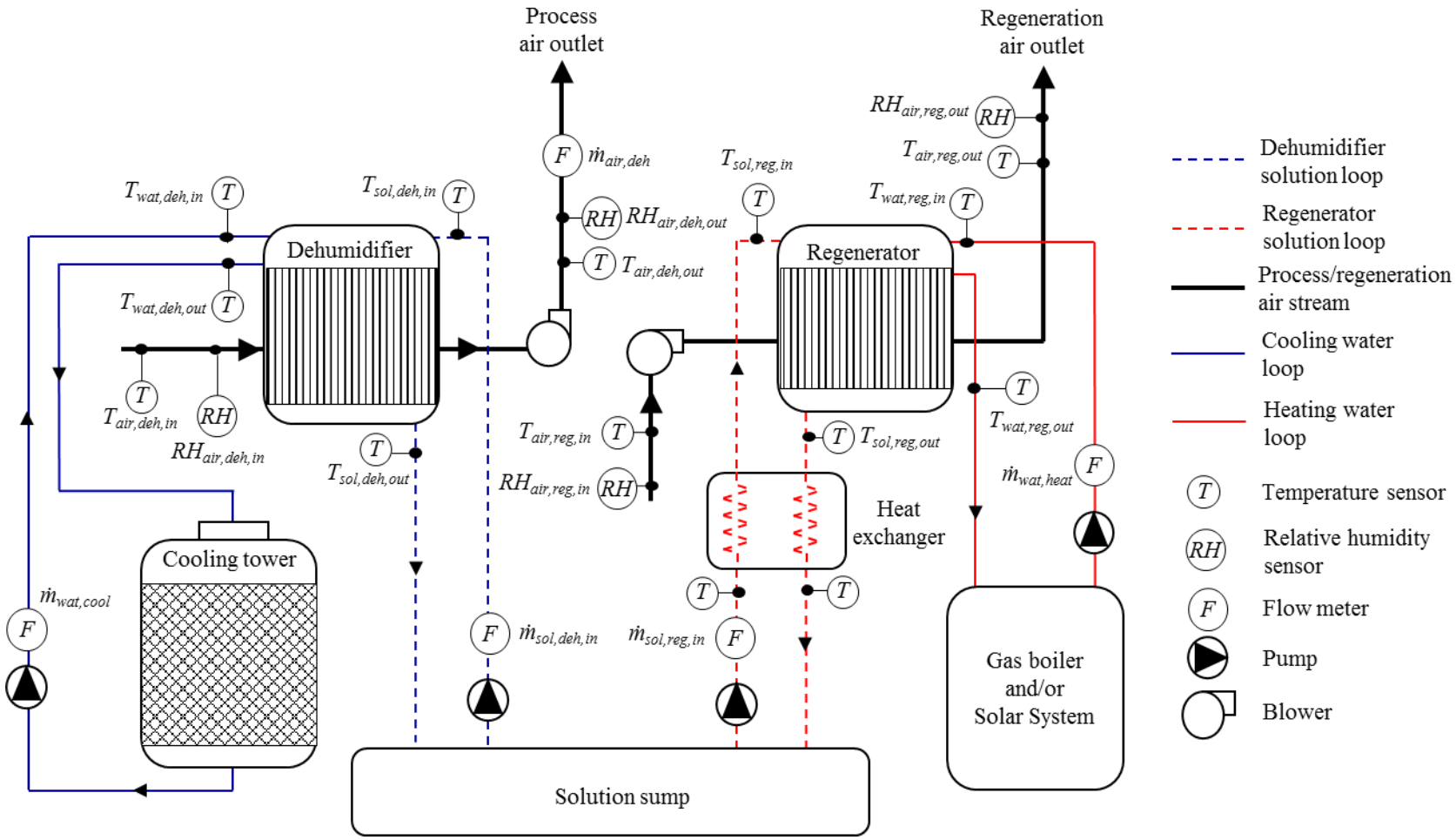

FIGURE 8.1. Schematic diagram of the experimental setup for the solar LDAC system.

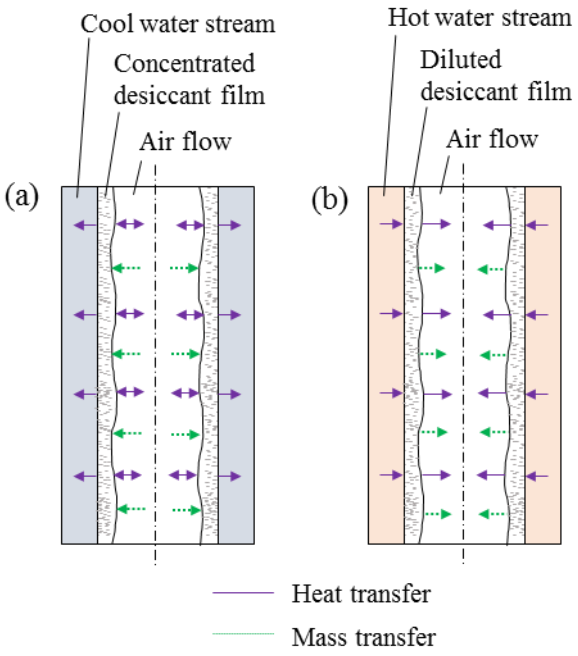

FIGURE 8.2. Conceptual schematics for the direction of heat and mass transfer in the low-flow (a) internally-cooled dehumidifier and (b) internally-heated regenerator. The dehumidifier dries the process air stream, while the regenerator dries the liquid desiccant.

8.5 EXPERIMENTAL SETUP

8.5.1 Specification of the tested LDAC system

The LDAC system was designed around a prototype low-flow internally-cooled/heated falling-film liquid desiccant unit produced by AIL Research Inc., see Figure 8.3. The unit is identified as model SOA3000. The unit is designed to condition 1416 L/s (3000 CFM) of process air. The unit contains the regenerator, dehumidifier, solution sump and pumps, solution-to-solution heat exchanger, as well as the process and regeneration air stream fans. The unit also contains a data logger and PLC controller.

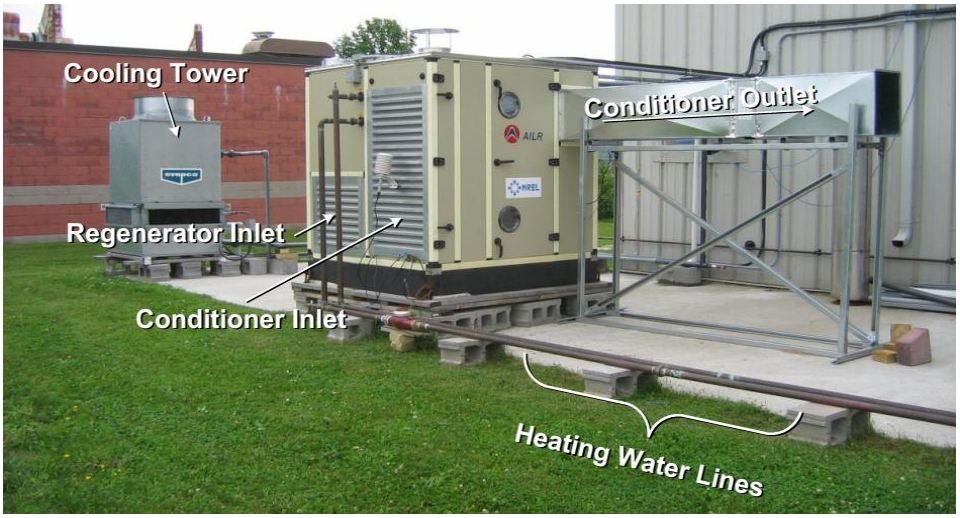

FIGURE 8.3. Photo showing the LDAC system (Jones, 2008).

8.5.2 Dehumidifier

Figure 8.4(a) shows the dehumidifier inside the LDAC system. It is made up of 96 curved parallel plates with internal passages for cooling water. These plates are joined by a header which both distributes the water into the plates and discharges the desiccant solution in a falling film over the plates. The outer surface of the plates is coated with a porous wicking material, approximately 0.5 mm thick, to aid in the even wetting of the plate by the desiccant solution (Lowenstein, 2006). A footer collects the desiccant and returns it to the sump. The cooling water enters the dehumidifier from the top and it flows through half of the plates in a parallel direction with the desiccant to the footer, where it is collected and then returned to the top of the unit through the other half of plates, providing counter flow to the falling desiccant. A cross section of one plate of the dehumidifier is shown in Figure 8.4(b) (Lowenstein, 2006). The process air stream is drawn through the gaps between the plates by a 1000W variable speed blower at approximately 1180 L/s (2500 CFM) providing a laminar flow with Re = 1250. The air stream comes into direct contact with the falling film of desiccant solution in a cross flow configuration. The desiccant is circulated from the solution sump by a 150W pump at a flow rate of 5.5 LPM as set by a manually operated control valve.

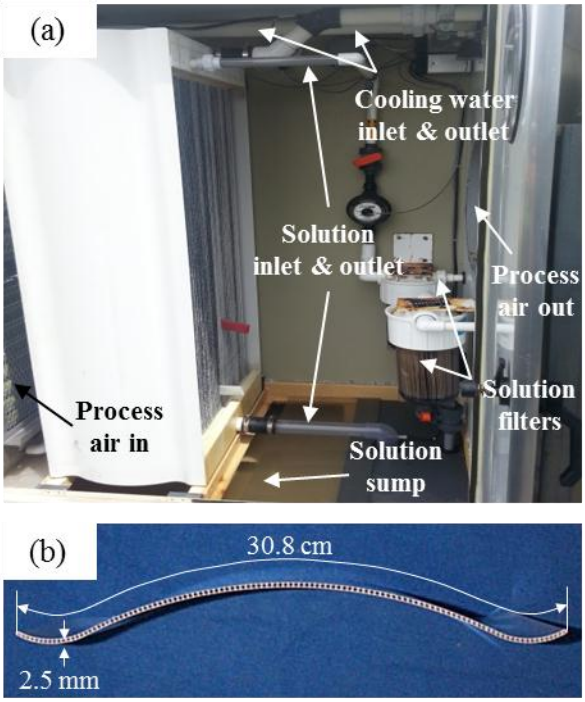

FIGURE 8.4. Photos showing (a) the low-flow internally-cooled dehumidifier, and (b) a cross section view of a single dehumidifier plate showing the internal water passages (Lowenstein, 2006).

Table 8.1 presents the important design variables for the dehumidifier. The surface area to volume ratio is 220 m^2/m^3, which indicates that the design has similar compactness to other flat-plate membrane energy exchangers with values between 200 and 250 m^2/m^3 (Abdel-Salam and Simonson, 2014a; Namvar et al., 2012; Moghaddam et al., 2014). The number of transfer units (NTU) for the heat and mass transfer between the air and liquid desiccant is presented in Table 8.1 as a function of the Nusselt number (Nu) since the convective heat and mass transfer coefficients are not exactly known for the air flow through the curved channels with porous sides. However, assuming that Nu = 8.24, which is for fully developed laminar flow with constant heat flux between two parallel plates (Moghaddam et al., 2013b; Incropera and Dewitt, 2002), NTU for the dehumidifier is 3.8. With the analogy between heat and mass transfer, the mass transfer and heat transfer NTU will be equal for this direct contact heat and moisture exchange (Simonson and Besant, 1999a, 1999b).

TABLE 8.1. Specifications of the dehumidifier and regenerator.

Parameter	Dehumidifier	Regenerator
Solution flow rate (LPM)	5.5	7.2
Air flow rate (L/s)	1180	236
Water flow rate (LPM)	110	88
Thickness of air gaps without wicking (mm)	2.5	3
Number of air gaps	95	74
Thickness of wicking material (mm)	0.5	0.5
Thickness of plates (cm)	2.5	3
Number of plates	96	75
Height of plates (cm)	125	120
Width of plates (cm)	30.5 (curved width)	11.5
Length (cm)	61	69
Width (cm)	38	18
Height (cm)	142	152
Surface area of heat and mass transfer (m^2)	72.4	20.4
Volume (m^3)	0.33	0.19
Surface area to volume ratio (m^2/ m^3)*	220	110
Re for air stream	1250	290
NTU between air and solution streams**	0.46·Nu	0.67·Nu

* The surface area to volume ratios for flat-plate membrane energy exchangers lie between 200 and 250 m^2/m^3 (Abdel-Salam and Simonson, 2014a; Namvar et al., 2012; Moghaddam et al., 2014). This indicates that the dehumidifier and regenerator used in this study have compactness that are similar to and lower than flat-plate membrane energy exchangers, respectively.

** For a fully developed laminar flow with constant heat flux between two plates, Nusselt number (Nu) is 8.23 (Moghaddam et al., 2013b; Incropera and Dewitt, 2002). In this case, the NTUs of the dehumidifier and regenerator are 3.8 and 5.5, respectively.

8.5.3 Regenerator

Figure 8.5 shows a photo for the regenerator inside the LDAC system. The specifications of the regenerator are given in Table 8.1. The regenerator requires a different design than the dehumidifier in order to account for the higher temperatures and greater thermal variation. The operation is similar to that of the dehumidifier, utilizing internally heated plates with a desiccant film flowing over the surface of 75 straight plates, coming into direct contact with a regeneration air stream flowing between the plates. The plates hang from the header and are not connected to a footer, unlike the dehumidifier. The desiccant drains off the plates and into a collection basin. The design air flow rate for the regenerator

is 236 L/s (500 CFM), and is drawn through the system by a 120 W blower. The airflow Re is 290 and the NTU is 0.67 Nu or approximately 5.5 (assuming Nu = 8.24 (Moghaddam et al., 2013b; Incropera and Dewitt, 2002)). The desiccant flows at 7.2 LPM, circulated and controlled by a pump and valve identical to the one used by the dehumidifier.

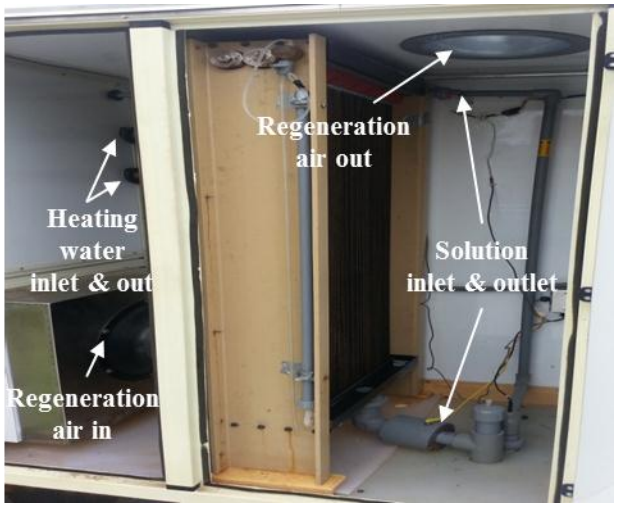

FIGURE 8.5. Photo showing the low-flow internally-heated regenerator.

8.5.4 Desiccant solution

The desiccant solution used in the current study is lithium chloride. In order to measure the solution concentration, samples are drawn from the inlet and outlets of the regenerator and dehumidifier. The density of the samples is measured using an Anton-Paar DMA 4000 density meter and then the concentration is calculated from the density.

8.5.5 Evaporative cooling tower

The cooling water is cooled with an Evapco evaporative cooling tower model ICT 3-63. This unit has a rated cooling capacity of 65 kW. The water is supplied at approximately 110 LPM by a 2 HP centrifugal pump.

8.5.6 Gas boiler

A Raypak Raytherm Type H3-400 natural gas boiler with a rated capacity of 90 kW is used to maintain the hot water inlet temperature to the regenerator at approximately 78.5ºC. This unit has a two stage firing mode to allow for better control of the water temperature.

8.5.7 Solar system

The solar system provides an alternate, low-environmental-impact heat source for the regenerator. The piping for the LDAC and solar systems has been designed so that a variety of flow paths are possible (Crofoot, 2012). The LDAC system can run using either the boiler, the solar array, or both the boiler and solar array in series. A photo for the solar array is presented in Figure 8.6, where it is located approximately 25 meters away from the LDAC regenerator. The solar array is divided into five parallel sections of collectors. Two different types of evacuated-tube heat pipe collectors are used with a total area of 95 m^2 and an absorber area of 61 m^2. A pair of insulated hot water tanks, each with a volume of 435 litres, are used to provide a buffer between the solar array and the LDAC system. Detailed information about the solar thermal system is presented by Crofoot (2012).

FIGURE 8.6. Photo showing the solar thermal array.

8.5.8 Controls

The LDAC system is controlled using a Direct Logic, model D0-06DR PLC controller. This system uses a separate set of sensors from the data acquisition system. For the tests in

this paper, the system is operated at full capacity which means that the air flow rates of the regenerator and dehumidifier are held at the maximum values capable by the fans rather than using the available PID control. The boiler set point temperature is set in the PLC program, and the PLC unit used this value to determine the temperatures at which the different boiler stages are fired. The system also has high and low level switches in the sump to prevent the sump from over flowing and to prevent over concentrating the desiccant, which would cause the lithium chloride to crystalize in the regenerator and possibly cause damage. The PLC contained instructions to improve the wetting of the plates, ensuring even desiccant coverage. On initial system start up, the desiccant pumps are pulsed on and off. During periods of extended deactivation, the regenerator desiccant pumps cycle on and off to make sure that when there is a call for regeneration the plates are evenly wetted. Other controls are in place for safety, such as fault detection and overheat controls. Programming and monitoring of the PLC control is done using the program DirectSoft 5.

8.5.9 Instrumentation and data acquisition

The locations of the instruments used in the setup are shown in Figure 8.1, and the types and uncertainties of the used instruments are given in Table 8.2. The data is collected by a Campbell Scientific CR10X in conjunction with an AM16 A multiplexer and a SDM-SW8A 8 channel pulse counter module. More details about the instrumentation and data acquisition system are presented by Jones (2008) and Crofoot (2012).

8.5.10 Uncertainty

The root mean square (RMS) method is used in this study to calculate the uncertainty in the calculated parameters as shown in equations (8.1) and (8.2) (ASME, 2005).

$$R = f\{x_1, x_2, x_3, \ldots\ldots, x_N\} \tag{8.1}$$

$$U_R = \pm \left[\sum_{i=1}^{N} \left(\frac{\partial R}{\partial x_i} U_{\bar{x}_i}\right)^2\right]^{1/2} \tag{8.2}$$

where, R is the calculated parameter, x_i represents the independent variables, U_R is the uncertainty in the calculated parameter R, and $U\bar{x}_i$ is the uncertainty in the independent variable x_i.

TABLE 8.2. Types and uncertainties of the instruments used in the field test.

Measured parameter		Uncertainty	Sensor
Flow rate (LPM)	Air	±3%	Ruskin AMS810
	Solution	±1.5%	Omega FTB6207-PS
	Hot water	±1.5%	AMCO M190 Hot Water Meter (1 1/2")
	Cold water	±1.5%	AMCO C700 Water Meter (1 1/2") Pulser Type SF
T (ºC)	Air	±0.3	Vaisala HMT330, Vaisala HMT331, Vaisala HMD60Y PT1000RTD and Campbell Scientific HMP45C-L25
	Solution	±0.3	10K thermistor (4159-1/8-6-25-TH44036-FEB)
	Water	±0.3	10K thermistor (4159-3/16-6-25-TH44036)
Air humidity (%RH)		±3.0%	Vaisala HMT330, Vaisala HMT331, Vaisala HMD60Y PT1000RTD and Campbell Scientific HMP45C-L25
Solution density (g/cm^3)		±0.0001	Anton-Paar DMA 4000 density meter
Power (kW)		±0.026	Watt Node WNB-3D-240-P

8.6 EXPERIMENTAL PROCEDURES

8.6.1 Transient conditions

The solar LDAC system was operated at full capacity for 20 test days during the summer of 2012 and the operating conditions were recorded for 10 hours (from 8AM to 6PM) per day at a one minute time step (Crofoot, 2012; Crofoot et al., 2014). Data was collected every five seconds and displayed on a live data display as well as being averaged into one minute time steps and saved to a data file.

8.6.2 Quasi-steady conditions

The transient data collected during the test days was post-processed in order to obtain data sets at which the inlet and outlet conditions to the dehumidifier did not vary by more than

the uncertainties of the used instruments for a time period of 30 minutes. Six quasi-steady operating conditions were obtained for the LDAC system as follows: three test conditions at constant ambient air humidity ratio (W_{amb}) and different ambient air dry bulb temperature ($T_{amb,db}$), and three test conditions at constant $T_{amb,db}$ and different W_{amb}. The values of $T_{amb,db}$ and W_{amb} at each of these six conditions are given in Table 8.3.

8.6.3 Energy and mass balances

The energy exchange inequality (EEI) and mass exchange inequality (MEI) used to check the energy and mass balances are shown in equations (8.3) and (8.4), respectively. The average EEI and MEI values for the six quasi-steady operating conditions tested are given in Table 8.3; it can be seen that the EEI and MEI lie within their uncertainty ranges (i.e. U_{EEI} and U_{MEI}).

$$EEI = \frac{\left|(\dot{m}\Delta h)_{air,deh}+(\dot{m}\Delta h)_{wat,deh}+(\dot{m}\Delta h)_{air,reg}+(\dot{m}\Delta h)_{wat,reg}\right|}{\left|(\dot{m}\Delta h)_{air,deh,max}\right|+\left|(\dot{m}\Delta h)_{air,reg,max}\right|} \tag{8.3}$$

$$MEI = \frac{\left|(\dot{m}\Delta W)_{air,deh}+(\dot{m}\Delta W)_{air,reg}\right|}{\left|(\dot{m}\Delta W)_{air,deh,max}\right|+\left|(\dot{m}\Delta W)_{air,reg,max}\right|} \tag{8.4}$$

where, $\dot{m}$ is the mass flow rate, W is the humidity ratio, and h is the enthalpy. Subscripts air and water refer to the air and water streams, respectively, while subscripts deh and reg refer to the dehumidifier and regenerator, respectively.

TABLE 8.3. The six quasi-steady-state test conditions and the average energy and mass exchange inequalities.

	Influence of temperature			**Influence of humidity**		
	T1	**T2**	**T3**	**W1**	**W2**	**W3**
$T_{air,db}$ (ºC)	22.8	29.7	34.3	27.7	27.8	27.9
W_{air} (g/kg)	16.2	16.4	16.3	12.8	15.1	17.2
EEI (%)	1.6	2.4	0.3	2.5	0.9	0.1
U_{EEI} (%)	4.2	4.3	4.5	4.8	4.5	4.2
MEI (%)	0.9	4.2	5.1	0.8	3.2	3.9
U_{MEI} (%)	4.1	4.5	5.3	4.9	5.5	6.3

8.6.4 Performance indices

The performance of the LDAC system is evaluated in this study using the following performance indices: (i) the inlet and outlet operating conditions for the air, solution and water streams; (ii) the rate of sensible (q_{sen}), latent (q_{lat}) and total (q_{tot}) heat transfer to/from the process air; (iii) the rate of heat transfer from/to the cooling/heating water ($q_{wat,cool}$/$q_{wat,heat}$), and (iv) the electrical (ECOP), thermal (TCOP), and total (COP) coefficients of performances for the LDAC system, equations (8.5) to (8.7).

$$TCOP = \frac{q_{tot}}{P_{thermal}} \tag{8.5}$$

$$ECOP = \frac{q_{tot}}{P_{electrical}} \tag{8.6}$$

$$COP = \frac{q_{tot}}{P_{thermal}+(P_{electrical}/0.33)} \tag{8.7}$$

where, $P_{thermal}$ is the rate of thermal energy input to the heating water (kW), $P_{electrical}$ is the rate of electrical energy input to the LDAC system (kW) The conversion coefficient from thermal energy to electric power is assumed to be 0.33. The COP of the LDAC system given in equation (8.7) is referenced to thermal energy, and it can be referenced to electricity by dividing it by the conversion coefficient from thermal energy to electricity.

8.7 RESULTS AND DISCUSSION

The influences of the ambient air dry bulb temperature ($T_{amb,db}$) and humidity ratio (W_{amb}) on the quasi-steady performance of the LDAC system are presented in Section 8.7.1, under the operating conditions given in Table 8.3. The results presented in Section 8.7.1 are calculated assuming that only the boiler is used to provide the heating energy requirements of the LDAC system. The influence of integrating the solar thermal system with the LDAC system and a daily transient profile for the solar LDAC system are presented in Section 8.7.2. A comparison between the quasi-steady and transient performances of the solar LDAC system is presented in Section 8.7.3. The prediction of the quasi-steady performance of the LDAC system using averaged transient data is presented in Section 8.7.4.

8.7.1 Quasi-steady parametric study

8.7.1.1 Influence of ambient air dry bulb temperature ($T_{amb,db}$)

Figure 8.7 presents the measured air, solution and water properties at the entrance and exit of the dehumidifier for the three tests with W_{amb} = 16.3 g/kg and $T_{amb,db}$ varying between 23ºC and 34ºC. For all the tests, the process air is dehumidified to the same humidity ratio and thus the dehumidification rate is independent of $T_{amb,db}$. On the other hand, the process air may be heated or cooled depending on $T_{amb,db}$, as presented in Figure 8.7(a). The process air stream undergoes heating and dehumidification when $T_{amb,db}$ is below a specific value and undergoes cooling and dehumidification when $T_{amb,db}$ exceeds this value. The value of $T_{amb,db}$ which determines whether the air is cooled or heated as it passes through the dehumidifier can be determined from Figure 8.7(a) at the intersection point between the inlet and outlet process air temperatures; it is found to be ~33ºC when W_{amb} is ~16.3 g/kg.

The humidity ratio of the process air leaving the dehumidifier remains almost constant with $T_{amb,db}$ as presented in Figure 8.7 (b), which is believed to be due to the following. The rate of mass transfer increases as the difference between the vapor pressures of air and solution streams increases. The solution concentration increases with $T_{amb,db}$ as shown in Figure 8.7(c), which decreases the solution vapor pressure, and thus increases the potential for mass transfer between the air and solution streams. On the other hand, the inlet temperatures for both the water and solution streams increase with $T_{amb,db}$ as shown in Figure 8.7(d) which decreases the potential for mass transfer from air to solution in the dehumidifier. Therefore, it can be depicted from the nearly constant supply humidity ratios shown in Figure 8.7(b) that in overall increasing $T_{amb,db}$ does not lead to a significant change in the potential for mass transfer in one specific direction due to the balancing natures of these effects.

Figure 8.7(d) shows that the temperature of the solution entering and leaving the dehumidifier increases with $T_{amb,db}$. This is attributed to the increase in temperature of the process air and cooling water entering the dehumidifier with $T_{amb,db}$. Since the cooling water is cooled using an evaporative cooling tower, the cooling water temperature at the dehumidifier inlet increases with $T_{amb,db}$ due to the direct proportionality between the dry

bulb temperature and wet bulb temperature at a constant humidity ratio. Additionally, the temperature of the cooling water leaving the dehumidifier (i.e. entering the cooling tower) increases with $T_{amb,db}$ due to the increased temperatures of the other fluids loops with the increase of $T_{amb,db}$. Figure 8.8 shows a psychrometric chart which summarizes the measured air, solution and water properties at the entrance and exit of the dehumidifier for the three tests with W_{amb} = 16.3 g/kg and $T_{amb,db}$ varying between 23ºC and 34ºC.

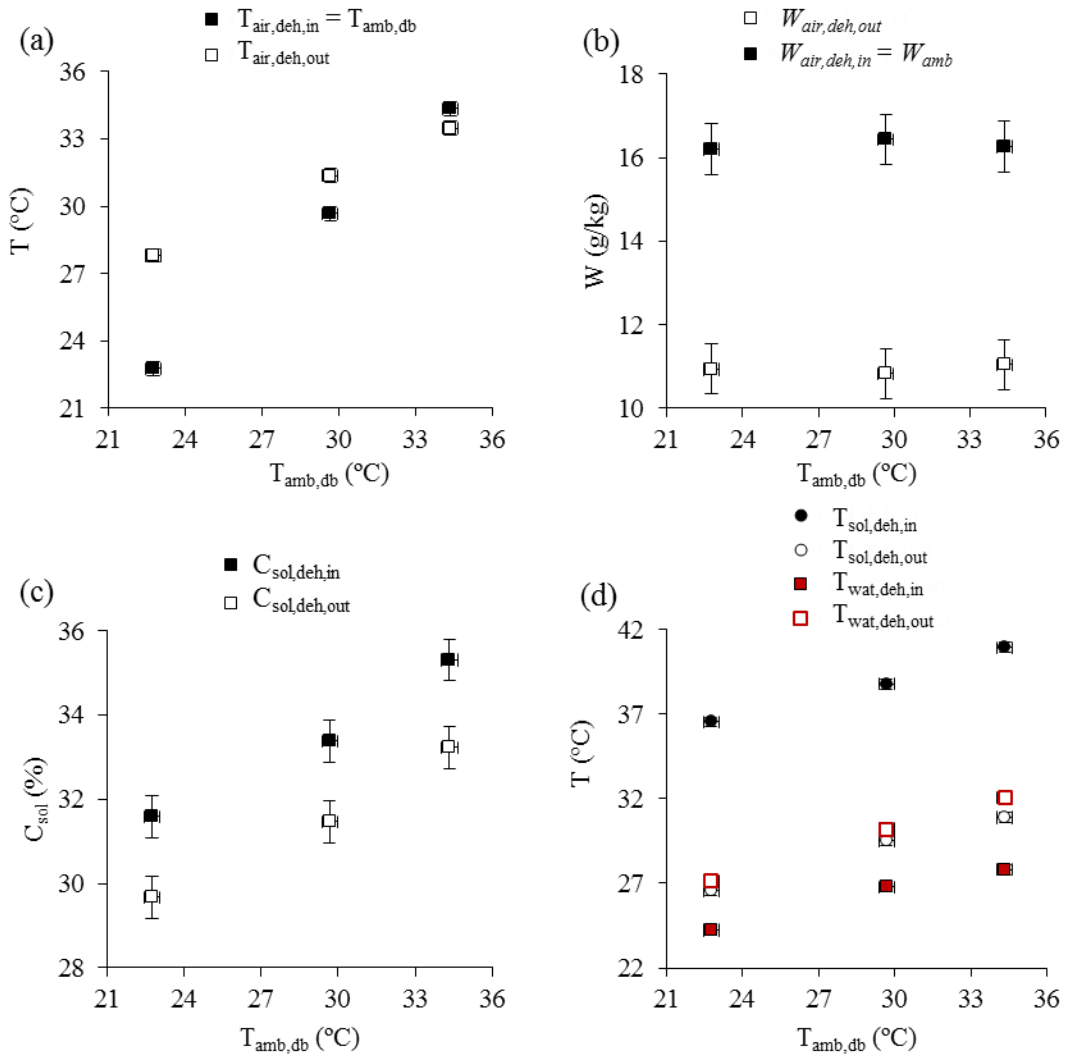

FIGURE 8.7. The influences of ambient air dry bulb temperature ($T_{amb,db}$) on the (a) temperature of air leaving the dehumidifier ($T_{air,deh,out}$), (b) humidity ratio of air leaving the dehumidifier ($W_{air,deh,out}$), (c) concentration of solution entering ($C_{sol,deh,in}$) and leaving ($C_{sol,deh,out}$) the dehumidifier, and (d) temperature of solution/water streams entering/leaving the dehumidifier.

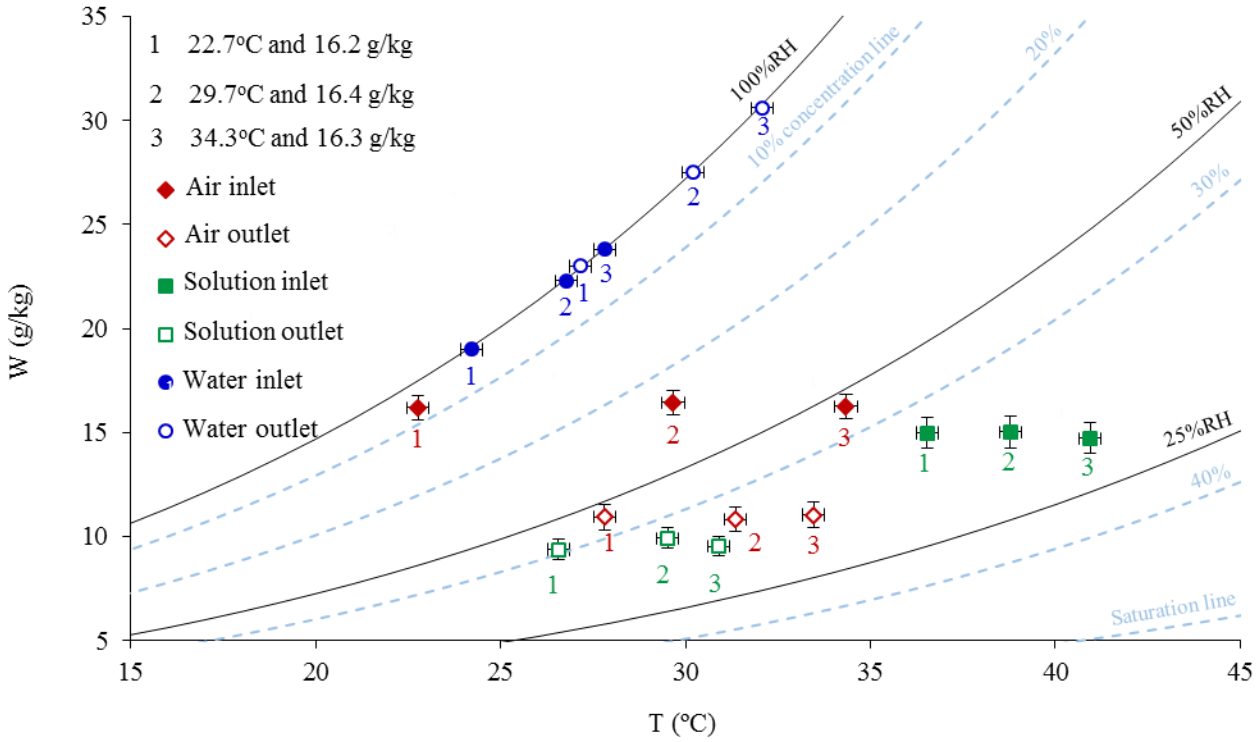

FIGURE 8.8. A psychrometric chart summarizes the influences of ambient air dry bulb temperature ($T_{amb,db}$) on the air and solution conditions entering/leaving the dehumidifier.

The amount of heat rejected from the cooling water in the cooling tower increases with $T_{amb,db}$ as presented in Figure 8.9. The temperature of heating water entering the regenerator is nearly constant with $T_{amb,db}$ because the set point temperature is maintained at a constant value by the boiler (i.e. ~78.5ºC). Since the temperatures of both the inlet regeneration air (i.e. $T_{amb,db}$) and the dilute solution entering the regenerator increases with $T_{amb,db}$, the heating water leaves the regenerator at slightly higher temperatures as $T_{amb,db}$ increases. This results in the reduction of the heating required to heat the heating water, as shown in Figure 8.9.

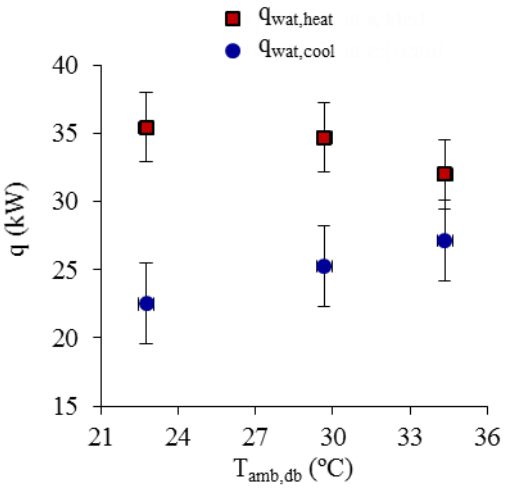

FIGURE 8.9. The influence of ambient air dry bulb temperature ($T_{amb,db}$) on the heat transfer rate to heating water ($q_{wat,heat}$) and from cooling water ($q_{wat,cool}$).

No mechanical cooling system is installed in the LDAC system studied in this paper. Thus, it is not possible to control neither the magnitude nor the direction (i.e. heating or cooling) of the sensible heat transfer between the solution and the process air in the dehumidifier. Figure 8.10(a) shows that at low $T_{amb,db}$, the process air is heated (i.e. $q_{sen} < 0$ kW) as it passes through the dehumidifier and this sensible heating gradually decreases as $T_{amb,db}$ increases until it switches to sensible cooling (i.e. $q_{sen} > 0$ kW). On the other hand, the latent capacity remains nearly constant with $T_{amb,db}$. Thus, the total capacity increases by a similar magnitude to the sensible capacity. Figure 8.10(b) shows the variations of TCOP, ECOP and COP of the LDAC system with $T_{amb,db}$. Since the total capacity of the LDAC system increases with T_{amb} while the thermal energy required for the dilute solution regeneration decreases, the TCOP, ECOP and COP increases with $T_{amb,db}$.

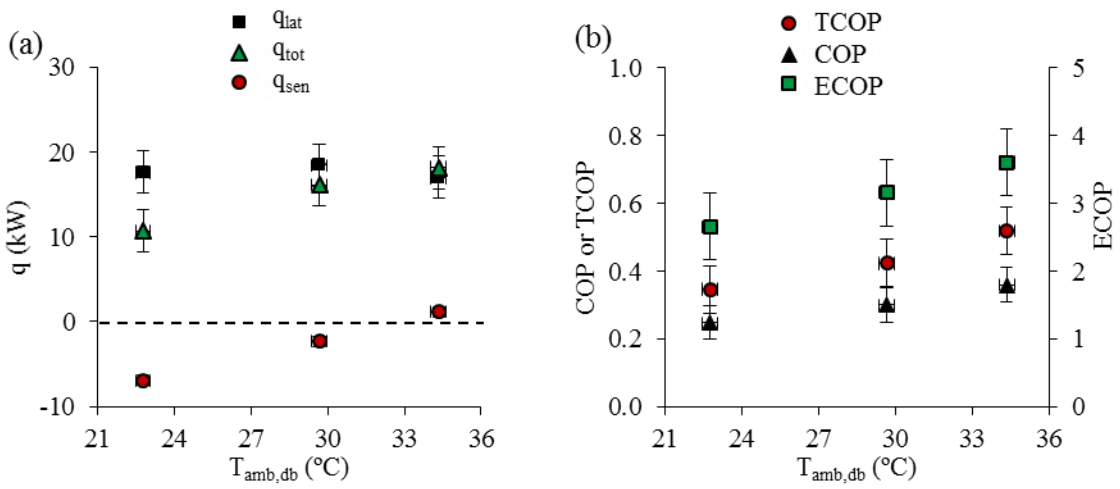

FIGURE 8.10. The influence of ambient air dry bulb temperature ($T_{amb,db}$) on (a) the sensible (q_{sen}), latent (q_{lat}) and total (q_{tot}) heat transfer rates, and (b) the TCOP, ECOP and COP of the LDAC system.

8.7.1.2 Influence of ambient air humidity ratio (W_{amb})

Figure 8.11 presents the measured air, solution and water properties at the entrance and exit of the dehumidifier for the three tests with $T_{amb,db}$ = 27.8ºC and W_{amb} varying between 12.8 g/kg and 17.2 g/kg. Figure 8.11(a) show that as W_{amb} increases, the temperature of process air leaving the dehumidifier ($T_{air,deh,out}$) increases. The measured data indicate that if W_{amb} decreases below a specific value (i.e. W_{amb}~12.8 g/kg at $T_{amb,db}$~27.8ºC), the temperature of the process air leaving the dehumidifier is expected to be lower than the process air inlet temperature. The humidity ratio of the process air leaving the dehumidifier is found to increase at a nearly constant slope with W_{amb}, as shown in Figure 8.11(b). On the other hand, the concentrations of solution streams entering and leaving the dehumidifier decrease as shown in Figure 8.11(c).

Figure 8.11(d) shows that the temperature of solution leaving the dehumidifier increases with W_{amb}. The temperature of the solution leaving the regenerator is found to be nearly constant at approximately 71ºC over the entire range of W_{amb}. This is expected because the inlet temperatures of the regeneration air (i.e. $T_{amb,db}$) and heating water remained almost constant at approximately 27.8ºC and 78.5ºC, respectively, over the entire range of W_{amb} values tested. Consequently, the inlet solution temperatures to the dehumidifier and

regenerator increases and remains constant, respectively, due to the nearly constant effectiveness of the solution-to-solution heat exchanger. The temperatures of the cooling water entering and leaving the dehumidifier increase with W_{amb}, as shown in Figure 8.11(d). This is due to the increase of the wet bulb temperature when W_{amb} increases at a constant dry bulb temperature. Figure 8.12 shows a psychrometric chart which summarizes the measured air, solution and water properties at the entrance and exit of the dehumidifier for the three tests with $T_{amb,db}$ = 27.8ºC and W_{amb} varying between 12.8 g/kg and 17.2 g/kg.

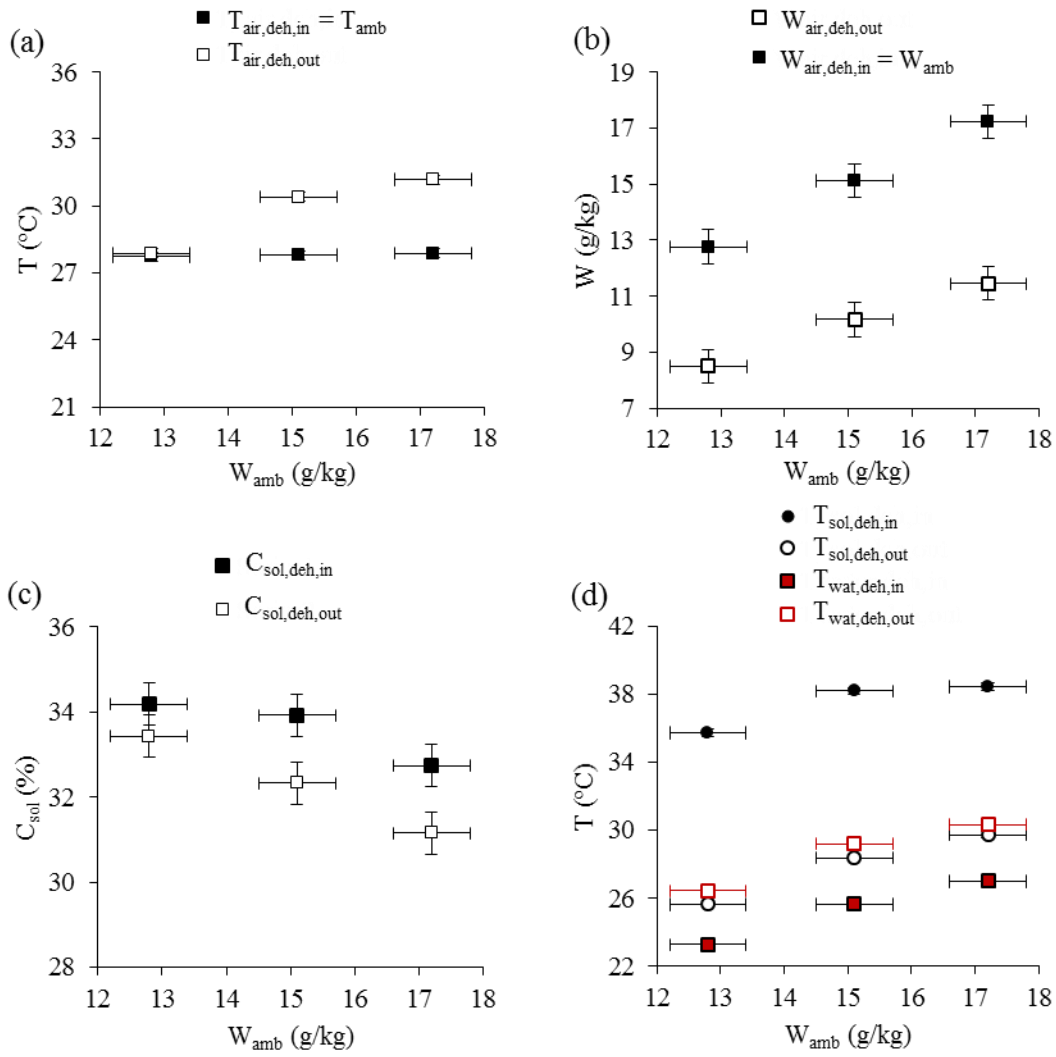

FIGURE 8.11. The influences of ambient air humidity ratio (W_{amb}) on the (a) temperature of air leaving the dehumidifier ($T_{air,deh,out}$), (b) humidity ratio of air leaving the dehumidifier ($W_{air,deh,out}$), (c) concentration of solution entering ($C_{sol,deh,in}$) and leaving ($C_{sol,deh,out}$) the dehumidifier.

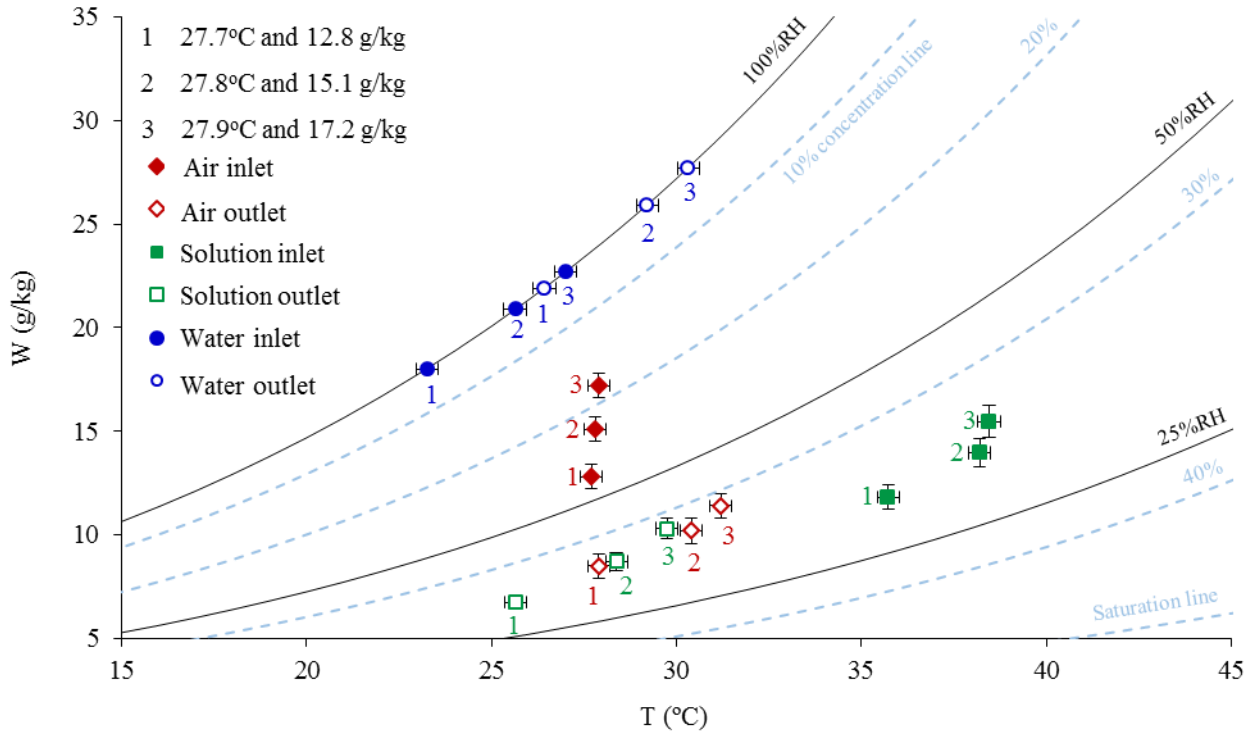

FIGURE 8.12. A psychrometric chart which summarizes the influences of ambient air dry humidity ratio (W_{amb}) on the air and solution conditions entering/leaving the dehumidifier.

The heat added to the heating water and heat rejected from the cooling water remain nearly the same with W_{amb}, as presented in Figure 8.13, unlike the relationships seen with $T_{amb,db}$ (see Figure 8.9). The temperature of the process air leaving the dehumidifier increases as W_{amb} increases and thus the sensible heating for the process air increases with W_{amb}, as shown in Figure 8.14(a). Although the humidity ratio of the process air leaving the dehumidifier increases with W_{amb} as shown in Figure 8.11(b), Figure 8.14(a) shows that the higher the W_{amb}, the larger the latent capacity. The total capacity of the LDAC system does not significantly change with W_{amb} due to the passive design of the system (i.e. no active mechanical cooling), which leads to the variation of latent and sensible capacities in opposite directions by close magnitudes when W_{amb} changes. The TCOP, ECOP and COP of the LDAC system show slight variation with W_{amb}, as shown in Figure 8.14(b).

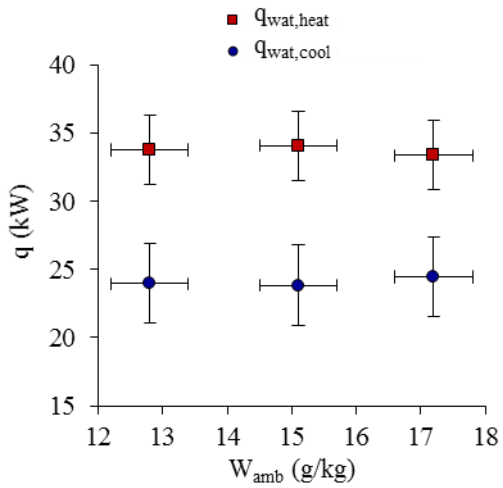

FIGURE 8.13. The influence of ambient air humidity ratio (W_{amb}) on the rate of heat transfer to heating water ($q_{wat,heat}$) and from cooling water ($q_{wat,cool}$).

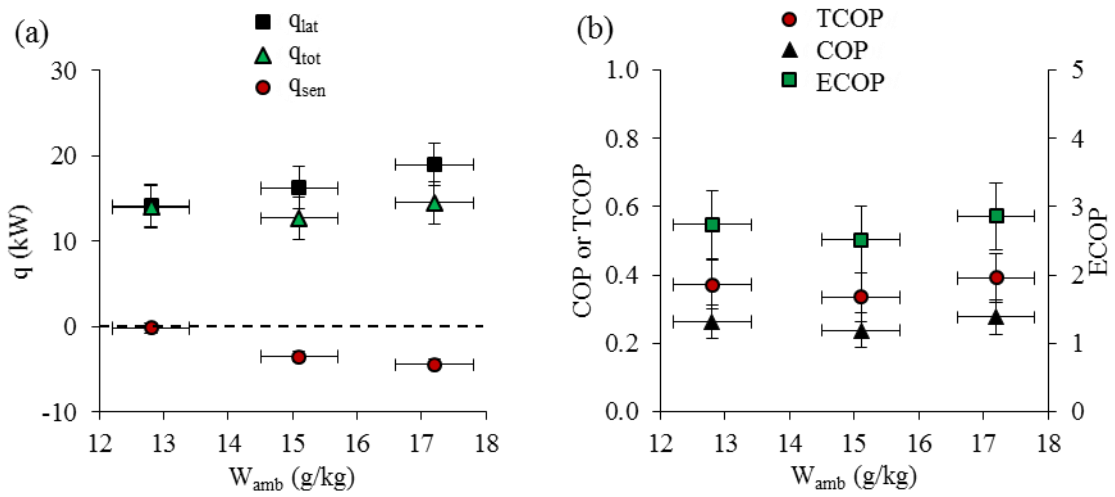

FIGURE 8.14. The influence of ambient air humidity ratio (W_{amb}) on (a) the sensible (q_{sen}), latent (q_{lat}) and total (q_{tot}) heat transfer rates, and (b) the TCOP, ECOP and COP of the LDAC system.

8.7.2 Transient daily profile

The advantage of a LDAC system is realized when a solar thermal system or a waste heat source is integrated with the LDAC system. The low COPs reported for the LDAC system in Figures 8.10 and 8.14 are attributed to the use of a gas boiler to provide all the thermal energy required for the regeneration of the dilute desiccant solution. The influence of integrating the 95 m^2 evacuated-tube solar thermal array, previously illustrated in Section 8.5.7, with the LDAC system is presented in this section. In order to quantify the improvements achieved in the COP of the LDAC system when it is integrated with the solar thermal array, equation (8.7) is used to calculate the COP of the LDAC system in two cases as follows.

- COP_{boiler}: assumes that all the thermal energy requirements of the LDAC system are provided using the gas boiler.
- COP_{solar}: considers the thermal energy delivered to the LDAC system by the solar thermal system and is counted as thermal energy input in the first term of the denominator of equation (8.7) only the auxiliary heating energy provided by the gas boiler.

Figure 8.15 shows the performance of the solar LDAC system for a complete test day from 8AM until 6PM on July 23, 2012. The outdoor air humidity ratio varied between 15 g/kg and 18 g/kg during the test day, and the outdoor air temperature varied between 24ºC and 31ºC. Figure 8.15(a) shows the temperatures and humidity ratios of the process air at the inlet and outlet of the dehumidifier, where it can be seen that the process air is heated and dehumidified during the whole test day. The solar fraction of the solar LDAC system is defined as the ratio between the thermal energy delivered to the LDAC system by the solar thermal system and the thermal energy consumed for the regeneration of dilute desiccant solution. The solar fraction of the solar LDAC system and the solar radiation during the test day are presented in Figure 8.15(b).

Figure 8.15(c) shows the COP_{boiler} and COP_{solar} during the test day. The percent improvement in the COP_{solar} compared to the COP_{boiler} is found to be strongly correlated with the solar radiation, as presented in Figure 8.15(d). The percent improvement in the COP reaches up to 270% (i.e. from COP_{boiler} = 0.3 to COP_{solar} = 1.1) during the peak solar radiation periods (i.e. approximately 950 W/m^2) of the test day. The lower values of COP_{solar} than COP_{boiler} between 8AM and 9AM are because the auxiliary boiler is used during the start-up of the solar thermal system to charge the buffer hot water tanks (Crofoot, 2012).

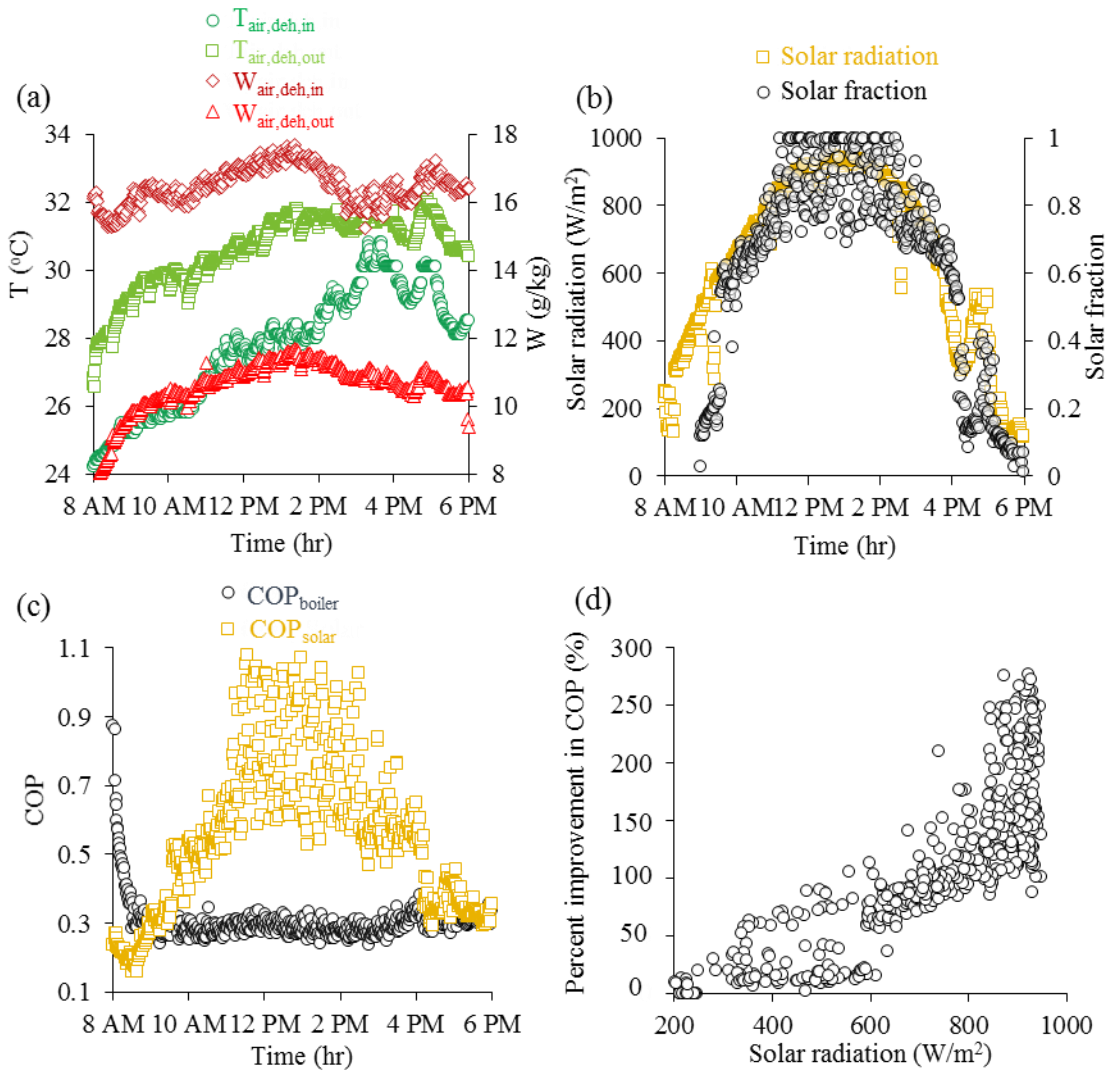

FIGURE 8.15. A daily transient profile for the solar LDAC system during a complete test day on July 23.

8.7.3 Comparison between quasi-steady and transient performances

Steady-state models are commonly used for performance evaluation of LDAC systems to decrease the computing effort and time associated with transient energy modelling. The influence of using steady-state performances of LDAC systems compared to if transient performances are considered need to be evaluated. To this aim, a comparison between the transient and quasi-steady supply air conditions and energy performances of the LDAC system under study is presented in this section. The quasi-steady performance of the LDAC system is estimated in this section based on regression correlations, equation (8.8), which

are developed based on the results presented in Figures 8.7 and 8.11. The regression correlations used in this section are applicable under specific outdoor air conditions, where either ambient air temperature is constant at 27.8ºC or ambient air humidity ratio is constant at 16.3 g/kg. The outdoor air conditions during the test day examined in this section (i.e. July 23) are within the ranges of validity for equation (8.8) and thus no extrapolation is used in the calculations presented in this section.

$$\left.\begin{array}{l}\left.\begin{array}{l} T_{air,deh,out} = 10.45(W_{amb})^{0.39} \\ W_{air,deh,out} = 0.64(W_{amb})^{1.01} \end{array}\right\} \text{ at } T_{amb,db} = 27.8^{o}C \\ \left.\begin{array}{l} T_{air,deh,out}=6.79\left(T_{amb,db}\right)^{0.45} \\ W_{air,deh,out}=0.0053\left(T_{amb,db}\right)^{2}-0.2932\left(T_{amb,db}\right)+14.87 \end{array}\right\} \text{ at } W_{amb} = 16.3 \text{ g/kg} \end{array}\right\} R^2 \geq 0.95 \quad (8.8)$$

Figure 8.16(a) shows the measured transient supply air conditions (temperature and humidity ratio of air leaving the dehumidifier) and the quasi-steady supply air conditions calculated using equation (8.8). It is found that the measured transient supply air conditions lie within the uncertainty bounds of the quasi-steady air conditions for majority of the test day. However, the deviation between the transient and quasi-steady supply air conditions exceeds the uncertainty bounds during the start-up of the system. Similarly, the transient and quasi-steady-state energy transfer rates in the dehumidifier of the LDAC system (Figure 8.16(b)) agree except for the first 2 hours of the day. Integrating these energy transfer rates gives the total energy transfer to the supply air (process air) stream during the test day (i.e. from 8AM until 6PM) as presented in Figure 8.16(c). It can be seen that the differences between the transient and quasi-steady results are low (11% for sensible, 5% for latent and 3% for total energy) and within the uncertainty bounds.

Figure 8.16(d) shows the quasi-steady and transient energy consumption of the LDAC system for the test day, assuming that the thermal energy required for the regeneration of dilute desiccant solution is provided by the gas boiler. This figure allows a comparison of the energy performance of a LDAC system when considering or neglecting the transient effects. Since the differences between the transient and quasi-steady results are low (less

than 10%) and within the uncertainty bounds, it can be concluded that a quasi-steady analysis, as applied in this experimental study and other numerical studies (Abdel-Salam et al., 2013a, 2014a; Abdel-Salam and Simonson, 2014a, 2014b; Crofoot, 2012; Li et al., 2009), is adequate to estimate the energy performance of LDAC systems. This is an important finding since this is the first paper in the literature to directly quantify the effects of transients on the energy performance of a LDAC system.

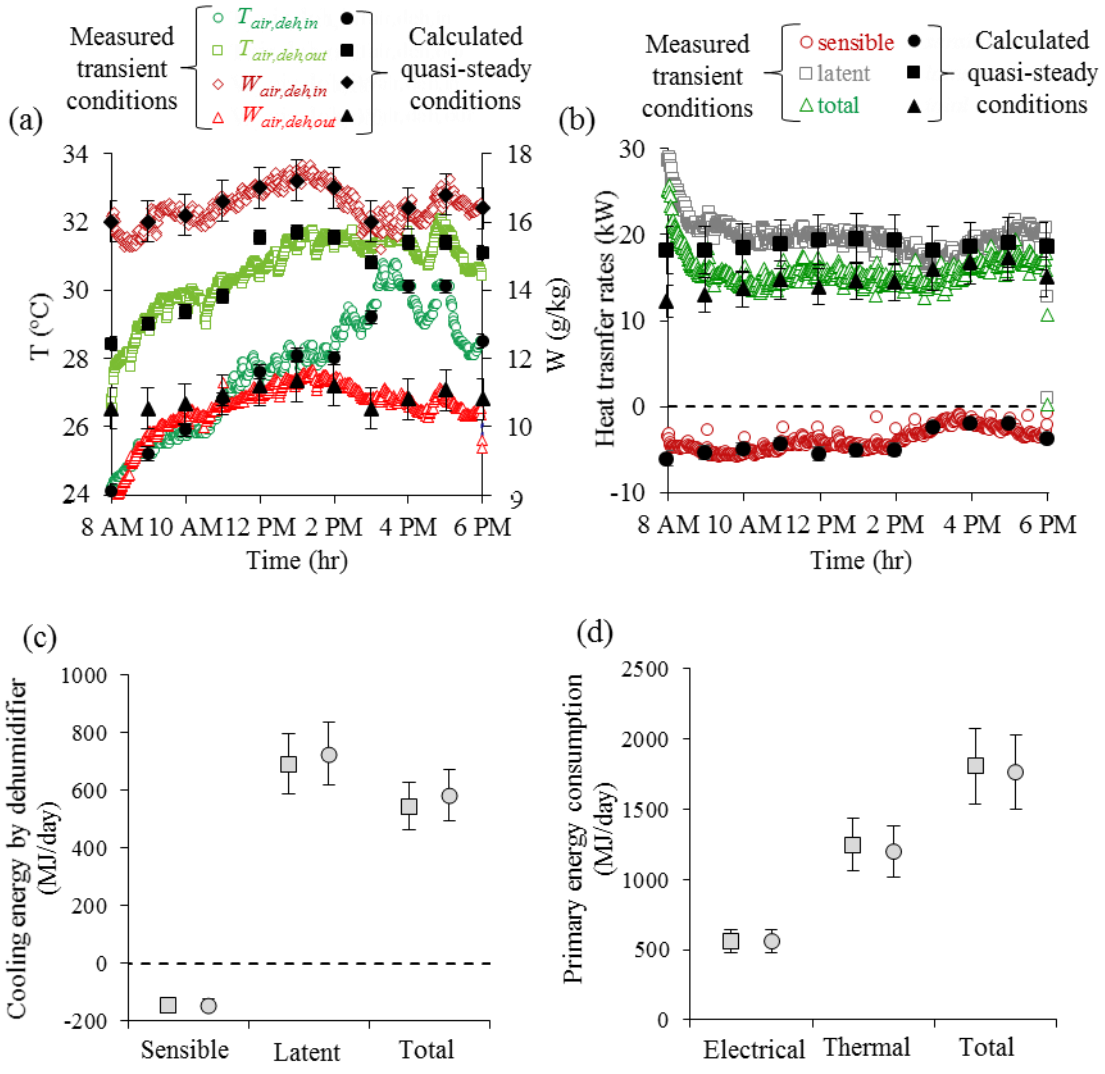

FIGURE 8.16. Comparisons between quasi-steady and transient (a) conditions of air leaving the dehumidifier, (b) heat transfer rates, (c) cooling energy by the dehumidifier, and (d) primary energy consumption of the LDAC system during a complete test day on July 23.

8.7.4 Quasi-steady performance evaluation using transient data

The evaluation of quasi-steady performance for a full-scale LDAC system is an expensive and challenging task. This is because there are a few certified test labs which are equipped with the necessary equipment to conduct tests for full-scale LDAC systems at steady-state conditions. In addition, manufacturers need to conduct field tests in different climates before commercializing a new system, which results in large sets of transient data. If averaged data collected from a field test can accurately predict the quasi-steady performance of LDAC systems, this would result in the reduction of the time and resources required to evaluate the quasi-steady performances LDAC systems.

For the field test in this paper, the average ambient air conditions for six hours on July 17 (T = 34ºC and W = 16.4 g/kg, see Figure 8.17(a)) and for 9 hours on July 31 (T = 27.2ºC and W = 15.1 g/kg, see Figure 8.18(a)) were found to be almost the same as the ambient air conditions for the quasi-steady tests T3 and W3 (see Table 8.3), respectively. Thus, these days are used to compare the quasi-steady and averaged transient performance of the LDAC system. The uncertainty of the averaged performance is assumed to be similar to the uncertainty of the quasi-steady performance.

Figure 8.17(b) shows that the averaged transient properties of the air, solution and water streams entering/leaving the dehumidifier on July 17 are almost identical to the quasi-steady properties for test T3. Furthermore, Figure 8.17(c) shows that the quasi-steady and average energy transfer rates agree within the experimental uncertainty bounds. Similarly, Figures 8.18(b) and 8.18(c) show good agreement (within uncertainty bounds) between the averaged transient values on July 31 and the quasi-steady values obtained from test W2. Therefore, it can be concluded that averaged transient data from field tests can be used to estimate the quasi-steady performance of LDAC systems under some operating and environmental conditions.

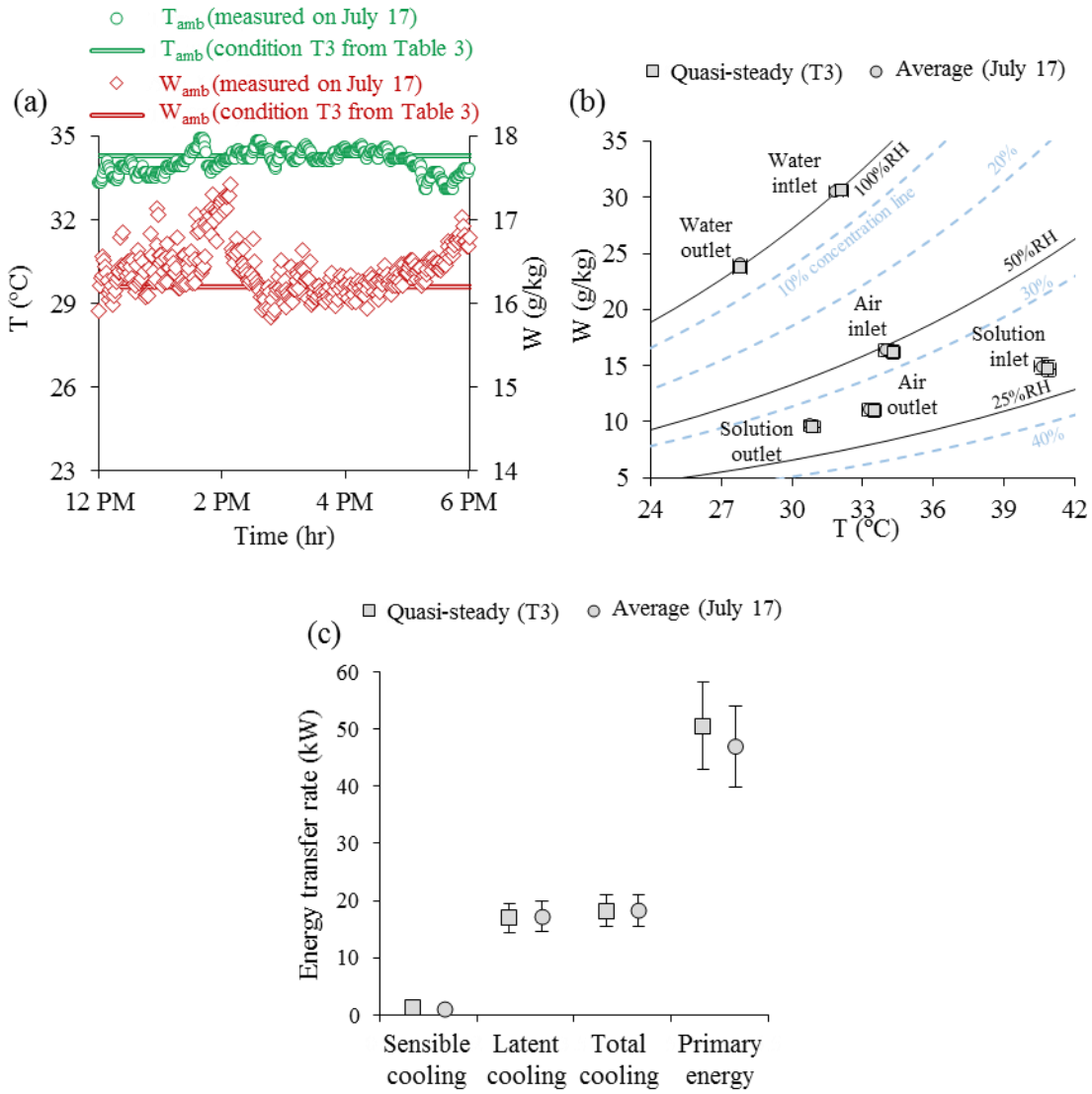

FIGURE 8.17. Comparison between performance evaluation using an average value of transients on July 17 and quasi-steady data at test condition T3 from Table 8.3. (a) Measured ambient air temperature and humidity ratio on July 17, (b) air, solution and water inlet and outlet conditions from the dehumidifier, (c) sensible, latent and total cooling energy by the dehumidifier, and rate of primary energy consumption by the LDAC system.

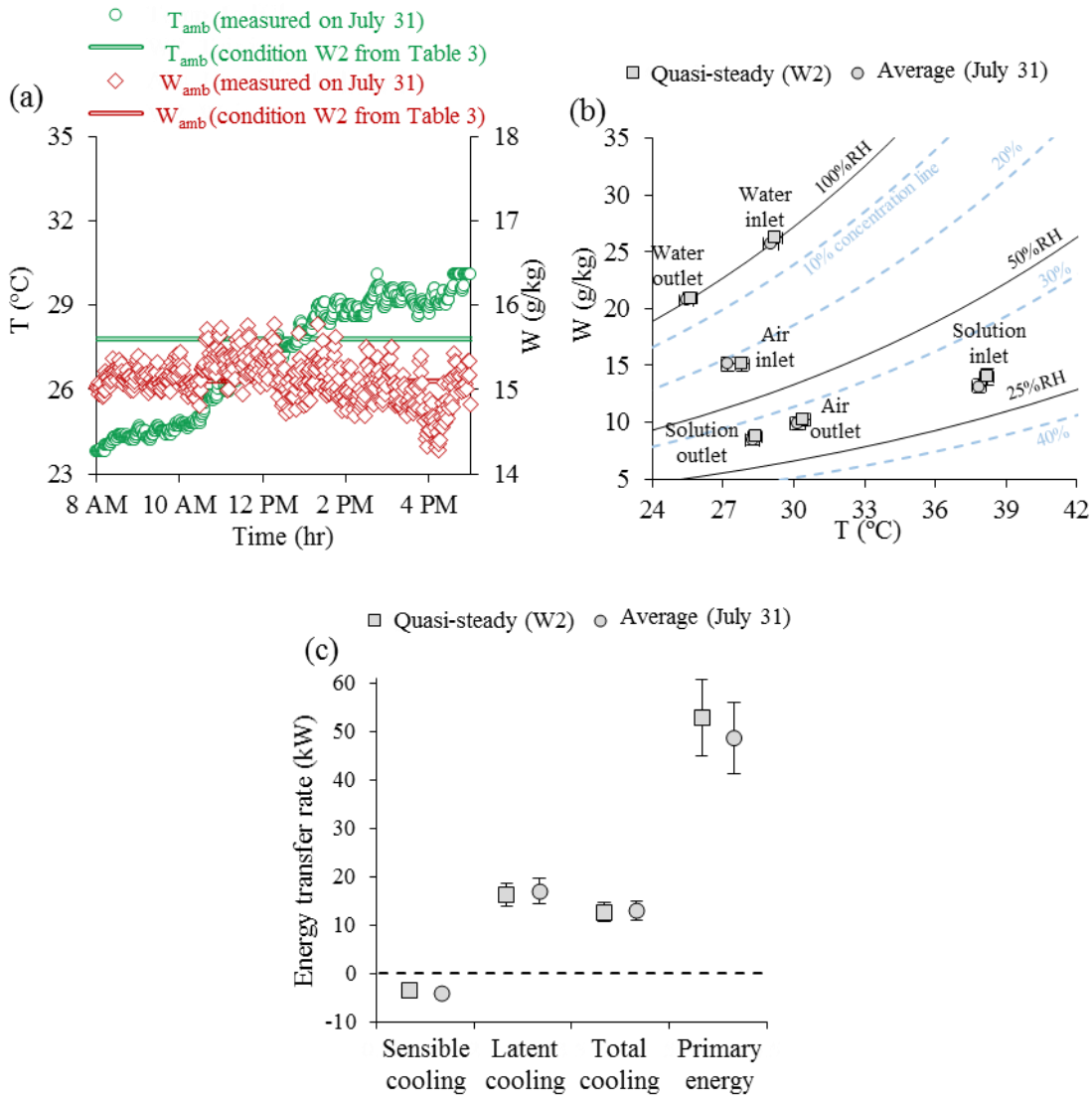

FIGURE 8.18. Comparison between performance evaluation using an average value of transients on July 31 and quasi-steady data at test condition W2 from Table 8.3. (a) Measured ambient air temperature and humidity ratio on July 31, (b) air, solution and water inlet and outlet conditions from the dehumidifier, (c) sensible, latent and total cooling energy by the dehumidifier, and rate of primary energy consumption by the LDAC system.

8.8 SUMMARY AND CONCLUSIONS

The performance of a low-flow internally-cooled/heated solar liquid desiccant air conditioning (LDAC) system is investigated in this study. Results from a field test are analyzed and discussed to evaluate the quasi-steady and transient performances of the solar LDAC system. Six quasi-steady operating conditions are presented to investigate the influences of ambient air temperature ($T_{amb,db}$) and humidity ratio (W_{amb}) on the performance of the LDAC system. The influence of integrating a 95 m^2 evacuated-tube solar thermal array with the LDAC system is investigated. The transient performance of the LDAC system is presented and compared to its quasi-steady performance, and the prediction of quasi-steady performance of the LDAC system using averaged transient data is evaluated.

It is found that $T_{amb,db}$ has observable influence on the COP of the LDAC system, while W_{amb} has no considerable influence on the COP of the LDAC system. The latent capacity of the LDAC system remains almost the same with increasing $T_{amb,db}$, while more sensible energy is removed; this leads to the increase of the total capacity removed from the process air. Thus, the COP of the LDAC system increases as $T_{amb,db}$ increases. On the other hand, increasing W_{amb} leads to an increase in the latent capacity, a decrease in the sensible cooling and a little change in the total capacity. Thus, the COP of the LDAC system remains nearly constant as W_{air} increases. The system's performance is found to be limited by the performance of the evaporative cooling tower. Under the six tested quasi-steady conditions, the latent and total capacities of the LDAC system are in the ranges of 14-19 kW and 11-18 kW, respectively. The thermal and electrical COPs are in the ranges of 0.35-0.52 and 2.7-3.6, respectively, and the combined COP ranges from 0.25 to 0.36 when referenced to thermal energy and 0.75 to 1.1 when referenced to electricity. The solar LDAC system has a significantly higher COP, up to 270% during peak solar radiation periods of 950 W/m^2, than a LDAC system which uses a gas boiler to provide the thermal energy required for the regeneration of dilute desiccant solution.

The transient and quasi-steady performances of the LDAC system have good agreement, except during the start-up, with a maximum deviation in supply air conditions of 1.5 g/kg

and 1.1ºC throughout the test day. The sensible, latent and total cooling energy of the LDAC system for the entire test day change by 11%, 5% and 3%, respectively, when the system is assumed to be operated under quasi-steady conditions compared to transient conditions. In addition, the deviation between the quasi-steady and transient primary energy consumption by the LDAC system during a complete test day is less than 10%. Thus, it can be concluded that steady-state models are reliable to evaluate energy performances of LDAC systems.

This paper demonstrates, for the first time, that data averaging for transient field tests can be used to predict the quasi-steady performances for a LDAC system with acceptable uncertainty. The findings of this paper are useful for practical applications of LDAC systems, and should be consulted by manufacturers as a reference for conducting field tests and evaluating the transient and quasi-steady performances of LDAC systems.

CHAPTER 9

SUMMARY, CONCLUSIONS, CONTRIBUTIONS AND FUTURE WORK

The main goal of this Ph.D. research is to propose and investigate novel solutions for limitations that hinder the wide spread use of LDAC systems in commercial and residential buildings. A summary of the important results and contributions of this thesis are presented in this chapter. In addition, some promising topics are suggested for future research.

9.1 SUMMARY AND CONCLUSIONS

Desiccant droplets carryover by the air streams is a major concern in most direct-contact LDAC systems. To eliminate this problem, a novel membrane LDAC technology is proposed and evaluated in this thesis. A steady-state TRNSYS model is developed for the membrane LDAC system in Chapter 2 to quantify the heat and mass transfer performance of the system. A parametric study is conducted and resulted in identifying the key control parameters, and their recommended operating ranges are identified. It is found that installing a solution-to-solution heat exchanger can decrease the solution cooling and heating loads by up to 26%, depending on the design and operating conditions. An efficient control system should be installed for the solution-to-solution heat exchanger because at some extreme operating conditions it is more beneficial to bypass solution flows around the exchanger.

Results in Chapter 2 show that the proposed membrane LDAC system is able to effectively remove latent loads in applications that require efficient humidity control. The performance of the LDAC system significantly improves with the increase of NTU and Cr^* until they reach specific maximum values. The moisture removal rate of the system can be increased by either increasing the solution inlet temperature to the regenerator or decreasing the solution inlet temperature to the dehumidifier. The NTU, Cr^*, and air inlet temperature and relative humidity are the most influential parameters on the effectivenesses of the LAMEEs used in the membrane LDAC system. The latent effectiveness of the LAMEE is always

lower than its sensible effectiveness, whether the LAMEE is used as a regenerator or a dehumidifier. This can be expected for membrane energy exchangers due to the fact that the mass transfer resistance is usually higher than that of heat transfer. The sensible and latent effectivenesses of the dehumidifier are always larger than those for the regenerator.

The thermal, economic and environmental performances of basic configurations for the membrane LDAC system are evaluated in Chapter 3 when it is installed in a small office building located in a hot-humid climate (Miami, FL). Results show that the annual primary energy consumption and the life cycle cost of the proposed membrane LDAC system are 19% and 12% lower than that of a conventional air conditioning system, and they reach 32% and 21% when an ERV is installed in the membrane LDAC system. It is concluded from Chapter 3 that the membrane LDAC system is a promising system from technical, environmental and economic points of views, and that more research should focus on investigating different types of solution heating equipment because solution heating contributes to a large portion of the energy consumption.º

Several configurations of solar membrane LDAC systems are investigated in Chapter 4, and the sizes of the solar thermal systems are optimized to give the lowest life cycle cost. It is concluded that using a solar thermal system to cover the solution heating loads significantly improves the thermal, economic and environmental performances of the LDAC systems studied, with more significant reductions when a natural gas boiler is used as the backup heating system and there is no energy recovery ventilator. In addition, it is found that counting on a natural gas boiler as the only heating source in a membrane LDAC system is not economical because this leads to higher initial, operating and life cycle costs than a conventional air conditioning system.

A heat-pump membrane LDAC system is investigated in Chapter 5, and its life cycle cost is found to be the lowest among all the systems studied in Chapters 3 and 4. It is found that there is no clear understanding for how capacity matching can be achieved in a heat-pump LDAC system. Thus, the focus of Chapter 6 is to define the fundamentals of capacity matching in heat-pump LDAC systems. Different configurations that were used in previous

heat-pump LDAC systems to achieve capacity matching are categorized into three general categories. A novel configuration for a heat-pump membrane LDAC system is proposed to eliminate the failure of achieving capacity matching under any operating condition. The capacity matching in this novel configuration is investigated by conducting a parametric study to evaluate the influences of the key design and operating parameters.

It is concluded from Chapter 6 that the solution inlet temperatures to the dehumidifier and regenerator are the most effective parameters to control the moisture removal rate, capacity matching and COP in heat-pump membrane LDAC systems. In addition, it is found that although the NTU and Cr^* do not have considerable direct influences on capacity matching, these two parameters are key parameters for the moisture removal rate of the system. This means that they, indirectly, affect capacity matching because the solution temperatures required to dehumidify the air to a specific humidity ratio vary accordingly with NTU and Cr^*.

The focus of Chapter 7 is to develop novel strategies for optimal control of the heat-pump membrane LDAC system investigated in Chapter 6. The main concept of the control strategies developed and presented in Chapter 7 is that there are infinite combinations of solution inlet temperatures to the regenerator and dehumidifier that can be used to meet a specific latent load. The proposed control strategy enables the operation of a heat-pump LDAC system under one of following three operating modes that aim to: (1) cover latent loads and optimize the system COP, (2) cover latent loads and achieve capacity matching, or (3) cover both the latent and sensible loads. At ambient air conditions of 35ºC and 12.5 g/kg, it is found that an improvement of up to 126% (i.e. from 1.9 to 4.3) can be achieved in the COP of the system when it is operated under the right combination of solution inlet temperatures to the regenerator and dehumidifier. The influences of the proposed control strategies on the performances of the main components of a heat-pump membrane LDAC system, as well as the performance of the whole system, are presented and discussed in detail. The proposed strategies are applied in this thesis on a heat-pump membrane LDAC system; however, it can be useful in controlling other types of LDAC systems with different heating and cooling equipment.

Although a majority of research conducted on LDAC systems, including this thesis, use steady-state models, no information was found in the literature about the importance of transients in evaluating the performance of LDAC systems. Thus, the focus of Chapter 8 is to evaluate the importance of transients in evaluating the performance of LDAC systems. A data set obtained from a field test on a solar LDAC system is analyzed in Chapter 8 to address this objective. A direct comparison of the transient and quasi-steady performance of the LDAC system is conducted. Results show that the sensible, latent and total cooling energy are changed by 11%, 5% and 3%, respectively, and the primary energy consumption is changed by less than 10% during an entire test day when transients are considered. Thus, a steady-state model may be used to predict the performance of LDAC systems with acceptable uncertainty. In addition, it is found that it is possible to quantify the quasi-steady performance of a LDAC system from transient field data using average data.

It is concluded from this thesis that there is high potential for membrane LDAC systems to achieve considerable energy savings compared to conventional systems, and to eliminate common concerns about direct-contact LDAC systems.

9.2 CONTRIBUTIONS

This thesis contains the following contributions to the scientific literature and practical appliactions of LDAC systems.

9.2.1 Performance and design of membrane LDAC systems

- Quantified the heat and mass transfer performance of a membrane LDAC system, and evaluated the energy savings compared to conventional air conditioning.
- Identified a preventive control strategy for the solution-to-solution heat exchanger in a LDAC system.
- Determined the energy, environmental and economic performances for sevreal membrane LDAC systems, and identifed the most promising configuration for future research.

9.2.2 Capacity matching and control of heat-pump LDAC systems

- Defined categories for different designs and strategies used to achieve capacity matching in heat-pump LDAC systems.
- Quantified the influences of key design and operating parameters on capacity matching in a heat-pump membrane LDAC system.
- Proposed a novel design to eliminate the failure of achieving capacity matching under any operating condition.
- Developed a novel dimensionless capacity-matching index (CMI) to quantify the degree of capacity matching in a heat-pump LDAC system.
- Developed novel optimal control strategies for heat-pump LDAC systems.

9.2.3 Field testing and modelling of LDAC systems

- Quantified the importance of transients in evaluating the performance of a LDAC system.
- Developed and verified a new method to quantify, with acceptable uncertainties, the quasi-steady performance of a LDAC system from transient field data using average data.

9.3. FUTURE WORK

9.3.1. Heating and humidification

The focus of this thesis is on achieving cooling and dehumidification using the membrane LDAC system. A membrane liquid desiccant heating and humidification (LDHH) system is recommended to be studied in future work.

9.3.2. Thermo-economic feasibility of optimally-controlled heat-pump LDAC system

The novel control strategies proposed in Chapter 7 for heat-pump LDAC systems are studied under fixed operating conditions. It is recommended that future research evaluate the thermo-economic feasibility of applying the proposed strategies in a heat-pump LDAC system during yearly operartion.

9.3.3. Two-fluid versus three-fluid membrane LDAC systems

A two-fluid LAMEE is used in this thesis as the dehumidifier/regenerator, where the desiccant solution is cooled/heated prior entering the two-fluid LAMEE. In a three-fluid LAMEE, the solution is heated/cooled as it passes through the LAMEE using internal tubes. Preliminary comparisons between the heat and mass transfer performances of the two-fluid and three-fluid LAMEEs show that higher sensible and latent effectivenesses can be attained using the three-fluid LAMEE (Abdel-Salam et al., 2015c). It is recommended that future work compare the economics and COPs of two-fluid and three-fluid membrane LDAC systems.

9.3.4. Advanced storage system

The continuous operation of a LDAC system requires the availability of concentrated desiccant solution, cold water and hot water. The feasibility of integrating a concentrated solution, cold water and hot water storage tanks is recommended to be studied. Although integrating advanced storage systems with the liquid desiccant technology will increase its complexity, several advantages are expected to be achieved as follows. (1) Assist to shift peak loads. (2) Decrease operating costs of the LDAC system by regenerating the storage system when energy is at low cost or when waste energy is available to be used at times when energy is expensive or waste energy is not available.

9.3.5. Indirect-evaporative and dew-point cooling technologies

Resutls presented in Chapter 8 of this thesis show that the use of a direct evaporative cooling towers hinders the performance of the LDAC system when the ambient wet bulb temperature increases. Since LDAC systems are expected to be mainly installed in humid climates (with high wet bulb temperatures), it is recommended that future work focus on integrating indirect-evaporative and dew-point cooling technologies with LDAC systems.

9.3.6. Different designs for the dehumidifier and regenerator

Majority of LDAC studies use similar designs for the dehumidifier and regenerator. It is recommended that future research investigate the feasibility of using different designs for the dehumidifier and regenerator. Different types of dehumidifiers and regenerators are presented in a recent review article by Abdel-Salam and Simonson (2015a). This review is recommended to be consulted to select possible combinations of dehumidifiers and regenerators.

9.3.7. Life cycle cost assessment

The economic results presented in this thesis show that the membrane LDAC technology can be more economic than the conventional air conditioning technology. However, some factors were not included in the economic analysis in this thesis such as the installation and maintenance costs, and salvage values. Further economic studies are recommended to be conducted to evaluate the membrane LDAC technology, and to include the installation and maintenance costs, salvage values and up-to-date components costs.

REFERENCES

Abdel-Salam, A.H., Ge, G., Simonson, C.J., 2013a. Performance analysis of a membrane liquid desiccant air-conditioning system. *Energy and Buildings*, **62**, 559-569.

Abdel-Salam, A.H., Ge, G., Fauchoux, M.T., Simonson, C.J., 2013b. Annual energy simulation of a novel membrane liquid desiccant air conditioning system in an office building located in a hot humid climate. Proceedings of the 5th International Conference on Solar Air-Conditioning, Bad Krozingen, Black Forest, Germany.

Abdel-Salam, A.H., Ge, G., Fauchoux, M.T., Moghaddam, D.G., Simonson, C.J., 2013c. Effectiveness evaluation of a liquid-to-air membrane energy exchangers as dehumidifier/regenerator in a liquid desiccant air-conditioning system. Proceedings of the 24th Canadian Conference of Applied Mechanics (CANCAM 2013), Saskatoon, SK, Canada.

Abdel-Salam, A.H., Abdel-Salam, M.R.H., Ge, G., Fauchoux, M.T., Simonson C.J., 2013d. Impacts of different air conditioning schemes on indoor air quality, energy consumption, environmental emissions and economics of a small office building in a hot-humid climate. Proceedings of the 17th ASHRAE IAQ Conference, Vancouver, Canada.

Abdel-Salam, A.H., Ge, G., Simonson, C.J., 2014a. Thermo-economic performance of a solar membrane liquid desiccant air conditioning system. *Solar Energy*, **102**, 56-73.

Abdel-Salam, M.R.H., Fauchoux, M.T., Ge, G., Besant, R.W., Simonson, C.J., 2014b. Expected energy and economic benefits, and environmental impacts for liquid-to-air membrane energy exchangers (LAMEEs) in HVAC systems: A review. *Applied Energy*, **127**, 202-218.

Abdel-Salam, M.R.H., Ge, G., Fauchoux, M.T., Besant, R.W., Simonson, C.J., 2014c. State-of-the-art in liquid-to-air membrane energy exchangers (LAMEEs): A comprehensive review. *Renewable Energy and Sustainable Reviews*, **39**, 700-728.

Abdel-Salam, A.H., Ge, G., Simonson, C.J., 2014d. TRNSYS modelling of a hybrid membrane liquid desiccant air conditioning system. Proceedings of IBPSA-Canada's 8th biennial conference (eSim 2014), Ottawa, ON, Canada.

Abdel-Salam, A.H., Simonson, C.J., 2014a. Annual evaluation of energy, environmental and economic performances of a membrane liquid desiccant air conditioning system with/without ERV. *Applied Energy*, **116**, 134-148.

Abdel-Salam, A.H., Simonson, C.J., 2014b. Capacity matching in heat-pump membrane liquid desiccant air conditioning systems. *International Journal of Refrigeration*, **48**, 166-177.

Abdel-Salam, A.H., Simonson, C.J., 2015a. State-of-the-art in liquid desiccant air conditioning equipment and systems. *Renewable Energy and Sustainable Reviews*, submitted.

Abdel-Salam, A.H., Simonson, C.J., 2015b. A novel control strategy for a heat-pump membrane liquid desiccant air conditioning system. *International Journal of Refrigeration*, submitted.

Abdel-Salam, A.H., Simonson, C.J., 2015c. COP evaluation for a membrane liquid desiccant air conditioning system using four different heating equipment. Proceedings of 2015 REHVA annual conference: Advanced HVAC & Natural Gas Technologies, Riga, Latvia.

Abdel-Salam, A.H., McNevin, C., Crofoot, L., Harrison, S.J., Simonson, C.J., 2015a. A field study of a solar liquid desiccant air conditioning system: Quasi-steady and transient. *ASME Journal of Solar Energy Engineering*, submitted.

Abdel-Salam, M.R.H., Besant, R.W., Simonson, C.J., 2015b. Sensitivity of the performance of a flat-plate liquid-to-air membrane energy exchanger (LAMEE) to the air and solution channel widths and flow maldistribution. *International Journal of Heat and Mass Transfer*, **84**, 1082-1100.

Abdel-Salam, M.R.H., Besant, R.W., Simonson, C.J., 2015c. Design and testing of a novel 3-fluid liquid-to-air membrane energy exchanger (3-fluid LAMEE). *International Journal of Heat and Mass Transfer*, submitted.

Advantix Systems (http://www.advantixsystems.com).

Afshin, M., 2010. Selection of the liquid desiccant in a run-around membrane energy exchanger, M.Sc. Thesis., Department of Mechanical Engineering, University of Saskatchewan, Saskatoon, SK.

Afshin, M., Simonson, C.J., Besant, R.W., 2010. Crystallization limits of LiCl-Water and $MgCl_2$-Water salt solutions as operating liquid desiccant in the RAMEE system. *ASHRAE Transactions*, **116**, 494–506.

Agra, Ö., 2011. Sizing and selection of heat exchanger at defined saving-investment ratio. *Applied Thermal Engineering*, **31**, 727-734.

Ahmed, S.Y., Gandhidasan, P., Al-Farayedhi, A.A, 1997. Thermodynamic analysis of liquid desiccants. *Solar Energy*, **62**, 11-18.

AHRI, 2005. ANSI/ARI Standard 1060: Standard for rating air-to-air exchangers for energy recovery ventilation equipment. Air-Conditioning & Refrigeration Institute, Arlington, VA.

AIL Research Inc. (http://www.ailr.com).

Akbari, S., Hemingson, H.B., Beriault, D., Simonson. C.J., Besant, R.W., 2012. Application of neural networks to predict the steady state performance of a run-around membrane energy exchanger. *International Journal of Heat and Mass Transfer*, **55**, 1628-1641.

Al-Alili, A., Islam, M.D., Kubo, I., Hwang, Y., Radermacher, R., 2012. Modeling of a solar powered absorption cycle for Abu Dhabi. *Applied Energy*, **93**, 160-167.

Alibaba Group, 2014 (http://www.alibaba.com/showroom/flat-plate-solar-collector-prices.html).

Alizadeh, S., 2008. Performance of a solar liquid desiccant air conditioner – An experimental and theoretical approach. *Solar Energy*, **82**, 563-572.

Alosaimy, A.S., Hamed, A.M., 2011. Theoretical and experimental investigation on the application of solar water heater coupled with air humidifier for regeneration of liquid desiccant. *Energy*, **36**, 3992-4001.

Andrusiak, M., Harrison, S.J., 2009. The modeling and design of a solar-driven liquid-desiccant air-conditioning system. Proceedings of the 4th annual Canadian solar buildings conference, Toronto, Canada.

Andrusiak, M., Harrison, S.J., 2009. The modeling of a solar thermally-driven liquid desiccant air conditioning system. Proceedings of the ASES national solar conference, Buffalo, USA.

Andrusiak, M., Harrison, S., Mesquita, L., 2010. Modeling of a solar thermally-driven liquid-desiccant air-conditioning system. Proceedings of ASES national solar conference, Pheonix, USA.

ASHRAE, 2007. ANSI/ASHRAE Standard 62.1-2007: Ventilation for acceptable indoor air quality. American Society of Heating, Refrigerating and Air-Conditioning Engineers Inc, Atlanta, Georgia.

ASHRAE, 2005. Handbook - Fundamentals 2005, Chapter 22: Sorbents and Desiccants. American Society of Heating, Refrigeration and Air-Conditioning Engineers, Inc., Atlanta Georgia.

ASHRAE, 2009. Handbook-Fundamentals. American Society of Heating, Refrigerating and Air-Conditioning Engineers, Inc., Atlanta, Georgia.

ASHRAE, 2004. ANSI/ASHRAE Standard 90.1-2004: Energy standard for buildings except low-rise residential buildings. American Society of Heating, Refrigerating and Air-Conditioning Engineers Inc, Atlanta, Georgia.

ASHRAE, 2008. ASHRAE Handbook–HVAC systems and equipment. American Society of Heating, Refrigerating and Air-Conditioning Engineers, Inc., Atlanta, Georgia.

ASHRAE, 2004. ANSI/ASHRAE Standard 55-2004: Thermal environmental conditions for human occupancy. American Society of Heating, Refrigerating and Air-Conditioning Engineers, Inc., Atlanta, Georgia.

ASHRAE, 2008. ANSI/ASHRAE Standard 84-2008: Method of testing air-to-air heat exchangers. American Society of Heating, Refrigerating and Air-Conditioning Engineers, Inc., Atlanta, Georgia.

ASME, 2005. PTC 19.1-2005: Test uncertainty. American Society of Mechanical Engineers, New York.

Assilzadeh, F., Kalogirou, S.A., Ali, Y., Sopian, K., 2005. Simulation and optimization of a LiBr solar absorption cooling system with evacuated tube collectors. *Renewable Energy*, **30**, 1143-1159.

Audah, N., Ghaddar, N., Ghali, K., 2011. Optimized solar-powered liquid desiccant system to supply building fresh water and cooling needs. *Applied Energy*, **88**, 3726–3736.

Bansal, P., Jain, S., Moon, C., 2011. Performance comparison of an adiabatic and an internally cooled structured packed-bed dehumidifier. *Applied Thermal Engineering*, **31**, 14-19.

Bassuoni, M.M., 2011. An experiment study of structures packing dehumidifier/regenerator operating with liquid desiccant. *Energy*, **36**, 2628-2638.

Beriault, D.A., 2011. Run-around membrane energy exchanger prototype 4 design and laboratory testing. M.Sc. thesis, Department of Mechanical Engineering, College of Engineering, University of Saskatchewan, Saskatoon, SK.

Bergero, S., Chiara, A., 2010. Performance analysis of a liquid desiccant and membrane contactor hybrid air-conditioning system. *Energy and Buildings*, **42**, 1976-1986.

Bergero, S., Chiari, A., 2011. On the performances of a hybrid air-conditioning system in different climatic conditions. *Energy*, **36**, 5261-5273.

Brown, J.S., Domanski, P.A., Lemmon, E.W., 2012. cycle_d: NIST vapor compression cycle design program version 5.0.

Burns, P.R., Mitchell, J.W., Beckman, W.A., 1985. Hybrid desiccant cooling system in supermarket applications. *ASHRAE Transactions*, **91**, 457–468.

Charles, N.T., Johnson, D.W., 2008. The occurrence and characterization of fouling during membrane evaporative cooling. *Journal of Membrane Science*, **319**, 44–53.

Cheng, Q., Zhang, X., 2013a. Review of solar regeneration methods for liquid desiccant air-conditioning system. *Energy and Buildings*, **67**, 426–433.

Cheng, Q., Zhang, X.-S., 2013b. A solar desiccant pre-treatment electrodialysis regeneration system for liquid desiccant air-conditioning system. *Energy and Buildings*, **67**, 434-444.

Cheng, Q., Xu, Y., Zhang, X.-S., 2013. Experimental investigation of an electrodialysis regenerator for liquid desiccant. *Energy and Buildings*, **67**, 419-425.

Chung, M., Park, J.-U., Yoon, H.-K., 1998. Simulation of a central solar heating system with seasonal storage in Korea. *Solar Energy*, **64**, 163-178.

Conde, M.R., 2004. Properties of aqueous solutions of lithium and calcium chlorides: Formulations for use in air conditioning equipment design. *International Journal of Thermal Sciences*, **43**, 367–382.

Crofoot, L., McNevin, C., Harrison, S., 2014. Performance evaluation of a liquid-desiccant solar air-conditioning system. Proceedings of ISES EuroSun international conference on solar energy and buildings, Aix-les-Bains, France.

Crofoot, L., 2012. Experimental evaluation and modeling of a solar liquid desiccant air conditioner, M.Sc. Thesis, Department of Mechanical and Materials Engineering, Queen's University, Kingston, ON.

Crofoot, L., Harrison, S., 2012. Performance evaluation of a liquid desiccant solar air conditioning system. *Energy Procedia*, **30**, 542-550.

Dai, Y.J., Wang, R.Z., Zhang, H.F., Yu, J.D., 2001. Use of liquid desiccant cooling to improve the performance of vapor compression air conditioning. *Applied Thermal Engineering*, **21**, 1185-1202.

Dai, Y.J., Zhang, H.F., 2004. Numerical simulation and theoretical analysis of heat and mass transfer in a cross flow liquid desiccant air dehumidifier packed with honeycomb paper. *Energy Conversion and Management*, **45**, 1343-1356.

Davies, P.A., 2005. A solar cooling system for greenhouse food production in hot climates. *Solar Energy*, **79**, 661-668.

Deru, M., Field, K., Studer, D., Benne, K., Griffith, B., Torcellini, P., Liu, B., Halverson, M., Winiarski, D., Rosenberg, M., Yazdanian, M., Huang, J., Crawley, D., 2011. US department of energy commercial reference building models of the national building stock. National Renewable Energy Laboratory, Colorado.

Domanski, P.A., Brown, J.S., Heo, J., Wojtusiak, J., McLinden, M.O., 2014. A thermodunamic analysis of refrigerants: Performance limits of the vapor compression cycle. *Internaltional Journal of Refrigeration*, **38**, 71-79.

Duffie, J.A., Beckman, W.A., 2006. Solar engineering of thermal processes, third ed. John Wiley and Sons Inc., Hoboken, New Jersey.

Elminir, H.K., Ghitas, A.E., El-Hussainy, F., Hamid, R., Beheary, M.M., Abdel-Moneim, K.M., 2006. Optimum solar flat-plate collector slope: case study for Helwan, Egypt. *Energy Conversion and Management*, **47**, 624-637.

Energy modelling of buildings, 2014 (http://energymodeling.pbworks.com).

Enteria, N., Yoshino, H., Takaki, R., Mochida, A., Satake, A., Yoshie, R., 2013. Effect of regeneration temperatures in the exergetic performances of the developed desiccant-evaporative air-conditioning system. *International Journal of Refrigeration*, **36**, 2323-2342.

Erb, B., Seyed-Ahmadi, M., Simonson, C.J., Besant, R.W., 2009. Experimental measurements of a run-around membrane energy exchanger with comparison to a numerical model. *ASHRAE Transactions*, **115**, 689-705.

Fan, H., 2005. Modeling a run-around heat and moisture recovery system. M.Sc. thesis, Department of Mechanical Engineering, College of Engineering, University of Saskatchewan, Saskatoon, SK.

Fauchoux, M.T., Simonson, C.J., Torvi, D.A., 2007. The effect of energy recovery on perceived air quality, energy consumption, and the economics of an office building. *ASHRAE Transactions*, **113**, 436–448.

Florida Public Service Commission. Facts and figures of the Florida utility industry 2012 - [cited 15 April 2013]. (http://www.floridapsc.com/publications/pdf/general/factsandfigures2013.pdf).

Florides, G.A.,Kalogirou, S.A., Tassou, S.A., Wrobel, L.C., 2002a. Modelling and simulation of an absorption solar cooling system for Cyprus. *Solar Energy*, **72**, 43-51.

Florides, G.A.,Kalogirou, S.A., Tassou, S.A., Wrobel, L.C., 2002b. Modelling, simulation and warming impact assessment of a domestic-size absorption solar cooling system. *Applied Thermal Engineering*, **22**, 1313-1325.

Fumo, N., Goswami, D.Y., 2002. Study of an aqueous lithium chloride desiccant system: air dehumidification and desiccant regeneration. *Solar Energy*, **72**, 351–361.

Ge, G., Xiao, F., Xu, X., 2011a. Model-based optimal control of a dedicated outdoor air-chilled ceiling system using liquid desiccant and membrane-based total heat recovery. *Applied Energy*, **88**, 4180-90.

Ge, G., Xiao, F., Niu, X.F., 2011b. Control strategies for a liquid desiccant air-conditioning system. *Energy and Buildings*, **43**, 1499-1507.

Ge, G., Abdel-Salam, M.R.H., Besant, R.W., Simonson, C.J., 2013a. Research and applications of liquid-to-air membrane energy exchangers in building HVAC systems at University of Saskatchewan: a review. *Renewable and Sustainable Energy Reviews*, **26**, 464-479.

Ge, G., Moghaddam, D.G., Namvar, R., Simonson, C.J., Besant, R.W., 2013b. Analytical model based performance evaluation, sizing and coupling flow optimization of liquid desiccant run-around membrane energy exchanger system. *Energy and Buildings*, **62**, 248-257.

Ge, G., Moghaddam, D.G., Abdel-Salam, A.H., Besant, R.W., Simonson, C.J., 2014a. Comparison of experimental data and a model for heat and mass transfer performance of a liquid-to-air membrane energy exchanger (LAMEE) when used for air dehumidification and salt solution regeneration. *International Journal of Heat and Mass Transfer*, **68**, 119–131.

Ge, G., Mahmood, G.I., Moghaddam, D.G., Simonson, C.J., Besant, R.W., Hanson, S., Erb, B., Gibson, P.W., 2014b. Material properties and measurements for semi-permeable membranes used in energy exchangers. *Journal of Membrane Science*, **453**, 328-336.

Gebreslassie, B.H., Guillen-Gosalbez, G., Jimenez, L., Boer, D., 2009. Design of environmentally conscious absorption cooling systems via multi-objective optimization and life cycle assessment. *Applied Energy*, **86**, 1712-1722.

Gommed, K., Grossman, G., 2007. Experimental investigation of a liquid desiccant system for solar cooling and dehumidification. *Solar Energy*, **81**, 131–138.

Gommed, K., Grossman, G., Ziegler, F., 2004. Experimental investigation of a LiCl-water open absorption system for cooling and dehumidification. *ASME Journal of Solar Eneergy Engineering*, **126**, 710-715.

Harriman, L.G., Plager, D. Kosar, D., 1997. Dehumidification and cooling loads from ventilation air. *ASHRAE Journal*, 37-45.

Hemingson, H.B., Simonson, C.J., Besant, R.W., 2011. Steady-state performance of a run-around membrane energy exchanger for a range of outdoor air conditions. *International Journal of Heat and Mass Transfer*, **54**, 1814-1824.

Hwang, Y., Radermacher, R., AlAlili, A., Kubo, I., 2008. Review of solar cooling technologies. *HVAC&R Research*, **14**, 507-528.

Incropera, F.P., Dewitt, D.P., 2002. Fundamentals of Heat and Mass Transfer, John Wiley & Sons Inc, New York.

International Energy Agency. Task 38 – Solar Air-Conditioning and Refrigeration (http://archive.iea-shc.org/task38).

Jain, S., Bansal, P.K., 2007. Performance analysis of liquid desiccant dehumidification systems. *International Journal of Refrigeration*, **30**, 861–872.

Jin, H., Spliter, J.D., 2002. A parameter estimation based model of water-to-water heat pumps for use in energy calculation programs. *ASHRAE Transactions*, **118**, 3-17.

Jones, B.M., 2008. Field evaluation and analysis of a liquid desiccant air handling system, M.Sc. Thesis, Department of Mechanical and Materials Engineering, Queen's University, Kingston, ON.

Jones, B.M., Harrison, S.J., 2008. First results of a solar-thermal liquid desiccant air conditioning concept. Proccedings of the 1st international congress on heating, cooling and buildings, Lisbon, Portugal.

Karlsson, F., Fahlen, P., 2007. Capacity-controlled ground source heat pumps in hydronic heating systems. *International Journal of Refrigeration*, **30**, 221-229.

Katejanekarn, T., Chirarattananon, S., Kumar, S., 2009. An experimental study of a solar-regenerated liquid desiccant ventilation pre-conditioning system. *Solar Energy*, **83**, 920–933.

Katejanekarn, T., Kumar, S., 2008. Performance of a solar-regenerated liquid desiccant ventilation pre-conditioning system. *Energy and Building*, **40**, 1252–1267.

Keßling, W., Lavemann, E., Kapfhammer, C., 1998. Energy storage for desiccant cooling systems component development. *Solar Energy*, **64**, 209–221.

Kessling, W., Laevemann, E., Peltzer, M., 1998. Energy storage in open cycle liquid desiccant cooling systems. *International Journal of Refrigeration*, **21**, 150-156.

Kim, M.-H., Park, J.-S., Jeong, J.-W., 2013. Energy saving potential of liquid desiccant in evaporative cooling-assisted 100% outdoor air system. *Energy*, **59**, 726-736.

Kim, Y.-D., Thu, K., Bhatia, H.K., Bhatia, C.S., Ng, K.C., 2012. Thermal analysis and performance optimization of a solar hot water plant with economic evaluation. *Solar Energy*, **86**, 1378-1395.

Klein, S.A., 2000. TRNSYS-A Transient System Simulation Program, Engineering Experiment Station Report 38-13, Solar Energy Laboratory, University of Wisconsin, Madison.

La, D., Dai, Y., Li, Y., Ge, T., Wang, R., 2011. Case study and theoretical analysis of a solar driven two-stage rotary desiccant cooling system assisted by vapor compression air-conditioning. *Solar Energy*, **85**, 2997-3009

Larson, M.D., 2006. The performance of membranes in a newly proposed run-around heat and moisture exchanger, MSc Thesis, Department of Mechanical Engineering, University of Saskatchewan, Saskatoon, SK.

Larson, M.D., Simonson, C.J., Besant, R.W. Gibson, P.W., 2007. The elastic and moisture transfer properties of polyethylene and polypropylene membranes for use in liquid-to-air energy exchangers. *Journal of Membrane Science*, **302**, 136-149.

Lee, C.K., Kam, H.N., 2014. Simplified explicit calculation algorithms for determining the performance of refrigerant coils in vapour-compression systems. *International Journal of Refrigeration*, **38**, 178-188.

Lemmon, E.W., Huber, M.L., McLinden, M.O., 2010. NIST reference fluids thermodynamic properties - REFPROP, Ver. 9.0, NIST standard reference database 23, National Institute of Standards and Technology, Gaithersburg, Maryland, USA.

Li, H.W.D., Yang, L., Lam, J.C., 2012. Impact of climate change in energy use in the built environment in different climate zones – A review. *Energy and Buildings*, **42**, 103-112.

Li, X.-W., Zhang, X.-S., 2009. Photovoltaic-electrodialysis regeneration method for liquid desiccant cooling system. *Solar Energy*, **83**, 2195-2204.

Li, Y., Lu, L., Yang, H., 2010. Energy and economic performance analysis of an open cycle solar desiccant dehumidification air-conditioning system for application in Hong Kong. *Solar Energy*, **84**, 2085-2095.

Li, Z., Liu, X., Jiang, Y., Chen, X., 2005. New type of fresh air processor with liquid desiccant total heat recovery. *Energy and Buildings*, **37**, 587-593.

Liu, X.H., Zhang, Y., Qu, K.Y., Jiang, Y., 2006. Experimental study on mass transfer performance of cross-flow dehumidifier using liquid desiccant. *Energy Conversion and Management*, **47**, 2682–2692.

Liu, X.H., Jiang, Y., Chang, X.M., Yi, X.Q., 2007. Experimental investigation of the heat and mass transfer between air and liquid desiccant in a cross-flow regenerator. *Renewable Energy*, **32**, 1623–1636.

Liu, X.H., Jiang, Y., Yi, X.Q., 2009a. Effect of regeneration mode on the performance of liquid desiccant packed bed regenerator. *Renewable Energy*, **34**, 209-216.

Liu, X.H., Chang, X.M., Xia, J.J., Jiang, Y., 2009b. Performance analysis on the internally cooled dehumidifier using liquid desiccant. *Building and Environment*, **44**, 299-308.

Löf, G.O.G., 1955. House heating and cooling with solar energy, Solar Energy Research, University of Wisconsin Press, Madison.

Lowenstein, A., 1994. Low-flow internally-cooled liquid-desiccant absorber, US patent #5351497, US patent and trademark office.

Lowenstein, A., Slayzak, S., Kozubal, E., 2006. A zero carryover liquid-desiccant air conditioner for solar applications. Proceedings of ISEC 2006 ASME international solar energy conference, Denver, USA.

Lowenstein, A., 2008. Review of liquid desiccant technology for HVAC applications. *HVAC&R Research*, **14**, 819-839.

Lstiburek, J.W., 1993. Humidity control in the humid south. Proceedings of the building enclosure technology and environment council (BETEC) workshop, Washington, USA.

Lychnos, G., Davies, P.A., 2012. Modeling and experimental verification of a solar powered liquid desiccant cooling system for greenhouse food production in hot climates. *Energy*, **40**, 116–130.

Ma, Q., Wang, R.Z., Dai, Y.J., Zhai, X.Q., 2006. Performance analysis on a hybrid air-conditioning system of a green building. *Energy and Buildings*, **38**, 447–453.

Mahmud, K., Mahmood, G.I., Simonson, C.J., Besant, R.W., 2010. Performance testing of a counter-cross-flow run-around membrane energy exchanger (RAMEE) system for HVAC applications. *Energy and Buildings*, **42**, 1139-1147.

Martin, V., Goswami, D.Y., 1999. Heat and mass transfer in packed bed liquid desiccant regenerators - an experimental investigation. *ASME Journal of Solar Energy Engineering*, **121**, 162-170.

McNevin, C., Harrison, S., 2014. Performance improvements on a solar thermally driven liquid desiccant air-conditioner. Proceedings of CSME International Congress, Toronto, Canada.

Mei, L., Dai, Y.J., 2008. A technical review on use of liquid-desiccant dehumidification for air-conditioning application. *Renewable and Sustainable Energy Reviews*, **12**, 662-689.

Mendes, L.F., Collares-Pereira, M., Ziegler, F., 1998. Supply of cooling and heating with solar assisted absorption heat pumps: as energetic approach. *Solar Energy*, **21**, 116-125.

Mesquita, L.C., 2007. Analysis of a flat-plate liquid-desiccant dehumidifier and regenerator. Ph.D. Thesis, Department of Mechanical and Materials Engineering, Queen's University, Kingston, ON.

Mesquita, L.C.S., Harrison, S.J., Thomey, D., 2006. Modeling of heat and mass transfer in parallel plate liquid-desiccant dehumidifiers. *Solar Energy*, **80**, 1475–1482.

Min, T., Cheng-Qin, R., Guang-Fa, T., Zhen-Sheng, Z., 2010. Performance comparison between two novel configuration of liquid desiccant air-conditioning system. *Building and Environment*, **45**, 2808–2816.

Misha, S., Mat, S., Ruslan, M.H., Sopian, K., 2012. Review of solid/liquid desiccant in the drying applications and its regeneration methods. *Renewable and Sustainable Energy Reviews*, **16**, 4686-4707.

Moghaddam, D.G., 2014. Testing small-scale and full-scale liquid-to-air membrane energy exchangers (LAMEEs), Ph.D. thesis, Department of Mechanical Engineering, College of Engineering, University of Saskatchewan, Saskatoon, SK.

Moghaddam, D.G., LePoudre, P.P., Besant, R.W., Simonson, C.J., 2013a. Evaluating the steady-state performance of a small-scale liquid-to-air membrane energy exchanger for different heat and mass transfer directions and liquid desiccant types and concentrations: experimental and numerical data. *ASME Journal of Heat Transfer*, **135**.

Moghaddam, D.G., Oghabi, A., Ge, G., Besant, R.W., Simonson, C.J., 2013b. Numerical model of a small-scale liquid-to-air membrane energy exchanger: parametric study of membrane resistance and air side convective heat transfer coefficient, *Applied Thermal Engineering*, **61**, 245-258.

Moghaddam, D.G, Mahmood, G., Ge, G., Besant, R.W., Simonson, C.J., 2013c. Steady-state performance of a prototype (200cfm) liquid-to-air membrane energy exchanger (LAMEE) under summer and winter test conditions. Proceedings of the ASME 2013 summer heat transfer conference, Minneapolis, USA.

Moghaddam, D.G., Oghabi, A., Ge, G., Besant, R.W., Simonson, C.J., 2013d. Numerical model of a small-scale liquid-to-air membrane energy exchanger: Parametric study of membrane resistance and air side convective heat transfer coefficient. *Applied Thermal Engineering*, **61**, 245-258.

Moghaddam, D.G., Ge, G., Abdel-Salam, A.H., Besant, R.W., Simonson, C.J., 2013e. Effects of solution inlet temperature on the effectiveness and moisture removal rate of a liquid-to-air membrane energy exchanger (LAMEE) during regenerator operating conditions. Proceedings of the 24th Canadian Conference of Applied Mechanics (CANCAM 2013), Saskatoon, SK, Canada.

Mohammad, A.T., Mat, S.B., Sulaiman, M.Y., Sopian, K., Al-abidi, A.A., 2013. Survey of liquid desiccant dehumidification system based on integrated vapor compression technology for building applications. *Energy and Buildings*, **62**, 1-14.

Molero-Villar, N., Cejudo-Lopez, J.M., Dominguez-Munoz, F., Carrillo-Andres, A., 2012. A comparison of solar absorption system configurations. *Solar Energy*, **86**, 242-252.

Mossman, M.J., 2010. RSMeans Mechanical Cost Data, Massachusetts: RSMeans.

Mumma, S.A., 2001a. Overview of integrating dedicated outdoor air systems with parallel terminal systems. *ASHRAE Transaction*, **107**, 542-552.

Mumma, S.A., 2001b. Dedicated outdoor air-dual wheel system control requirements. *ASHRAE Transactions*, **107**, 147–155.

Namvar, R., 2012. Transient and steady-state performance of a liquid-to-air membrane energy exchanger (LAMEE). M.Sc. thesis, Department of Mechanical Engineering, College of Engineering, University of Saskatchewan, Saskatoon, SK (http://ecommons.usask.ca/bitstream/handle/10388/etd-2012-09-635/NAMVAR-THESIS.pdf).

Namvar, R., Pyra, D., Ge, G., Simonson, C.J., Besant, R.W., 2012. Transient characteristics of a liquid-to-air membrane energy exchanger (LAMEE) experimental data with correlations. *International Journal of Heat and Mass Transfer*, **55**, 6682-6694.

Natural Gas Supply Association - [cited 15 April 2013]. Available from: (http://www.naturalgas.org/environment/naturalgas.asp).

Nayak, S.M., Hwang, Y., Radermacher, R., 2009. Performance characterization of gas engine generator integrated with a liquid desiccant dehumidification system. *Applied Thermal Engineering*, **29**, 479–490.

Niu, X., Xiao, F., Ge, G., 2010. Performance analysis of liquid desiccant based air-conditioning system under variable fresh air ratios. *Energy and Buildings*, **42**, 2457-2464.

Niu, X., Xiao, F., Ma, Z., 2012. Investigation on capacity matching in liquid desiccant and heat pump hybrid air-conditioning systems. *International Journal of Refrigeration*, **35**, 160-170.

Oberg, V., Goswami, D.Y., 1998. Experimental study of the heat and mass transfer in a packed bed liquid desiccant air dehumidifier. *ASME Journal of Solar Energy Engineering*, **120**, 289-297.

Peng, D., Zhang, X., 2011. Modelling and simulation of solar collector/regenerator for liquid desiccant cooling systems. *Energy*, **36**, 2543-2550.

Perez-Lombard, L., Ortiz, J., Pout, C., 2008. A review on buildings energy consumption information. *Energy and Buildings*, **40**, 394-398.

Pineda, S.M., Diaz, G., 2011. Performance of an adiabatic cross-flow liquid-desiccant absorber inside a refrigerated warehouse. *International Journal of Refrigeration*, **34**, 138-147.

Qi, R., Lu, L., Yang, H., 2012. Investigation on air-conditioning load profile and energy consumption of desiccant cooling system for commercial buildings in Hong Kong. *Energy and Buildings*, **49**, 509-518.

Qi, R., Lu, L., Yang, H., Qin, F., 2013. Investigation on wetted area and film thickness for falling film liquid desiccant regeneration system. *Applied Energy*, **112**, 93-101.

Qi, R., Lu, L., Qin, F., 2014. Model development for the wetted area of falling film liquid desiccant air-conditioning system. *International Journal of Heat and Mass Transfer*, **74**, 206–209.

Radhwan, A.M., Gari, H.N., Elsayed, M.M., 1993. Parametric study of a packed bed dehumidifier/regenerator using $CaCl_2$ liquid desiccant. *Renewable energy*, **3**, 49-60.

Rasouli, M., Akbari, S., Hemingson, H., Besant, R.W., Simonson, C.J., 2011. Application of a run-around membrane energy exchanger in an office building HVAC system. *ASHRAE Transactions*, **117**, 686-703.

Rasouli, M., Simonson, C.J., Besant, R.W., 2010. Applicability and optimum control strategy of energy recovery ventilators in different climatic conditions. *Energy and Buildings*, **42**, 1376–1385.

Rattner, A.S., Nagavarapu, A.K., Garimella, S., Fuller, T.F., 2011. Modeling of a flat plate membrane-distillation system for liquid desiccant regeneration in air-conditioning applications. *International Journal of Heat and Mass Transfer*, **54**, 3650-3660.

Rhodes, J.D., Stephens, B., Webber, M.E., 2012. Energy audit analysis of residential air-conditioning systems in Austin, Texas. *ASHRAE Transactions*, **118**, 143-150.

Rushing, A.S., Kneifel, J.D., Lippiat, B.C., 2011. Energy price indices and discount factors for life-cycle cost analysis, Maryland: National Institute of Standards and Technology.

Salimizad, D., McNevin, C., Harrison, S., 2014. Evaluation of cooling water storage for liquid-desiccant air conditioning system. Proceedings of ASME International Mechanical Engineering Congress and Exposition, Montreal, Canada.

Sarbu, I., 2014. A review on substitution strategy of non-ecological refrigerants from vapour compression-based refrigeration, air-conditioning and heat pump systems. *International Journal of Refrigeration*, **46**, 123-141.
Simonson, C.J., Besant, R.W., 1999. Energy wheel effectiveness: part I—development of dimensionless groups. *International Journal of Heat and Mass Transfer*, **42**, 2161 - 2170.

Simonson, C.J., Besant, R.W., 1999. Energy wheel effectiveness: part II-correlations. *International Journal of Heat and Mass Transfer*, **42**, 2171-2185.

Sterling, E.M., Arundel, A., Sterling, T.D., 1985. Criteria for human exposure to humidity in occupied buildings. *ASHRAE Transactions*, **91**, 611-622.

Sullivan, C., 2011. Liquid desiccant dehumidification for challenging environments. *Engineering Systems*, **28**.

Syed, A., Izquierdo, M., Rodriguez, P., Maidment, G., Missenden, J., Lecuona, A., Tozer, R., 2005. A novel experimental investigation of a solar cooling in Madrid. *International Journal of Refrigeration*, **28**, 859-871.

Trane Corporation (www.trane.com/commercial).

TRNSYS-version 17, 2010. Solar Energy Laboratory, University of Wisconsin, Madison, Wisconsin.

Tu, R., Liu, X.-H., Jiang, Y., 2014. Performance analysis of a two-stage desiccant cooling system. *Applied Energy*, **113**, 1562-1574

US Department of Energy. 2010 buildings energy data book - [cited 15 April 2013]. Available from: (http://buildingsdatabook.eren.doe.gov/docs/DataBooks/2010_BEDB).

US Energy Information Administration. Independent statistics & analysis - [cited 15 April 2013]. Available from: (http://www.eia.gov/state).

Vali, A., Simonson, C.J., Besant, R.W., Mahmood, G.I., 2009. Numerical model and effectiveness correlations for a run-around heat recovery system with combined counter and cross flow exchangers. *International Journal of Heat and Mass Transfer*, **52**, 5827-5840.

Welty, J.R., Wicks, C.E., Wilson, R.E., 2001. Fundamentals of Momentum, Heat and Mass Transfer, John Wiley & Sons Inc., New York.

Xiao, F., Ge, G., Niu, X., 2011. Control performance of a dedicated outdoor air system adopting liquid desiccant dehumidification. *Applied Energy*, **88**, 143-149.

Yadav, Y.K., 1995. Vapour-compression and liquid-desiccant hybrid solar space-conditioning system for energy conservation. *Renewable Energy*, **6**, 719-723.

Yamaguchi, S., Jeong, J., Saito, K., Miyauchi, H., Harada, M., 2011. Hybrid liquid desiccant air-conditioning system: Experiments and simulations. *Applied Thermal Engineering*, **31**, 3741-3747.

Yin, Y., Zhang, X., Wang, G., Luo, L., 2008. Experimental study on a new internally cooled/heated dehumidifier/regenerator of liquid desiccant systems. *International Journal of Refrigeration*, **31**, 857-66.

Yin, Y., Zhang, X., 2010. Comparative study on internally heated and adiabatic regenerators in liquid desiccant air conditioning system. *Building and Environment*, **45**, 1799-807.

Yutong, L., Hongxing, Y., 2008. Investigation on solar desiccant dehumidification process for energy conservation of central air-conditioning systems. *Applied Thermal Engineering*, **28**, 1118-1126.

Zhang, L.-Z., Niu, J.L., 2001. Energy requirements for conditioning fresh air and the long-term savings with a membrane-based energy recovery ventilator in Hong Kong. *Energy*, **26**, 119-35.

Zhang, L.-Z., Zhu, D.S., Deng, X.H., Hua, B, 2005. Thermodynamic modeling of a novel air dehumidification system. *Energy and Buildings*, **37**, 279–286.

Zhang, L., Dang, C., Hihara, E., 2010a. Performance analysis of a no-frost hybrid air conditioning system with integrated liquid desiccant dehumidification. *International Journal of Refrigeration*, **33**, 116-124.

Zhang, L.-Z., Liang, C., Pei, L., 2010b. Conjugate heat and mass transfer in membrane-formed channels in all entry regions. *International Journal of Heat and Mass Transfer*, **53**, 815-824.

Zhang, L.-Z., 2011. An analytical solution to heat and mass transfer in hollow fiber membrane contactors for liquid desiccant air dehumidification. *ASME Journal of Heat Transfer*, **133**, 1-8.

Zhao, K., Liu, X.-H., Zhang, T., Jiang, Y., 2011. Performance of temperature and humidity independent control air-conditioning system in an office building. *Energy and Buildings*, **43**, 1895-1903.

Zhang, T., Liu, X., Jiang, Y., 2012a. Performance optimization of heat pump driven liquid desiccant dehumidification systems. *Energy and Buildings*, **52**, 132-144.

Zhang, L.Z., Zhang, X.R., Miao, Q.Z., Pei, L.X., 2012b. Selective permeation of moisture and VOCs through polymer membranes used in total heat exchangers for indoor air ventilation. *Indoor Air*, **22**, 321–330.

Zhang, T., Liu, X.-H., Jiang, Y., 2013a. Performance comparison of liquid desiccant air handling processes from the perspective of match properties. *Energy Conversion and Management*, **75**, 51-60.

Zhang, T., Liu, X., Jiang, J., Chang, X., Jiang, Y., 2013b. Experimental analysis of an internally-cooled liquid desiccant dehumidifier. *Building and Environment*, **63**, 1-10.

Zhang, L.-Z., Zhang, N., 2014. A heat pump driven and hollow fiber membrane-based liquid desiccant air dehumidification system: Modelling and experimental validation. *Energy*, **65**, 441-451.

<http://joyceriver.com.sg>

<http://www.engineeringvillage.com>

<http://www.sulzer.com>

<http://www.yugie.com>

<http://www.floridapsc.com/publications/pdf/general/factsandfigures2013.pdf>

<http://www.naturalgas.org/environment/naturalgas.asp>

<http://www.epa.gov/ozone/title6/phaseout/22phaseout.html>

APPENDIX

COPYRIGHT PERMISSIONS

This Appendix includes the copyright permissions for the published and coauthored manuscripts presented in this thesis. For manuscripts that form part of a thesis, the College of Graduate Studies and Research (CGSR) requires a written request from:

- the publisher (copyright holder) for previously published manuscripts, and
- the co-author(s) for unpublished manuscripts.

The permissions for using the published manuscripts in this thesis are presented in Sections A.1 and A.2, and the permission for using the unpublished manuscripts are presented in Sections A.3 and A.4.

A.1 Permission for manuscripts used in Chapters 2, 3, 4 and 6

The manuscripts used in Chapters 2, 3, 4 and 6 are published by Elsevier. For manuscripts published by Elsevier, the authors retain the right to include their publication in a thesis without requesting a written permission as mentioned at the publisher's website as follows.

"As an author, you retain rights for a large number of author uses, including use by your employing institute or company. These rights are retained and permitted without the need to obtain specific permission from Elsevier. These include: the right to include the article in full or in part in a thesis or dissertation (provided that this is not to be published commercially); the right to use the article or any part thereof in a printed compilation of works of the author, such as collected writings or lecture notes (subsequent to publication of the article in the journal); and the right to prepare other derivative works, to extend the article into book-length form, or to otherwise re-use portions or excerpts in other works, with full acknowledgement of its original publication in the journal."

~Source: http://support.elsevier.com/app/answers/detail/a_id/565/session/L3RpbWUv

A.2 Permission for manuscript used in Chapter 5

The manuscript used in Chapter 5 is published in the proceedings of the esim2014 conference. A written permission for using the published manuscript in this thesis has been permitted by the conference chair by email on June 16, 2015 s follows.

"*Dear Mr. Abdel-Salam:*

It is my pleasure to grant you permission to use the paper titled "TRNSYS Moelling of a Hybrid Membrane Liquid Desiccant Air Conditioning System" from the esim 2014 proceedings. The paper is to be used in your Ph.D. thesis, which is to be published by the University of Saskatchewan.

Sincerely,
William (Liam) O'Brien, PhD
Assistant Professor
Architectural Conservation and Sustainability Engineering
Carleton University
Canal Building, 5208
PI, Human Building Interaction Laboratory (carleton.ca/hbilab)
Phone: (613) 520-2600 ext. 8037
Email: liam.obrien@carleton.ca"

A.3 Permission for manuscript used in Chapter 7

The manuscript used in Chapter 7 is unpublished, and thus a copyright permission is obtained from the coauthor of the paper (Dr. Carey Simonson) as follows.

Copyright Permission Request Form

I am preparing the publication of a manuscript titled "A novel control strategy for a heat-pump membrane liquid desiccant air conditioning system" to be published as the seventh chapter of my Ph.D. thesis, and to be submitted to the Department of Mechanical Engineering at the University of Saskatchewan. The authors contributing in the completion of this manuscript are Ahmed H. Abdel-Salam and Carey J. Simonson.

I am requesting permission to use the materials described in aforementioned manuscript in my Ph.D. thesis and all subsequent editions that may be prepared at the University of Saskatchewan. Please indicate agreement by signing below.

Sincerely,
Ahmed Abdel-Salam
June 16, 2015

Permission granted by: Carey J. Simonson
Signature:
Date:

A.4 Permission for manuscript used in Chapter 8

The manuscript used in Chapter 8 is unpublished, and thus copyright permissions are obtained from the coauthors of the paper (Mr. Chris McNevin, Ms. Lisa Crofoot, Dr. Stephen Harrison, and Dr. Carey Simonson) as follows.

Copyright Permission Request Form

I am preparing the publication of a manuscript titled "A field study of a solar liquid desiccant air conditioning system: Quasi-steady and transient performance" to be published as the seventh chapter of my Ph.D. thesis, and to be submitted to the Department of Mechanical Engineering at the University of Saskatchewan. The authors contributing in the completion of this manuscript are Ahmed H. Abdel-Salam, Chris McNevin, Lisa Crofoot, Stephen J. Harrison and Carey J. Simonson.

I am requesting permission to use the materials described in aforementioned manuscript in my Ph.D. thesis and all subsequent editions that may be prepared at the University of Saskatchewan. Please indicate agreement by signing below.

Sincerely,
Ahmed Abdel-Salam
June 16, 2015

Permission granted by: Chris McNevin
Signature:
Date:

Copyright Permission Request Form

I am preparing the publication of a manuscript titled "A field study of a solar liquid desiccant air conditioning system: Quasi-steady and transient performance" to be published as the seventh chapter of my Ph.D. thesis, and to be submitted to the Department of Mechanical Engineering at the University of Saskatchewan. The authors contributing in the completion of this manuscript are Ahmed H. Abdel-Salam, Chris McNevin, Lisa Crofoot, Stephen J. Harrison and Carey J. Simonson.

I am requesting permission to use the materials described in aforementioned manuscript in my Ph.D. thesis and all subsequent editions that may be prepared at the University of Saskatchewan. Please indicate agreement by signing below.

Sincerely,
Ahmed Abdel-Salam
June 16, 2015

Permission granted by: Lisa Crofoot
Signature:
Date:

Copyright Permission Request Form

I am preparing the publication of a manuscript titled "A field study of a solar liquid desiccant air conditioning system: Quasi-steady and transient performance" to be published as the seventh chapter of my Ph.D. thesis, and to be submitted to the Department of Mechanical Engineering at the University of Saskatchewan. The authors contributing in the completion of this manuscript are Ahmed H. Abdel-Salam, Chris McNevin, Lisa Crofoot, Stephen J. Harrison and Carey J. Simonson.

I am requesting permission to use the materials described in aforementioned manuscript in my Ph.D. thesis and all subsequent editions that may be prepared at the University of Saskatchewan. Please indicate agreement by signing below.

Sincerely,
Ahmed Abdel-Salam
June 16, 2015

Permission granted by: Stephen Harrison
Signature:
Date:

Copyright Permission Request Form

I am preparing the publication of a manuscript titled "A field study of a solar liquid desiccant air conditioning system: Quasi-steady and transient performance" to be published as the seventh chapter of my Ph.D. thesis, and to be submitted to the Department of Mechanical Engineering at the University of Saskatchewan. The authors contributing in the completion of this manuscript are Ahmed H. Abdel-Salam, Chris McNevin, Lisa Crofoot, Stephen J. Harrison and Carey J. Simonson.

I am requesting permission to use the materials described in aforementioned manuscript in my Ph.D. thesis and all subsequent editions that may be prepared at the University of Saskatchewan. Please indicate agreement by signing below.

Sincerely,
Ahmed Abdel-Salam
June 16, 2015

Permission granted by: Carey Simonson
Signature:
Date: